An investigation into the role of MeCP2 in sleep-related brain rhythms and memory consolidation

Grace Louise Cowen

PhD

University of York
Biology

November 2021

In loving memory of *Miles A Whittington*

The kindest soul, the quickest wit and the most brilliant mind I've ever met.

Abstract

Methyl-CpG binding protein 2 (MeCP2) is a chromatin-associated protein which functions in epigenetic gene regulation. Mutations in MeCP2 lead to a variety of neurological disorders, including Rett Syndrome (RTT). Learning and memory deficits are prevalent in RTT, as are sleep disturbances: throughout the night, RTT patients spend less time in Stage 3 non-rapid eye movement (NREM) sleep. Delta oscillations (0.5 – 4 Hz) are the main constituent of Stage 3 NREM sleep, and are thought to be vital for sleep-related memory consolidation.

In this thesis, the mechanisms and networks involved in delta oscillation generation were studied in a mouse model of RTT. In isolated sections of somatosensory cortex, loss of MeCP2 function resulted in the disruption of pharmacologically-induced cortical delta oscillations. In contrast, delta oscillations that arise via the thalamic generator remained intact. Pre-symptomatic *Mecp2*-null animals showed partial preservation of cortical delta oscillations, suggesting that neurological deficits precede phenotype onset.

Intracellular current clamp recordings revealed that loss of MeCP2 function impairs the firing pattern of layer V intrinsically bursting pyramidal neurons, the cells responsible for generating the cortical delta rhythm. The bursting mechanism of these cells was restored by reducing the intracellular calcium ion concentration in these cells, which was also sufficient to reinstate the cortical delta rhythm.

Finally, delta oscillations, sleep spindles and hippocampal sharp-wave ripples were studied *in vivo* during NREM sleep, since the coupling of these rhythms is thought to facilitate sleep-related memory consolidation. Rhythm coupling was unaffected by the loss of MeCP2 function, however the incidence of all three rhythms was significantly reduced, resulting in impaired performance on a hippocampus-dependent spatial memory task.

The implication of these results on our understanding of the precise role of MeCP2 in coordinating NREM-associated brain rhythms and on the development of learning and memory deficits in RTT are discussed.

Contents

DEDICATION **2**

ABSTRACT **3**

CONTENTS **4**

LIST OF FIGURES AND TABLES **10**

ACKNOWLEDGEMENTS **13**

AUTHOR'S DECLARATION **15**

CHAPTER 1 – GENERAL INTRODUCTION **16**

1.1 DNA METHYLATION AND MECP2 ..... **16**

1.1.1 DNA methylation 16

1.1.2 MeCP2 and gene repression 19

1.1.3 Other possible functions of MeCP2 22

1.1.4 MeCP2 domain organisation and mutations 24

1.1.5 MeCP2 splice variants 25

1.2 CLINICAL RELEVANCE OF MECP2 ..... **27**

1.2.1 Rett syndrome (RTT) 27

1.2.2 Gender differences in RTT 29

1.2.3 Other MeCP2-related disorders 30

1.2.4 Sleep disturbances in RTT and other MeCP2-related disorders 33

1.3 SLEEP **34**

1.3.1 The sleep cycle 34

1.3.1.1 Wakefulness 34

1.3.1.2 Non-rapid eye movement (NREM) sleep 35

1.3.1.3 Rapid eye movement (REM) sleep 36

1.3.2 Biological function of sleep 36

1.3.3 Sleep and memory consolidation 37

1.3.4 Consequences of sleep deprivation 38

1.3.5 Sleep-cycle changes in RTT 39

1.4 NEURONAL OSCILLATIONS **40**

1.4.1 Electroencephalogram (EEG) 40

1.4.2 Neuronal oscillations 40
1.4.3 Neuronal oscillations associated with wakefulness 41
1.4.3.1 Gamma oscillations (30 - 80 Hz) 41
1.4.3.2 Beta II (20 - 30 Hz) and Beta I (12 - 20 Hz) oscillations 42
1.4.3.3 Alpha oscillations (8 - 12 Hz) 42
1.4.4 Neuronal oscillations associated with REM sleep 43
1.4.4.1 Theta oscillations (4 - 8 Hz) 43
1.4.5 Neuronal oscillations associated with NREM sleep 43
1.4.5.1 Sleep spindles (7 - 14 Hz) 43
1.4.5.2 Delta oscillations (0.5 - 4 Hz) 44
1.4.5.3 Slow wave oscillations (<1 Hz) 48
1.4.5.4 Hippocampal sharp-wave ripples (100 - 200 Hz) 48
1.4.6 The Two-Stage theory of memory consolidation 49
1.4.7 Neuronal oscillations in RTT 51
1.5 NEURONAL NETWORKS 52
1.5.1 Structure and function of the neocortex 52
1.5.2 The Somatosensory Cortex 55
1.5.3 Intrinsically bursting (IB) pyramidal neurons 56
1.5.4 Calcium ions in neuronal signalling 58
1.5.4.1 Voltage-gated calcium channels (VGCCs) 61
1.5.5 Changes in neuronal connectivity in RTT 62
1.6 AIMS AND OBJECTIVES 65

CHAPTER 2 – MATERIALS AND METHODS 66

2.1 *MECP2*-STOP MICE 66
2.1.1 Animal housing and husbandry 66
2.1.2 Licensing 66
2.1.3 Genotyping 66
2.1.4 Immunohistochemistry 68
2.2 SOLUTIONS AND DRUGS 69
2.3 ISOLATED SLICE ELECTROPHYSIOLOGY 72
2.3.1 Anaesthesia and surgical procedures 72
2.3.2 Preparation of neocortical brain slices 72
2.3.2.1 Coronal sections 73
2.3.2.2 Thalamocortical sections 73
2.3.3 Maintenance of brain slices 73
2.3.4 Extracellular recording technique 75

2.3.5 Intracellular recording technique 76
2.3.6 Data acquisition, processing and analysis 77
2.4 *IN VIVO* PROTOCOLS 77
2.4.1 Pre-surgery acclimatisation 77
2.4.2 Surgical techniques 77
2.4.3 Post-surgery care and acclimatisation 79
2.4.4 Longitudinal recordings 79
2.4.5 Data acquisition, processing and analysis 79
2.4.6 Electrode location confirmation 80
2.5 BEHAVIOURAL STUDIES 80
2.5.1 Pre-test acclimatisation 80
2.5.2 Novel Location Recognition Task 80
2.5.3 Data acquisition and analysis 82
CHAPTER 3 – CORTICAL AND THALAMOCORTICAL DELTA OSCILLATIONS IN ISOLATED BRAIN SLICES 83
3.1 AIMS 83
3.2 RESULTS 83
3.2.1 Loss of MeCP2 impairs the generation of cortical delta oscillations 83
3.2.2 Cortical delta rhythms are partially preserved in pre-symptomatic *Mecp2*$^{Stop/y}$ mice 88
3.2.3 Thalamocortical delta rhythms are preserved in *Mecp2*$^{Stop/y}$ mice 90
3.3 DISCUSSION 91
3.3.1 The *in vitro* model of cortical delta oscillations 91
3.3.2 Delta oscillations in the absence of MeCP2 function 93
3.3.3 Functional differences between the cortical and thalamocortical delta oscillation generators 94
3.3.4 Age-dependent changes in neuronal oscillations and the role of MeCP2 98
3.4 SUMMARY 100
CHAPTER 4 – CELLULAR CONSEQUENCES OF LOSS OF MECP2 FUNCTION IN LAYER V PYRAMIDAL NEURONS 102
4.1 AIMS 102
4.2 RESULTS 102
4.2.1 Loss of MeCP2 decreases bursting in IB pyramidal neurons 102
4.2.2 Action potential generation and baseline synaptic transmission is normal in regular spiking neurons from *Mecp2*$^{Stop/y}$ mice 106

4.2.3 Proportionally fewer *Mecp2*-null IB cells were recorded compared to WT cells 109
4.3 DISCUSSION 109
4.3.1 MeCP2 function has cell-type specificity 109
4.3.2 Resting membrane potential modulates IB cell bursting 112
4.3.3 Fewer IB cells were recorded from *Mecp2*-null brain slices compared to WT 113
4.3.4 Interneuron function following MeCP2 loss and implications for delta oscillations 114
4.3.5 MeCP2 mutations in distinct neuronal circuits and generalisability of results 116
4.4 SUMMARY 118
CHAPTER 5 – MOLECULAR CONSEQUENCES OF LOSS OF MECP2 FUNCTION IN LAYER V PYRAMIDAL NEURONS 119
5.1 AIMS 119
5.2 RESULTS 119
5.2.1 Increasing intracellular Ca2+ concentrations inhibit the bursts of spike generation that characterise IB neurons 119
5.2.2 Increasing intracellular Ca^{2+} concentration inhibits the generation of cortical delta oscillations 122
5.2.3 Reducing intracellular calcium concentration restores the bursting potential of *Mecp2*-null IB cells 124
5.2.4 Cortical delta oscillations are restored in *Mecp2*$^{Stop/y}$ mice by pharmacological blockade of voltage-gated calcium channels 126
5.2.5 Intracellular calcium concentrations must be tightly regulated for delta oscillations to be generated 130
5.3 DISCUSSION 131
5.3.1 The role of Ca^{2+} in burst generation during IB cell firing 131
5.3.2 Gene expression changes and Ca^{2+} regulation in *Mecp2*-null neurons 135
5.3.3 The relationship between MeCP2 and Ca^{2+} 138
5.3.4 Ca^{2+}-modulating drugs as a therapeutic target for sleep disturbances in RTT 140
5.3.4.1 Pharmacological properties of Ca^{2+} modulating drugs 143
5.4 SUMMARY 146

CHAPTER 6 – *IN VIVO* ASSESSMENT OF THE ROLE OF MECP2 ON SLEEP-RELATED BRAIN RHYTHMS AND MEMORY CONSOLIDATION 148

6.1 AIMS 148

6.1.1 Detection of Delta Waves 148

6.1.2 Detection of Spindles 149

6.1.3 Detection of Sharp Wave-Ripples (SPW-Rs) 150

6.2 RESULTS 151

6.2.1 Loss of MeCP2 decreases the number of cortical delta waves during NREM sleep 151

6.2.2 The incidence and amplitude of sleep spindles is decreased in *Mecp2*$^{Stop/y}$ mice 153

6.2.3 Loss of MeCP2 results in a decrease in the frequency and incidence of CA1 ripple oscillations during NREM sleep 153

6.2.4 Hippocampo-cortical oscillatory coupling is normal in *Mecp2*$^{Stop/y}$ mice ... 156

6.2.5 *Mecp2*-null mice exhibit impaired performance in a novel location recognition task 157

6.3 DISCUSSION 159

6.3.1 Reduced delta oscillation incidence following loss of MeCP2 function 159

6.3.2 Loss of MeCP2 function also affects the properties of other NREM-associated brain rhythms 162

6.3.3 Coupling of NREM-associated rhythms is unaffected by the loss of MeCP2 function 165

6.3.4 The importance of MeCP2 function for performance on a hippocampus-dependent learning and memory task 166

6.4 SUMMARY 168

CHAPTER 7 – GENERAL DISCUSSION 170

7.1 OVERVIEW 170

7.1.1 Summary of findings 170

7.2 WIDER IMPLICATIONS 171

7.3 STRENGTHS AND WEAKNESSES OF THIS PROJECT 172

7.4 FUTURE DIRECTIONS 174

7.4.1 Differential influence of MeCP2 on cortical and thalamocortical networks 174

7.4.2 Age-dependent reduction in delta oscillation power 176

7.4.3 Delta oscillations in other brain regions 177

7.4.4 Delta oscillations during wakefulness 177
7.4.5 Delta oscillations couple to higher frequency rhythms 178
7.4.6 Loss of MeCP2 function on beta oscillations 179
7.4.7 Effect of Ca^{2+}-modulating drugs *in vivo* during sleep and on hippocampus-dependent memory consolidation 180
7.4.8 Quantification of intracellular Ca^{2+} concentration misregulation in *Mecp2*-null cells 181
7.4.9 Further exploration into the effect of MeCP2 on sleep spindles 182
7.4.10 Further exploration into the effect of MeCP2 on hippocampal SPW-Rs 183

LIST OF ABBREVIATIONS 184

BIBLIOGRAPHY 186

List of figures and tables

Chapter 1

Figure 1.1	DNA methylation of cytosine residues at CpG sites	18
Figure 1.2	Proposed functions of MeCP2	23
Figure 1.3	Alternative splice variants of MeCP2	26
Figure 1.4	Clinical progression and life expectancy as a result of MeCP2 mutations in humans and mice	31
Figure 1.5	The sleep cycle	35
Figure 1.6	Laminar structure of the neocortex	54
Figure 1.7	Calcium regulation in neurons	60

Chapter 2

Figure 2.1	*Mecp2*$^{Stop/y}$ mouse model	67
Table 2.1	List of chemicals, compounds and pharmacological agents	69
Figure 2.2	Schematic representation of brain slice preparations used in *in vitro* electrophysiological experiments	74
Figure 2.3	Schematic representation of recording equipment used for S1-CA1 *in vivo* experiments	78
Figure 2.4	Novel location recognition task	81

Chapter 3

Figure 3.1	Loss of MeCP2 impairs the generation of cortical delta oscillations across the S1 somatosensory cortex	84
Figure 3.2	Current source density analysis reveals the generation of delta oscillations specifically from layer V of the somatosensory cortex, the source of which is lost in *Mecp2*-null mice	86
Figure 3.3	Loss of MeCP2 impairs the generation of cortical delta oscillations	87
Figure 3.4	Cortical delta oscillations are partially preserved in pre-symptomatic *Mecp2*$^{Stop/y}$ mice	89
Figure 3.5	Thalamocortical delta oscillations are preserved in *Mecp2*$^{Stop/y}$ mice	92

Chapter 4

Figure 4.1	Loss of MeCP2 decreases bursting in intrinsically bursting (IB) neurons	103
Figure 4.2	Cellular characteristics of *Mecp2*-null IB neurons are significantly altered compared to WT IB cells	105
Figure 4.3	Action potential generation and baseline synaptic transmission is normal in regular spiking neurons from *Mecp2*$^{Stop/y}$ mice	107
Figure 4.4	Proportionally fewer IB cells were recorded from *Mecp2*-null brain slices compared to WT slices	109

Chapter 5

Figure 5.1	Inhibition of the SERCA pump via CPA application	120
Figure 5.2	Increasing the intracellular concentration of calcium ions extinguishes the bursting potential of WT IB neurons	121
Figure 5.3	Increasing the intracellular concentration of calcium ions abolishes the pre-existing cortical delta rhythm	123
Figure 5.4	Reduction of intracellular calcium ion concentration via the addition of the calcium chelator EGTA	124
Figure 5.5	Reducing the intracellular concentration of calcium ions is sufficient to re-establish the bursting potential of KO IB neurons, but does not alter the firing patterns of KO RS cells	125
Figure 5.6	Pharmacological blockade of voltage gated calcium channels inhibits calcium ion entry into the cell	127
Figure 5.7	Reducing the intracellular concentration of calcium ions is sufficient to re-establish the neocortical delta rhythm in *Mecp2*-null coronal brain slices	128
Figure 5.8	WT delta oscillations cannot be generated when intracellular calcium ion concentrations are too low	132

Chapter 6

Figure 6.1	Detection of delta waves during NREM sleep	149
Figure 6.2	Detection of sleep spindles during NREM sleep	150

Figure 6.3	Loss of MeCP2 decreases the number of cortical delta waves during NREM sleep	152
Figure 6.4	The power and incidence of sleep spindles is decreased in Mecp2-Stop mice	154
Figure 6.5	Loss of MeCP2 results in a decrease in the frequency and incidence of CA1 ripple oscillations during NREM sleep	155
Figure 6.6	Hippocampo-cortical oscillatory coupling is normal in *Mecp2*$^{Stop/y}$ mice	157
Figure 6.7	Loss of MeCP2 function impairs performance on a hippocampus-dependent spatial memory task	159

Acknowledgements

I would like to dedicate my thesis to one of my supervisors, Professor Miles Whittington, who sadly passed away in October 2021. Miles, your passion for research was inspiring and your sense of humour always kept us on our toes. I'm gutted you didn't get to see this project to the end – I think you would have really loved the final product.

To my main supervisor, Darren. Thank you for all your help, for always believing in me and for pushing me to reach my fullest potential, even when I didn't know it was there. Also, thank you for bringing me that bread roll and can of coke during the worst hangover of my life in Rome – I think you might have actually saved my life that day! To Will, your help, guidance and support as both my TAP member and then supervisor have meant so much. Also, to Sean and Sangeeta for their support during TAP and progression meetings, I can't thank you enough.

To Annie, Grace, Jess and Sarah – the Long Boi's Gals! I am so glad we got to share this experience together; you guys have got me through the hardest of times during this process and I love you all so much for that. I hope we will still be dancing 'til the lights come on in Flares when we're old and grey. To Annie especially, it's been you and me since day one, I don't know what I would have done without you by my side.

To Nick, for not rolling your eyes every time I asked a MATLAB question (even 18 months after you left), and more importantly, for teaching me the rules of NFL – thank you! I look forward to many years of Packers vs Seahawks rivalry. To Steve, the last few years really haven't been the same without your crude jokes and witty northern charm. Thank you for your constant piss-taking, only you could get away with it. To Iain, Anna, Alex, Jack, Lizzie and everyone else that has come and gone during my time in the lab – you're all awesome! To Chris, Carl and everyone in the BSF – you guys are the unsung heroes of this project.

To the Seshlington Road Gang who were part of my York journey before I even started my PhD – you guys are just the best! To Anna, your unwavering support means more than I could ever put into words – love you, Banana! To the GILS from home, thank you for not hating me when I said for the 100th time in a row that I wouldn't be able to attend another one of our get-togethers – I'm excited to spend more time with you all from now on! To Holly, Jenny and everyone else who has welcomed me into the Academy family,

thank you for making this transition into the next stage of my life on of the best decisions I've ever made.

To Ellie, the best housemate, musical-duet partner and co-founder of Lasagne Day I could ever have wished for. Thank you for letting me burden you with four years' worth of PhD rants. Always remember: a pint, a pint and half an ounce… right?

To my incredible family: the Thompson clan (Hey Nan, you finally got a Dr in the family!), and the Cuttifords and Feehans, I love you all. To Laura, my best friend and greatest supporter, thank you for always believing in me and for sending me an endless stream of dog videos on Instagram, you always know exactly how to cheer me up. Love ya, mean it! To Mum, Dad and Chris, the three best parents I could ever have wished for. Your love and support (both emotional and financial, lol) have been my rock throughout this whole experience. I love you all so much and I hope I can continue to make you proud in everything I do.

And finally, to you, the reader: I once heard the following quote: "Neurobiology is just the study of grey squishy stuff" – while I can't deny this may be true in a literal sense, I hope I can prove to you that it's also infinitely more exciting than that.

So all that is left to say is: good luck and please enjoy…

Author’s declaration

I declare that this thesis is a presentation of original work and I am the sole author. This work has not previously been presented for an award at this, or any other, University. All sources are acknowledged as References.

Chapter 1 – General introduction

1.1 DNA methylation and MeCP2

1.1.1 DNA methylation

DNA methylation is the biological process of adding a methyl ($–CH_3$) group to a cytosine residue via the activity of methyltransferase enzymes (review: Moore et al. 2012). Methylation of adenine residues occurs in prokaryotic nuclei (Vanyushin et al. 1968), though little evidence exists for this modification in eukaryotes (Douvlataniotis et al. 2020). In mammals, methylation typically occurs through the addition of a methyl group to the 5 position on the pyrimidine ring of cytosine residues to form 5-methylcytosine (mC; Fig 1.1 A). mC is almost exclusively found in CpG dinucleotides, where the cytosines on both the forward and reverse strand are usually methylated (Figure 1.1 B). This modification occurs with high frequency in the mammalian genome: although mC makes up only 1% of DNA bases in the vertebrate genome, 70-80% of CpG dinucleotides are methylated (Jang et al. 2017). In the human genome, CpG dinucleotides are under-represented: they occur at just one-fifth of the expected frequency. This likely occurs because mC residues can spontaneously deaminate to form thymine residues (Coulondre et al. 1978; Bird, 1980). The repair mechanisms that recognise the resulting T:G mismatch will replace the guanine residue with adenine, turning the original C:G pair into a T:A pair. In contrast, spontaneous deamination of unmethylated cytosine residues gives rise to uracil residues, which are recognised, repaired and restored to their original format by the cell.

In mammals, the only exception for this global CpG depletion resides in CpG-rich sequences known as CpG islands (Figure 1.1 C; Bird, 1986). These typically occur at the promoter region of a gene, or in the gene body where they serve as alternative promoters. Over 70% of genes within the human genome contain promoters that lie within CpG islands (Saxonov et al. 2006), including many housekeeping genes (Gardiner-Garden & Frommer, 1987). Methylation of gene promoters negatively correlates with gene expression levels (Moore et al. 2012), suggesting that DNA methylation functions in epigenetic gene regulation. However, the overall importance of DNA methylation in gene repression is not well understood, with much of the existing literature appearing to contradict itself. Although CpG-dense promoters of actively transcribed genes have low

levels of mC, transcriptionally silent genes do not necessarily have a highly methylated promoter. Furthermore, although methylation of CpG islands has been linked to gene repression, most CpG islands remain unmethylated independent of the transcriptional activity of the gene. In fact, it is thought that the majority of CpG islands are constitutively unmethylated (Bird et al. 1985; review: Deaton & Bird, 2018). In addition, DNA methylation is enriched in the gene body of highly transcribed genes (Hellman and Chess, 2007; Ball et al. 2009; Aran et al. 2011). DNA methylation, however, does play an important role in many forms of stable, long-term epigenetic repression, including in genes that are inherited via imprinting and those under the control of X chromosome inactivation, and in the silencing of repetitive DNA elements (Jones, 2012; Schübeler, 2015).

It is important to note that methylation of cytosine residues is not solely restricted to CpG dinucleotides. Interestingly, the proportion of CX dinucleotides (where X = A, T, C or G) throughout the genome is not evenly distributed among the four bases, and methylation levels within each group is also not proportionate to the abundance of each dinucleotide type. For example, although CA represents the most abundant CX dinucleotide (approximately 36%), relatively few of these are methylated at any one time (less than 2%). On the other hand, CG is generally under-represented in the genome (only 4% of CX), but these sites are highly methylated (approximately 80%; Lagger et al. 2017). Methylation of cytosine residues (in any CX context) is unaffected by the identity of the nucleotide preceding the mC residue in question (Laurent et al. 2010).

DNA methylation in the non-CG context (mCH, where H = A, C or T) occurs across the entire genome (Patil et al. 2014; Jang et al. 2017), and increases during postnatal development where, in the neuronal genome, it approaches the number of mCG sites (Xie et al. 2012; Lister et al. 2013; Guo et al. 2014). During development, mCA accumulation coincides with a large phase of developmentally-driven synaptogenesis (Lister et al. 2013). mCH, particularly mCA, has been identified in several stem cell lines, including human embryonic stem cells (hESCs; Lister et al. 2009; Lister et al. 2011), induced pluripotent stem cells (iPSCs; Ziller et al. 2011), and germ cells (Ichiyanagi et al. 2013). During cellular differentiation, modest yet significant changes in methylation patterns occur (Bock et al. 2012; Nazor et al. 2012), though it is unclear whether this relates to mC levels as a whole, or to any specific mCX subtype. Several stem cell marker genes become heavily methylated during hESC differentiation (Yeo et al. 2007), a process in which these genes are eventually silenced, suggesting that changes in DNA

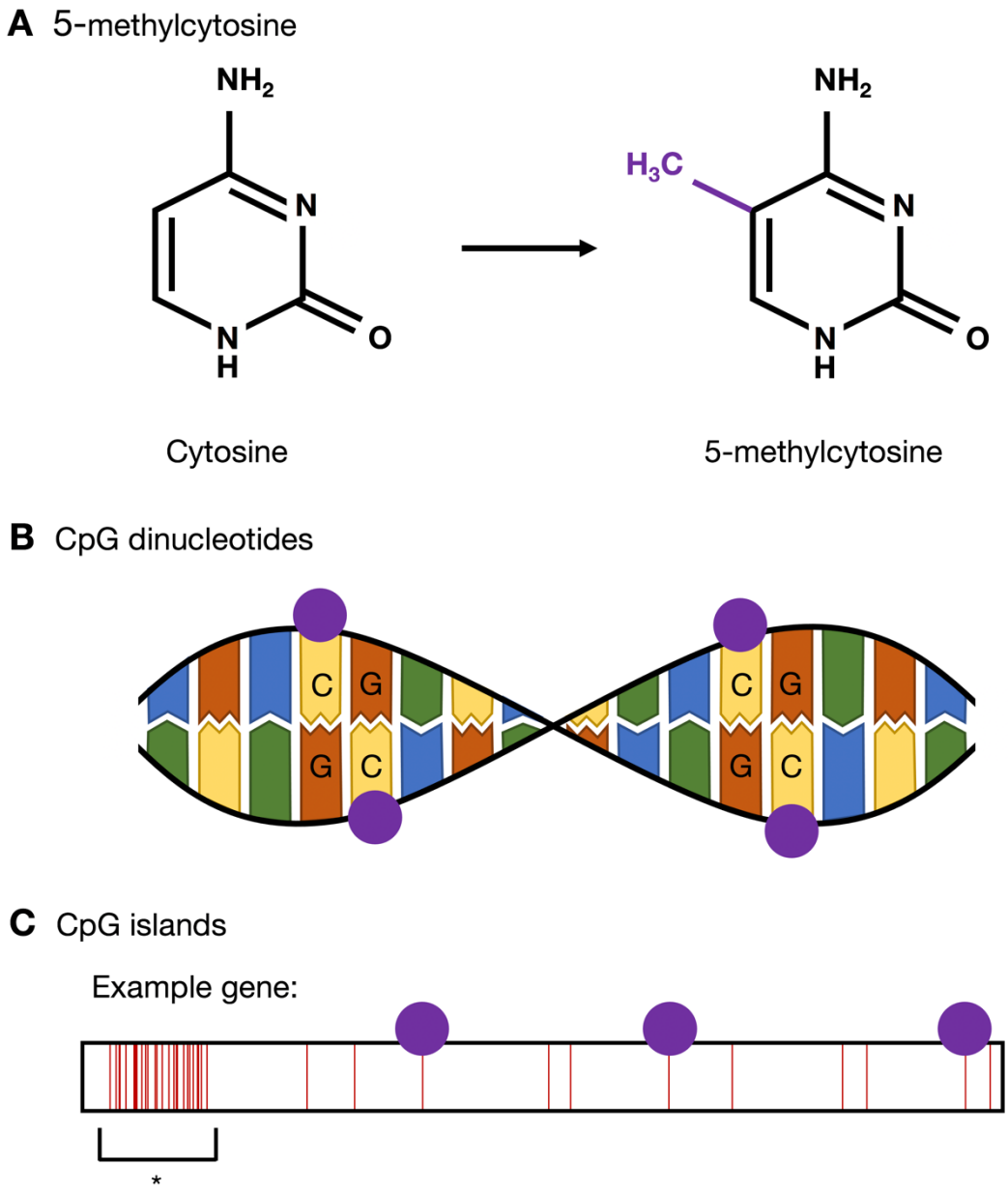

Figure 1.1: DNA methylation of cytosine residues at CpG sites. (A) A methyl group (-HC_3; purple) is added to the fifth carbon atom of the pyrimidine ring of the cytosine molecule, producing 5-methylcytosine. **(B)** 5-methylctosine is almost exclusively found in CpG dinucleotides, where a cytosine molecule is followed by a guanine molecule in the 5' to 3' direction. Yellow: cytosine; orange: guanine; blue: thymine; green: adenine. Purple circle: methyl group. **(C)** Clustering of CpG dinucleotides (red line) at a CpG island (denoted by *) at the beginning or promoter region of the gene. CpG sites outside of this island are less densely packed, and more likely to be methylated (purple circle). CpG sites within the island are often constitutively unmethylated.

methylation patterns are an important component of gene regulation in cellular differentiation during embryonic development. Interestingly, mCH residues in the adult human brain occur at different loci to those observed in hESCs (Varley et al. 2013), again highlighting how methylation patterns vary over time, and suggesting that the role that DNA methylation plays in epigenetic gene regulation is not solely restricted to processes involving differentiation and development. In support of this, mCH levels are highly abundant in the frontal cortex of adult mice, where the abundance of this modification was negligible in fetal animals (Lister et al. 2011). Like mCG, the presence of mCH has been linked to gene repression (Guo et al. 2014): highly expressed genes are generally depleted of mCH, with quantified levels of mCH inversely correlated with transcript abundance of the associated gene (Lister et al. 2011). It has been postulated that the location of mCH within the gene alters its effect on gene expression: while mCH within gene promoters has been linked to gene repression, mCH residues within the gene body have shown positive correlation with expression levels (Lister et al. 2009). However, others refute this idea, stating that mCH levels inversely correlate with gene expression regardless of location within the gene (Xie et al. 2012).

DNA methylation may affect the transcription of a gene in several ways (Bird, 2002). Firstly, the addition of the methyl group itself may physically impede the binding of transcriptional proteins to the gene (Moore et al. 2012). Secondly, there exists a family of proteins known as methyl-CpG binding proteins (Hendrich and Bird, 1998), which bind to methylated DNA and recruit additional protein complexes that influence the transcriptional activity of the bound gene. For example, histone deacetylases (HDACs) and chromatin remodelling proteins are recruited to modify the DNA-histone interaction and therefore induce changes in chromatin conformation. Acetylation of histone tails has been shown to weaken the binding of a stretch of DNA to its histone-octamer within the nucleosome, and hence leaves the DNA more accessible to the binding of transcription factors. Histone deacetylation on the other hand strengthens the DNA-histone interaction, therefore preserving chromatin conformation and resulting in reduced gene expression (Grunstein, 1997). One of the most important members of the methyl-CpG binding protein family is Methyl-CpG Binding Protein 2 (MeCP2), who's function and role in neurological disease will remain the focus of this thesis.

1.1.2 MeCP2 and gene repression

MeCP2 is a chromatin-associated protein that binds with high affinity to methylated DNA (Lewis et al. 1992; Meehan et al. 1992). First discovered in 1992 due to its specific

binding to mC residues in CpG dinucleotides (Lewis et al. 1992), in neurons, MeCP2 is expressed at near-histone levels, and binds across the entire neuronal genome (Skene et al. 2010; Cohen et al. 2011; Gabel et al. 2015). Its sister protein, MeCP1 (previously known simply as MeCP), was discovered in 1989 and binds widely across the mammalian genome at symmetrically-methylated CpGs (Meehan et al. 1989). Despite being discovered second, MeCP2 soon became the more popular methyl-CpG binding protein in research due to its relevance in health and disease: mutations in MeCP2 lead to a variety of neurological disorders, the most commonly known of which is Rett syndrome (RTT; see Chapter 1.2).

Although MeCP2 was discovered in the context of mCG binding, it has since been shown that MeCP2 is also capable of binding to mCH sequences, particularly to residues in the mCA context (Guo et al. 2014; Chen et al. 2015; Gabel et al. 2015). As well as coinciding with synaptogenesis (Lister et al. 2013), the mCA mark is postnatally deposited at the same time that MeCP2 levels increase (Akbarian et al. 2001; Shahbazian et al. 2002; Skene et al. 2010), suggesting that mCA is likely to play an important role in the recruitment of MeCP2 to chromatin during development. As well as being essential for embryonic development (Tate et al. 1996), MeCP2 expression also increases during development of the central nervous system and is required for neuronal maturation (Na and Monteggia, 2011). During development, the binding of MeCP2 to mC switches from predominantly mCG, to an equally high affinity for mCH (Chen et al. 2015), coinciding with the postnatal accumulation of mCH. Indeed, genes which acquire increased levels of mCA throughout development become dysregulated in *Mecp2*-null mice (Chen et al. 2015; Gabel et al. 2015), suggesting that MeCP2 is required for the control of gene expression levels at these loci. Moreover, the degree of MeCP2-induced gene repression was found to be proportional to the number of mCG and mCA sequences across the body of a gene (Kinde et al. 2016). It has been postulated that MeCP2 binding can act as both a transcriptional repressor and activator (Chahrour et al. 2008). In this study, which looked only at MeCP2 binding in the mCG context, genes that were up-regulated by MeCP2 were shown to have more CpG islands than those that are down-regulated. However, the proportion of CpG sites within each gene that are methylated is higher in those that are down-regulated by MeCP2 compared to those that are up-regulated.

While it is widely accepted that MeCP2 is capable of binding mCA dinucleotides, evidence now suggests that this binding is preferential to specific trinucleotide sequences, usually where a second cytosine nucleotide follows mCA. mCAC

trinucleotides, and to a lesser extent mCAT, effectively bind MeCP2 *in vitro*, while mCAA and mCAG exhibit little difference in binding affinity compared to non-methylated control DNA (Lagger et al. 2017). This study suggested that all possible mCGH trinucleotide sequences are bound with equal affinity to MeCP2, suggesting that the binding of MeCP2 to mCG is unaffected by the identity of the third nucleotide in the sequence. Interestingly, chimeric mice that are capable of binding only mCG and not mCAC develop severe neurological and behavioural deficits that replicate the RTT-like phenotype seen in other *Mecp2*-knockout models (Tillotson et al. 2021). These mice were called "chimeric" as their MeCP2 protein contained, in place of the conserved MBD, the MBD of a closely related protein, MBD2, which only allows binding to mCG and no other conformation of mCH. The results from this study reveal that binding of MeCP2 to mCG alone is insufficient to preserve neurological function. Furthermore, approximately one third of genes whose expression was dysregulated by the loss of MeCP2-mCAC binding are also dysregulated in *Mecp2*-knockout models, and many of these shared genes have previously been associated with neurological disorders.

MeCP2 also has the ability to bind sequences of otherwise-modified DNA, including methylation-independent chromatin binding (Baubec et al. 2013) and G-T rich motifs (Connelly et al. 2020), although binding here was shown only *in vitro*, and without *in vivo* support. The MeCP2 protein also contains at least three known AT-hooks within its sequence (Baker et al. 2013), which provide further opportunity for methylation-independent interaction with DNA, although the importance of this feature is called into question given that no known RTT-causing mutations are found within the AT-hook sequence (Lyst et al. 2016). One methylation-independent MeCP2 binding target of particular relevance is 5-hydroxymethylcytosine (hmC; Mellén et al. 2012), which is structurally similar to mC except that a hydroxymethyl group (-CH_2OH) is attached to the fifth carbon atom instead of a methyl group (Kriaucionis and Heintz, 2009). hmC is found throughout the brain where its abundance varies among different locations and cell types (Münzel et al. 2010; Mellén et al. 2012). The abundance of hmC increases postnatally (Szulwach et al. 2011), and it has been suggested that hmC aids development by regulating brain-region specific patterns of transcriptional activity. MeCP2 binds hmC and mC with equal affinity, despite their differences in location: while mC tends to be depleted in active genes, hmC is highly abundant at these loci (Mellén et al. 2012). MeCP2-mC binding is thought to prevent the conversion of mC to hmC, which is corroborated by the findings that hmC levels are increased in *Mecp2*-knockout mice, and decreased in *Mecp2*-overexpressing mice (Szulwach et al. 2011). MeCP2-hmC binding is unlikely to occur at CpG dinucleotides (Szulwach et al. 2011), but rather

binds preferentially in the hmCAC context (Lagger et al. 2017), similar to the binding of mCAC as previously described. While some believe, due to the rarity of hmCAC, that hmC is unlikely to represent a major binding target for MeCP2, others have shown that a specific RTT-causing mutation, MeCP2-R133C, preferentially disrupts MeCP2-hmC binding over MeCP2-mC binding (Mellén et al. 2012), suggesting that MeCP2-hmC binding is critical for neurological function.

mC residues recruit MeCP2 to chromatin through a methyl-CpG binding domain (MBD; Nan et al. 1993). Missense mutations located in the MBD disrupt the binding of MeCP2 to mC and lead to RTT, suggesting that interactions with methylated DNA via the MBD are necessary for MeCP2 (and neurological) function (Ballestar et al. 2000; Yusufzai and Wolffe 2000; Baubec et al. 2013). Biochemical assays revealed MeCP2 also contains a transcriptional repression domain (TRD) which interacts with the histone deacetylase-containing co-repressor complexes SIN3A (Nan et al. 1998; Jones et al. 1998), NCoR and SMRT (Kokura et al. 2001; Stancheva et al. 2003; Lyst et al. 2013). The presence of both an MBD and TRD suggests that MeCP2 functions to bridge the gap between DNA and repressor complexes, and therefore facilitate gene silencing (Fig. 1.2 A; review: Lyst and Bird, 2015). MeCP2 binding can specifically repress methylated reporter genes *in vitro* (Baubec et al. 2013). This theory is supported by the findings that deacetylation of histone protein tails is strongly correlated with transcriptional repression (Grunstein, 1997). Furthermore, one of the most common non-MBD MeCP2 missense mutations that also leads to RTT, R306C, disrupts the interaction between MeCP2 and NCoR, again suggesting that a key function of MeCP2 is to mediate transcriptional repression (Lyst et al. 2013). Despite these findings, it is worth noting that changes in gene expression levels following the loss of MeCP2 are relatively subtle (Tudor et al. 2002).

1.1.3 Other possible functions of MeCP2

Several studies looking at the gene expression profiles in mouse models that either lack or over-express MeCP2 have shown that MeCP2 can also activate gene expression (Chahrour et al. 2008; Ben-Shachar et al. 2009). There is evidence that MeCP2 associates with the transcriptional activator CREB1 at the promoter of genes that are up-regulated by MeCP2 (Fig. 1.2 B), and that this interaction does not occur at the promoter of genes that are down-regulated by MeCP2 (Chahrour et al. 2008). However, findings from this study are called into question given that few people have been able to replicate these results. MeCP2 has also been implicated in regulating chromatin remodelling by inducing the formation of heterochromatin aggregates (Brero et al. 2005;

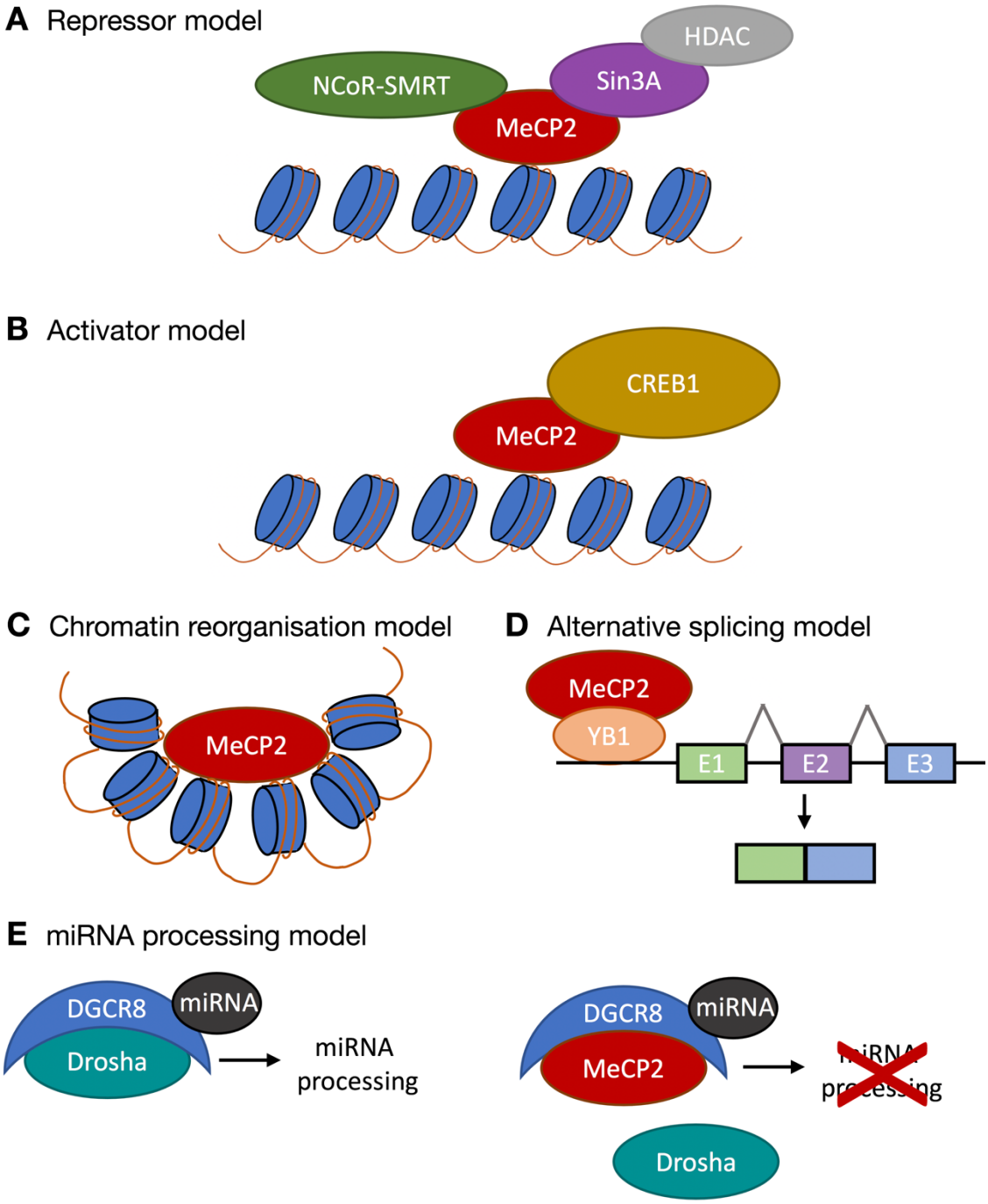

Figure 1.2: Proposed functions of MeCP2. Figure adapted from Lyst & Bird (2015). **(A)** MeCP2 initiates transcriptional repression by recruiting the NCoR-SMRT complex and the HDAC-containing Sin3A complex to the promoter of bound genes. **(B)** MeCP2 activates transcription by recruiting CREB1 to the promoter of bound genes. **(C)** MeCP2 initiates chromatin remodelling by inducing the formation of heterochromatin loops and chromocenters. **(D)** MeCP2 regulates gene expression post-transcriptionally by initiating alternative splicing events through its interaction with YB1. **(E)** Binding of MeCP2 to DGCR8 disrupts the formation of the DGCR8-Drosha complex, which in turn inhibits miRNA processing.

Fig. 1.2 C). Indeed, *Mecp2*-deficient mice exhibit a lack of chromatin looping (Horike et al. 2005). Given that MeCP2 forms RNA-binding complexes *in vitro* (Jeffery and Nakielny, 2004), it has been proposed that MeCP2 may regulate gene expression at the post-transcriptional stage, by regulating alternative splicing events (Young et al. 2005; Maunakea et al. 2013; see Fig 1.2 D), and / or by controlling the processing of micro-RNAs (Cheng et al. 2014; see Fig. 1.2 E).

1.1.4 MeCP2 domain organisation and mutations

MeCP2 has previously been described as an "intrinsically disordered protein", meaning it can undergo a degree of structural rearrangement due to its general lack of secondary or tertiary structure (Claveria-Gimeno et al., 2017). Structural plasticity such as this permits the interaction of MeCP2 with a large number of binding partners by transiently exposing different protein binding regions in different conformations. The result of this is the variety of MeCP2 functions that have previously been discussed (see Fig. 1.2). The MeCP2 protein is organised into five domains, beginning with the N-terminal domain, then the MBD at amino acid number 90, followed by the intervening domain at amino acid number 174, the TRD begins at amino acid 219, and then the MeCP2 protein ends with a C-terminal domain from amino acid 322 to the end (Claveria-Gimeno et al., 2017; Kyle, Vashi and Justice, 2018). Note that the amino acid number at which these domains begin is stated for the MeCP2_e1 isoform, and these domain boundaries occur 12 amino acids earlier in the MeCP2_e2 isoform due to the MeCP2_e1 N-terminal domain being 12 amino acids longer (Good, Vincent and Ausió, 2021; see below, Chapter 1.1.5, for more information on MeCP2 splice variants).

To date there have been several hundred different mutations identified within the MeCP2 gene of RTT patients. Despite the heterogeneity of MeCP2 functions described earlier, the majority (>90%) of RTT-causing mutations occur within either the MBD or the TRD (Cheadle et al., 2000; Philippe et al., 2006), highlighting the importance of the role that MeCP2 plays in gene expression regulation on neurological function. For example, in one mutational-landscape study comprised of 424 RTT patients, the eight most common point mutations occurred at the following sites (frequencies shown in brackets): R168X (11.5%), R270X (9%), R255X (8.7%), T158M (8.3%), R306C (6.8%), R294X (5.9%), R133C (4.2%), R106W (4.2%), all of which lie within either the MBD or TRD (Philippe et al., 2006). These mutations are consistently reported among the most common mutation types in other mutational analysis studies, though their frequencies sometimes vary,

likely due to varying sample sizes (Wan et al., 1999; Buyse et al., 2000; Dragich, Houwink-Manville and Schanen, 2000; Huppke et al., 2000; Vacca et al., 2001).

There are fewer RTT-causing mutations in the MeCP2 gene that relate to the other functions of MeCP2. For example, the binding of MeCP2 to both YB1 and the DGCR8 complex is thought to occur within the MeCP2 C-terminal domain (Gonzales et al., 2012; Cheng et al., 2014). C-terminus mutations do occur in RTT patients and make up a significant proportion of the ~10% of RTT-causing mutations that occur outside of the MBD and TRD (Vacca et al., 2001; Philippe et al., 2006). To date, none of these mutations have been specifically linked to the disruption of a specific MeCP2 function. The interactions between MeCP2 and YB1 or the DGCR8 complex are facilitated by the phosphorylation of serine 80 which acts to activate the MeCP2 protein. The rapid phosphorylation and dephosphorylation of S80 in response to neuronal activity causes swift alterations in MeCP2 structure that allow interaction with different binding partners. To the best of my knowledge, mutations at this S80 site have not been reported and are not common in patients diagnosed with RTT.

1.1.5 MeCP2 splice variants

MeCP2 was originally purified from rat brain samples as a single 84kDa protein (Lewis et al. 1992) and mapped to the Xq28 loci in the mouse genome (Quaderi et al. 1994). MeCP2 exists as two isoforms, MeCP2e1 and MeCP2e2, that occur through alternative splicing and differ in the sequence of their N terminus (Fig. 1.3). The MeCP2e1 transcript contains coding regions from exons 1, 3 and 4, but does not include exon 2. On the other hand, the MeCP2e2 transcript contains coding regions from all four exons of the *MECP2* gene (Kriaucionis and Bird, 2004). The MeCP2e1 transcript produces a protein of 498 amino acids, while the MeCP2_e2 transcript, despite containing an additional exon, has its translation initiation point within exon 2 and produces a slightly smaller protein of 486 amino acids (Martínez de Paz et al. 2019).The precise functional roles of these two isoforms is unknown, since the two major functional domains of MeCP2, the MDB and the TRD, are coded for by exons 3 and 4, respectively, and are therefore included in both isoforms of the protein (Fig. 1.3). The MeCP2e1 isoform is regularly described as the major isoform of MeCP2 protein, since it is more abundant than MeCP2e2 in almost all tissues, including the brain where in mouse tissue it is thought to outnumber MeCP2e2 by 10:1. Furthermore, sequence alignment studies showed that non-mammalian databases never expressed the MeCP2e2 isoform, suggesting that the

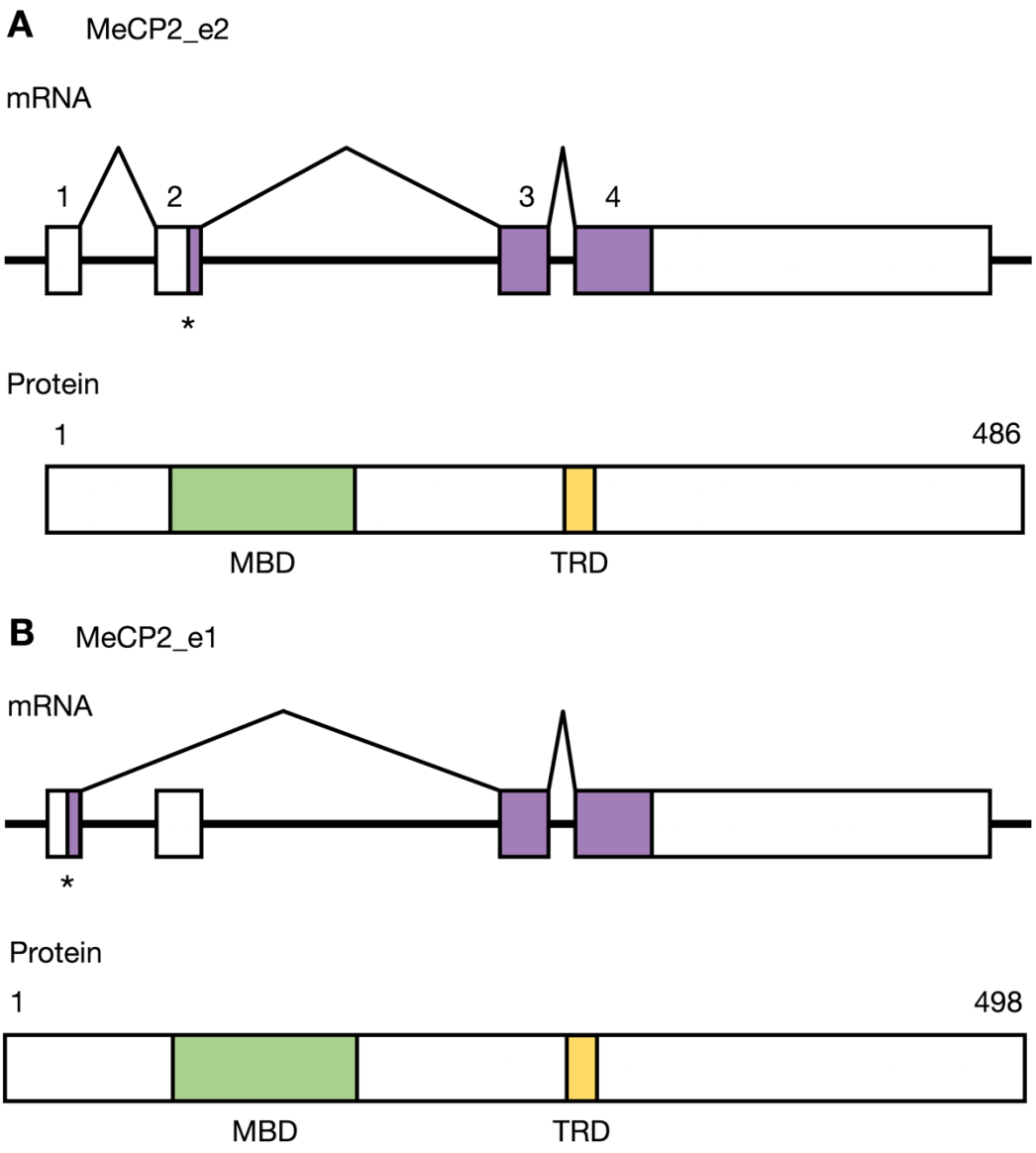

Figure 1.3: Alternative splice variants of MeCP2. Figure adapted from Kriaucionis and Bird (2004) and Martìnez de Paz et al. (2019). **(A)** The MeCP2_e2 isoform is 486 amino acids in length and contains all known exons in the *MECP2* gene. **(B)** The MeCP2_e1 isoform is 498 amino acids long, despite lacking exon 2. Translation initiation points denoted by *. Purple boxes denote protein coding regions, open boxes represent non-coding regions. Note that the coding regions for the methyl-binding domain (MBD; green boxes) and the transcriptional repression domain (TRD; yellow boxes) are located with exons 3 and 4 respectively, and therefore are both present in each MeCP2 variant.

MeCP2e1 isoform more closely resembles the ancestral MeCP2 gene (Kriaucionis and Bird, 2004).

In newborn mice (postnatal day 1, P1), riboprobe signals of MeCPe2 overlapped with total MeCP2 throughout the brain, including in the forebrain, sensory cortical areas, striatum, hippocampus, thalamus and hypothalamus, suggesting that MeCP2e1 is hardly expressed at this time. However, in the postnatal mouse brain (P21 and P60), there are marked differences between the abundance and distribution of total MeCP2 and MeCP2e2: while total MeCP2 continued to label structures throughout the brain, MeCP2e2 signal was restricted to the thalamus and cortical layer V (Dragich et al. 2007). Quantitative RT-PCR from P30 whole mouse brain samples again showed that MeCP2e1 was more abundant than its sister isoform, a finding consistent with previous reports (Mnatzakanian et al. 2004; Kriaucionis and Bird, 2004). There are no reports of any spatial or temporal differences in the distribution of either MeCP2 variant between sexes. The difference in expression of MeCP2e1 and MeCP2e2 during postnatal development suggests a mechanism for brain-region specific splicing, although it is currently unknown what function this plays in brain development.

The vast majority of RTT-causing mutations occur within the MBD or TRD, which are coded for by exons 3 and 4 respectively. Therefore, RTT-causing mutations tend to alter the function of both MeCP2e1 and MeCP2e2 equally. To date, only a few individuals carrying an MeCP2e1 isoform-specific mutation have been identified (Amir et al. 2005; Quenard et al. 2006; Saunders et al. 2009), and no MeCP2e2-specific mutations have ever been found. Loss of MeCP2e1 alone is sufficient to recapitulate many RTT-associated behavioural deficits in mice (Yasui et al. 2014), however the effects of this on humans is yet to be fully evaluated. Given the time course of RTT disease progression and the fact that MeCP2e1 transcripts appear late on in postnatal development, it is perhaps not surprising that the MeCP2e1 isoform appears to be more pathologically relevant than its sister variant.

1.2 Clinical relevance of MeCP2

1.2.1 Rett syndrome (RTT)

Rett syndrome (RTT) is a devastating neurological disorder primarily affecting females during early childhood. In 1966, Andres Rett, a neurodevelopmental paediatrician from Vienna, reported the discovery of a unique neurodevelopmental disorder based on distinctive symptomatic features among a cohort of 22 patients (Rett, 1966; history of

RTT reviewed in Percy, 2014). However, due to his findings being published only in German literature, initial recognition of Rett's discovery was low. In 1983, Bengt Hagberg, a child neurologist from Sweden, published in English his own findings from a cohort of 35 female patients who all presented with similar features to that which Rett had previously discovered (Hagberg et al. 1983). Hagberg described a "uniform and striking progressive encephalopathy" and named the syndrome after Rett in recognition of his early contribution to the field.

It is estimated that 1 in every 10,000 live female births worldwide are affected by RTT (Chahrour and Zoghbi, 2007). Affected females exhibit normal development for the first 6-18 months of their lives, possibly reaching several developmental milestones such as crawling, walking, babbling, talking, feeding themselves and recognition of their own name. At 6-18 months of age, RTT-patients enter a period of developmental regression, where they progressively lose all acquired language and motor skills. The four main criteria for a diagnosis of classical RTT are: loss of purposeful hand movements, loss of acquired spoken language skills, development of gait abnormalities (dyspraxia or absence of ability) and hand stereotypies, which may include wringing, squeezing, clapping, tapping, mouthing, washing and / or rubbing automatisms (Neul et al. 2010). After the initial period of regression, a stage of stabilisation and potentially even improvement ensues, with some individuals partially regaining some skills. Additional symptoms that are not required for diagnosis of classical RTT, include: breathing disturbances, bruxism, impaired sleeping patterns, abnormal muscle tone, scoliosis, kyphosis, growth retardation, inappropriate laughing and/or screaming spells, diminished response to pain and intense eye communication (known as the 'Rett gaze'). These supportive criteria are used to guide clinicians towards the correct diagnosis. There is also a set of exclusion criteria (including, but not exclusive to: prematurity, meningitis, trisomy 21 and traumatic brain injury), which must all be absent for a diagnosis of RTT. This excludes any other possible cause of neurological disease (Neul et al. 2010). By definition, all individuals with RTT experience developmental regression. Some individuals present with some but not all of the main criteria for classical RTT; they are given a diagnosis of atypical RTT assuming they meet at least 2 of the 4 main criteria and 5 of the 11 supportive criteria. Patients with atypical RTT have been found to cluster in distinct clinical groupings, such as preserved speech variant, early seizure variant and congenital variant (Neul et al. 2010).

Patients who suffer RTT tend to be smaller than other children of the same age, and they often exhibit decelerated head growth relative to the rest of their body (Armstrong et al.

1999; Neul et al. 2010). Their brains are disproportionately small, with marked grey matter atrophy. However, post-mortem brain examination revealed the absence of gross morphological or anatomical abnormalities, which distinguished RTT from other progressively debilitating conditions, and ruled it out as being a neurodegenerative disorder (Neul and Zoghbi, 2004). Interestingly, studies involving rodent models of RTT showed that restoration of MeCP2 expression in an otherwise null background reverses the neurological symptoms associated with the loss of MeCP2 function (Guy et al. 2007; Robinson et al. 2012). This corroborates the theory that brain development is not dependent on functional MeCP2 expression in early life, and that loss of MeCP2 disrupts neurological function without causing atrophy or neurodegeneration.

RTT is primarily caused by mutations in the X-linked gene that encodes MeCP2 (Amir et al. 1999). However, MeCP2 mutations only account for 95% of classical RTT cases, and 50-70% of atypical RTT cases, making the presence of an MeCP2 mutation alone insufficient for the proper diagnosis of RTT (Neul et al. 2010). Hence, diagnosis of RTT is based on the presentation of clinical features, with DNA mutation analysis used only for clarity and support. Mutations in several other genes have been implicated in specific variants of atypical RTT, including CDKL5 mutations in the early seizure variant (Evans et al. 2005; Mari et al. 2005), and FOXG1 mutations in the congenital variant (Ariani et al. 2008; Mencarelli et al. 2010; Philippe et al. 2010).

1.2.2 Gender differences in RTT

RTT is considered to be a disorder which almost exclusively affects females, owing to the location of the affected gene, *MECP2* (Amir et al. 1999), within the X chromosome (Quaderi et al. 1994). Heterozygous females only express 50% mutant protein due to the random pattern of X-chromosome inactivation (Xi; D'Esposito et al. 1996), whereas male hemizygosity means that all of their cells express the same *MECP2* allele. Due to the toxic effects of 100%-mutant MeCP2, RTT-associated mutations in males tend to lead to prenatal or early-postnatal lethality (Kankirawatana et al. 2006; Villard, 2007). This suggests that Xi provides protection against the lethal effects of total MeCP2 loss, and explains why the vast majority of individuals diagnosed with RTT are female.

In recent years, the identification of males carrying MeCP2 mutations has increased, although in most cases additional genetic manipulation occurs to circumvent the lethal effects of mutant *MECP2* hemizygosity (Moog et al. 2003). This includes somatic

mosaicism (Topçu et al. 2002), and instances of a 47,XXY karyotype (Schwartzman et al. 2001). As a result of these additional genetic complications, males carrying RTT-associated mutations exhibit a highly diverse range of phenotypic traits, from mild mental retardation to severe cognitive encephalopathy, often with neurological comorbidities (Moog et al. 2003).

Although the majority of classical RTT cases are seen in females, RTT-based research utilises both female and male animal models, including Drosophila (Kudo et al. 2001) primate (Liu et al. 2016), rat (Patterson et al. 2016) and mouse models (Chen et al. 2001; Guy et al. 2001). Male mice develop fewer complications from mutant MeCP2 hemizygosity compared to humans, and therefore are less likely to suffer prenatal or early postnatal lethality. The timeline of disease pathology differs between mice and humans, with mice developing RTT-like symptoms at a much later stage of their respective development (see Fig. 1.4; Guy et al. 2001). RTT mouse models are able to effectively recapitulate many of the symptoms commonly associated with RTT in both males and females (Chen et al. 2001; Guy et al. 2001; Guy et al. 2007), making them a useful model for understanding how loss of MeCP2 leads to the phenotypic traits we see in humans.

1.2.3 Other MeCP2-related disorders

Although the majority of MeCP2-related literature is given in the context of RTT, MeCP2 has been linked to several other neurological disorders. RTT was previously considered an autism-spectrum disorder (Neul, 2012). However, due to its genetic origin and distinct clinical features, RTT was later reclassified with the recognition that many of its features overlap with autism, but RTT itself is not an autistic disorder. Since then, several studies have reported females who carry *MECP2* mutations but fail to meet the criteria for RTT, who have instead been issued a clinical diagnosis of autism (Carney et al. 2003). *MECP2* mutations have also been implicated in cases of developmental delay and non-specific mental retardation (Kleefstra et al. 2004; Harvey et al. 2007). Xi studies of three female patients with very mild RTT-like phenotypes showed that heavily skewed Xi sufficiently protects against the negative consequences of mutant MeCP2. These patients carried *MECP2* mutations previously found in RTT but exhibited a phenotype that was so mild they did not meet the necessary diagnostic criteria (Huppke et al. 2006).

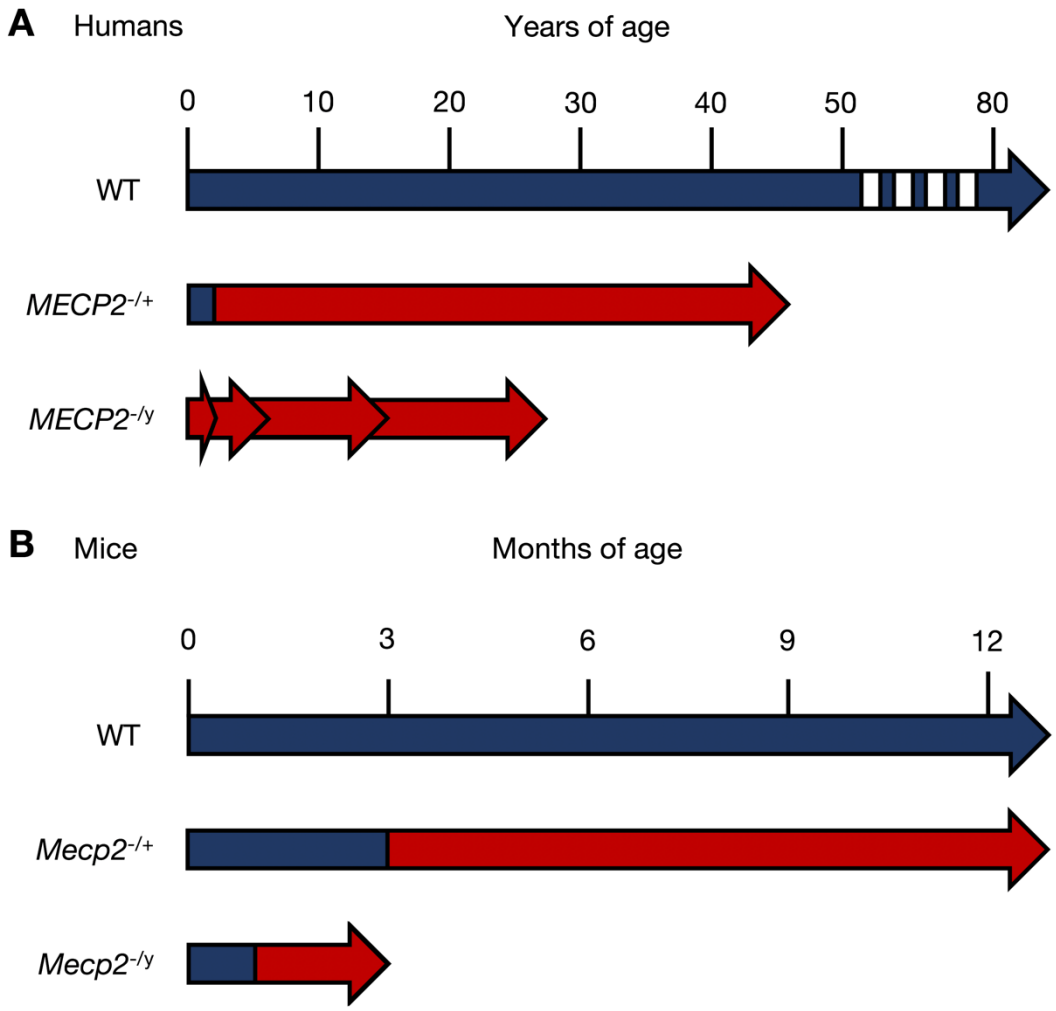

Figure 1.4: Clinical progression and life expectancy as a result of MeCP2 mutations in humans and mice. (A) RTT disease progression in females (*MECP2*$^{-/+}$; middle band) and males (*MEPC2*$^{-/y}$; lower band) carrying *MECP2* mutations compared to wild-type (WT; upper band). **(B)** Phenotype progression and life expectancy changes in female (*Mecp2*$^{-/+}$; middle band) and male (*Mecp2*$^{-/y}$; lower band) mutant mice compared to their wild-type (WT; upper band) littermates. Blue bars = non-phenotypic period of life. Red bars = phenotypic period of life. Life expectancy depicted by each arrowhead. Multiple arrow heads in A, *MECP2*$^{-/y}$, depict variations in life expectancy due to heterogeneity caused by comorbidities and differences in disease severity.

It has previously been reported that males with a less severe non-RTT phenotype carry a subset of *MECP2* mutations that are never shown in males or females suffering RTT (Neul and Zoghbi, 2004). This suggests that these mutations alter the function of MeCP2 in such a way that the consequences are milder than those seen in RTT. These males

exhibit a broad range of phenotypes, with few commonalities among all patients: most suffer some degree (usually moderate) of mental retardation (Meloni et al. 2000; Orrico et al. 2000; Couvert et al. 2001; Dotti et al. 2002), while others presented with features of Angelman syndrome (Imessaoudene et al. 2001) or neuropsychiatric disorders such as psychosis (Klauck et al. 2002) or schizophrenia (Cohen et al. 2002). Often the obligate female carriers of these less-severe *MECP2* mutations suffered mild mental retardation, and did not meet the diagnostic criteria for RTT, while others were considered phenotypically normal.

While all of the neurological disorders discussed so far have related to loss-of-function MeCP2 mutations, it has been shown that gain-of-function mutations can be equally detrimental to neurological function. A transgenic mouse model overexpressing human *MEPC2* by a factor of two experienced severe seizures and hypoactivity by 20 weeks of age and many suffered a reduced life span compared to their wild-type (WT) littermates (Collins et al. 2004). In humans, MeCP2 duplication syndrome (MDS) most often occurs in males: duplications in the Xq28 region of the X chromosome are thought to account for 1% of patients suffering unexplained X-linked mental retardation, and 2% of severe encephalopathy in males (Lugtenberg et al. 2009). Patients suffering MDS exhibit a range of symptoms including moderate-to-severe mental retardation, delayed or absent speech, seizures, progressive spasticity, ataxia and recurrent respiratory infections (Van Esch et al. 2005; del Gaudio et al. 2006). MeCP2 duplications have also been found in a small number of individuals diagnosed with autism (Ramocki et al. 2009). In one study, a patient carrying an MeCP2 triplication genotype suffered the most severe phenotype of all the patients assessed (del Gaudio et al. 2006). Similar to MeCP2 loss-of-function disorders, it is often the case in MDS that the mother proves to be an asymptomatic obligate carrier for the duplication but is protected by severely skewed Xi (Van Esch et al. 2005; del Gaudio et al. 2006). In mothers that do not exhibit heavily skewed Xi, psychiatric conditions such as generalised anxiety and depression are often present (Ramocki et al. 2009). In summary, MeCP2 function is highly sensitive to protein abundance; both increases and decreases in MeCP2 dosage can have severe implications on neurological and cognitive function. Hence, MeCP2 abundance must be tightly controlled in order to avoid neurological disease.

1.2.4 Sleep disturbances in RTT and other MeCP2-related disorders

Abnormal sleeping patterns and behaviours are common features of many MeCP2-related disorders. It is estimated that over 80% of RTT patients experience regular sleep disturbances and impaired sleeping patterns (Young et al. 2007; Wong et al. 2015), hence its inclusion on the list of supportive diagnostic criteria for RTT (Neul et al. 2010). The clinical manifestations of these sleep disturbances are broad and similar across all MeCP2-related disorders, and include irregular sleep-cycle patterns, long periods of wakefulness during the night, significant increases in daytime napping compared to age-matched controls, and abnormal sleeping behaviours such as teeth grinding, laughing and screaming (Nomura, 2005; Young et al. 2007). It has also been shown that RTT patients do not experience the age-related decrease in both total and daytime sleeping that is typical of normal development (Ellaway et al. 2001). MDS patients also tend to exhibit abnormal sleep behaviours (Signorini et al. 2016), most often manifested through sleep apneas (Ramocki et al. 2010; Breman et al. 2011).

Often in RTT, mutation type dictates symptom architecture and subsequently clinical severity (Neul et al. 2008; Cuddapah et al. 2014). For example, some mutations such as *MECP2* R294X, R306C and three-prime truncations generally present a less severe phenotype, while others such as *MECP2* T158M and larger deletion mutations result in more severe presentations of the disease (Schanen et al. 2004; Cuddapah et al. 2014). The occurrence of sleep disturbances in RTT is highest in patients carrying the R294X or R306C mutations, or large deletions of the *MECP2* gene (Young et al. 2007), suggesting that the frequency of sleep disturbances in RTT correlates with mutation type, but irrespective of clinical severity. Despite overall clinical severity for most RTT cases increasing with age (Cuddapah et al. 2014), the occurrence of sleep disturbances, particularly night laughing, screaming and waking, decreases with age, although they are still present among older patients (Wong et al. 2015).

In *Drosophila*, reduced expression of endogenous MBD-containing proteins and overexpression of the human *MECP2* gene, both result in changes in sleep circuitry, including sleep fragmentation (Gupta et al. 2016), highlighting the role of MBD-containing proteins in mediating sleep behaviours. Circadian rhythms govern almost all biological processes, including sleep, with this 24-hour rhythm being partly under the control of epigenetics (Qureshi and Mehler, 2014). Genome-wide DNA methylation levels undergo regular 24-hour fluctuations (Bönsch et al. 2007), and many clock genes

regularly undergo DNA methylation (Ji et al. 2010; Belden et al. 2011). MeCP2 is required to convey this epigenetic message. Disruptions in clock gene DNA methylation patterns have been reported in a number of neurological disorders exhibiting sleep disturbances (Qureshi and Mehler, 2014). Furthermore, MeCP2 itself is phosphorylated in the suprachiasmatic nucleus (a sub-structure of the hypothalamus, and the brain region responsible for setting the circadian rhythm) in response to light signalling (Zhou et al. 2006). This suggests that, not only does MeCP2 interact with genes that are affected by the circadian rhythm, but also that the activity of MeCP2 itself follows a 24-hour cycle. Therefore, the function of MeCP2 likely involves, at least in part, coordinating patterns of sleep-wake behaviours. Indeed, several studies have observed poor maintenance of the intrinsic circadian rhythm in *Mecp2*-null animals compared to WT controls (Wither et al. 2012; Li et al. 2015; review: Zhang et al. 2021). *Mecp2*-null mice also exhibit increased latency to the onset of sleep (Johnston et al. 2014; Li et al. 2015), which in the latter study was directly attributable to the observed deficits in maintaining the circadian clock.

1.3 Sleep

1.3.1 The sleep cycle

During the night, our brains cycle through several different phases of sleep in a pattern that is known as the sleep cycle. Each stage is thought to be functionally independent and is characterised by the type and frequency of neuronal activity that occurs within them (see Chapter 1.4). In humans, each cycle generally lasts around 1-2 hours, with up to 5 or 6 cycles occurring each night (McCarley, 2007). The sleep cycle can include periods of wakefulness, but is mostly predominated by periods of rapid eye movement (REM) and non-rapid eye movement (NREM) sleep (Fig. 1.5). The sleep cycle is distinct from the sleep-wake cycle which refers to the 24-hour pattern of sleep and wakefulness which almost all animals experience and is determined by their natural circadian rhythm.

1.3.1.1 Wakefulness

A period of wakefulness occurs when an individual is in an awake state of consciousness or awareness. During this time, they engage with their environment, consciously (and subconsciously) process sensory information and actively make decisions. Awake states are initiated by activation of the ascending reticular activating system (a bundle of neurons that project from the brainstem up to the thalamus, hypothalamus and cerebral cortex, among other brain structures), and naturally occurs following a period of REM

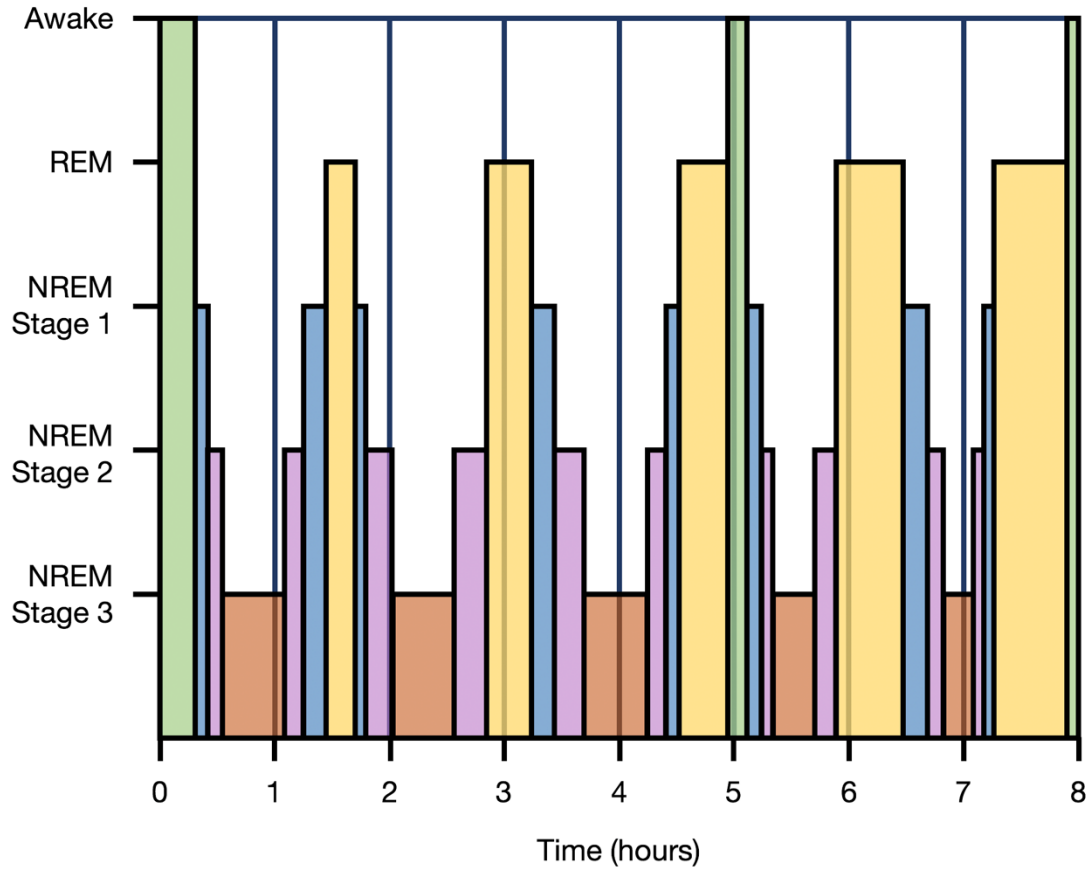

Figure 1.5: The sleep cycle. Figure adapted from Purves et al, Neuroscience 5th edition, Chapter 28 (2012). Graphical representation of a typical human pattern of sleep cycles during an average 8 hour sleep period. Bar width represents time spent in each phase. Non-rapid eye movement sleep (NREM; blue, pink and orange bars) predominates the sleep-wake cycle at the start of the night, whereas rapid eye movement sleep (REM; yellow bars) predominates in the latter hours of sleep. Brief periods of wakefulness (green bars) are common, and always followed by NREM sleep. REM sleep occurs at the end of each cycle, and before any periods of natural wakefulness.

---

sleep (Fig. 1.5). During wakefulness, the brain exhibits epochs of high frequency, low amplitude neuronal activity (see Chapter 1.4).

1.3.1.2 Non-rapid eye movement (NREM) sleep

NREM sleep comprises three sub-stages of sleep, each of which confers a deeper state of unconsciousness. Dreaming is rare during NREM sleep; heart rate and breathing rate drop, there is very little eye movement and only occasional body movements (McCarley, 2007). The transition into sleep from an awake state always begins with Stage 1 NREM sleep, followed by Stage 2 and then Stage 3, where the cycle then reverses. At the end

of a sleep cycle, NREM sleep transitions into REM sleep. NREM sleep generally predominates the sleep cycle in the early stages of the night, while latter sleep cycles contain a smaller proportion of time spent in NREM sleep (Fig. 1.5; Colten et al. 2006). The brain exhibits reduced neuronal activity as NREM sleep progresses: Stage 1 NREM, which occurs during the transition into sleep, comprises a mixture of rhythms common to wakefulness, as well as some sleep-specific rhythms. Stage 2 NREM is characterised by sleep spindles (7 - 14 Hz) and K complexes. Stage 3 NREM sleep is characterised by the presence of delta (0.5 - 4 Hz) and slow-wave (<1 Hz) oscillations (see Chapter 1.4).

1.3.1.3 Rapid eye movement (REM) sleep

REM sleep occurs at the end of each sleep cycle, when the brain is in its most active sleep state and closely mimics the awake state. During REM sleep, the eyes move rapidly from side to side, while muscle tone throughout the rest of the body remains low. Almost all vivid dreaming occurs during REM sleep, and heart rate is markedly increased in REM sleep compared to NREM (McCarley, 2007). Although the length of each sleep cycle is generally maintained throughout the night, the proportion of time spent in REM sleep per cycle starts off low and increases throughout the night (Fig. 1.5; Colten et al. 2006). REM sleep is associated with increased brain activity, with epochs of high frequency neuronal activity that are generally associated with wakefulness. The main electrophysiological characteristic of REM sleep is the presence of theta oscillations (4 - 8 Hz), although these too can also be seen during wakefulness (see Chapter 1.4).

1.3.2 Biological function of sleep

Sleep is an evolutionarily-preserved behaviour that carries vital functions for survival. Sleep-like behaviours have been observed in almost all animals studied to-date (Zimmerman et al. 2008): most animals exhibit phases of NREM-like brain activity during rest periods. In both *Drosophila* and *C. elegans* these rest periods are under the control of genes that are homologous to the mammalian genes which regulate sleep (Cirelli, 2009). REM sleep appears to be a mammalian-specific feature of sleep, with simplistic REM-like brain states seen in reptiles and birds (Siegel et al. 1998).

Historically, the function of sleep has been subject to great debate, with many scientists struggling to see the overall advantage of becoming unconscious (and therefore more vulnerable) for long periods at a time. Replenishment of energy stores (and conservation of energy in the case of animals that hibernate) is a common theory: cerebral metabolic

rate (CMR) of oxygen and glucose are reduced by 25% and 44% respectively during sleep compared to CMR during periods of wakefulness (Madsen et al. 1991; Maquet, 1995). Sleep is also thought to play a crucial role in metabolic homeostasis, as it aids the removal of waste products that accumulate during periods of wakefulness, which may be neurotoxic if not efficiently removed from the central nervous system quickly (Xie et al. 2013). Another theory is that sleep aids the immune system in fighting infection, given that high-quality sleep has been shown to enhance the function of cytokines and promote white blood cell relocation to the sight of infection (Besedovsky et al. 2012), and also that an increase in sleep is often a symptom of ill health (Brown et al. 2012). Sleep is thought to be important for development, as it is a predominant behaviour in babies and young children, as well as many juvenile animals. Indeed, the neuronal networks responsible for controlling sleep and wakefulness mature during early development, and in humans specifically, the brain rhythms specific to each behavioural state during sleep continue to mature even during adolescence (Brown et al. 2012).

In the brain, sleep has long been implicated in learning: it allows us to process information that has been gathered during wakefulness by regulating synaptic plasticity and reinforcing long-term potentiation (LTP) that occurred during wakefulness (Campbell et al. 2002; Shaffery et al. 2002; Rosanova and Ulrich, 2005, Cooper and Bear, 2012). The synaptic homeostasis hypothesis suggests that synaptic potentiation in awake states induces slow-wave (<4.5 Hz) neuronal activity in cortical circuits during NREM sleep, which in turn induces synaptic downscaling (Tononi and Cirelli, 2003). This is a crucial process, as the potentiation of these synapses during learning tasks in wakefulness leads to an increase in metabolic demand, which must be downscaled during sleep to a level that is energetically efficient and, more importantly, sustainable (Tononi and Cirelli, 2006). Furthermore, when synaptic strengths are substantially increased, the ability of neurons to selectively respond to each input is reduced, and as a consequence, so is the ability to learn from the input. Therefore, the renormalisation of synaptic strength during sleep not only reduces the metabolic burden of synaptic potentiation on neurons and other cells, but also fine-tunes the signal-to-noise ratios that aid the consolidation and integration of memories (Tononi and Cirelli, 2014).

1.3.3 Sleep and memory consolidation

The processes of sleep and memory consolidation are so interwoven that the individual stages of sleep have previously each been implicated in the processing of different types of memories (Walker and Stickgold, 2004). REM sleep is thought to enhance non-

declarative (or “implicit”) memory formation (Fischer et al. 2002), whereas NREM sleep is generally associated with the consolidation of declarative (or “explicit”) memories (Gais and Born, 2004; Marshall et al. 2006). Slow frequency neuronal oscillations became increasingly coherent following a declarative word-pairing memory task immediately prior to sleep (Mölle et al. 2004). Similarly, slow-wave transcranial stimulation of cortical regions during NREM sleep prior to memory recall resulted in better outcomes on a similar word-pairing task, compared to both control participants who underwent placebo stimulation during sleep and those who were given the same stimulation during wakefulness (Marshall et al. 2004). Further evidence exists that implicates NREM sleep in non-declarative memory formation (Ackermann and Rasch, 2014). Following simple motor tasks, sleep spindles increased in both incidence and duration during the following sleep period (Fogel et al. 2007), while suppression of slow oscillations during NREM sleep results in poorer performance on a texture discrimination task (Aeschbach et al. 2008).

1.3.4 Consequences of sleep deprivation

Factors that impede the quality and continuity of sleep, such as the type of sleep disturbances previously mentioned in Chapter 1.2.4, can lead to sleep deprivation, which has been identified as a precursor for numerous health conditions (Medic et al. 2017). Cognitively, sleep deprivation can lead to lack of concentration, blurred vision, impaired reaction time, reduced performance ability and increased rate of error (Orzeł-Gryglewska, 2010). Sleep deprivation also leads to alterations in attention span and working memory, and can have significant effects on decision making, and long-term memory formation and retrieval (Alhola and Polo-Kantola, 2007). In mice, five hour periods of sleep deprivation lead to structural changes relating to synaptic connectivity in the hippocampal CA1 region, including reduction in the number of dendritic spines (Havekes et al. 2016). These structural alterations are quickly ameliorated when normal sleeping patterns resume. Sleep deprivation in rats causes a significant decrease in the amplitude of cortical event-related potentials, and can have long-term effects on neuronal excitability (Borbély et al. 2018). These studies highlight the importance of obtaining high-quality, uninterrupted sleep for brain function and learning and memory.

1.3.5 Sleep-cycle changes in RTT

Patients suffering RTT often experience disruptions in the architecture of sleep cycle patterns, which is undoubtedly linked to the sleep disturbance behaviours they exhibit. Compared to age-matched controls, RTT patients have significantly fewer sleep cycles per night and spend significantly less time in Stage 3 NREM sleep, also known as "slow-wave sleep" (SWS; Ammanuel et al. 2015). In this study, RTT patients also experienced less time where delta oscillations were the major constituent of the electroencephalogram (EEG; see Chapter 1.4.1), which is perhaps not surprising given that delta oscillations are the main constituent of SWS (Chauvette et al. 2011). Like humans, *Mecp2*-deficient mice exhibit fewer sleep cycles and overall spend less time in SWS (Wither et al. 2012). Total sleep duration does not differ significantly between RTT patients and control groups, nor is there any significant difference in the duration of individual bouts of SWS (Ammanuel et al. 2015). Therefore, reduced SWS and delta oscillations throughout the night is directly attributed to the reduction in the number of sleep cycles.

Although there is ample evidence to suggest that loss of MeCP2 affects the structure of sleep cycles, evidence for the effect of MeCP2 loss on delta power is more contentious. Quantification of EEG delta power during SWS revealed heightened power in RTT patients compared to controls (Ammanuel et al. 2015). Furthermore, in control subjects, there was a noticeable decrease in both SWS duration and corresponding delta power in consecutive sleep cycles as the night progressed, which was not seen in RTT patients. In contrast to human studies, the overall power of delta oscillations during periods of SWS did not significantly differ between *Mecp2*-null and WT animals (Wither et al. 2012). However, in contradiction to this, a further study using the same animal model found significant attenuation of delta power in *Mecp2*-null mice (Johnston et al. 2014). Here, the reduction in delta power with respect to control animals correlated with poor quality of SWS in knock-out (KO) mice. The authors suggest that the reduction in SWS quality served as a biomarker for uncompensated sleep deprivation.

1.4 Neuronal oscillations

1.4.1 Electroencephalogram (EEG)

In humans, an electroencephalogram (EEG) can be used to assess both quantity and quality of sleep by measuring changes in the electrical activity of the brain. This non-invasive method of recording rhythmic patterns of brain activity was first used by German psychiatrist Hans Berger in the 1920s (review: Kaiser, 2005), and involves the placement of small disk-shaped electrodes on the surface of the skull which measure extracellular fluctuations in voltage as a result of neuronal activity. Rhythmic activity is present throughout the brain at all times, and can be influenced by sensory stimulation and by the behavioural state of the subject. EEG is a useful tool for recording changes in brain activity in real-time, however, its lack of defined spatial resolution makes it difficult to identify the precise brain region of interest from the graphical outputs. Hence, with the invention of alternative methods of measuring brain activity, EEG is now typically used in conjunction with other techniques to provide a more precise output with both spatial and temporal resolution (Mulert et al. 2004; Ebersole and Ebersole, 2010; Vulliemoz et al. 2010).

1.4.2 Neuronal oscillations

The rhythmic patterns of brain activity seen in the human EEG arise from groups of neurons firing in synchrony and are termed “neuronal oscillations”. Oscillations are grouped according to their frequency and each band of oscillation frequency has a distinct function (Buzsaki, 2006). Many have sought to discover the precise role and mechanisms underlying each of these oscillations. Using isolated regions of animal (often rodent) brain tissue *in vitro*, it is possible to establish network oscillations that are equivalent to those seen in the human EEG, hence providing a useful model for studying these rhythms in isolation. These rhythms correlate with the neuronal oscillations that can be studied in an *in vivo* setting also. *In vitro* models are particularly useful, as they allow for easy pharmacological manipulation and/or electrical stimulation of the network in order to assess the mechanisms that underlie the rhythm. Indeed, these techniques are often used to establish the rhythm itself: transient oscillations can be evoked through electrical stimulation of the cells responsible for their generation, and persistent oscillations can be induced with pharmacological entities that mimic the activity of neurotransmitters *in vivo*.

1.4.3 Neuronal oscillations associated with wakefulness

1.4.3.1 Gamma oscillations (30 - 80 Hz)

Gamma oscillations represent one of the most common and fastest groups of network oscillations within the human EEG, with a frequency of 30 - 80 Hz. Gamma oscillations are found throughout the cerebral cortex (Chrobak and Buzsáki, 1998; Gross et al. 2007; Hermes et al. 2015) and in several subcortical regions of the brain, including the hippocampus (Traub et al. 1996). It is thought that gamma oscillations play a role in higher cognitive functions including sensory and pain perception, selective attention and perceptual grouping (Fries et al. 2001; Henrie and Shapley, 2005; Gross et al. 2007; Panagiotaropoulos et al. 2012). Gamma oscillations facilitate the synchronicity of neuronal activity across spatially distinct networks and across hemispheres (Engel et al. 1991a; Engel et al 1991b; Bibbig et al. 2002). It is thought that gamma oscillations here help to integrate information relating to a single stimulus that originated in distinct neuronal networks.

Gamma oscillations are associated with awake states and consciousness: power is highest during wakefulness, at intermediate levels during REM sleep and lowest during NREM sleep (Gross and Gotman, 1999). Gamma oscillations are highly synchronous during REM sleep, as the brain closely resembles the awake state (Steriade et al. 1996). However, in both human EEG (Valderrama et al. 2012) and animal *in vivo* studies (Steriade et al. 1996), gamma oscillations have been shown to be present during NREM sleep too. Evidence from these studies suggests that bursts of gamma activity occur during the depolarising component (or “UP state”) of slow oscillations. Gamma oscillations have been implicated in learning and memory (Carr et al. 2012; Yamamoto et al. 2014). Heightened gamma power is associated with the formation of long-term coherent representations of learnt information in the brain (Tallon-Baudry and Bertrand, 1999). Gamma oscillations increase with memory load (Howard et al. 2003; van Vugt et al. 2010), and are able to predict the successful encoding of new memories (Sederberg et al. 2007). Learning and memory is enhanced by the coupling of gamma oscillations to other bands of neuronal oscillations, particularly theta:gamma (Osipova et al. 2006; Tort et al. 2008; review: Nyhus and Curran, 2010) and alpha:gamma coupling (Park et al. 2016).

1.4.3.2 Beta II (20 - 30 Hz) and Beta I (12 - 20 Hz) oscillations

Beta II oscillations (20 - 30 Hz) are associated with activation of the motor cortex and occur in the pre-motor cortex during the preparation period immediately before movement (MacKay and Mendonca, 1995; Baker et al. 1999). Beta II oscillations can even be evoked simply by the illusion of movement (Keinrath et al. 2006), but are replaced with gamma oscillations when movement begins. Beta II oscillations are able to traverse significant distances across the brain in order to synchronise with spatially distinct brain regions (Kopell et al. 2000). A second, slower type of beta oscillation, beta I oscillations (12 – 20 Hz), aid the integration of information from different regions of the neocortex for multimodal processing (von Stein et al. 1999). When gamma and beta II oscillations occur concurrently, they combine via a period concatenation process (Roopun et al. 2008), resulting in a single rhythm of beta I frequency (Faulkner et al. 1999; Olufsen et al. 2003). These rhythms are associated with the presentation of a novel stimulus (Bibbig et al. 2001) and begin to habituate when the same stimulus is presented repeatedly (Haenschel et al. 2000). It has been postulated that beta I oscillations act as a substrate for memory: their characteristics influence the synchronisation of neuronal activity among spatially distinct networks, and hence may provide a mechanism for storage and retrieval of stimulus-specific information across multiple brain regions (Whittington et al. 1997).

1.4.3.3 Alpha oscillations (8 - 12 Hz)

Once nicknamed “The Berger Rhythm”, alpha oscillations (8 - 12 Hz) were discovered by Hans Berger and were noted to occur within the EEG during “idling” awake states (Adrian and Matthews, 1934). Alpha oscillations have been linked to meditative behavioural states; their power is greatly reduced opening of the eyes, the onset of movement and the initiation of conscious thought and cognitive tasks. Alpha oscillations also occur during the transition to sleep, as synchronous activity throughout the brain shifts from predominantly high to predominantly low frequency (De Gennaro et al. 2001a; De Gennaro et al. 2001b). Alpha oscillations have also been implicated in the learning and memory process (Jensen et al. 2002), particularly in relation to their coupling with theta rhythms (Khader et al. 2010; Riddle et al. 2020). Since alpha oscillations are diminished during sensory stimulation, it is postulated that the alpha rhythm serves as a mechanism to filter task-relevant information post-stimulus and inhibit populations of neurons that convey task-irrelevant information (Jensen and Mazaheri, 2010).

1.4.4 Neuronal oscillations associated with REM sleep

1.4.4.1 Theta oscillations (4 - 8 Hz)

Theta oscillations (4 - 8 Hz) are the defining feature of REM sleep (Jouvet, 1969). They occur throughout the hippocampus (Winson, 1974; Bullock et al. 1990) and are one of the fastest rhythms that predominantly occur during sleep. Theta oscillations have also been seen in cortical regions such as the entorhinal cortex (Mitchell and Ranck, 1980; Alonso and García-Austt, 1987) and subcortical regions such as the amygdala (Paré and Collins, 2000); however, none of these regions can generate a theta rhythm on their own, and instead rely on theta frequency inputs for distant rhythm generators (Buzsáki, 2002). Theta oscillations can be seen during wakefulness, and are associated with the initiation of higher motor acts, such as locomotor activity. The occurrence of theta oscillations in the hippocampus is often seen in conjunction with gamma oscillations, where cross frequency phase-phase coupling occurs (Canolty et al. 2006; Belluscio et al. 2012). The function of theta oscillations in the human EEG has been subject to intense investigation, with evidence for a role in spatial navigation and learning, attention, and memory (Winson, 1978; Kahana et al. 1999; Tesche and Karhu, 2000; Jensen and Tesche, 2002; Rizzuto et al. 2006; review: Sauseng et al. 2010). As previously described, theta:gamma coupling has been implicated in working memory and in the encoding of long-term episodic memories (review: Nyhus and Curran, 2010).

1.4.5 Neuronal oscillations associated with NREM sleep

1.4.5.1 Sleep spindles (7 - 14 Hz)

Stage 2 NREM sleep combines activity of multiple frequencies, however its defining feature is the presence of sleep spindles (7 - 14 Hz; Loomiset al. 1935). Sleep spindles represent one of the few types of brain activity that is unique to sleep, though not necessarily unique to Stage 2 NREM. A sleep spindle can be recognised as a transient flurry of oscillations with a “waxing and waning” characteristic. Sleep spindles occur in the thalamus and throughout the cerebral cortex, either in isolation, or coupled to delta oscillations, sharp wave ripples (SPW-Rs) or K-complexes (De Gennaro & Ferrara, 2003). Auditory evoked responses are significantly reduced during periods of spindle activity (Yamadori, 1971), suggesting that sleep spindles play an important role in promoting sleep continuity by inhibiting sensory input to the cortex. The duration and density of spindles, as well as the duration of Stage 2 NREM sleep in general, are increased

following both declarative and non-declarative memory tasks, and recall performance is correlated with this rate of increase (Schabus et al. 2004; Fogel and Smith, 2006; Fogel et al. 2007).

Sleep spindles are thought to rely on reciprocal connections between the thalamus and neocortex, as rhythms within these regions occur in phase (Contreras and Steriade, 1996). Thalamocortical neurons provide a major source of input to the neocortex and present an avenue for bi-directional corticothalamic feedback. This is thought to account for the long-range synchrony of spindle activity between the thalamus and cortex (Destexhe et al. 1998). Spindle generation survives dissociation from the cortex (Morison and Bassett, 1946) and can be modelled in isolated thalamic networks (Destexhe et al. 1994), which is suggestive of a thalamic generator. Later studies revealed thalamic spindles were markedly disorganised and had low spatiotemporal coherence following decortication (Contreras et al. 1996), suggesting a role for neocortical feedback in the maintenance of sleep spindles. Reticular thalamic neurons generate spindle-like activity in isolation (Steriade et al. 1987), and their absence prevents thalamic nuclei from generating this rhythm (Steriade et al. 1985). Thalamocortical relay cells are reciprocally connected to reticular thalamic cells in this network and robustly project to pyramidal cells in the neocortex where spindle activity is prevalent, further consolidating the importance of thalamocortical connections for the production and maintenance of sleep spindles (Andrillon et al. 2011). Synchronous spindle activity also occurs in the cortex following dissociation from the thalamus (Contreras et al. 1996), suggesting that a cortical generator also exists.

1.4.5.2 Delta oscillations (0.5 - 4 Hz)

During Stage 3 NREM sleep, the human EEG mainly consists of delta oscillations (0.5 - 4 Hz; Chauvette et al. 2011). These are predominantly found in regions of the frontal and parietal cortex during deep sleep, with somatosensory areas being of particular interest to both human (Ioannides et al. 2009) and rodent studies (Carracedo et al. 2013). Delta activity predominates each sleep-cycle during the early stages of sleep, declines as the period of sleep progresses and is increased in line with the duration and intensity of prior wakefulness (Borbély et al. 1981; Hanlon et al. 2009; Rodriguez et al. 2016). Delta oscillations enhance sleep-related memory consolidation (review: Walker, 2009) and occur during sleep in a use-dependent manner: they are increased in cortical regions in which notable sensory experiences have been encoded during the previous awake state (Kattler et al. 1994; Huber et al. 2004). They are also reduced in cortical areas that were

suppressed during wakefulness (Huber et al. 2006). When delta activity is increased during NREM sleep, memory performance is enhanced during a post-sleep memory task (Huber et al. 2004; Marshall et al. 2006). Conversely, suppression of delta activity during sleep resulted in poorer performance on a texture-discrimination task, as well as reduced overall EEG power density in cortical areas where learning occurred (Aeschbach et al. 2008). As previously mentioned, slow oscillatory activity (<4.5 Hz) has been associated with synaptic downscaling, as part of the synaptic homeostasis hypothesis (see Chapter 1.3.2; Tononi & Cirelli, 2003). This theory is supported by the findings that NREM sleep induces an overall reduction in cortical firing rates (Vyazovskiy et al. 2009, Watson et al. 2016), as well as the number of dendritic spines in mouse cortical areas (Maret et al. 2011). It has also been hypothesised that the reduction in cortical firing rates allows individual neurons within the network to undergo periods of rest and undertake vital cellular maintenance processes (Vyazovskiy and Harris, 2013). Furthermore, delta oscillations correlate with a reduction in ATP consumption and therefore increase ATP availability (Dworak et al. 2011), in preparation for more energy-demanding behavioural states following NREM.

Delta oscillations are known to interact with other higher frequency rhythms to facilitate information processing. Notably, delta and theta oscillations have a synergistic effect on memory consolidation: the synaptic rescaling that occurs during NREM sleep with periods of delta activity relies on the theta-facilitated strengthening of synaptic connections during previous REM phases (Diekelmann and Born, 2010). Given the role of theta oscillations in LTP (Larsonet al. 1986) and the role of delta oscillations in the depression of previously potentiated synapses (Staubli and Lynch, 1990), these two rhythms function in a reciprocal manner to upregulate important synaptic connections and down-regulate those that are unwanted in the long-term. Not only do these two rhythms work together in a temporally-distinct manner, delta:theta coupling occurs throughout the sleep cycle (Borbély et al. 1981) and theta oscillations are found to be nested within the cortical column during periods of delta activity (Carracedo et al. 2013). The coupling of delta oscillations to other rhythms during wakefulness is discussed in Chapter 7.4.5.

Delta oscillations can be generated through one of two mechanisms. Firstly, a sensory-modified generator of delta oscillations is seen in the thalamus (Leresche et al. 1991; Amzica et al. 1992; Steriade et al. 1993a), whose main function is to relay sensory information between the cortex and subcortical structures such as the brain stem. Thalamically-generated delta oscillations are projected onto the neocortex through

reciprocal thalamocortical connections. Secondly, local generators exist within the neocortex itself where delta oscillations can be induced in the absence of thalamocortical connections (Steriade et al. 1993a; Timofeev et al. 2000). It is believed that each region of the cortex contains its own local rhythm generator (Mormann et al. 2008) which communicates reciprocally with the thalamic generator through projections to thalamocortical and thalamic reticular cells via the corticothalamic tract (Steriade, 2003). The following sections will describe the mechanisms by which thalamocortical and cortical delta oscillations are each generated.

Thalamocortical delta oscillations

Delta rhythms in the thalamus originate from a network of hyperpolarised thalamocortical cells, which receive inhibitory input from reticular thalamic cells (Steriade et al. 1991). Thalamic delta rhythms are governed by two intrinsic cellular mechanisms: the I_h, a hyperpolarisation-activated inward cation current, and the I_t current, a low threshold calcium ion (Ca^{2+}) current (Deschênes et al. 1982; McCormick and Pape, 1990; Soltesz et al. 1991; Steriade et al. 1993a) which together mediate low-threshold spiking activity in these cells. These relatively slow processes reciprocally activate one-another, which results in the firing of thalamocortical cells at delta frequency in a clock-like manner (Amzica et al. 1992). As thalamocortical cells project to cortical regions, delta oscillations occur here phase-locked to the thalamic rhythm. Cortical neurons project back to the thalamus, rhythmically activating a network of thalamic reticular cells. Excitation of these cells activates a phase of gamma-aminobutyric acid (GABA)-induced inhibition onto thalamocortical cells, thus restoring the hyperpolarised nature of these cells and establishing a feedback loop to the thalamic generator (Steriade, 2003). Once the thalamocortical cell membrane potential is sufficiently hyperpolarised, the I_h and I_t conductances are activated once more, and hence the cyclic pattern within the network is established (Steriade et al. 1991).

The thalamus receives a large amount of input from the reticular activating system during the control of sleep and wakefulness. During sleep, inhibitory inputs into the reticular activating system result in reduced cholinergic activity received by the thalamus. Low cholinergic tone is important for sleep-related memory consolidation during NREM sleep and the transition between different sleep states is modulated cholinergic signalling. It is unsurprising then that low cholinergic tone is also required for the maintenance of the brain rhythms that occur during the deepest phases of sleep (Steriade et al. 1991; review: Steriade, 2006): stimulating cholinergic synapses that project from the brainstem onto

the thalamus abolished the thalamocortical delta rhythm and induced high frequency spiking activity that is indicative of awake-state brain rhythms.

Cortical delta oscillations

Due to the sheer volume of projections that extend between the thalamus and the neocortex, it was previously believed that all delta oscillations were generated by the thalamus and superimposed onto the cortex via these reciprocal connections. However, it was later discovered that a subset of these oscillations were able to persist in the cortex despite dissociation from the thalamus (Steriade et al. 1993a; Timofeev et al. 2000), indicating that their origin lay elsewhere. Indeed, isolated regions of the neocortex are able to induce and maintain delta oscillations in the absence of any subcortical connection (Amzica and Steriade, 1998), confirming the presence of a purely cortical generator. Furthermore, some of the delta oscillations present in the thalamus are thought to arise from cortical generators that have been projected backwards via corticothalamic axonal tracts (Amzica and Steriade, 1998). During sleep, delta oscillations occur in many regions across the neocortex and do not necessarily occur in phase with each other (Mormann et al. 2008), suggesting that each cortical region contains its own local generator that functions independently to adjacent generators.

Cortical delta oscillations have been characterised in an *in vitro* model in the rat somatosensory cortex (Carracedo et al. 2013). While these rhythms occur in phase across the entire cortical column, the greatest power is recorded in layer V. Here, delta oscillations originate in an NMDA-driven network of layer V intrinsically bursting (IB) pyramidal cells, and are sensitive to mACh, NMDA and AMPA-plus-kainate receptor antagonisation, as well as blockade of gap junction conductances. IB cells, which produce excitatory outputs, fire bursts of action potentials concurrently with the phase of the field delta rhythm as a result of the summed effect of compound somatic EPSPs. Fast spiking interneurons (also found in layer V) also fire at delta frequency and provide inhibitory feedback to the IB cells in the form of fast IPSPs during the active phase of the delta oscillation that result in burst termination in the IB cells. During the quiescent phase of the delta oscillation, IB cells receive a secondary type of inhibitory input in the form of slow $GABA_B$ receptor-mediated inhibition. Nested within the cortical delta rhythm, some fast spiking interneurons also fire at theta frequency, which is reflected in layer V regular spiking (RS) pyramidal neurons, and projects upwards to superficial layers II and III, where outputs from IB cells are also received in the form of $GABA_B$ receptor-mediated IPSPs.

1.4.5.3 Slow wave oscillations (<1 Hz)

Slow wave oscillations (SWOs) represent the slowest form of coherent activity seen in the human EEG (< 1 Hz) and are seen throughout the cortex and thalamus in Stage 3 NREM. SWOs have been recorded in both IB and RS pyramidal cells in layers III and IV of sensory, motor and association cortex regions (Steriade et al. 1993b). Further investigation revealed that RS SWOs are often coupled to spindle activity, whereas IB SWOs are often coupled to delta oscillations and spindles together (Steriade et al. 1993c), suggesting cell-type specificity exists in SWO function.

SWOs have the ability to modulate oscillatory activity from multiple higher bandwidths, including delta oscillations and sleep spindles (Steriade et al. 1993d), as well as fast oscillations, including gamma (Steriade et al. 1996). This provides a function for SWOs in learning and memory: facilitating the integration and temporal coordination of faster rhythms in the neocortex and hippocampus serves as a substrate for memory consolidation (Sirota and Buzsáki, 2005). Hippocampal gamma oscillations and sharp-wave ripples, two forms of neuronal activity integral to the learning and memory process, self-organise and temporally reset in accordance with the SWO that is projected from the neocortex to the hippocampus (Isomura et al. 2006). Furthermore, during sleep the SWO acts as a "travelling wave", originating in a defined location and propagating outwards in an anteroposterior manner, which is thought to aid sleep-related synaptic plasticity via the temporal correlation of spike-timing (Massimini et al. 2004).

1.4.5.4 Hippocampal sharp-wave ripples (100 - 200 Hz)

Sharp-wave ripples (SPW-Rs) have been identified in the hippocampus during deep sleep and periods of immobile wakefulness (Buzsáki et al. 1983; Buzsáki, 1986; Buzsáki et al. 1992). These events consist of a sharp-wave burst followed by a very high frequency oscillation known as a ripple. The incidence of SPW-Rs is very irregular and each event lasts between 50 - 100 ms. The sharp-wave component of the SPW-R is generated through build-up of excitatory activity within a network of CA3 pyramidal cells. This occurs through the activity of hippocampal interneurons that replay compressed fragments of sequences encoded in the awake state, and hence provides a mechanism for how these networks function in the consolidation of memories during sleep (Buzsáki, 2015). Temporary disinhibition of CA3 pyramidal cells by blocking $GABA_A$-mediated inhibition allows for the generation of the high amplitude sharp-wave event (Buzsáki, 1986). The excitatory output of CA3 pyramidal cells during the sharp-wave is delivered

to the CA1 region via schaffer collateral projections (Csicsvari et al. 2000), and drives a network of reciprocally linked CA1 pyramidal cells and parvalbumin-positive interneurons (Schlingloff et al. 2014). The outcome of this is fast synchronous activity at ripple frequency, and ripple frequency inhibition is provided through $GABA_A$-mediated currents, which coordinate the phase-locking of pyramidal cells within the network. Indeed, blocking $GABA_A$-mediated signalling abolishes the hippocampal ripple oscillation (Stark et al. 2014).

The hippocampus is considered the central hub for memory formation: gamma oscillations in the awake state enable the encoding of information relating to sensory and perceptual experiences, while SPW-Rs during sleep facilitate the reactivation of these systems and the transfer of information to the neocortex for long-term storage (Axmacher et al. 2006; review: Ferrara et al. 2012). Hippocampal circuits are reactivated during post-learning sleep and mimic the sequences elicited in response to sensory stimuli in prior wakefulness (Ji and Wilson, 2006). Following a hippocampus-dependent spatial memory task in rodents, selectively suppressing SPW-R during the following consolidation period resulted in poorer task performance (Ego-Stengel and Wilson, 2010; van de Ven et al. 2016), highlighting the importance of hippocampal SPW-Rs in memory consolidation. Induction of LTP via experimental high-frequency stimulation of the hippocampal CA3 region also induced SPW-Rs in the same network (Behrens et al. 2005), suggesting that the processes of LTP induction and SPW-R generation are functionally linked. While evidence for the importance of SPW-Rs in sleep-related memory consolidation is plentiful, it is believed that the specific interaction of these events with neocortical delta oscillations and sleep spindles is required for fine tuning this process.

1.4.6 The Two-Stage theory of memory consolidation

The Two-Stage theory of memory consolidation suggests that an interplay exists between hippocampal activity (the site of initial memory encoding) and neocortical activity (the location of long-term memory storage) during sleep, which has large implications for sleep-related memory consolidation (Buzsáki, 1989). Communication between the two neuronal networks is essential for newly-formed memories to be successfully reinforced, stored and retrieved at a later date. Specifically, this dialog consists of the coupling between neocortical delta waves, neocortical sleep spindles and hippocampal SPW-Rs (Buzsáki, 1986). These three rhythms are known to couple to one-another in temporal succession (Sirota et al. 2003), with local networks in the neocortex, thalamus and hippocampus working together to form synchronous activity

across these regions (review: Adamantidis et al. 2019). Here, the amplitudes of each event are thought to support rhythm coupling. During NREM sleep, several variations of coupling occur, including delta:SPW-Rs, delta:spindles, spindles:SPW-Rs, and delta:spindle:SPW-Rs (Siapas and Wilson, 1998; Sirota et al. 2003; Staresina et al. 2015). Typically, delta-coupled-spindle events occur with a delta wave preceding the sleep spindle, and hippocampal SPW-Rs occur before and after, but rarely during the delta event (Sirota et al. 2003; Maingret et al. 2016). SPW-Rs occur coupled to the trough, or active phase, of the spindle, with the duration and amplitude of both spindle and ripple events significantly increased when coupled to one another (Azimi et al. 2021). During a hippocampal SPW-R, cortical regions are activated in temporal coordination, while thalamic inhibition occurs immediately prior to each ripple (Logothetis et al. 2012). Reasons for this are thought to be that suppression of thalamic activity enhances the strength of communication between the hippocampus and cortex by temporarily dampening the input of unwanted sensory information.

Although each of the three rhythms have individually been implicated in processes relating to memory consolidation, their occurrence in isolation is thought to be insufficient for successful large-scale consolidation. Instead, the effect of triplet coupling of these rhythms is considered to be the main driver of sleep-related memory consolidation during NREM sleep (review: Navarrete et al. 2020). The relationship between these neuronal activities allows for the transformation of learnt information initially encoded in the hippocampus into long-term memories stored in the neocortex, in a post-learning, time-dependent manner (Inostroza and Born, 2013). The interplay between these rhythms is thought to lead to an overall increase in cortical plasticity and a reduction in the representation of learnt information in the hippocampus (Navarrete et al. 2020).

In support of the Two-Stage theory, several studies have shown that the coupling of these rhythms is directly correlated with improved memory performance. The degree of delta:spindle, ripple:delta and ripple:delta:spindle coupling during the post-training sleep was positively correlated with performance on a hippocampus-dependent memory task (Maingret et al. 2016). Also in this study, experimental stimulation of the neocortex following an endogenous hippocampal SPW-R during deep sleep both enhanced hippocampo-cortical coupling and improved memory performance. During a memory consolidation task based on the recollection of pre-learnt information prior to sleep, the number of ripples superimposed from the hippocampus onto the neocortex during sleep was positively correlated with memory performance during the recall task

after sleep (Axmacher et al. 2008). Thalamic spindle stimulation in-phase with the cortical delta oscillation increases the coupling of thalamic, hippocampal and cortical events and enhances hippocampus-dependent memory performance (Latchoumane et al. 2017).

1.4.7 Neuronal oscillations in RTT

Many studies have sought to understand the function of MeCP2 in the coordination of different brain rhythms. Unfortunately, due to the variability among studies - with respect to experimental procedure, subject type, recording techniques and brain regions of interest - some of the results appear to contradict each other, and it is still not clear exactly how each oscillation type is affected by the loss of MeCP2 function. Furthermore, the corroboration of results from mouse models with parallel studies in RTT patients is limited.

I have previously discussed how delta power was heightened during NREM sleep in RTT patients compared to age-matched controls, with gamma, beta, alpha and theta oscillation power unaffected (Ammanuel et al. 2015). Furthermore, the typical regression of delta power in consecutive sleep-cycles was absent in RTT patients. In another study, an overall reduction in EEG power of middle-frequency (alpha and beta) oscillations was observed across four brain regions of interest, as well as an increase in the relative power of delta oscillations (Roche et al. 2019). Here, changes in oscillation power were significantly correlated with severity of disease progression among the RTT patients, corroborating the idea that neuronal oscillations are vital for neurological function.

Studies using mouse models of RTT have also found neuronal oscillation abnormalities. *Mecp2*$^{-/y}$ and *Mecp2*$^{T158A/y}$ mice exhibited significantly reduced event-related power in both high- and low-frequency oscillation bandwidths (Goffin et al. 2011). In *Mecp2*$^{T158A/y}$ mice, reductions in the power of delta, theta and alpha oscillations occurred at post-natal day (P) 30, before the establishment of behavioural deficits associated with RTT, suggesting that neurological abnormalities precede the onset of neuropathological phenotypes. These mice also exhibited a significant increase in the power of gamma oscillations at the symptomatic (P90) stage. Given the influence of gamma oscillations in epilepsy and seizure-like activity, the authors here note that the observed increase in high gamma power likely reflects the overall hyperexcitability seen in MeCP2-deficient brains. However, as this effect was not seen at the pre-symptomatic stage, it is likely this phenomenon occurs in an age-dependent manner as a result of (rather than a precursor for) RTT-like phenotypes. Resting EEG power was evaluated from female mice

carrying the R225X mutation: an increase in delta power during both awake and NREM states, an increase in theta power during REM sleep, and a decrease in alpha power in almost all experimental conditions (Dong et al. 2020). Despite increased epileptiform activity which is consistent with previous findings, this study found a trend towards a decrease in gamma power and that this decrease was correlated with phenotypic severity, which is not consistent with previous findings. As previously mentioned, other studies using mouse models of RTT have shown a significant reduction in delta power compared to WT (Johnston et al. 2014), while others have found there to be no difference (Wither et al. 2012). Another study found abnormalities in gamma and beta frequency rhythms, with theta and delta unaffected (Liao et al. 2012). Finally, as with WT animals, *Mecp2*-deficient mice exhibited a significant increase in spontaneous activity within the theta range during exploratory behaviours, however, the frequency of these evoked oscillations was significantly reduced with respect to WT controls (D'Cruz et al. 2010). This study noted that the activity of delta oscillations and hippocampal SPW-Rs was normal with respect to the WT.

Overall, the body of research relating to MeCP2 and oscillations is large and at times contradictory. Each bandwidth of oscillations has its own precise function and mechanism of generation, which often differs between distinct brain regions. Furthermore, each bandwidth of oscillations also occurs with a degree of temporal specificity that must be so precisely controlled for neurological function to proceed. Many of the studies mentioned above assessed neuronal activity through EEG analysis, which although provides a useful non-invasive method for assessing neurological function in RTT patients and mouse models, does not provide precise spatial resolution for studying individual networks. Hence, further investigation using animal models where individual brain regions can be probed and dissected, and where the mechanisms that underlie oscillations can be manipulated, will provide better insight into how MeCP2 affects each oscillation type. This can then be brought together to understand how all of these affected oscillations work together in the MeCP2-deficient brain.

1.5 Neuronal networks

1.5.1 Structure and function of the neocortex

The neocortex represents one of the newest structures in the evolutionary development of the brain. It is believed that intelligence among mammals is correlated with the number and density of cortical neurons (Dicke and Roth, 2016). The structure of the neocortex

is complex, but exquisitely organised such that it can support multiple processes of high-level brain function at once, including sensory perception, motor coordination, cognition, spatial recognition and language comprehension and production. The neocortex has a laminar structure with six layers, labelled I – VI from most to least superficial, each with its own distinct cellular composition. Pyramidal neurons within each layer project axons and dendrites vertically to connect with cells in other layers, and horizontally to connect to neighbouring cells of the same lamina, hence establishing an efficient network within the cortical column (Mountcastle, 1997). Cells also extend long range horizontal projections which allow the relay of information between adjacent or even distal regions of the cortex. There are two main types of neurons in the cortex: excitatory pyramidal cells and inhibitory interneurons, both of which possess many subtypes. Pyramidal cells outnumber interneurons by approximately 4:1, and are restricted to layers II, III, V and VI; though their axons can project within and beyond the column, to other cortical and subcortical regions, including those in the contralateral hemisphere. Interneurons on the other hand are found in all layers of the column and have axon projections that are restricted within local circuits. A complementary schematic of the laminar structure of the neocortex is shown in Fig 1.6.

Layer I contains the fewest cell bodies of all the lamina layers, 95% of which are GABAergic interneurons (Gabbot and Somogyi, 1986). It is devoid of excitatory cell soma, and mostly comprises the most superficial apical dendrites of pyramidal cells from deeper layers (Marin-Padilla and Marin-Padilla, 1982). Layer I receives afferent input from the thalamus and other cortical regions, and plays a crucial role in propagating sensory information through the cortical column with specialised top-down modulation. Layers II and III are histologically very similar and are often described and studied as a single entity. These layers contain pyramidal cell soma, with axons projecting downwards to innervate other regions of the same column, horizontally to neighbouring columns or protruding beyond layer VI, across, and back up to innervate distal cortical regions, including regions in the contralateral hemisphere (Chovsepian et al. 2017). Pyramidal cells in layer III are generally bigger than those in layer II, though smaller than those in layer V. Interneuron populations in layer II/III comprise of fast-spiking, late-spiking and low threshold spiking interneurons (Kawaguchi, 1995). Layer IV consists mainly of spiny stellate cells interspersed with some pyramidal cells (Staiger et al. 2004), which receive a large proportion of thalamic input via thalamocortical relay neurons (Benshalom and White, 1986). Given that the majority of sensory information is delivered to the cortex via the thalamus, the main role of layer IV is thought to be in processing the majority of this afferent input. Information received by layer IV is generally

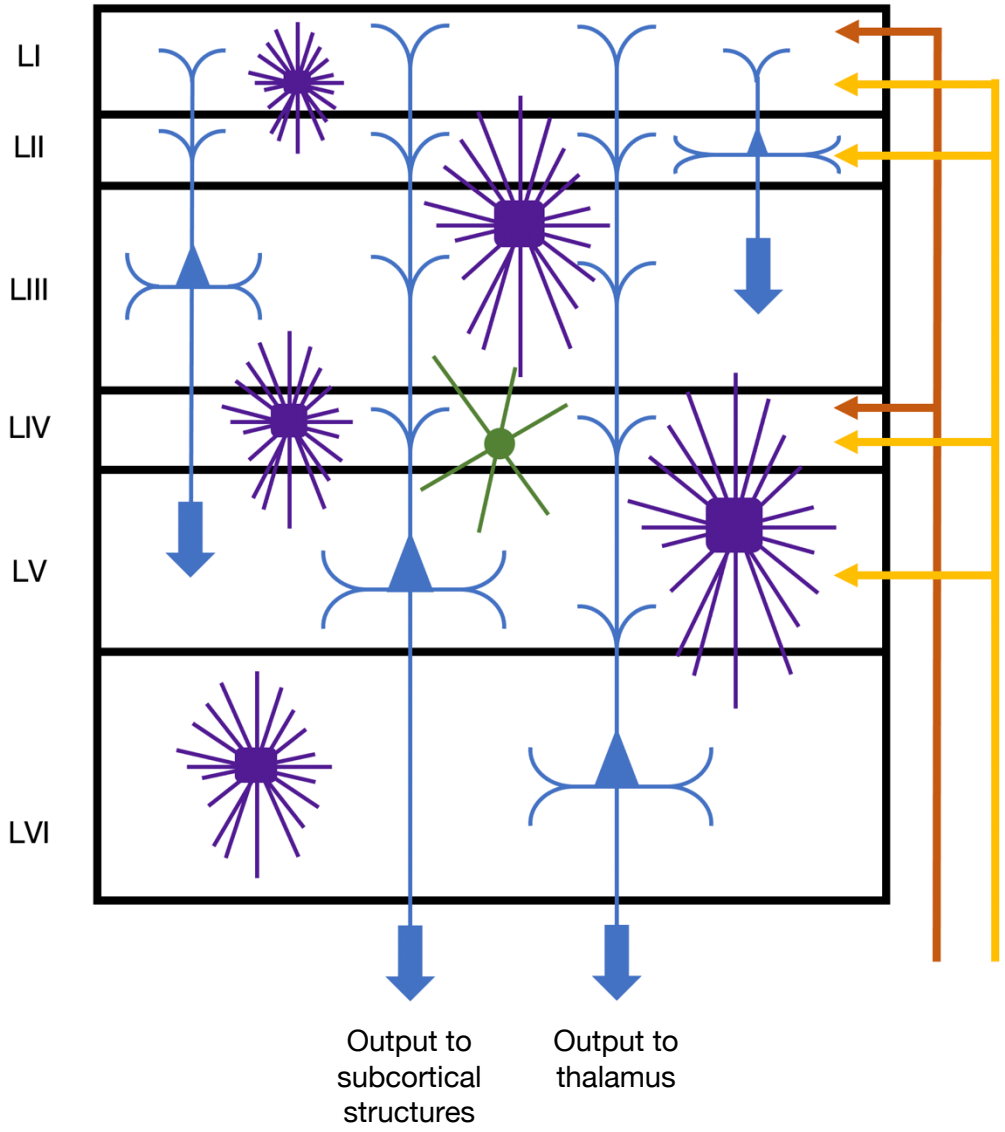

Figure 1.6: Laminar structure of the neocortex. Basic schematic depicting the main cell types in each layer of the neocortex. Blue: pyramidal cells; excitatory neurons with pyramidal-shape soma (triangle) with apical dendrites projecting upwards (terminating in layer I), and basal dendrites projecting horizontally within the lamina. Axons project downwards, as depicted by blue arrows. Layer V pyramidal cells project to subcortical structures, while layer VI pyramidal cells project to the thalamus. Orange: input from other cortical regions. Red: input from the thalamus. Green: stellate cells; excitatory cells with spiny dendrites, mainly found in layer IV though sparsely found in layer II/III also (not shown). Stellate cells receive most of the thalamic input and relay information to pyramidal cells in other lamina. Purple: interneurons; inhibitory cells which synapse onto pyramidal cell dendrites and regulate their excitatory output.

---

relayed directly to layer VI (Tarczy-Hornoch et al. 1999), or to layer II/III, where it may then be projected to layer V (Thomson et al. 2002). Layer IV also contains an array of

interneurons, which also receive input from the thalamus (Miller, 2003). Layer V contains the largest of all pyramidal cells in the neocortex, whose axons project to either subcortical or contralateral cortical regions (Kasper et al. 1994; Levesque et al. 1996; Aronoff et al. 2010; Chovsepian et al. 2017). Layer V receives information from higher up in the column via top-down processing, and can also be innervated by inputs from other cortical and subcortical regions, including the thalamus (Agmon and Connors, 1992). Interneurons in this layer are largely fast-spiking, and regulate the firing of pyramidal cells through synaptic connections at both the soma and the dendrites (Naka and Adesnik, 2016). The composition of layer VI is similar to that of layer V, with large pyramidal cells that receive inputs from superficial layers and project predominantly to the thalamus (Levesque et al. 1996; Gentet and Ulrich, 2004). Interneurons in this layer possess aborisations that are restricted to layer VI, suggesting that these cells provide very localised inhibition (Briggs, 2010).

1.5.2 The Somatosensory Cortex

The somatosensory cortex is located posterior to the central gyrus, and receives information relating to tactile, nociceptive and proprioceptive sensation. In contrast to other localised sensory systems such as sight, hearing and taste, the somatosensory system integrates information pertaining to all areas of the body, via the “cortical homunculus” (Penfield and Boldrey, 1937; Nakamura et al. 1998). The somatosensory cortex is divided into two distinct regions known as the primary (S1) and secondary (S2) somatosensory areas. The S1 cortex receives global information relating to pressure, temperature and pain (Ploner et al. 2000; Shaw et al. 2001), which is projected to the neocortex from the thalamus (Jones and Friedman, 1982). Information is relayed from the S1 to the S2 cortex for higher-order processing events, including learning, memory formation and attention (Chen et al. 2008), and can also be projected to subcortical regions including the thalamus and basal ganglia (Künzel, 1977). During a behavioural task designed to assess attention during tactile performance, an increase in neuronal activity is seen in both somatosensory sub-regions, however this increase was greater in S2 compared to S1 (Hsiao et al. 1993). Following nociceptive stimuli, the response in S1 cortical areas was linearly correlated with the intensity of laser stimulation, suggesting a role for S1 in coding the magnitude of sensory input (Timmermann et al. 2001). The S1 cortex can also discriminate between different types of somatosensory input (Ploner et al. 2000; Bornhövd et al. 2002). In the case of the S2 cortex, increases in nociceptive stimulation resulted in an S-shaped response in activity in this area, with a sharp increase in response reported at the point where the pain threshold was reached and a

tapering off of response was seen after this threshold was exceeded (Timmermann et al. 2001). This suggests a role for S2 in distinguishing between harmful and non-harmful sensory inputs, which aids higher-order processes involved in coordinating the appropriate responses to nociception, and learning from these inputs to avoid painful stimulation in the future.

The somatosensory cortex has been subject to investigation since it was discovered that a range of different oscillation types can be generated in this brain region. In human MEG studies, gamma oscillations were induced following nociceptive stimuli, with gamma power increasing linearly with increasing stimulus intensity (Gross et al. 2007; Rossiter et al. 2013). Recent evidence from mice suggests that experimental induction of gamma oscillations in this region increases sensitivity to painful stimuli and promotes avoidance behaviours (Tan et al. 2019), suggesting a protective role of gamma oscillations in avoiding painful stimuli. During the latter stages of NREM sleep, increases in low frequency oscillations are observed in sensorimotor areas of the cortex (Ioannides et al. 2009). Notably, delta oscillations have been observed in the S1 cortex of the resting rat brain (Lu et al. 2007). Pre-sleep somatosensory stimulation resulted in enhanced delta oscillations during NREM sleep in the first hour of subsequent sleep in the contralateral somatosensory cortex (Kattler et al. 1994), implicating a role for delta oscillations in reinforcing the previously-activated neuronal circuitry. The somatosensory cortex has proven to be incredibly useful for modelling these brain rhythms *in vitro*, including gamma oscillations (Buhl et al. 1998), Beta I and Beta II oscillations (Kramer et al. 2008), and delta oscillations (Carracedo et al. 2013).

1.5.3 Intrinsically bursting (IB) pyramidal neurons

As previously mentioned, layer V of the cortical column consists of large pyramidal neurons whose apical dendrites extend upwards to superficial layers and whose axons project downwards to either subcortical or contralateral cortical regions (Kasper et al. 1994; Levesque et al. 1996; Aronoff et al. 2010; Chovsepian et al. 2017). Basal dendrites extend horizontally with a width approximately equal to the width of one subunit of the cortical column (Wang et al. 2018), suggesting a role for these cells in integrating information from neighbouring circuits. Pyramidal cell somas have a rounded pyramidal shape, with the apical dendrites extending upwards from the tip. Pyramidal cells are not specific to the cortex; they are also present in subcortical structures including the hippocampus, and subtle differences in pyramidal cell morphology exist between locations (Bekkers, 2011). In layer V of the somatosensory cortex, there are two subtypes of pyramidal neurons: intrinsically bursting (IB) and regular spiking (RS) cells (Agmon and

Connors, 1989). These cells are characterised by their distinctive firing patterns: IB neurons fire bursts of action potentials followed by periods of silence, whereas RS cells fire single action potentials at regularly spaced intervals (McCormick et al. 1985). These two cellular subtypes also exhibit subtle differences in their morphology: IB cells have large cell somas, tufted apical dendrites and axonal projections extending to subcortical regions, while RS cells have a smaller soma size, smaller and shorter apical dendrites that contain fewer branches and axonal projections that extend to the contralateral hemisphere via the corpus callosum and to the striatum (Hattox and Nelson, 2007). This study also showed that when IB cells fired only one singular action potential, the event also contained an after-depolarisation (ADP) phase following the initial spike, whereas RS cells rarely possessed this feature. In hippocampal CA1 pyramidal neurons, the ADP phase is a prominent feature of cellular activity, and is associated with action potential bursting (Jensen et al. 1996), both of which were abolished following the blockade of calcium ion (Ca^{2+}) signalling (Magee and Carruth, 1999).

It has been further postulated that the generation of spike bursts in pyramidal neurons is dependent on the kinetics of Ca^{2+} signalling. In hippocampal CA1 pyramidal cells, lowering the intracellular Ca^{2+} concentration was sufficient to induce bursting in previously-non-bursting cells, while increasing Ca^{2+} levels terminated the bursting potential of previously-bursting cells (Su et al. 2001). In these cells, ion conductance through R-type calcium channels is thought to drive the ADP phase of the action potential and is therefore integral to the bursting potential of these cells (Metz et al. 2005). In the midbrain, cellular bursting was induced following blockade of T-type calcium channels, which was shown to activate a subset of Ca^{2+}-activated potassium channels (Wolfart and Roeper, 2002). Similarly, low threshold calcium currents through T-type calcium channels at the distal dendrites were responsible for bursting properties of thalamic reticular cells (Destexhe et al 1996). Ca^{2+} currents have been implicated in cortical pyramidal cell bursting also (Rhodes and Gray, 1994; Wang, 1998; Kole et al. 2007), where layer V pyramidal cell bursting is dependent on a large influx of Ca^{2+} at the apical dendrites (Helmchen et al. 1999). Furthermore, IB cell bursting is thought to be modulated by the cell's resting membrane potential, which is itself modulated by Ca^{2+}-activated potassium conductance (Wang and McCormick, 1993). It is thought that IB neurons mature postnatally in line with increased deposition of Ca^{2+}-activated potassium channels in the somatosensory cortex (Franceschetti et al. 1993).

1.5.4 Calcium ions in neuronal signalling

Calcium ions (Ca^{2+}) act as second messenger molecules that activate various binding partners and induce a plethora of signal transduction pathways that are vital to each cell's function. Given the involvement of calcium signalling in so many cellular processes, Ca^{2+} homeostasis must be precisely controlled to ensure survival of the cell and tissue. In excitable cells, Ca^{2+} signalling helps convey information regarding membrane depolarisation and synaptic activity to the cell's biochemical machinery. One such process in which this occurs is the release of neurotransmitters from the synaptic terminal following the arrival of an action potential: voltage-gated calcium channels (VGCCs) are activated upon membrane depolarisation, causing an influx of Ca^{2+} which in turn activates the quantal release of neurotransmitters from synaptic vesicles via the binding of Ca^{2+} to synaptotagmin (Südhof, 2012). In neuronal cell populations, the extracellular Ca^{2+} concentration is approximately 10,000 fold higher than the intracellular concentration: ~1mM vs ~100nM respectively (Gleichmann & Mattson, 2011). This results in a large influx of Ca^{2+} when plasma membrane channels are opened, and requires the action of several ATPase channels to pump Ca^{2+} out of the cytoplasm when the need for calcium signalling has ended, in order to restore the original concentration gradient. Therefore, calcium signalling is a high energy-demanding process, another reason why it must be tightly regulated.

Within the neuron there are several locations where the intracellular levels of Ca^{2+} can be regulated (see Fig. 1.7 for a complimentary schematic). Firstly, Ca^{2+} can enter and leave the cell through specialised channels at the plasma membrane. Depolarisation-induced calcium entry occurs at the sight of VGCCs, and allows Ca^{2+} to flow into the cell down its electrochemical gradient. This happens during the repolarisation phase of an action potential, and leads to the initiation of activity-dependent signalling within the cell, including regulation of gene expression (Brosenitsch and Katz, 2001) and trafficking neurotransmitter receptors to and from the plasma membrane (Hayashi et al. 2000). Increases in Ca^{2+} at this point activates calcium-dependent potassium channels, which initiate potassium ion (K^{+}) conductances that shape the afterhyperpolarisation (AHP) phases of the action potential (Hoston and Prince, 1980). Ca^{2+} can also enter the postsynaptic terminal via the activation of several glutamate receptors, both ionotropic and metabotropic. Due to the large transmembrane electrochemical gradient that drives Ca^{2+} into the cell, calcium ions have to be extruded from the cytosol through the plasma membrane Ca^{2+}-ATPase (PMCA) pump. This process occurs at the expense of one ATP molecule, and can be activated by the binding of calmodulin. Since calmodulin is activated by Ca^{2+}, this is a mechanism whereby increased Ca^{2+} signalling negatively

regulates itself by inducing the extrusion of Ca^{2+} from the cell (Monesterolo et al. 2008). Ca^{2+} can also be removed from the cytosol indirectly by the activity of the Na^{+}/Ca^{2+} exchanger (NCX) channel which exchanges three Na^{2+} ions for one Ca^{2+} ion.

Neuronal Ca^{2+} modulation can also occur when Ca^{2+} is taken up or released from the endoplasmic reticulum (ER). The ability of cells to take up extracellular Ca^{2+} and sequester it away into these organelles is an evolutionarily-advanced property that provides a buffering mechanism whereby intracellular Ca^{2+} levels can be increased and decreased when needed irrespective of changes to extracellular ion concentrations (Koch, 1990). Ca^{2+} is taken up into the ER via the sarco/endoplasmic reticulum Ca^{2+}-ATPase (SERCA) pump, which is structurally similar to the PMCA pump, but differs in several features including that it transports two Ca^{2+} across the ER membrane and hydrolyses one ATP molecule in the process. This makes the SERCA pump metabolically more efficient at lowering intracellular Ca^{2+} levels than the PMCA pump. The concentration of Ca^{2+} in the ER is much higher than in the cytosol (~500μM; Vandecaetsbeek et al. 2011), which generates the luminal environment necessary for enzymatic activity relating to localised cellular functions (Wuytack and Missiaen, 2002). Ca^{2+} is released from the ER following the binding of inositol triphosphate (IP_3) to its receptor on the ER membrane, or through ryanodine receptors (RyRs) that are activated by Ca^{2+} entry through VGCCs at the plasma membrane via the process of calcium-induces calcium release.

Finally, Ca^{2+} can also be stored and released from the mitochondria. Ca^{2+} is transported into the mitochondrial matrix via the mitochondrial Ca^{2+} uniporter. This serves not only to reduce the intracellular Ca^{2+} concentration, but also to increase the activity of the three main enzymes involved in the TCA cycle (Brini et al. 2014). Therefore, Ca^{2+} storage makes the mitochondria more efficient at producing ATP and increases the cell's energy output. Ca^{2+} can be extruded from the mitochondria via NCX channels, the mitochondrial Ca^{2+} proton exchanger channel, or following the opening of the mitochondrial permeability transition pore.

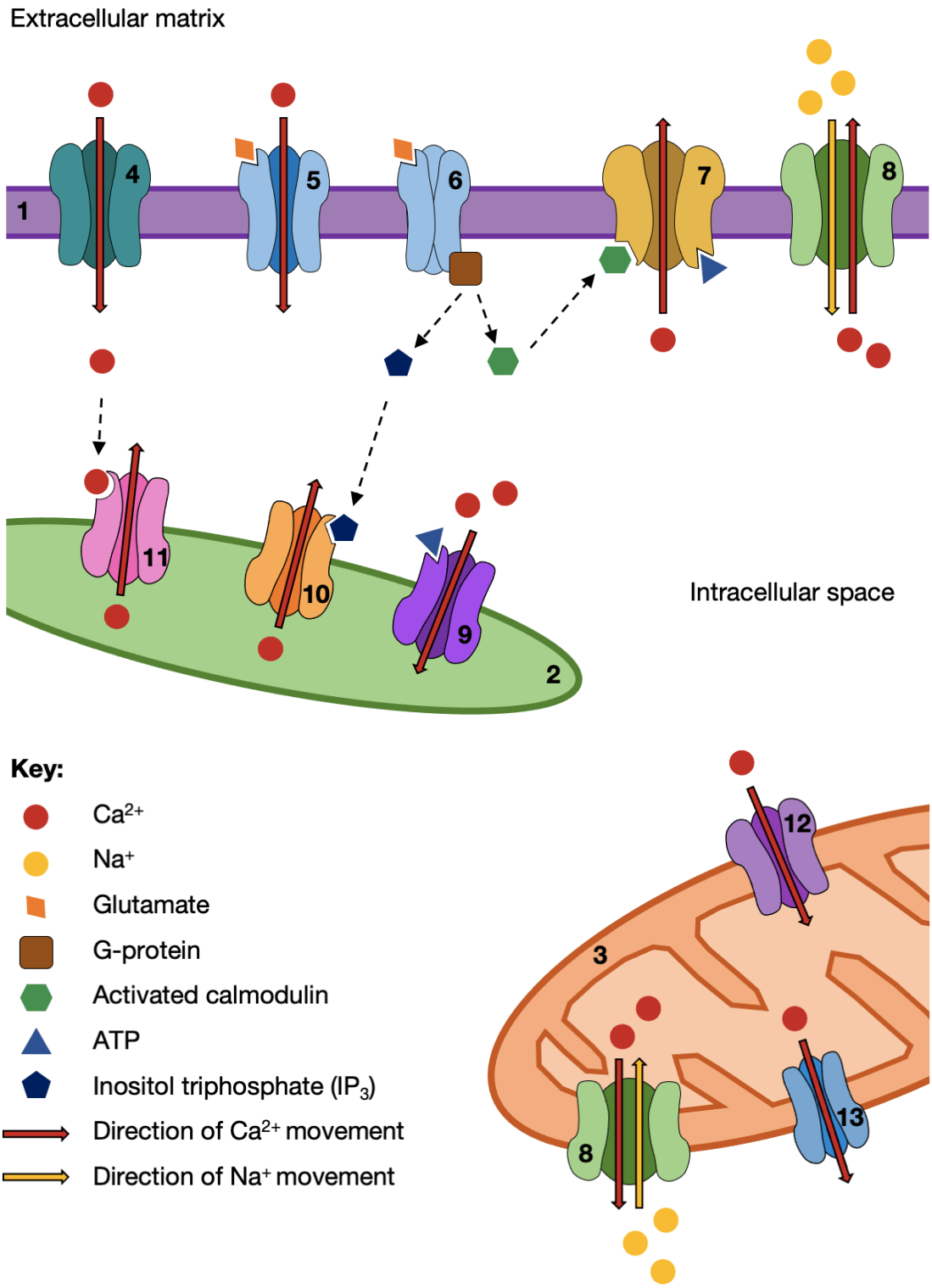

Figure 1.7: Calcium regulation in neurons. Schematic diagram depicting the mechanisms by which intracellular (cytosolic) calcium concentration can be increased or decreased through movement across the plasma (1), endoplasmic reticulum (ER; 2) or mitochondrial (3) membranes. Ca^{2+} enters the cell through the plasma membrane via the depolarization-induced activation of voltage-gated calcium channels (VGCCs; 4), or via the activation of ionotropic glutamate receptors (5). Activation of metabotropic (GPCR) glutamate receptors (6) leads to the production of calmodulin and IP_3. The

plasma membrane calcium ATPase (PMCA; 7) removes Ca^{2+} from the cytoplasm and can be activated by calmodulin. Ca^{2+} can also leave the neuron via the Na^{+} / Ca^{2+} exchanger channel (NCX; 8). On the ER membrane, the sarco-endoplasmic reticulum calcium ATPase (SERCA; 9) pumps two Ca^{2+} into the lumen of the ER at the expense of one ATP molecule. Ca^{2+} is released from the ER via the activation of IP_3 receptors (10) or the opening of ryanodine receptors (RyRs; 11) via the process of calcium-induced calcium release. Finally, at the mitochondrial membrane, Ca^{2+} is pumped into the mitochondria via the Ca^{2+} uniporter (12) and leaves the mitochondria via NCX channels (8) or the mitochondrial permeability transition pore (13).

1.5.4.1 Voltage-gated calcium channels (VGCCs)

There are several known variants of the VGCC, that are structurally and functionally distinct from each other, and are expressed in different cell and tissue types to fulfil these functions. N-type VGCCs are named the “neuronal” type because they are exclusively expressed in neurons, though they have been found in both the central and peripheral nervous system (Witcher et al. 1993; Molderings et al. 2000; Sann et al. 2008). N-type channels are primarily found at the neuronal presynaptic terminal where they function in coordinating NT release through the binding of syntaxin (Lipscombe et al. 1989; Sheng et al. 1994; Mochida et al. 1996), however these channels are also expressed at the neuronal soma and dendritic spines (Mills et al. 1994; Jones et al. 1997). The majority of literature regarding N-type VGCCs speaks of their role in initiating the release of synaptic vesicles, however there is also evidence for a role in modulating synaptic growth at the presynapse (Rieckhof et al. 2003), in regulating LTP and LTD at the dendritic postsynaptic membrane (Normann et al. 2000; Ahmed and Siegebaum, 2009), in controlling neurite outgrowth in the peripheral nervous system (Sann et al. 2008) and in directing the migration of immature neurons during development (Komuro and Rakic, 1992). These channels have a high-voltage threshold for Ca^{2+}-conductance, meaning they only open when the plasma membrane is significantly depolarised (Helton et al. 2005).

L-type VGCCs have a high-voltage threshold for opening, though they open at lower membrane potentials compared to N-type channels (Helton et al. 2005). L-type VGCCs are named due to their long-lasting period of activation: they open quickly and the slow kinetics that lead to channel inactivation means that Ca^{2+}-conductance persists for a long time (Helton et al. 2005). These channels can be found outside the nervous system,

in myocytes and cardiomyocytes where they are located at the membrane of T-tubules and aid muscle contraction through excitation-contraction coupling (Tanabe et al. 1988; Tanabe et al. 1990), and in endocrine cells where they regulate hormone release (Ashcroft et al. 1994). In neurons, L-type VGCCs are involved in depolarisation-induced Ca^{2+} influx during the latter stages of an action potential, and increases in Ca^{2+} concentration via these channels regulate neuronal excitability (Gamelli et al. 2011; Moore and Murphy, 2020), LTP (Weisskopf et al. 1999), LTD (Christie et al. 1997; Lei et al. 2003), gene expression (Graef et al. 1999; Weick et al. 2003) and cellular survival (Galli et al. 1995; Marshall et al. 2003).

Compared to the L-type channel, T-type VGCCs are termed “transient” because of their low-voltage threshold for activation and their fast voltage-dependent inactivation (Randall and Tsien, 1997; Perez-Reyes et al. 1998). They are activated at more negative membrane potentials compared to other VGCCs, and are required for the repetitive firing of action potentials in cells that require rhythmic firing patterns. They are most prevalent in myocardiocytes and thalamic neurons (Perez-Reyes, 2003).

R-type VGCCs have an intermediate-to-high voltage threshold for activation and have been located in many regions throughout the brain, including the cortex, hippocampus, striatum and amygdala, at presynaptic, postsynaptic and somatic locations (Parajuli et al. 2012). Interestingly, R-type VGCCs have been shown to be resistant to most known drugs that block other forms of VGCC, and hence these channel types were termed “residual” as they account for the residual calcium current following the application of the selective VGCCs channel toxins. These channels are thought to be involved in presynaptic LTP (Myoga and Regehr, 2011), and contribute to fast excitatory synaptic transmission (Gasparini et al. 2001).

1.5.5 Changes in neuronal connectivity in RTT

Despite the severe neurological abnormalities seen in both RTT patients and animal models, evidence for overt changes in neuroanatomy of MeCP2-deficient brains is minimal. This led to the theory that the neurological symptoms seen in RTT are more likely a result of changes at the cellular and subcellular level, which alter neuronal connectivity within the network. Consistent with this idea are the findings that cortical and hippocampal neuronal populations in *Mecp2*-deficient mice exhibit hyperexcitability and seizure-like activity (Calfa et al. 2011; Zhang et al. 2014), which is indicative of

alterations in neuronal connectivity and a shift in the balance of excitatory and inhibitory input into the system.

As a means of assessing neuronal connectivity, several studies have measured event-related potentials (ERPs): neurological responses that occur as a result of sensory stimulation that manifest as isolated deflections in EEG and other forms of recordings. In RTT patients and the associated mouse models, both visual and auditory ERPs are attenuated, with smaller ERP amplitude and longer ERP latency (Stauder et al. 2006; LeBlanc et al. 2015; Key et al. 2019; Dong et al. 2020). In *Mecp2*^{T158A} mice, auditory brain stem responses were unaffected with respect to WT animals, as is the case with *Mecp2*-null mice too (Goffin et al. 2011). This preservation of brain stem function suggests that loss of MeCP2 affects cortical processing of sensory information, and leaves hearing abilities intact. Interestingly, auditory ERPs in a mouse model where MeCP2 was lost from only forebrain GABAergic interneurons revealed significantly reduced ERP power, while preservation of MeCP2 function in these cells alone was sufficient to maintain ERP responses (Goffin et al. 2014). Furthermore, loss of MeCP2 function only from forebrain GABAergic interneurons resulted in cortical hyperexcitability, as well as both behavioural and electrophysiological seizures. Together these findings suggest that MeCP2 maintains cortical circuitry by influencing inhibitory cells within the network.

In a post-mortem study of brains from RTT patients, pyramidal cells in the cortex exhibited fewer dendritic aborisations, with shorter and less complex branching structures compared to non-RTT pyramidal cells (Armstrong et al. 1995). Both apical and basal dendritic spines appeared to be affected across multiple regions of the cortex and multiple layers within the cortical column. In support of this, activation of MeCP2 via phosphorylation was shown to mediate dendritic patterning and induce spine development (Zhou et al. 2006). Furthermore, MeCP2 has previously been implicated in aiding cellular maturation in post-migratory neurons, which included regulating dendritic branching, rather than in deciding cell fate (Kishi and Macklis, 2004). Interestingly, dendritic spine morphology changes also occur in layer V pyramidal cells of the somatosensory cortex in a MeCP2-duplication syndrome model (Jiang et al. 2013), suggesting that MeCP2 levels must be tightly controlled for normal dendritic morphology.

Fewer and shorter dendritic spines in the brains of RTT patients is indicative of reduced synaptic connectivity, and a number of electrophysiological studies have provided evidence to back this up. Spontaneous firing of layer V RS pyramidal neurons from the

S1 cortex was significantly reduced in *Mecp2*-null brain slices compared to WT, although the intrinsic properties of these excitatory neurons was not altered (Dani et al. 2005). These findings were attributed to alterations in the balance of excitatory and inhibitory drive onto these cells: total excitation was reduced, with smaller EPSP amplitudes, while total inhibition was increased. Similar findings have also been reported in *Mecp2*-deficient hippocampal cultured neurons (Nelson et al. 2006), but whether these changes were a direct result of impaired synaptic connectivity remained unclear. Further research again using layer V RS pyramidal cells from the S1 cortex revealed weaker excitatory synapses in this microcircuit due to reduced quantal release at these sights (Dani and Nelson, 2009). In cultured hippocampal cells, loss of MeCP2 resulted in significantly reduced synaptic responses, whereas a two-fold overexpression line exhibited increased responses, and these changes were directly attributed to the number of synaptic connections formed (Chao et al. 2007).

Interestingly, despite the observed deficits in synaptic connectivity, the mechanisms that underlie LTP are preserved in *Mecp2*-null pyramidal cell microcircuits (Dani and Nelson, 2009). However, given that the induction of LTP is dependent on the strength of synaptic connectivity, LTP deficits are consistently seen in *Mecp2*-null mouse models. Both high-frequency tetanic stimulation and theta-burst stimulation failed to induce the quantity of synaptic potentiation needed to induce LTP in both hippocampal and cortical regions, consistent with smaller average length of postsynaptic densities, and poor performance on a hippocampus-dependent spatial memory task (Moretti et al. 2006). Short term synaptic plasticity was also significantly attenuated following loss of MeCP2 through the assessment of paired-pulse facilitation (Weng et al. 2011). The effect of MeCP2 overexpression on learning and memory remains elusive, with some research showing an enhancement of LTP (Collins et al. 2004), and other showing the opposite (Na et al. 2012). Overall, these findings suggest that optimal expression of MeCP2, while not involved in neuronal differentiation or cellular longevity, is important for the maintenance of subcellular structures that promote healthy network connectivity and aid the processes of synaptic plasticity during learning and memory.

Synaptic plasticity is itself a mechanism involved in development of the brain, as wiring and rewiring neuronal circuits is important for network formation, particularly in the early stages of life. Indeed, experience-dependent plasticity during the critical period of visual cortex development is significantly attenuated in *Mecp2*-null mice (Krishnan et al. 2015), owing to the accelerated maturation of inhibitory networks that prematurely close the window of plasticity. The fact that RTT-like symptoms in *Mecp2*-deficient animal models

begin to emerge during a period of development where synaptic plasticity is crucial (Lohmann and Kessels, 2014) suggests that MeCP2-related deficits in synaptic plasticity may play a role in the presentation of RTT-like features in these animals.

1.6 Aims and objectives

I have thus far given an overview of the current understanding of MeCP2-related disorders, sleep disturbances, and the electrophysiology, neurobiology and neuroanatomy relating to sleep and sleep-related behaviours. By studying the electrophysiological patterns of sleep-related brain rhythms in a mouse model of RTT, this project aims to determine the effect of loss of MeCP2 function on these neuronal networks, and better understand how sleep disturbance behaviours in RTT arise. Specifically, there are four main aims:

Aim 1: To establish whether loss of MeCP2 affects the generation of delta oscillations in isolated brain slices.

Aim 2: To determine whether loss of MeCP2 affects the function of intrinsically bursting neurons in layer V of the somatosensory cortex.

Aim 3: To establish whether pharmacological inhibition of voltage-gated Ca^{2+} channels can rescue cortical delta oscillations in isolated brain slices.

Aim 4: To determine whether loss of MeCP2 affects the generation of sleep-related neuronal oscillations in the cortex and hippocampus *in vivo*.

Chapter 2 – Materials and methods

2.1 *Mecp2*-Stop mice

All animals in this project were from the same mouse model of RTT, whereby the endogenous *Mecp2* gene was silenced via the insertion of a lox-Stop cassette, generating *Mecp2*$^{Stop/y}$ and *Mecp2*$^{Stop/+}$ mice (Guy et al. 2007). With acknowledgment that the coding regions for the MBD and TRD are located within exons 3 and 4 respectively, the lox-Stop cassette was inserted up-steam to these exons (Fig 2.1). As a result, premature termination of translation occurred, and a truncated, non-functional MeCP2 protein was produced (Guy et al. 2007). These mice exhibit robust RTT-like phenotypes that are similar to those observed in *Mecp2*-null mice (Guy et al. 2007; Robinson et al. 2012). Throughout the rest of this thesis, the terms *Mecp2*$^{Stop/y}$, *Mecp2*-null, and *Mecp2*-knockout (KO) are used interchangeably to refer to mutant animals.

2.1.1 Animal housing and husbandry

All mice used in this study were bred and maintained at the University of York Biological Services Facility (BSF) under standard conditions (12-hour light/dark cycle, with access to food and water *ad libitum*). Breeding cages were set-up and maintained by BSF staff: one male was placed in a cage with two dams and the resulting pups were weaned at approximately three weeks of age. Same-sex littermates were grouped housed with up to five mice per cage.

2.1.2 Licensing

All procedures were conducted in accordance with the regulations laid out by the UK Animals (Scientific Procedures) Act, 1986, and all appropriate project and personal licenses were granted by the UK Home Office and obtained prior to embarking on this project.

2.1.3 Genotyping

Genomic DNA was prepared from ear notch or tail snip samples from experimental animals. Tissue samples were digested overnight at 55°C in a tissue lysis buffer containing: 25 mM Tris, pH 8.0; 10 mM EDTA, pH 8.0; 1% (v/v) SDS; and 20 mg/ml proteinase K. Protein precipitation occurred by adding 7.5M ammonium acetate followed by centrifugation. The resulting supernatant was decanted into a fresh tube,

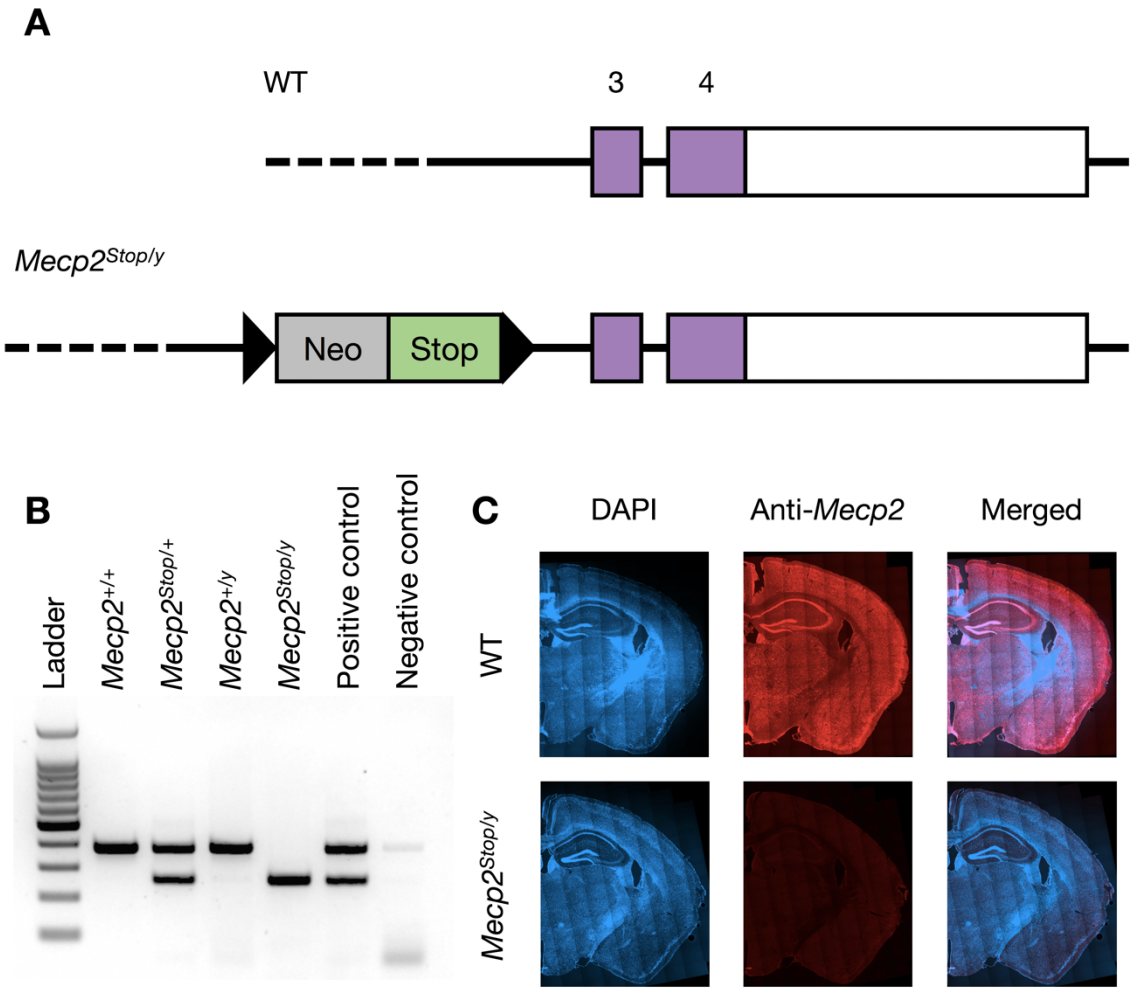

Figure 2.1: *Mecp2*$^{Stop/y}$ mouse model. (A) Figure adapted from Guy et al 2007. Schematic diagram of the endogenous *Mecp2* gene highlighting exons 3 and 4 (purple boxes) and part of the 3' untranslated region (white box). The Neo-Stop cassette is inserted upstream of exon 3. **(B)** Example image from genotyping protocols confirming genetic knockout of *Mecp*2 in mutant animals. Upper band: WT allele, 379 bp; lower band: mutant allele, 222 bp. Image shows 100 base-pair ladder (left) then: WT female, heterozygous female, WT male, hemizygous male, positive control, negative (H_2O) control. **(C)** Example images from immunohistochemistry assay confirming loss of MeCP2 protein in male *Mecp2*-null mice. Images show WT (upper panels) and *Mecp2*$^{Stop/y}$ (lower panels). Left: DAPI; middle: anti-MeCP2; right: merged.

---

where DNA was precipitated with isopropanol and pelleted by centrifugation. DNA was washed with 70% (v/v) ethanol, pelleted by centrifugation, and rehydrated in ddH_2O at 65°C for 1 hour. Genomic DNA was stored at 4°C until use.

PCR amplification of genomic DNA was performed using the following primers: 5'-AAC AGT GCC AGC TGC TCT TC-3', 5'-CTG TAT CCT TGG GTC AAG CTG-3', 5'-GCC AGA GGC CAC TTG TGT AG-3', and under the following protocol: template denaturation at 94°C for 30 seconds, primer annealing at 60°C for 30 seconds, extension phase at 72°C for 60 seconds, repeated 32 times. PCR products were run on a 2% agarose in 1x TAE buffer gel (which also contained SYBR-safe for DNA detection), and separated by gel electrophoresis at ~180 V for 30 minutes. The gel was then visualised using a Gel Doc EZ Imager (Bio Rad, UK) and Image Lab 5.2.1 software (Bio Rad, UK). Fig 2.1 B shows the expected PCR results from both WT and mutant animals. The WT band is 379 bp long while the mutant band is 222 bp, resulting in the mutant band moving faster than the WT band during electrophoresis. Female mutants are heterozygous, while male mutants are hemizygous. DNA extraction and PCR was completed twice per animal to provide full confidence that genotype assessment was current: firstly at the point of weaning from ear snip tissue samples and secondly post-experimentally from tail snip tissue samples.

2.1.4 Immunohistochemistry

Immunohistochemistry (IHC) was performed for two purposes in this project: for additional confirmation of genetic model knockout and for confirmation of electrode localisation in *in vivo* experiments (see Chapter 2.4.6). Below is the full IHC protocol for staining for MeCP2 to confirm the genetic knock-out in the $Mepc2^{Stop/y}$ model.

Preparation of brain tissue for IHC followed the same anaesthesia and surgical procedures as those detailed in Chapter 2.3, with the exception that the catheter here was used to perfuse the circulatory system with 4% paraformaldehyde (PFA) instead of sucrose-based artificial cerebrospinal fluid (sACSF; see Chapter 2.2). PFA is a fixative and therefore terminates any ongoing biochemical reactions within cells, preserving the sample in its natural form and with little damage from autolysis. PFA also helps to increase the structural integrity of the brain making it easier to manipulate in the following steps without damaging the tissue. The dissected brain tissue was immersed immediately in 4% PFA for 24 hours, after which it was transferred to a 30% sucrose solution for a further 24 hours. Brain tissue was embedded in O.C.T. compound and placed immediately into -80 °C. Once frozen solid, the embedded tissue was sliced into 40 µm thick coronal sections using a cryostat (Leica CM1900), placed into a solution of phosphate buffer (PB, 80.5 mM K_2HPO_4, 19.5 mM NaH_2PO_4) and 0.005% sodium azide, and stored at 4°C.

Sections were washed in phosphate buffer saline (PBS, diluted from 10X stock to 1X working solution), and then soaked in a solution of PBS and 0.2% Triton to permeabilise the cellular membrane. 10% methanol was used to permeabilise the nuclear membrane, which would allow antibodies to enter the nucleus during the staining processes. Non-specific binding was blocked using 3% (v/v) normal goat serum (NGS) for one hour at room temperature, and then incubated overnight at 4°C with a rabbit anti-MeCP2 primary antibody (1:1000 dilution; Zhou et al. 2006) diluted in PBS containing 1% (v/v) NGS and 0.1% (w/v) sodium azide. The following day, sections were washed three times in PBS for 5 minutes, and then incubated for two hours at room temperature with an anti-rabbit Alexa595 secondary antibody (Invitrogen) diluted in PBS containing 1% (v/v) NGS. Sections were washed again in PBS, briefly incubated with Hoechst 33342 (2 $\mu g.ml^{-1}$ in PBS), washed with PBS, then with PB, and finally mounted on microscope slides with fluoromount. Samples were imaged using a slide scanner (Zeiss Axio Scan.Z1) at the Bioscience Technology Facility at the University of York, and visualised using Zen (Zen Digital Imagine, Zeiss).

2.2 Solutions and Drugs

Table 2.1 lists all chemicals, compounds and pharmacological agents used in this project. Drugs were dissolved in double-distilled H_2O wherever possible, and in dimethyl sulfoxide where solutes were insoluble in H_2O. Stock solutions were stored according to the instructions given by the supplier. During *in vitro* protocols, drugs were introduced to the brain tissue via direct application to the 50 ml of nACSF circulating through the recording chamber. During *in vivo* protocols and surgical procedures, drugs were administered through injection as described.

Table 2.1: List of chemicals, compounds and pharmacological agents

Chemical / compound	**Supplier**
Agarose	Melford, Suffolk, UK
Ammonium acetate	Sigma-Aldrich Ltd., Dorset, UK
Calcium chloride	Sigma-Aldrich Ltd., Dorset, UK
Dimethyl sulfoxide (99.9%)	Sigma-Aldrich Ltd., Dorset, UK
Dipotassium phosphate	Thermo-Fisher Scientific Ltd., Leicestershire, UK

EDTA	Thermo-Fisher Scientific Ltd., Leicestershire, UK
EGTA	Sigma-Aldrich Ltd., Dorset, UK
Ethanol	VWR International Ltd., Leicestershire, UK
Fluoromount	Sigma-Aldrich Ltd., Dorset, UK
Glucose	Thermo-Fisher Scientific Ltd., Leicestershire, UK
Hoechst 33342	Tocris Biosciences Ltd., Bristol, UK
Isopropanol	Sigma-Aldrich Ltd., Dorset, UK
Magnesium sulfate	Thermo-Fisher Scientific Ltd., Leicestershire, UK
Methanol	Sigma-Aldrich Ltd., Dorset, UK
OCT Compound	VWR International Ltd., Leicestershire, UK
Paraformaldehyde (4%)	Thermo-Fisher Scientific Ltd., Leicestershire, UK
Phosphate buffer saline (10x)	Thermo-Fisher Scientific Ltd., Leicestershire, UK
Potassium acetate	VWR International Ltd., Leicestershire, UK
Potassium chloride	Thermo-Fisher Scientific Ltd., Leicestershire, UK
SDS solution (20% w/v)	Bio-Rad, California, USA
Sodium azide	Thermo-Fisher Scientific Ltd., Leicestershire, UK
Sodium bicarbonate	Sigma-Aldrich Ltd., Dorset, UK
Sodium chloride	Thermo-Fisher Scientific Ltd., Leicestershire, UK
Sodium dihydrogen phosphate	Thermo-Fisher Scientific Ltd., Leicestershire, UK
Sucrose	Thermo-Fisher Scientific Ltd., Leicestershire, UK
TAE (50x)	Thermo-Fisher Scientific Ltd., Leicestershire, UK
Triton	Sigma-Aldrich Ltd., Dorset, UK

Pharmacological agent	Supplier	Stock concentration	Working concentration
Amlodipine	Tocris Biosciences Ltd., Bristol, UK	4 mM	4 μM
Bupravet (Buprenorphine)	Virbac, UK	0.5 $mg.ml^{-1}$	0.1 $mg.kg^{-1}$
Carbamylcholine chloride (Carbachol, or CCH)	Tocris Biosciences Ltd., Bristol, UK	10 mM	4 μM
Cyclopiazonic acid	Tocris Biosciences Ltd., Bristol, UK	20 mM	20 μM
Isoflurane (Vetflurane)	Virbac, UK	1000 $mg.ml^{-1}$	
Ketavet (Ketamine)	Zoetis Ltd, UK	100 $mg.ml^{-1}$	100 $mg.kg^{-1}$
Nifedipine	Tocris Biosciences Ltd., Bristol, UK	100 mM	20 μM
NNC 55-0396	Tocris Biosciences Ltd., Bristol, UK	10 mM	4 μM
Rimadyl (Carprofen)	Zoetis Ltd, UK	50 $mg.ml^{-1}$	5 $mg.kg^{-1}$
Rompun (Xylazine)	Bayer, UK	20 $mg.ml^{-1}$	12.5 $mg.kg^{-1}$
SCH-23390 hydrochloride	Tocris Biosciences Ltd., Bristol, UK	10 mM	10 μM
SNX-482	Tocris Biosciences Ltd., Bristol, UK	3 μM	3 nM

2.3 Isolated slice electrophysiology

2.3.1 Anaesthesia and surgical procedures

Male mice were selected for experimentation based on age and genotype. Adult male mice (approximately 60 days) or juvenile mice (maximum 28 days) were placed in a bell jar and exposed to the anaesthetic isoflurane via inhalation at a concentration sufficient to abolish the righting reflex. This was followed by an intraperitoneal injection of 100 $mg.kg^{-1}$ ketamine and 12.5 $mg.kg^{-1}$ xylazine. Sensory responses were assessed via pedal withdrawal and corneal reflex until all reflexes had been completely abolished. Next, the skin of the abdomen was cut open to reveal the thoracic cavity, where the ribs were removed to expose the heart. A catheter was inserted into the left ventricle of the heart, followed by an incision in the right atrium. The circulatory system was then perfused with approximately 30 ml of ice-cold, oxygenated sucrose-based artificial cerebrospinal fluid (sACSF), via the catheter at a rate of approximately 1 $ml.s^{-1}$. sACSF contained the following: 252 mM sucrose, 3 mM KCl, 1.25 mM NaH_2PO_4, 24 mM $NaHCO_3$, 2 mM $MgSO_4.7H_2O$, 2mM $CaCl_2$ and 10 mM glucose. This solution was used for intracardial perfusion as it improves the viability and longevity of neurons in the resulting brain slices. Through a low NaCl concentration and high sucrose content, this solution prevents the entry of sodium and chloride ions into the cells, therefore minimising the associated effects of swelling and cell lysis, which can be toxic to neurons (Aghajanian and Rasmussen 1989, Ting et al 2014). Once the intracardial perfusion was complete, the spinal cord was severed via decapitation at the neck. An incision was made along the midline of the top of the head to reveal the skull, which was cut along the midline in a caudal to rostral direction and then removed, along with the dura, to expose the brain. The brain was then excised and immediately immersed in ice-cold oxygenated sACSF.

2.3.2 Preparation of neocortical brain slices

The brain tissue was cut using a scalpel blade according to which type of brain slices were required (see below), and then glued to the plate of a Leica VT1000 Vibratome (Leica Microsystems LTD, Milton Keynes, UK), which was placed into the cutting chamber and re-submerged in ice-cold oxygenated sACSF, ready for slicing. Neocortical slices were cut to a thickness of 450 μm. This thickness was chosen as it is thin enough to allow sufficient oxygenation of all cells in the resulting brain slice while still being thick enough to preserve the integrity of the local neuronal circuits required to induce oscillatory activity. Referencing visual aids to a mouse brain atlas (Paxinos & Franklin, 2001) was used to identify slices that contained the correct regions of primary

somatosensory cortex (see Fig. 2.2). Approximately three full slices were obtained per brain, resulting in six individual isolated neocortical tissue slices.

2.3.2.1 Coronal sections

Brain tissue was trimmed along the coronal plane, removing the cerebellum and creating a flat cut edge at the caudal end of the brain. The brain was then immediately glued down with this fresh edge against the surface of the vibratome plate, such that the frontal cortex was pointing upwards. 450 µm thick slices were taken along the coronal plane, with the blade cutting through more dorsal brain tissues first. Once slicing was finished, coronal slices were trimmed such that they contained only somatosensory neocortex and no other brain tissue (see Fig. 2.2).

2.3.2.2 Thalamocortical sections

Similar to coronal slices, preparation of thalamocortical slices also began with removal of the cerebellum. A second cut was then performed along the sagittal axis through the midline, producing two separate hemispheres of the brain. Each hemisphere was then cut along the thalamocortical plane (Agmon and Connors, 1991) and promptly glued to the vibratome plate with the fresh cut flat to the vibratome plate. The resulting slices from this method of preparation are cut on a specific angle so that they not only contain both the ventrobasal nucleus of the thalamus and the somatosensory cortex, but also maintain viable connections between these two brain regions (see Fig. 2.2). These connections would have been severed if the brain had been sliced along more traditional planes (ie coronal, horizontal or sagittal).

2.3.3 Maintenance of brain slices

Once slicing was complete, brain slices were transferred to a holding chamber containing normal artificial cerebrospinal fluid (nACSF) where they were allowed to acclimate for at least one hour at room temperature at the interface between oxygenated nACSF and carbogen gas (95% O_2: 5% CO_2). nACSF contained the following: 126 mM NaCl, 3 mM KCl, 1.25 mM NaH_2PO_4, 24 mM $NaHCO_3$, 1 mM $MgSO_4.7H_20$, 1.2 mM $CaCl_2$, and 10 mM glucose. This solution increases the intrinsic excitability of neurons within the brain slice: reducing the $MgSO_4$ (and therefore Mg^{2+}) concentration relieved the magnesium block imposed on NMDA-receptors (Nowak et al. 1984), while reducing $CaCl_2$ (and therefore Ca^{2+}) concentration increased cellular activity (Su et al. 2001). For

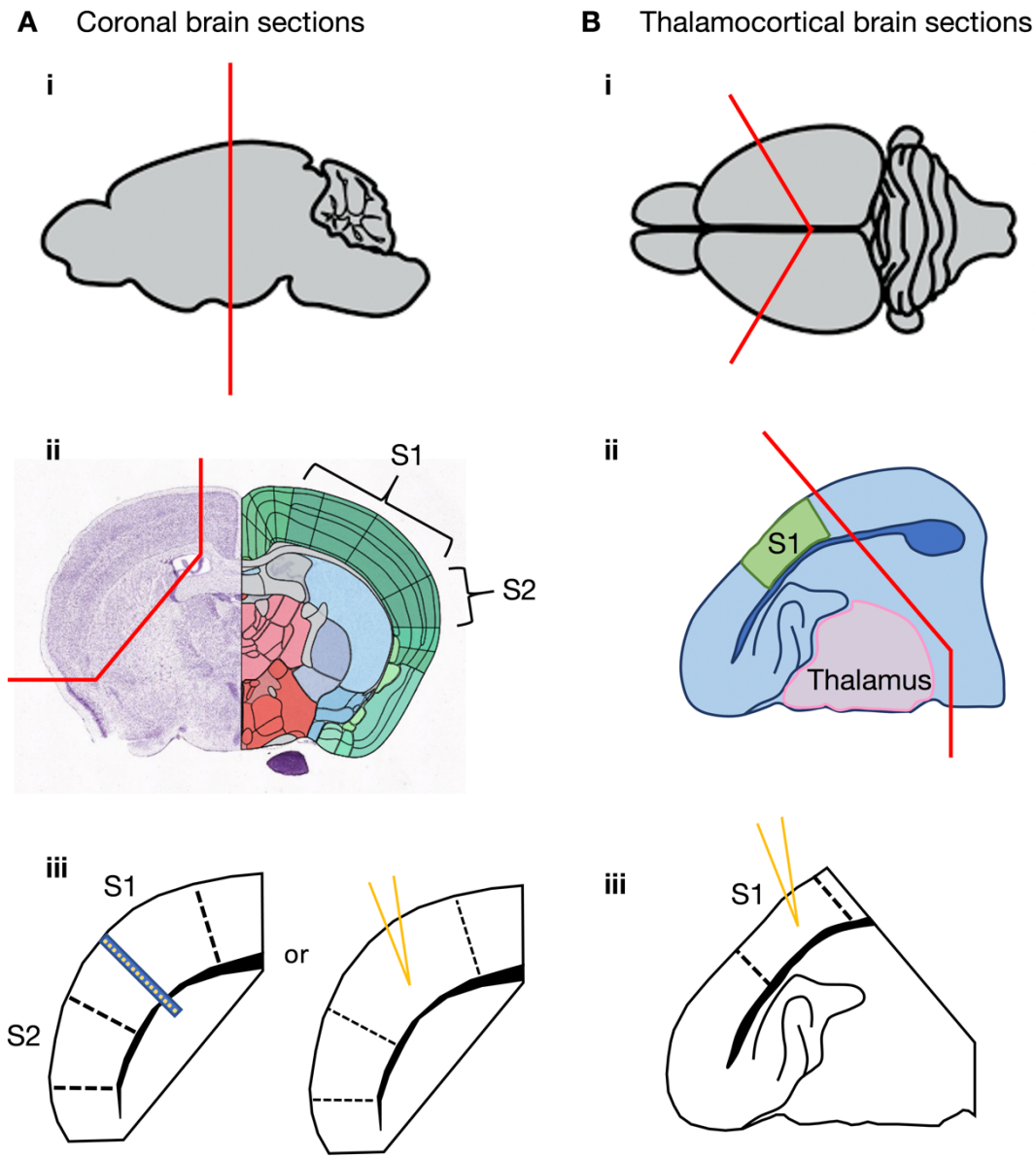

Figure 2.2: Schematic representation of brain slice preparations used in *in vitro* electrophysiological experiments. (A) Coronal slices: i) Mouse brain outline in sagittal view. Red line depicts the plane of cutting. ii) Example of a full coronal brain slice containing the cortical regions of interest (somatosensory areas). Image taken from Allen Brain Atlas, Allen Institute for Brain Science, 2021. Red lines represent incision lines to produce cortical sections (seen in iii) containing isolated somatosensory cortex. iii) left: blue rectangle represents placement of a multi-electrode array, with yellow dots representing 16 electrode contact points. iii) right: yellow arrowhead depicts the location of electrode implantation to record from layer V of the primary somatosensory cortex (S1). **(B)** Thalamocortical slices: i) Mouse brain outline viewed from above. Red lines depict the plane of cutting. ii) Schematic example of thalamocortical slice from one brain hemisphere. Red lines represent incision lines to produce thalamocortical sections (seen

in iii) containing somatosensory cortex (green) reciprocally connected to the thalamus (pink). Yellow arrow head in iii depicts the location of electrode implantation to record from layer V of the S1 somatosensory cortex.

---

experimentation, slices were transferred to a recording chamber and a peristaltic pump (Watson Marlow, UK) was used to ensure oxygenated nACSF constantly perfused over the surface of the brain tissue at a rate of approximately 1.6 $ml.min^{-1}$. The temperature of the recording chamber was set to 31°C using a water bath (Grant Instruments LTD, Cambridge, UK).

2.3.4 Extracellular recording technique

Extracellular local field potential (LFP) recordings were taken through one of two ways. Firstly, by inserting a horizontal silicon probe containing 16 micro-electrodes (100 µm spacing; Neuronexus) across the cortical column, with approximately 14 electrodes spanning the cortical column and approximately two electrodes protruding into the white matter (Fig. 2.2, A iii left). Secondly, neuronal activity local to layer V of the somatosensory cortex was recorded by inserting a micropipette (Fig. 2.2 A iii right) which was pulled from thin glass capillaries (1.2 mm outer diameter, 0.94 mm inner diameter; Harvard Apparatus, Kent, UK) and filled with the same nASCF solution as that which the slices were maintained in. A P-1000 Flaming / Brown horizontal puller (Sutter Instruments Co., California, USA) was used to pull all glass electrodes. Slice visualization was achieved using a stereo microscope and a head stage manipulator (Hs-9A, Axon Instruments) for accurate electrode positioning. For these extracellular recordings, glass electrodes had a micropipette resistance of 2 - 10 MΩ. A silver wire was passed through the centre of the glass pipette and therefore immersed in the nACSF, which facilitated the conductance of electrical signals to the amplifier electronics. Pipettes were placed in holders and attached to head stages (HS-9A, Axon Instruments) that could be finely moved through the use of micromanipulators. Electrical signals from brain slices were conducted via the silver wire, amplified (Axoclamp 900A, Axon Instruments), digitised at a 2000 Hz sampling rate (ITC018 A/D converter, HEKA Instruments), and filtered according to the following metrics: high-pass: 0.1 Hz, low-pass: 300 Hz. Electrical noise and interference was removed (Humbug, Quest Scientific), and the resulting signals were visualised and saved using Axograph (Axograph, USA).

Baseline recordings were taken from the somatosensory cortex once the tissue slices had been allowed sufficient time to acclimatise and the water bath had reached a temperature of 31°C. These recordings were taken prior to the application of any drugs which would serve as a reference by which to compare later recordings and confirm that any oscillatory activity was a direct result of the pharmacological agents that would next be applied to the system. To induce delta oscillations (0.5 – 4 Hz), a low concentration of the muscarinic and nicotinic cholinergic receptor agonist carbachol (4 μM, aka CCH) was added in conjunction with the D1-receptor antagonist SCH-23390 (10 μM). CCH was used at approximately 1/5th of the concentration that would be required to generate the neuronal activity typical of awake brain states, while suppression of dopaminergic pathways reduced the input from reward and arousal pathways which would naturally be silenced during SWS. These drug concentrations were used as they effectively mimic the idle state of the brain during SWS and have previously been shown to induce delta oscillations in rat brain slices containing somatosensory cortex (Carracedo et al. 2013). A two minute recording was taken every ten minutes following CCH and SCH-23390 application, and stable oscillations were recorded within two hours.

2.3.5 Intracellular recording technique

Intracellular recordings were taken using sharp micropipettes (75 - 150 MΩ) filled with a 2M potassium acetate solution. This is because when the neuronal cell membrane is punctured, potassium (K^+) ions will naturally flow out of the cell, therefore a high concentration of free K^+ ions in the solution within the electrode is required to replenish K^+ stores in the intracellular space. The same electrode manipulator as described before was used to track the tip of the electrode gently through the slice. A constant tuning step (-0.2 nA at 2 Hz) was applied throughout the tracking-down process, as well as a hyperpolarising holding current (-0.1 - -0.4 nA) where necessary. Piercing the cell membrane of neurons close to the electrode tip was facilitated by 'buzzing' the electrode with every tracking-down motion that was made. Cells were allowed up to 5 minutes to stabilise, in which time (if stabilisation was successful) the membrane should have formed a seal around the tip of the penetrating electrode. Holding current was reduced and eventually turned off in order to record the cell's resting membrane potential and spontaneous activity. Data was sampled at 2000 Hz, with no high-pass filter and a low-pass filter of 2 kHz. Other than that, all experimental set up was the same as that for extracellular recordings.

2.3.6 Data acquisition, processing and analysis

Data acquired using the 16-channel micro-electrode array was recorded using the Neuronexus SmartBox system, and the subsequent data was analysed using Matlab (R2018a, MathWorks). For both single channel extracellular experiments and intracellular experiments, data was acquired via Axograph (version 1.7.2, J. Clements) and analysed using Matlab (R2018a, MathWorks). Fast Fourier transformations (FFT) were used to generate power spectra, and delta oscillation peaks were identified between 0.5 - 4 Hz. Microsoft Excel (2016) and GraphPad Prism (version 8.2.1 for Windows, GraphPad Software, California USA) were used to analyse the data from these experiments and generate the appropriate figures.

2.4 *In vivo* protocols

2.4.1 Pre-surgery acclimatisation

Animals were selected for experimentation at approximately 60 days of age, on the basis that they weighed in excess of 20 g on the day of surgery. Animals were acclimated for up to one hour every day for one week prior to the start of surgical procedures. This included manual handling of the animals, and placing the home cage in the recording environment where conditions mimicked the recording setup as closely as possible.

2.4.2 Surgical techniques

On the morning of surgery, mice were given a subcutaneous injection of 5 $mg.kg^{-1}$ carprofen and 0.1 $mg.kg^{-1}$ buprenorphine, and anaesthetised with ~1.5 % isoflurane combined with 1.5 $L.min^{-1}$ O_2 throughout the procedure. Under anaesthesia, the animal's head was shaved and the skin on top of the head cut with a scalpel blade along the midline to expose the skull. Using coordinates relative to bregma, (AP: -1.7mm, ML: +/- 1.9mm) a small craniotomy was performed and a linear 16-channel single shank electrode (A1x16-3mm-100-177-H16_21mm, Neuronexus) was implanted across the entire primary somatosensory cortex and the CA1 region of the hippocampus, at an angle of 17° relative to the midline (see Fig. 2.3). Electrode sites were linearly spaced 100 µm apart, and connected to a moveable microdrive (dDrive-m, Neuronexus). Grounding and reference wires were attached to two screws implanted in the cerebellum and coated in silver paint to ensure connectivity. A third screw was implanted above the frontal plate to act as an anchor point for the head cap. The probe was lowered to a

A *In vivo* recording equipment

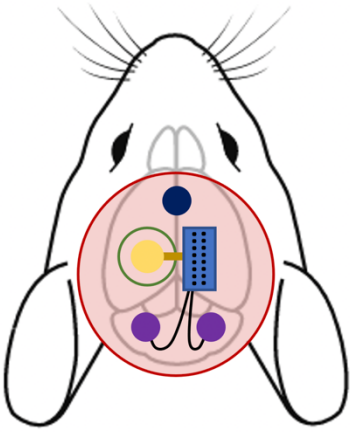

B Electrode location

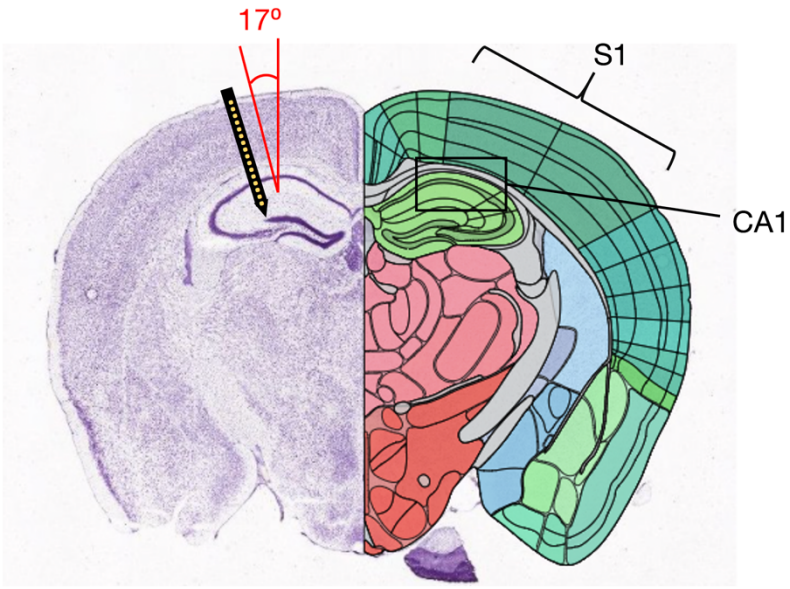

Figure 2.3: Schematic representation of recording equipment used for S1-CA1 *in vivo* experiments. (A) View of electrode set-up from above, consisting of: electrode (yellow circle) implanted following craniotomy; protective case (green) placed around and over the top of the electrode; microdrive (light blue) containing contact points for connection to recording equipment; gold wire (gold) connecting electrode to microdrive; grounding and reference wires (black) attached to silver-coated screws (purple) in the cerebellum; screw implanted above the frontal plate for anchorage (navy blue); and head cap made of dental cement (red/pink). **(B)** Electrode location (black arrow) within the brain from a coronal view. Schematic shows the position of 16 recording sites (yellow dots) spanning the length of the primary (S1) somatosensory cortex and CA1 region of the hippocampus, at an angle of 17^0 perpendicular to the midline. Image taken from Allen Brain Atlas, Allen Institute for Brain Science, 2021.

depth of approximately 1.6 mm below the surface of the brain, such that the top electrode contact point was located just below the pial surface. Finally, a head-cap was built around the microdrive, ensuring all wires and screws were covered (see Fig. 2.3).

2.4.3 Post-surgery care and acclimatisation

Following surgery, animals were individually housed to allow safe recovery, and appropriate analgesia was provided where necessary, including a further 5 $mg.kg^{-1}$ carprofen and 0.1 $mg.kg^{-1}$ buprenorphine injected subcutaneously once a day for three days post-surgery. At three days post-surgery, animals were allowed more time to acclimatise to the recording environment, this time with their head-cap connected to the recording equipment. During this time, short recordings (2 x 15 minutes) were used to ensure the probe worked properly and to identify the hippocampal pyramidal cell layer through localisation of SPW-R bursts (130 - 200 Hz), which were usually found around channel 14 (where channel 1 represents the most superficial electrode).

2.4.4 Longitudinal recordings

Five longitudinal recordings were taken per animal, approximately every other day starting from one week post-surgery. Probes were connected to a headstage (Intan RHD2000 amplifieR), and data was recorded using the SmartBox system (Neuronexus). All data was sampled at 20 kHz (high-pass filter: 0.1 Hz, low-pass filter: 10 kHz). Recordings were taken continuously for seven hours in 15 minute epoch data files, with the animal in their home cage, with the lid, food and water bottle removed to allow access and free movement of the tether, and the lights dimmed.

2.4.5 Data acquisition, processing and analysis

Analysis of data from these experiments was performed using Matlab (R2018a, MathWorks). Firstly, data was down-sampled to 1.25 kHz. Sleep-score analysis was used to identify sections of the recording when the animal was awake, in REM sleep and in NREM sleep. When high frequency oscillations correlated between the top and bottom electrodes, the animal was presumed to be moving and therefore awake - this is electromyography data. Periods of REM sleep were identified through the presence of theta oscillations (5 - 12 Hz). Broad-band slow wave oscillations were used as the main identifiable characteristic of NREM sleep, and were taken between 0.5 - 6 Hz. Spindle

frequency was identified as 9 - 17 Hz, and SPW-Rs were identified as 130 - 200 Hz. Microsoft Excel (2016) and GraphPad Prism (version 8.2.1 for Windows, GraphPad Software, California USA) were used to analyse the data from these experiments and generate the appropriate figures.

2.4.6 Electrode location confirmation

To confirm electrode localisation, animals were transcardially perfused with ice-cold 4% PFA, and the brain was carefully dissected out of the skull and away from the electrode. The brain was embedded in O.C.T., frozen and cryo-sliced (Leica CM1900) to 40 µm. Sections were stained with 2 $\mu g.ml^{-1}$ Hoechst 33342 for five minutes at room temperature and mounted onto slides. Fluorescent photomicrographs were taken using a slide scanner (Zeizz Axio Scan.Z1).

2.5 Behavioural studies

2.5.1 Pre-test acclimatisation

All behavioural tests took place in the same dimly lit room as longitudinal sleep studies. To encourage habituation to the behavioural test cage, animals were given three opportunities to become acclimated to the test cage prior to the start of the behavioural test, by placing them in the empty cage for 20 minutes at a time. For animals that were simultaneously used for *in vivo* sleep studies (see Chapter 2.4), this occurred prior to placing in the home cage for longitudinal recording, on the first, second and third day of recording. For the animals that were not undergoing simultaneous *in vivo* studies, acclimatisation took place Monday, Tuesday and Wednesday, with the encoding and recall phases (see below) taking place on Thursday and Friday respectively. The empty test cage used for acclimatisation was the same as the one used for the encoding and recall phase; a white piece of card with a large black cross was placed at one end of the cage to encourage spatial recognition during the test. Subjects were not introduced to the test objects until the start of the encoding phase.

2.5.2 Novel Location Recognition Task

The novel location recognition task used in this project is adapted from Maingret et al. (2016). The test environment consisted of a large empty cage (approximately 30 cm x

30 cm) in which a white piece of card with a large black cross was placed at one end to serve as a visual reference cue (see Fig. 2.4). The novel location recognition task consisted of an encoding phase and a recall phase, each lasting 20 minutes and separated by 24 hours (for animals used simultaneously for *in vivo* sleep studies, these occurred immediately before recordings four and five respectively). During each phase, two identical objects were placed in the test cage. Between the encoding and recall phase, one object was displaced to a new location, while the other remained in the same place (see Fig. 2.4). At the start of each test phase, animals were gently placed in the middle of the two objects. A 20 minute video recording was taken from above, to record the animals movement and exploration behaviours during the task. At the end of each test phase, the animal was moved back to their home cage.

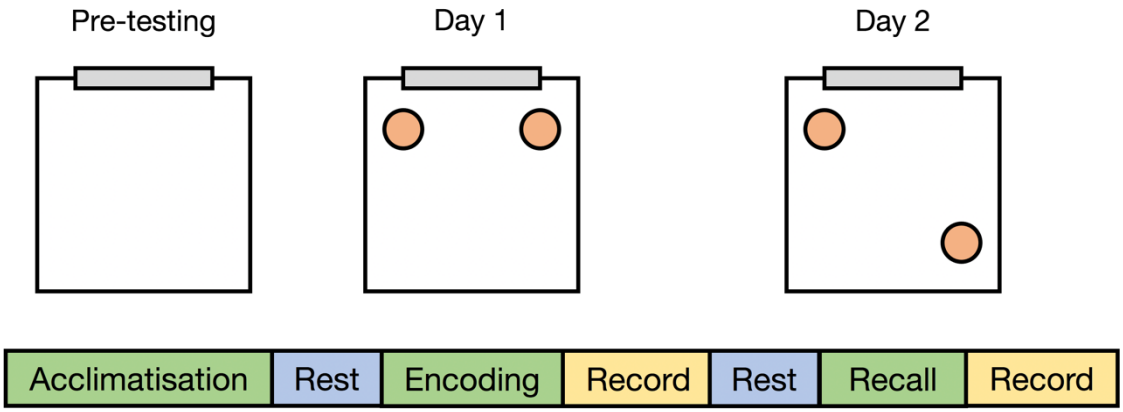

Figure 2.4: Novel location recognition task. Schematic representation of behavioural test protocol designed to assess spatial memory consolidation. Mice were allowed to acclimatise to the test cage (a clean, empty cage with a piece of white card with a black cross placed at one end, denoted by thin grey box at the top of the cage) for twenty minutes, on three occasions prior to testing. During the encoding phase, two objects (orange circles) identical in size, colour, shape and material, were placed in the test cage in the locations shown above. During the recall phase, one object (the stationary object) remained in its original location, while the other object (the displaced object) was moved. Encoding and recall phases lasted twenty minutes each and were video recorded. Between acclimatisation periods and tests, the animal was returned to their home cage.

2.5.3 Data acquisition and analysis

Video analysis of the first five minutes of each phase allowed quantification of behavioural data by assessing the number of interactions each animal had with either object and total exploration time of each object. Data from each video was then used to calculate the discrimination index. This highlights the degree to which each animal favoured the displaced object: overall time spent exploring the displaced object was divided by the total time spent exploring either object. An interaction was defined as an event lasting more than 0.5 seconds, where the animal was facing the object in close proximity, sniffing, touching or in any way exploring the object. Climbing onto the object was taken as an interaction, however once the animal stopped actively exploring the object, the interaction was deemed to have ended, even if they were still sitting on the object. Microsoft Excel (2016) and GraphPad Prism (version 8.2.1 for Windows, GraphPad Software, California USA) were used to analyse the data from these experiments and generate the appropriate figures.

Chapter 3 – Cortical and thalamocortical delta oscillations in isolated brain slices

3.1 Aims

Neocortical delta rhythms are generated in the somatosensory cortex through a network of Intrinsically Bursting (IB) pyramidal neurons located in layer V of the cortex that activate a source of $GABA_B$ receptor-mediated inhibition (Carracedo et al. 2013). Loss of MeCP2 has been previously shown to decrease excitatory input onto Regular Spiking (RS) pyramidal neurons located in layer V of the somatosensory cortex (Dani et al. 2005; Dani and Nelson, 2009). It is reasonable, therefore, to hypothesise that loss of MeCP2 function also decreases the excitability of IB neurons and impairs the generation of cortical delta rhythms. Thus, in this chapter, I will determine whether loss of MeCP2 affects cortical delta rhythms in neocortical slices containing isolated somatosensory cortex.

3.2 Results

3.2.1 Loss of MeCP2 impairs the generation of cortical delta oscillations

Cortical delta oscillations have previously been generated *in vitro* in rat brain slices containing isolated somatosensory cortex with low levels of cholinergic activation and blocking constitutive dopaminergic activity at D1 receptors – conditions thought to mimic the neuromodulatory tone of NREM sleep (Carracedo et al. 2013; Hall et al. 2018). I first wanted to determine whether I could model delta oscillations using neocortical slices from mice. To this end, I prepared cortical slices from male wild-type (WT) mice at 8 – 10 weeks of age and recorded extracellular local field potentials (LFPs) across all layers of the S1 somatosensory cortex using a horizontal, 16-electrode (100 µm spacing) silicon probe. Cortical slices were maintained in nACSF containing 4 µM carbachol (CCH) and 10 µM SCH-23390. After approximately 40 minutes, I observed the emergence of robust oscillatory activity, which reached peak power within two hours (Fig. 3.1A). Through power spectral density analysis, I show that these oscillations occurred within the 0.5 – 4 Hz delta band frequency (Fig. 3.1C and D) and exhibited

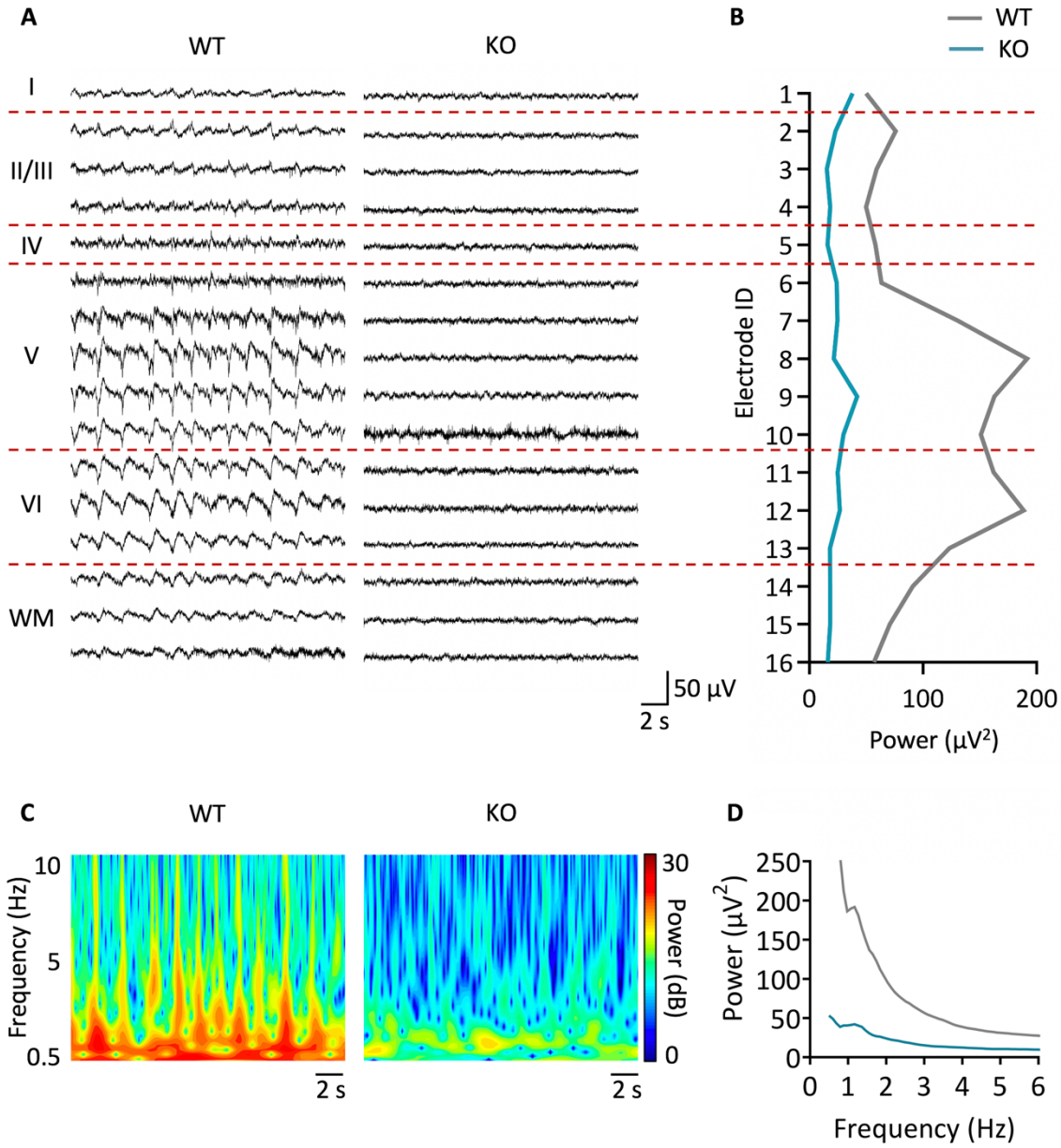

Fig. 3.1: Loss of MeCP2 impairs the generation of cortical delta oscillations across the S1 somatosensory cortex. Local field potentials (LFPs; filtered 0.3–100 Hz) were recorded across all cortical layers of the S1 somatosensory cortex using neocortical brain slices obtained from wild-type mice (WT, left) or *Mecp2*$^{Stop/y}$ (KO, right) mice. **(A)** Example LFPs from slices maintained in nACSF containing CCH (4 µM) and SCH-23390 (10 µM) for 120 minutes. The approximate positions of cortical layer boundaries are marked by horizontal red lines and each band corresponds with the label on the left: I - VI = cortical layers I - VI, WM = white matter. **(B)** Peak power of oscillations within the 0.5 – 4 Hz bandwidth recorded at each electrode position. **(C)** Wavelet-based spectrogram of LFP data shown in A. **(D)** Power spectral density of LFP data shown in A.

greatest spectral power within layers V and VI (Fig. 3.1B). I found similar results in two other WT mice (data not shown). These results demonstrate that I could generate persistent cortical delta oscillations in wild-type mice.

Next, I wanted to determine whether I could observe similar cortical delta oscillations using male *Mecp2*$^{Stop/y}$ (KO) mice at 8 – 10 weeks of age, since RTT-like phenotypes are heavily established at this age. Surprisingly, I found no discernible delta oscillations in any layer of cortical KO slices maintained in nACSF containing 4 μM CCH and 10 μM SCH-23390 for up to two hours (Fig. 3.1A–D). I found similar results in two other WT mice (data not shown). These results suggest that loss of MeCP2 impairs the generation of cortical delta oscillations.

I also show using current source density (CSD) analysis that delta oscillations in WT slices are generated in layer V of the cortex (Fig. 3.2, left), in line with that of previous findings (Carracedo et al. 2013). Clear epochs of source and sink activity occurred in layer V, which correlates with the channel in which the delta oscillations of greatest power were recorded in Fig. 3.1. Given that oscillatory activity across the entire cortical column is disrupted following the loss of MeCP2 function, I was unsurprised to find the lack of source and sink activity in KO slices in the corresponding layer V (Fig. 3.2, right). I saw a small intensity increase around the lower half of layer V, where the electrode with the peak power was recorded in Fig. 3.1, however, the power of these events is markedly reduced compared to WT, consistent with reduced power in oscillatory activity in these slices also.

It is possible that the absence of delta oscillations in KO cortical slices is due to damage from the electrode array. To mitigate this possibility, I selectively recorded from layer V of the S1 somatosensory cortex using a glass micropipette as described in Chapter 2.3.4. I observed robust cortical delta oscillations in WT slices maintained in nACSF containing 4 μM CCH and 10 μM SCH-23390, but not when maintained in nACSF alone (Fig. 3.3 A-C). The power of cortical delta oscillations increased in a time-dependent manner with the highest power at approximately 90 minutes post-drug application. These results support earlier findings that isolated cortical slices from WT mice are capable of generating persistent delta oscillations.

In contrast, I observed no overt delta oscillations in cortical slices from KO mice maintained in nACSF containing CCH and SCH-23390 for up to two hours (Fig. 3.3 A, B

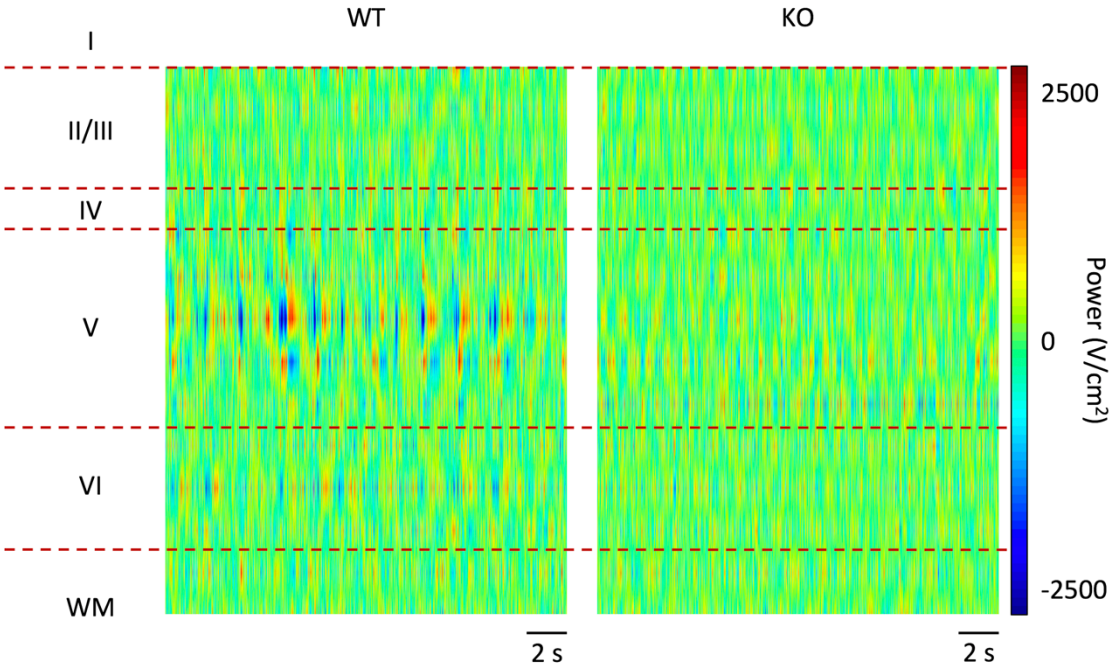

Fig. 3.2: Current source density analysis reveals the generation of delta oscillations specifically from layer V of the somatosensory cortex, the source of which is lost in *Mecp2*-null mice. CSD analysis of the corresponding LFP recordings shown in Fig. 3.1. Left = WT, right = KO. The approximate positions of cortical layer boundaries are marked by horizontal red lines and each band corresponds with the label on the left. I - VI = cortical layers I - VI, WM = white matter.

---

and D). Using spectral analysis, I found a statistically significant decrease in the power of pharmacologically-induced delta oscillations in KO mice compared to WT mice (WT: n=12, KO: n=10, $p<0.0001$, two-way ANOVA with Tukey's multiple comparisons test; Figure 3.3 E right). Despite KO delta oscillations being significantly reduced in power, the frequency at which the greatest delta power occurred was not significantly different between WT and KO mice in either control conditions or following CCH and SCH-23390 treatment, and neither did drug application affect delta frequency (WT: n=12, KO: n=10, p=ns for all comparisons, 2-way ANOVA with Tukey's multiple comparisons test; Figure 3.3 F). Together, these results suggest that loss of MeCP2 function impairs the generation of cortical delta oscillations.

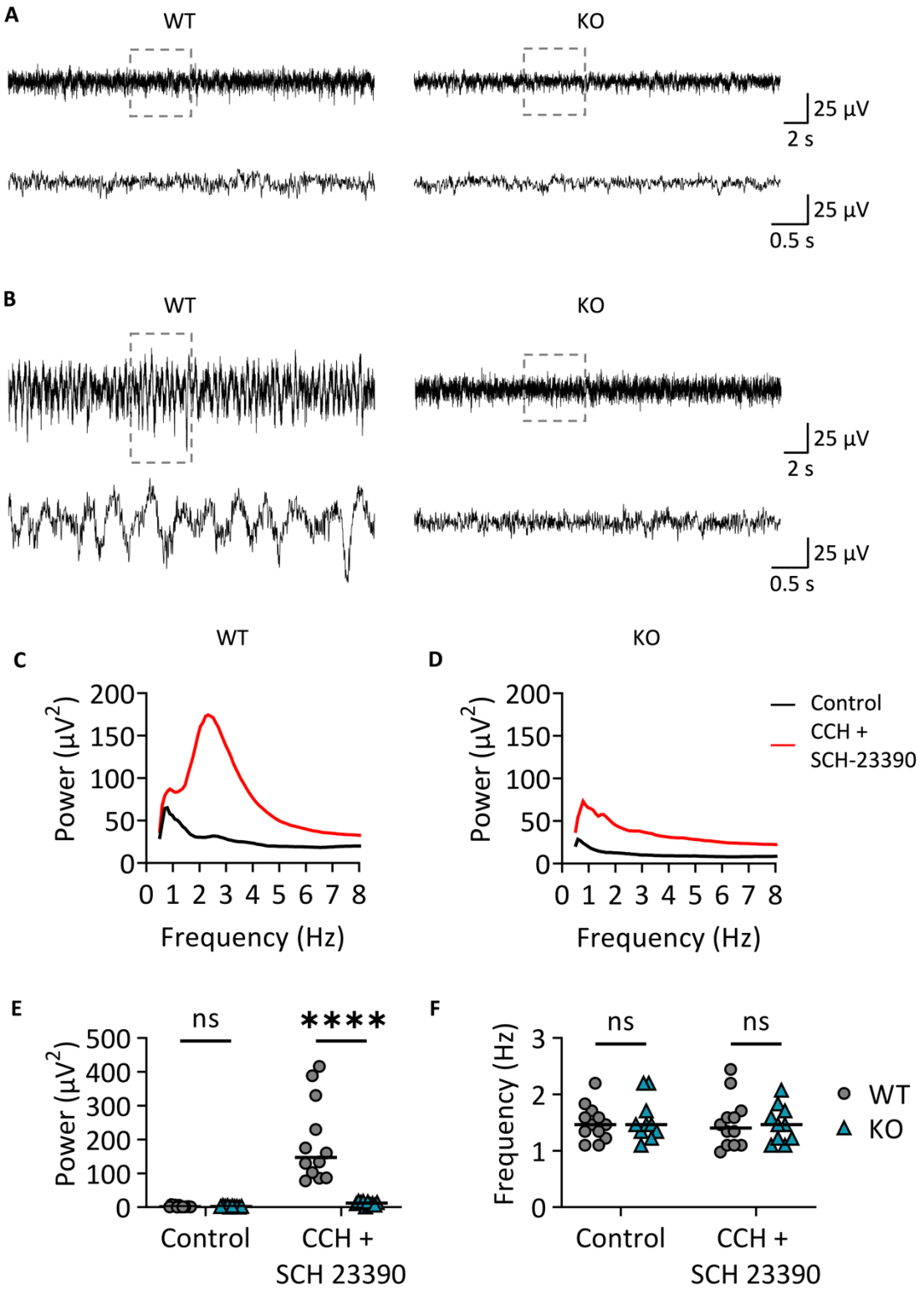

Fig. 3.3: Loss of MeCP2 impairs the generation of cortical delta oscillations. Neocortical brain slices were prepared from wild-type mice (WT, left) and *Mecp2*$^{Stop/y}$ (KO, right) mice at 8 – 10 weeks of age. Local field potentials (LFPs; filtered 0.3–100 Hz) were recorded from layer V of the S1 somatosensory cortex in the absence (Control) or presence of CCH (4 µM) and SCH-23390 (10 µM). **(A)** Example LFPs from slices maintained in nACSF alone. Lower traces represent expanded traces of regions

highlighted using dashed boxes. **(B)** Example LFPs from slices maintained in nACSF containing CCH and SCH-23390. **(C and D)** Example power spectral density of LFPs from a WT mouse (C) or KO mouse (D). **(E and F)** Group data showing peak power (E) and peak frequency (F) before and after treatment with CCH and SCH-23390 in WT (n = 12) and KO mice (n = 10). Symbols represent data from one animal; horizontal lines represent median. Statistics were performed using two-way ANOVA with Sidak post-test analysis. **** = $p<0.0001$, ns = not significant.

3.2.2 Cortical delta rhythms are partially preserved in pre-symptomatic *Mecp2*$^{Stop/y}$ mice

RTT is characterised by a period of typical development for 6 – 18 months of life, followed by regression of purposeful hand use and spoken language (Neul et al. 2010). Similarly, male mice lacking functional MeCP2 are phenotypically normal for the first 3 – 4 weeks of life, after which they develop progressive RTT-like phenotypes (Guy et al. 2007; Robinson et al. 2012). Therefore, I next wanted to determine whether the impaired generation of cortical delta rhythms in *Mecp2*-null mice occurs before or after the manifestation of RTT-like phenotypes. To this end, I prepared neocortical slices from juvenile (less than 28 days old) male *Mecp2*$^{Stop/y}$ mice and their WT littermates. Importantly, *Mecp2*$^{Stop/y}$ mice were phenotypically indistinguishable from WT mice at this age according to established phenotypic scoring (Guy et al. 2007). I recorded LFPs from layer V of the S1 somatosensory cortex as described earlier.

In juvenile WT mice, I observed robust delta rhythms in neocortical slices maintained in nACSF containing CCH (4 μM) and SCH-23390 (10 μM), but not when maintained in nACSF alone (Fig. 3.4 A-C). I found that the peak power of delta rhythms in juvenile WT mice was significantly higher than those recorded from adult WT mice ($p<0.0001$, two-way ANOVA with Tukey's multiple comparisons test; Fig. 3.4 G). In contrast, I found no change in delta frequency between juvenile and adult mice (Fig. 3.4 H). Therefore, these data show an age-dependent decrease in the power of neocortical delta rhythms in WT mice.

In juvenile KO mice, I also observed robust delta oscillations in neocortical slices maintained in nACSF containing CCH (4 μM) and SCH-23390 (10 μM), but not when maintained in nACSF alone (Fig. 3.4 A-C). I found that the peak power of delta rhythms

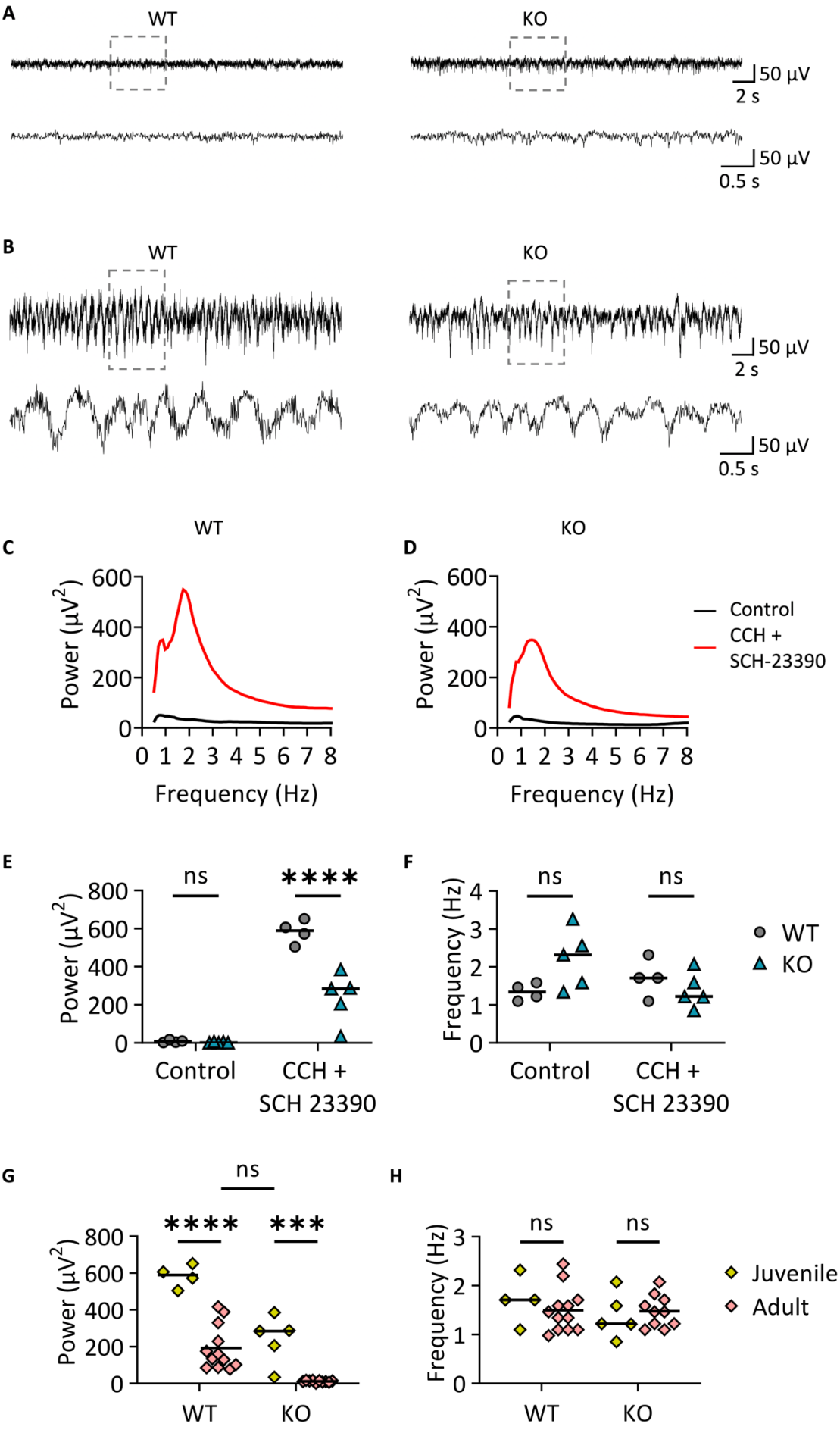
A
WT
KO
50 µV
2 s
50 µV
0.5 s
B
WT
KO
50 µV
2 s
50 µV
0.5 s
C
WT
D
KO
Power (µV²)
600
400
200
0
0 1 2 3 4 5 6 7 8
Frequency (Hz)
Control
CCH +
SCH-23390
E
ns
****
Power (µV²)
800
600
400
200
0
Control
CCH +
SCH 23390
F
ns
ns
Frequency (Hz)
4
3
2
1
0
Control
CCH +
SCH 23390
WT
KO
G
ns
****
***
Power (µV²)
800
600
400
200
0
WT
KO
H
ns
ns
Frequency (Hz)
3
2
1
0
WT
KO
Juvenile
Adult

Fig. 3.4: Cortical delta oscillations are partially preserved in pre-symptomatic *Mecp2*$^{Stop/y}$ mice. Local field potentials (LFPs; filtered 0.3–100 Hz) were recorded from layer V of the S1 somatosensory cortex using cortical brain slices obtained from wild-type mice (WT, left) or MeCP2-Stop (KO, right) mice at 3 – 4 weeks of age. **(A)** Example LFPs from slices maintained in nACSF alone. Lower traces represent expanded traces of regions highlighted using dashed boxes. **(B)** Example LFPs from slices maintained in nACSF containing CCH (4 μM) and SCH-23390 (10 μM). **(C and D)** Example power spectral density of LFPs from a WT mouse (C) or KO mouse (D). **(E and F)** Group data showing peak power (E) and peak frequency (F) before and after treatment with CCH and SCH-23390 in WT (n = 12) and KO mice (n = 10). **(G and H)** Group data comparing peak power (G) and peak frequency (H) in WT and KO at juvenile and adult ages. Symbols represent data from one animal; horizontal lines represent median. Statistics were performed using two-way ANOVA with Sidak post-test analysis. **** = $p<0.0001$, *** = $p<0.001$, ns = not significant.

---

in juvenile KO mice was significantly higher than those recorded from adult KO mice ($p<0.001$, two-way ANOVA with Tukey's multiple comparisons test; Fig. 3.4 G), mimicking the age-dependent decrease in delta power seen in WT animals. I also found that the peak delta power in juvenile KO mice was significantly lower compared to juvenile WT mice ($p<0.0001$, two-way ANOVA with Tukey's multiple comparisons test; Fig. 3.4 E), but not significantly different from adult WT mice (Fig. 3.4 G). In contrast, I found no change in delta frequency across age or genotype (Fig. 3.4 H). Together, these data show that delta oscillations are partially preserved before the onset of overt RTT-like phenotypes, and that *Mecp2*$^{Stop/y}$ mice show the same age-dependent decrease in delta rhythm power as seen in WT, although at both stages the power of delta oscillations is reduced in the absence of functional MeCP2.

3.2.3 Thalamocortical delta rhythms are preserved in *Mecp2*$^{Stop/y}$ mice

Previous studies have shown that there are two generators of delta oscillations within the brain: firstly, local generators exist within the neocortex itself (Mormann et al. 2008), and secondly a separate generator exists in the thalamus which projects these rhythms of neuronal activity onto the neocortex from distal regions (Amzica et al. 1992). So far in this chapter I have assessed the implications of MeCP2 loss on the production of

cortically generated delta oscillations through the use of *in vitro* electrophysiological experiments on regions of isolated somatosensory cortex. I next sought to determine whether thalamically-generated delta oscillations are equally affected by the loss of MeCP2 function in KO mice, and hence used a thalamocortical slice preparation (see Chapter 2.3.2.2) where connections between the thalamus and somatosensory cortex were maintained. As with previous experiments, control recordings were taken before the addition of 4 μM CCH and 10 μM SCH-23390 through bath application to the slices, following which a two minute recording was taken every ten mins thereafter.

Thalamocortical slices were prepared from adult (8 - 10 weeks of age) male *Mecp2*$^{Stop/y}$ mice and their WT littermates. I confirmed reciprocal connections between thalamus and cortex using stimulation prior to experimentation. I then recorded LFPs from layer V of the S1 somatosensory cortex as described earlier. To my surprise, I observed robust delta rhythms in thalamocortical slices maintained in nACSF containing CCH (4 μM) and SCH-23390 (10 μM) from both *Mecp2*$^{Stop/y}$ mice and their WT littermates (Fig. 3.5 A-D). In contrast, delta rhythms were absent from slices maintained in nACSF alone (Fig. 3.5 A-D), confirming that these oscillations are pharmacologically-induced. I found that there was no statistically significant difference between peak delta power or frequency in *Mecp2*$^{Stop/y}$ mice and their WT littermates. (Fig. 3.5 E and F). Together, these data suggest that thalamocortical delta rhythms are preserved in *Mecp2*$^{Stop/y}$ mice.

3.3 Discussion

3.3.1 The *in vitro* model of cortical delta oscillations

The opening experiments in this chapter were used to validate the *in vitro* model of delta oscillations in the mouse somatosensory cortex, which had previously been established in the rat somatosensory cortex (Carracedo et al. 2013). The basis of this model is in replicating the neuromodulatory tone during Stage 3 NREM sleep. Cholinergic tone is reduced though not completely silenced during deep sleep (Platt and Riedel, 2011). Consequently, in previous studies, low level activation of ACh-receptors through CCH application (at a concentration approximately 10 fold smaller than is required for the activation of awake-state rhythms) alone was sufficient to induce delta oscillations in the rat somatosensory cortex (Carracedo et al. 2013). However, the chance of successfully inducing delta oscillations was increased when CCH was added in conjunction with the D1 dopamine receptor antagonist SCH-23390, as was delta power. The effect of SCH-23390 application on the generation of NREM-associated rhythms is representative of

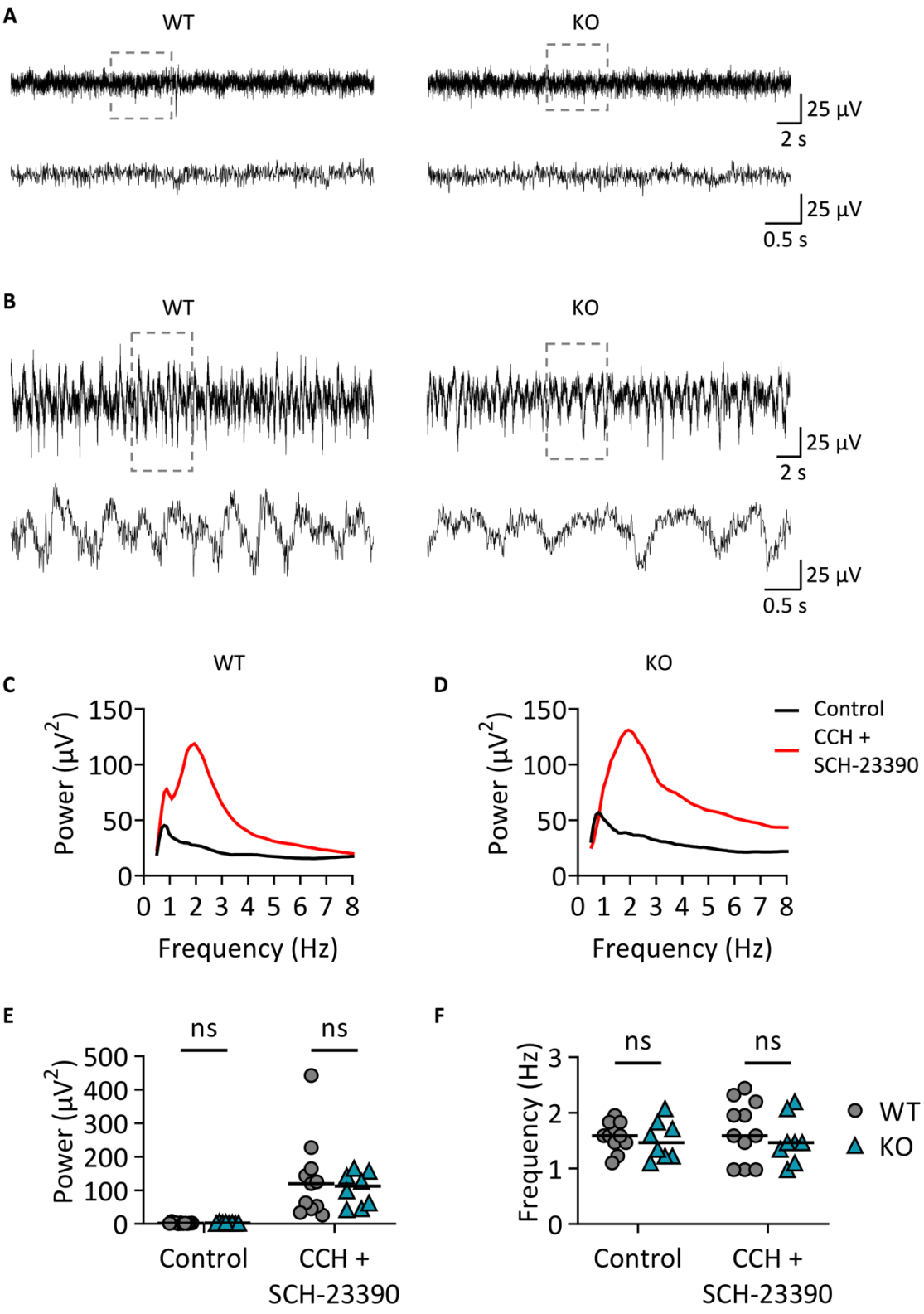

Fig. 3.5: Thalamocortical delta oscillations are preserved in *Mecp2*$^{Stop/y}$ mice. Local field potentials (LFPs; filtered 0.3–100 Hz) were recorded from layer V of the S1 somatosensory cortex using thalamocortical brain slices obtained from wild-type mice (WT, left) or *Mecp2-Stop* (KO, right) mice at 8 – 10 weeks of age. Reciprocal connections between thalamus and cortex were checked using stimulation prior to recordings. **(A)** Example LFPs from slices maintained in nACSF alone. Lower traces represent

expanded traces of regions highlighted using dashed boxes. **(B)** Example LFPs from slices maintained in nACSF containing CCH (4 μM) and SCH-23390 (10 μM). **(C and D)** Example power spectral density of LFPs recorded before (control) or after treatment with CCH and SCH-23390 from a WT mouse (C) or KO mouse (D). **(E and F)** Group data showing peak power (E) and peak frequency (F) before and after treatment with CCH and SCH-23390. Symbols represent data from one animal; horizontal lines represent median. Statistics were performed using two-way ANOVA with Sidak post-test analysis. ns = not significant.

---

the inhibition of reward and arousal pathways that are silenced during deep sleep and are governed by dopaminergic signalling (Schultz, 1998; Kume et al. 2005; Lena et al. 2005). These findings during the establishment of the *in vitro* model of delta oscillations confirm that NREM-associated brain rhythms found in the EEG can be replicated *in vitro* in isolated sections of the neocortex by replicating the neuromodulatory tone of the brain during NREM sleep. Therefore, these *in vitro* delta oscillations are an equivalent model of the *in vivo* rhythm. To my knowledge, I present here the first study whereby this *in vitro* model has been used in the mouse somatosensory cortex. It was important to start these experiments by validating this model in WT mouse brain slices to confirm that delta oscillations could indeed be induced in the isolated mouse somatosensory cortex. Once this was achieved, the model was then used in *Mecp2*-null mouse brain slices to determine the role of MeCP2 in the generation of cortical delta oscillations.

3.3.2 Delta oscillations in the absence of MeCP2 function

There have been several studies that have previously looked at the role of MeCP2 in the generation of delta oscillations. Unfortunately, a large portion of this data contradicts itself: some studies showed an increase in delta power following the loss of MeCP2 function (Ammanuel et al. 2015; Roche et al. 2019; Dong et al. 2020), some found a decrease (Johnston et al. 2014), and others found no significant difference (Liao et al. 2012; Wither et al. 2012). These studies comprised data from both RTT patients and *Mecp2*-null animals, but importantly they all used EEG as their primary recording technique. The authors of these studies do not comment on delta oscillations with respect to their mode of generation (cortical or thalamocortical), which is likely due to the difficulty of studying each rhythm generator in isolation *in vivo* (see below). As a result, the experiments presented in this thesis represent the first study where the effects

of MeCP2 function on the individual generators of delta oscillations has been investigated.

Previous studies have looked at the electrophysiological consequences of loss of MeCP2 function in the somatosensory cortex, though not specifically in relation to delta oscillations. Neuronal networks within the somatosensory cortex exhibit reduced axonal connectivity (Dani and Nelson, 2009), likely owing at least in part to the alterations in dendritic morphology in the absence of MeCP2 (Armstrong et al. 1995; Stuss et al. 2012; Rietveld et al. 2015). These networks also exhibit an imbalance of excitatory and inhibitory drive, whereby total excitation is reduced and total inhibition is increased (Dani et al. 2005). With excitatory input reduced within the somatosensory network in *Mecp2*-null brain slices, it is perhaps not surprising that delta oscillations whose origin exists specifically within this network are equally disrupted, especially considering the cells required to generate this rhythm require NMDA-receptor mediated excitation in order to function in this process (Carracedo et al. 2013).

3.3.3 Functional differences between the cortical and thalamocortical delta oscillation generators

The results presented in this chapter reveal that the loss of MeCP2 function impairs the generation of cortical, but not thalamocortical, delta oscillations. The expression and function of MeCP2 differs with regional and cell-type specificity (see Chapter 4.3.1) and hence it is not unrealistic to conclude that loss of MeCP2 function has differential effects on each rhythm generator.

Although the distinct mechanisms that underlie the cortical and thalamocortical delta rhythms have previously been identified (see Chapter 1.5.4.2), the temporal distribution of each rhythm and the processes that they are involved in have yet to be elucidated. This is likely due to the difficulties in studying the two rhythm generators in isolation in an *in vivo* setting. Specifically, you cannot establish an *in vivo* model of neocortical delta oscillations without input from the thalamus, which makes it incredibly difficult to determine whether the delta waves observed in the cortex at any given time point possess a cortical or thalamocortical origin. For this reason, previous studies that have assessed the functional role of delta oscillations have not distinguished between delta waves that arise from each rhythm generator. To circumvent these challenges, researchers would need to study both regions at the same time *in vivo* in order to

determine whether the thalamus is activated simultaneously with the cortex during periods of delta activity. This would provide insight into the differences in temporal distribution of thalamically-generated and cortically-generated delta oscillations during different neurological processes and behavioural states. Only once this has been achieved can we determine further the function of MeCP2 in coordinating different types of oscillatory activity throughout the brain.

It is worth noting here that some of the delta oscillations observed in the thalamus actually arise from cortical generators that have been projected backwards onto thalamic neurons via corticothalamic axonal tracts (Amzica and Steriade, 1998). These findings are supported by the knowledge that axonal projections from the cortex to the thalamus are more numerous than those projecting from the thalamus to the cortex (Steriade, 2006). This is an additional factor that would need to be considered if the thalamus and cortex were to be studied concurrently in an *in vivo* setting: even with cortically-generated delta oscillations the thalamus would be activated, and so the presence of thalamic activity alone would be insufficient to determine the origin of the delta rhythm at any given time point. To account for this, researchers would need to study precise sequences of spike timing and phase-coupling with an incredibly high degree of temporal resolution to determine which brain region was activated first during the delta wave. This would identify which region was responsible for generating each delta wave, and which region simply received the delta wave as a projection.

It is also worth noting that while the studies proposed above sound simple, in reality it can be very difficult to study the thalamus in an electrophysiological setting *in vivo* due to the depth at which it is located within the brain. Superficial brain regions such as the cortex are relatively easy to study *in vivo*: they are positioned in close proximity to EEG electrodes on the surface of the skull, and can also be implanted with an electrode following a craniotomy with relative ease and without damaging other brain regions. It would be difficult to record thalamic activity *in vivo* via electrode implantation as this is an incredibly invasive technique and would involve tracking the electrode through other brain regions in order to reach the thalamus, which may be damaging to neurological function. Furthermore, although the site and depth of electrode implantation could be calculated using a brain atlas and coordinates relative to bregma, once the electrode is in the brain it is difficult to know for certain (at least until post-mortem analysis can be conducted) that it is in the correct location. Given the depth that would need to be achieved to record from the thalamus, there is therefore likely to be a large amount of variability between experimental repeats and potentially a large amount of error involved.

With the thalamus being positioned so close to the centre of the brain, the lack of spatial resolution in EEG recordings makes it difficult to identify electrical activity from subcortical regions, and even if this were possible, it is unlikely that thalamic activity would be recorded without interference from more superficial regions at the same time. EEG can be used in conjunction with other techniques to provide better spatial and temporal resolution, including functional magnetic resonance imaging (fMRI; Vulliemoz et al. 2010) and magnetoencephalography (MEG; Ebersole and Ebersole, 2010). Perhaps the combination of these techniques would be the best option for studying the temporal and functional differences of thalamically-generated and cortically-generated delta oscillations.

The functional role of the thalamus outside of delta oscillation generation may aid the understanding of the different functions of each delta rhythm generator. It is well accepted that during wakefulness the thalamus functions in gating external stimuli and conducting these inputs to the relevant cortical regions (Gisiger and Boukadoum, 2011). During this process, cholinergic activation of thalamocortical neurons is thought to be responsible for cortical activation (Hirata and Castro-Alamancos, 2010). This could potentially help explain the need for low levels of cholinergic activation via CCH application for the generation of delta oscillations in the brain slice preparations used in this project. However, during sleep, the brain becomes less responsive to external stimuli, and the thalamus plays an active role in preventing sensory information from reaching the cortex. This is thought to be important to allow the cortex to reactivate networks during memory consolidation without interference from unwanted sensory stimuli. With this information, one might infer that thalamically-generated delta oscillations occur primarily during wakefulness (see Chapter 7.4.4 for more information on delta oscillations during wakefulness) and are silenced during phases of sleep when thalamocortical communication is reduced. If this is the case, cortically-generated delta oscillations would predominate the brain during less active states, including Stage 3 NREM. The findings presented in this chapter show that loss of MeCP2 function disrupts the generation of cortical delta oscillations only. Given the high abundance of delta oscillations in Stage 3 NREM sleep (Chauvette et al. 2011) and the fact that RTT patients spend less time in Stage 3 NREM sleep compared to age matched controls (Ammanuel et al. 2015), the findings of this chapter support the idea that the cortical generator of delta oscillations is responsible for NREM-associated rhythms.

One of the most striking results from the data presented in this chapter is that loss of MeCP2 function affects the networks involved in cortically-generated delta oscillations

and not those involved in thalamic delta oscillations. The implications of this are that, during periods of thalamic delta, the thalamocortical cells which fire like clock-work and project this onto cortical regions, as well as the cortical neurons that project back to the thalamic reticular nucleus and the thalamic reticular cells which in turn provide inhibitory feedback to the thalamocortical cells (see Chapter 1.4.5.2), function in the *Mecp2*-null brain in the same way they do in WT brains. While this may seem like a fairly simple conclusion based on the results presented here, it is supported by the findings of other studies, for example that evoked thalamocortical excitatory outputs onto the cortical layer IV are unaffected by the loss of MeCP2 function (He et al. 2014). This theory is however complicated by the fact that during periods of cortically-generated delta, the somatosensory cortex relies on excitatory input from the thalamus via these same thalamocortical projections. Given the disruption of cortically-generated delta oscillations as shown by the data in this chapter, this would therefore suggest that cells within the thalamocortical network are in fact affected by the loss of MeCP2 function.

In support of this, it has previously been shown that the somatosensory cortex experiences reduced excitatory input and increased GABAergic transmission following the loss of MeCP2 function (Dani et al. 2005). The majority of thalamic input received by the somatosensory cortex is delivered from the ventrobasal complex, which comprises the ventral posteromedial nucleus and the ventral posterolateral nucleus. Cortical cells project back to thalamic reticular neurons which in turn provide inhibitory feedback to cells in the ventrobasal complex. Previously, MeCP2 has shown to be important for regulating GABAergic transmission in this network, with MeCP2 differentially regulating GABAergic innervations at excitatory and inhibitory synapses (Zhang, Zak, and Liu 2010). The findings in this study were attributed to fewer GABAergic synapses on ventrobasal neurons and more on reticular thalamic neurons compared to age-matched controls. The authors conclude that MeCP2 function is required for the development of GABAergic innervations, given that GABAergic transmission was shown to be defective in neonatal mice. Altered expression levels of GABA-receptors have also been shown in layer IV somatosensory neurons at presynaptic terminals where thalamic projections are received (Lo, Blue, and Erzurumlu 2016). Together these findings suggest that MeCP2 functions to regulate GABAergic transmission in thalamocortical networks, thus providing context to the loss of cortically-generated delta oscillations in *Mecp2*-null brain slices given the dependency of the mouse somatosensory cortex on thalamic input which is in turn reliant on GABAergic transmission.

3.3.4 Age-dependent changes in neuronal oscillations and the role of MeCP2

The data presented in this thesis reveal that a natural reduction in cortical delta oscillation power occurs during the progression from juvenile to adulthood. Indeed, these results are supported by the findings of previous studies: delta wave activity is shown to undergo significant decreases during late development (Campbell and Feinberg, 2009; Baker et al. 2012; Zhang et al. 2013) and during aging (Vlahou et al. 2014). During development, the decrease in delta activity reflects a simultaneous decrease in the amount of time spent in SWS (Tarokh and Carskadon, 2010; De Vivo et al. 2014), as well as an overall reduction in total sleep duration. Several studies have shown that delta power actually increases in the very early stages of infancy and then subsequently decreases during the transition to adulthood, which is thought to reflect network maturation and structural changes during this time (Feinberg and Campbell, 2010; Chu et al. 2014). The initial increase in delta oscillations is indicative of a large phase of synaptogenesis that occurs during early postnatal development, and the later decrease in delta activity is suggestive of a synaptic pruning process that occurs during the fine-tuning of neuronal activity during late development (Cirelli and Tononi, 2015). Delta oscillations are not the only frequency band affected by the development or aging process: it is thought that all frequency bandwidths undergo a general age-related pattern of reduced activity (Michels et al. 2013). However, despite these changes, the coherence of neuronal oscillations throughout the brain increases with age (Tarokh et al. 2010), which supports this idea that developmentally-regulated changes in synaptic connectivity are required to fine tune neuronal activity throughout the brain. Indeed, changes in neuronal activity of delta frequency have been shown to correlate with processes involved in cortical restructuring and maturation (Buchmann et al. 2011; Kurth et al. 2010).

At the cellular level, neurons undergo a large phase of maturation during development. Layer V pyramidal cells in the mouse neocortex experience significant changes in the first month after birth, including alterations in dendritic morphology and basal intrinsic properties (Kroon et al. 2019). The results of this paper show that resting membrane potential of these cells becomes more negative as development progresses, while the balance between excitatory and inhibitory input is restructured. The apical dendrites of these cells are continually growing in both length and complexity during the transition from juvenile to adulthood in both the rat neocortex (Wise et al. 1979; Zhu, 2000) and

human neocortex (Koenderink and Uylings, 1995). It has previously been shown that MeCP2 plays a functional role in neuronal cell maturation: *Mecp2*-null neurons exhibit delayed maturation processes, including the developmentally-induced increase in dendritic size and complexity (Kishi and Macklis, 2004; Kishi and Macklis, 2010). *Mecp2*-null mouse brains do not exhibit typical increases in cortical thickness after the age of 4 weeks, as is seen in control animals (Fukuda et al. 2005), again highlighting the role of MeCP2 in coordinating developmental changes in neuronal networks and brain anatomy. Indeed, increases in MeCP2 expression are thought to coincide with the timing of a large phase of maturation of the central nervous system in general (Shahbazian et al. 2002).

With this information alone, one might predict that delta oscillations in the adult brain would be affected by the loss of MeCP2 function, and would appear more similar to that of the juvenile brain. However, this is a contrasting theory to the results presented in this chapter. As described in Chapter 3.2.2, both WT and *Mecp2*-null mice exhibit the same age-dependent reduction in the power of cortically generated delta oscillations. This suggests that the age-dependent change in delta oscillation architecture occurs independently of MeCP2 function, and is unaffected by the deficits in neuronal maturation observed in *Mecp2*-null neurons. The implications of this are that neuronal maturation state (particularly the processes of maturation under the control of MeCP2) surprisingly do not affect the fine-tuning of oscillatory activity during the development from juvenile to adulthood.

The results shown in Chapter 3.2.2 do however highlight some significant differences between WT and *Mecp2*-null brains during delta oscillation generation: loss of MeCP2 function causes a significant reduction in the power of cortically generated delta oscillations at both ages. The most striking conclusion to be drawn from this is that the neurological deficits relating to rhythm generation occur at the pre-symptomatic stage, as they pre-date the onset of RTT-like phenotypes in *Mecp2*-null mice.

The findings that *Mecp2*-null brain slices from juvenile animals have the ability to produce robust delta oscillations (albeit at a reduced power to juvenile WT animals) reveal that cortical networks within the somatosensory cortex do indeed possess the ability to generate these rhythms, at least at this age. Together with the knowledge that adult *Mecp2*-null brain slices are incapable of generating cortical delta oscillations, this data further suggests that, while neurological deficits are already established at the pre-symptomatic stage, the mechanisms involved in generating these rhythms cease to

function entirely around the same time as the RTT-like phenotype begins to establish itself. This suggests that there are multiple stages at which different levels of neurological deficits begin to emerge in brains lacking MeCP2 function. However, the fact that juvenile *Mecp2*-null brain slices can produce some form of cortical delta oscillation is reassuring, as it suggests that the loss of this rhythm in adulthood is a "degenerative" process, rather than "developmental". In order to re-establish the cortical delta rhythm, researchers would need to find a way to switch the mechanism back on, which although challenging, poses less difficulties than attempting to rewire an entire network. The mechanisms involved in the generation of cortical delta oscillations are examined in further detail in the following two chapters.

As mentioned above, some neurological deficits exist before the onset of the RTT-like phenotype in *Mecp2*-null mice, since the power of cortically generated delta oscillations is significantly reduced at the juvenile stage compared to WT. Despite several studies suggesting that MeCP2 functions in neuronal maturation, it is not clear at what exact stage the maturation process becomes affected by the loss of MeCP2. The processes involved in neuronal development begin pre-birth, and while most studies looked at the consequences of MeCP2 loss on neuronal maturation in adulthood, some studies suggest that these deficits (including reduced cortical thickness) exist at the juvenile stage (<28 days in mice; Fukuda et al. 2005). With this in mind, the reduction in delta oscillation power in juvenile *Mecp2*-null brain slices could be attributed to deficits in maturation that pre-date this age. It has previously been discussed how these alterations in neuronal maturation do not affect the age-dependent reduction in delta power. Nevertheless, they may be responsible for the reduced delta power compared to WT animals at either age, assuming they do indeed pre-date both ages.

Interestingly, calcium ion signalling is involved in EPSP generation in these cells at the post-maturation stage, but not before (Zhu, 2000). Furthermore, during development, there is a simultaneous increase in calcium current oscillations, pyramidal cell maturation and the synchronicity of neuronal activity (Opitz et al. 2002), highlighting the role of calcium ion signalling in the process of network maturation. The significance of this will be discussed in Chapter 5.

3.4 Summary

In this chapter I used *in vitro* electrophysiological recording techniques to assess the capabilities of the two delta oscillation generators in the presence and absence of

functional MeCP2 protein. Specifically, brain slice preparations containing either isolated or thalamically-linked somatosensory cortex were taken from WT and *Mecp2*-null mice and subject to pharmacological manipulation previously shown to induce delta oscillations. I have shown that functional MeCP2 is crucial for the establishment of cortically-generated delta oscillations: local generators within layer V of the somatosensory cortex are unable to produce coherent, high-powered delta oscillations, and oscillatory activity across the entire cortical column is reduced as a result. Using juvenile mice, I have shown that cortical delta oscillations are partially preserved at the pre-symptomatic stage, suggesting that some neurological deficits coincide with phenotype establishment. Interestingly, rhythm generators that reside within the thalamus are seemingly unaffected by the loss of MeCP2 function, as delta oscillations are maintained in the somatosensory cortex when reciprocal connections to the thalamus are preserved. Given that delta oscillations are the main constituent of Stage 3 NREM sleep, the results presented in this chapter shed light on the underlying causes of the disrupted sleep cycle patterns and sleep disturbances that occur in 80% of RTT patients.

In the next chapter, I will investigate further the mechanisms that underlie the generation of cortical delta oscillations. Specifically, I will study the specific cell types involved in this rhythm, including layer V IB pyramidal cells, and aim to understand the precise role that MeCP2 plays in maintaining their function.

Chapter 4 – Cellular consequences of loss of MeCP2 function in layer V pyramidal neurons

4.1 Aims

In the previous chapter, I demonstrated that the generation of neocortical delta rhythms is impaired in isolated cortical slices from *Mecp2*$^{Stop/y}$ mice. Given the critical role of layer V IB pyramidal neurons in the generation of cortical delta oscillations (Carracedo et al. 2013), I hypothesise that loss of MeCP2 function impairs the firing of these cells. Thus, in this chapter, I will characterise the firing patterns and cellular characteristics of layer V IB pyramidal neurons in *Mecp2*$^{Stop/y}$ mice.

4.2 Results

To examine whether the function of IB neurons is affected by the loss of MeCP2, I performed intracellular, current-clamp recordings of layer V pyramidal neurons, as described in Chapter 2.3.5. All-together, I recorded 38 IB pyramidal neurons from 4 WT mice and 44 IB pyramidal neurons from 6 KO mice.

4.2.1 Loss of MeCP2 decreases bursting in IB pyramidal neurons

In WT mice, I could readily classify neurons into two main groups. The first group of neurons generated a complex train of three to five action potentials in response to a current pulse, with an increase in duration and decrease in amplitude of each subsequent action potential within the burst (Fig. 4.1A, top row). Based on these properties, I classified these neurons as intrinsically bursting (IB) neurons (McCormick et al. 1985). These neurons either generated spontaneous bursts of action potentials in the absence of current pulses (Fig. 4.1A, middle row) or generated a single spontaneous action potential that was associated with a large after-depolarisation (ADP) component (Fig. 4.1A, bottom row). I therefore also classified neurons with a single action potential associated with a large ADP as IB neurons.

In KO mice, I also recorded from putative IB neurons, with their classification based on the generation of a complex train of three to five action potentials in response to a current pulse (Fig. 4.1B, top row). However, I found that the number of bursts per current pulse was markedly reduced in KO mice compared to WT mice (Fig. 4.1C and D). These

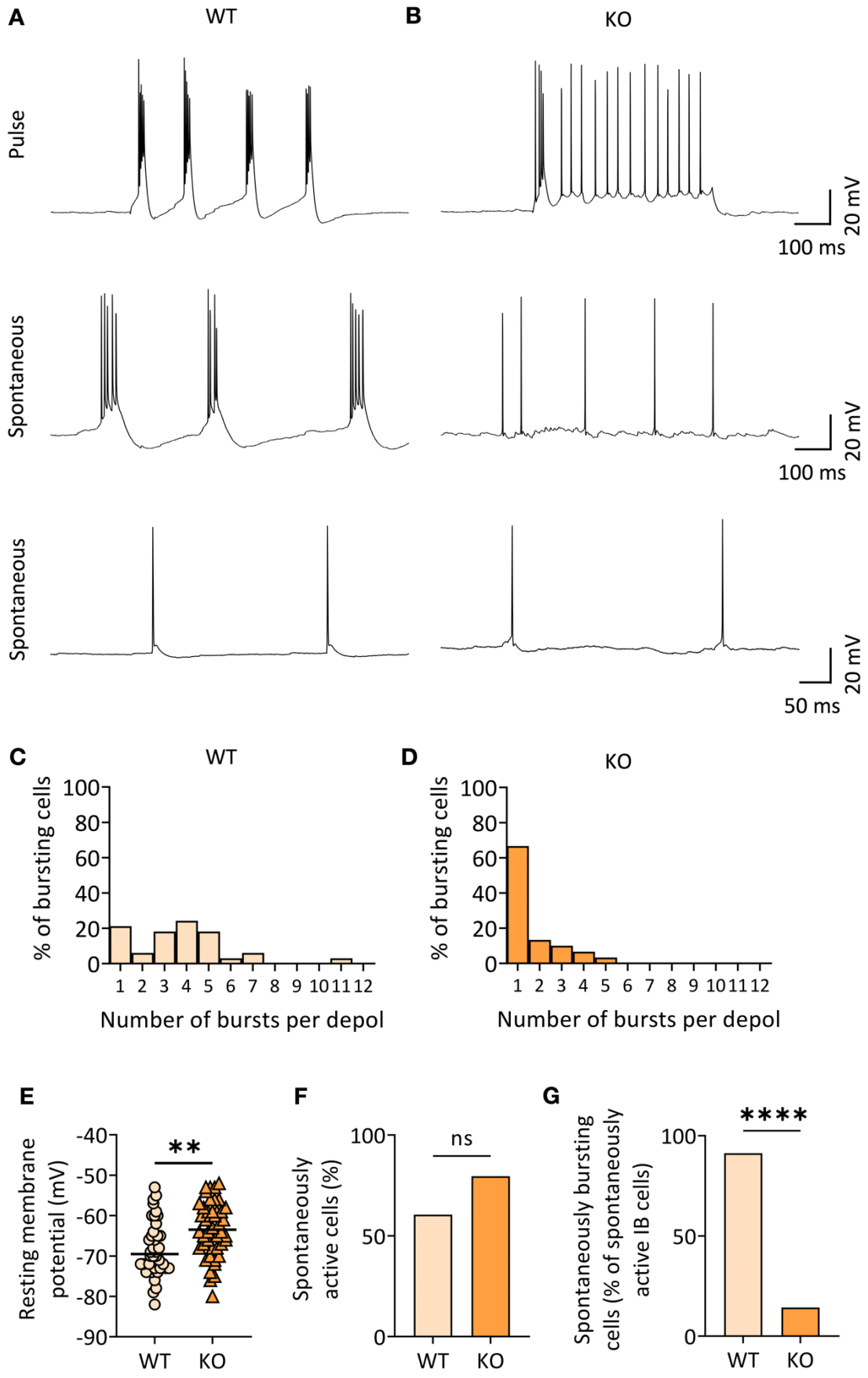

Fig. 4.1: Loss of MeCP2 decreases bursting in intrinsically bursting (IB) neurons. (A and B) Example intracellular recordings from putative intrinsically bursting (IB) neurons in layer V of S1 cortex from WT (A) and KO (B) brain slices. Top: step depolarization with

0.2 nA (500 ms) current pulse reveals the intrinsic bursting behaviour of this cell type. Middle: spontaneous bursts of spike generation at resting membrane potential phase in the same neuron shown above. Bottom: IB neurons also show spontaneous single spikes with an ADP component. **(C and D)** Histogram showing the number of bursts per depolarising pulse of current in WT (C) and KO (D) cells. **(E)** Resting membrane potential of IB neurons. Symbols represent individual neurons; horizontal lines represent median. **(F)** Percentage of IB neurons exhibiting spontaneous activity. **(G)** Percentage of cells represented in F that exhibit spontaneous bursts of spike generation. **** = $p<0.0001$, ** = $p<0.01$, ns = not significantly different.

---

putative IB neurons very rarely burst spontaneously, but instead exhibit large single action potential associated with a large ADP (Fig. 4.1B, middle and bottom row). There was no change in the percentage of IB neurons that exhibited spontaneous activity (p=ns, Fisher's exact test, Fig. 4.1F). However, I found a statistically significant decrease in the proportion of spontaneously active IB neurons that spontaneously burst in KO mice compared to WT ($p<0.0001$, Fisher's exact test, Fig. 4.1G). Interestingly, I also found a statistically significant increase in the resting membrane potential (RMP) of IB neurons in KO mice compared to those in WT mice ($p<0.01$, Mann-Whitney test, Fig. 4.1E).

Of cells that possessed an ADP component to their single action potentials, I found significant differences in both the amplitude and duration of these events between WT and KO cells. KO ADP events occurred with a significantly greater amplitude compared to WT ADPs (WT: n=19, KO: n=34, $p<0.01$, Mann-Whitney test, Fig. 4.2 A left), and for a significantly longer duration (WT: n=19, KO: n=34, $p<0.01$, Mann-Whitney test, Fig. 4.2 A right). AHP events were also significantly altered in KO IB cells: AHP amplitude was significantly reduced compared to WT cells (WT: n=38, KO: n=44, $p<0.05$, Mann-Whitney test, Fig. 4.2 B left), as was AHP duration (WT: n=38, KO: n=44, $p<0.001$, Mann-Whitney test, Fig. 4.2 B right). The average amplitude of EPSP events per cell was significantly reduced in KO IB cells compared to WT cells (WT: n=36, KO: n=41, $p<0.01$, Mann-Whitney test, Fig. 4.2 C left). Finally, EPSP frequencies did not differ significantly between genotypes (WT: n=36, KO: n=41, p=ns, Mann-Whitney test, Fig. 4.2 C right).

I also measured the amplitude, duration and spike gradient of both single action potential events and burst events in WO and KO IB cells. The amplitudes of these events were

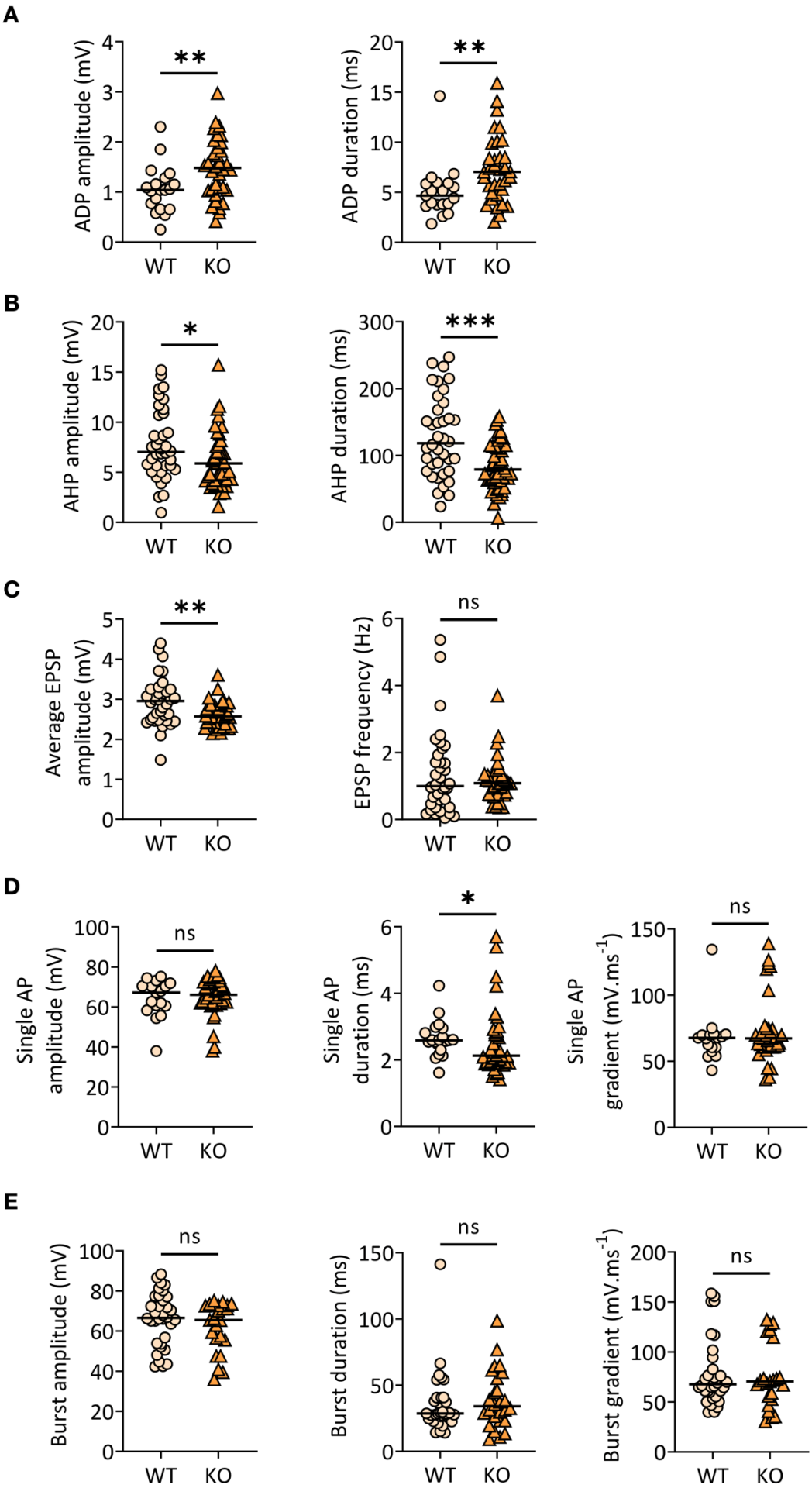
A
ADP amplitude (mV)
**
WT
KO
ADP duration (ms)
**
B
AHP amplitude (mV)
*
AHP duration (ms)
***
C
Average EPSP amplitude (mV)
**
EPSP frequency (Hz)
ns
D
Single AP amplitude (mV)
ns
Single AP duration (ms)
*
Single AP gradient (mV.ms-1)
ns
E
Burst amplitude (mV)
ns
Burst duration (ms)
ns
Burst gradient (mV.ms-1)
ns

Fig. 4.2: Cellular characteristics of *Mecp2*-null IB neurons are significantly altered compared to WT IB cells. (A) ADP amplitude (left) and duration (right). **(B)** AHP amplitude (left) and duration (right). **(C)** Average EPSP amplitude (left) and EPSP frequency (right). **(D)** Amplitude (left), duration (middle) and spike gradient (right) of single action potential events. **(E)** Amplitude (left), duration (middle) and initial spike gradient (right) of bursting events. Each symbol represents one data point (one cell), horizontal lines represent median values. *** = $p<0.001$, ** = $p<0.01$, * = $p<0.05$, ns = not significantly different.

---

taken as the difference between RMP and the peak of the action potential, or in the event of a burst, the peak of the spike which reached the greatest amplitude. Duration was measured as the time between the start of the initial depolarisation phase to the end of the repolarisation phase, before an ADP or AHP component began. The gradient of these events was measured as the steepness of the depolarisation phase of a single action potential, or in the event of a burst, of the initial depolarisation phase of the event. I found that only the duration of single action potentials differed significantly between WT and KO IB cells, with KO IBs exhibiting a significantly shorter single action potential duration compared to WT cells (WT: n=17, KO: n=40, $p<0.05$, Mann-Whitney test, Fig. 4.2 D middle). The amplitude and gradient of single action potential events were not significantly different between WT and KO IB cells (WT: n=17, KO: n=40, p=ns for both, Mann-Whitney test, Fig. 4.2 D left and right respectively), as were the amplitude, duration and gradient of bursting events (WT: n=34, KO: n=30, p=ns for all, Mann-Whitney test, Fig. 4.2 E left, middle and right respectively).

4.2.2 Action potential generation and baseline synaptic transmission is normal in regular spiking neurons from *Mecp2*$^{Stop/y}$ mice

Regular spiking (RS) pyramidal neurons located in layer V of the cortex are also active during delta oscillations, although they are not required for its generation. Instead, RS neurons produce theta-frequency spike outputs phase-locked to the delta rhythm (Carracedo et al. 2013). I therefore wanted to examine whether loss of MeCP2 affects

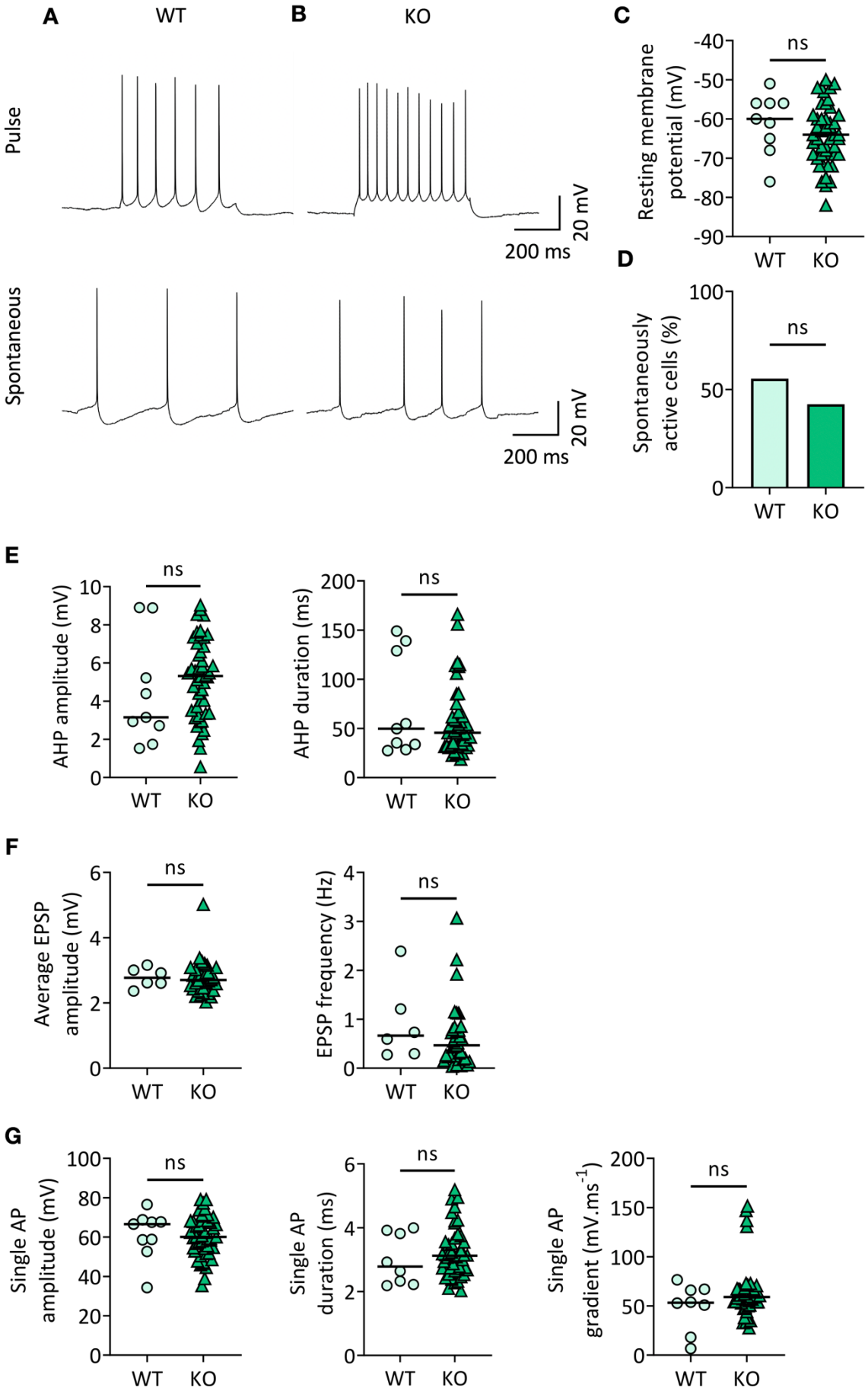
A
WT
B
KO
Pulse
20 mV
200 ms
Spontaneous
20 mV
200 ms
C
Resting membrane potential (mV)
ns
WT
KO
D
Spontaneously active cells (%)
ns
WT
KO
E
AHP amplitude (mV)
ns
WT
KO
AHP duration (ms)
ns
WT
KO
F
Average EPSP amplitude (mV)
ns
WT
KO
EPSP frequency (Hz)
ns
WT
KO
G
Single AP amplitude (mV)
ns
WT
KO
Single AP duration (ms)
ns
WT
KO
Single AP gradient (mV.ms-1)
ns
WT
KO

Fig. 4.3: Action potential generation and baseline synaptic transmission is normal in regular spiking (RS) neurons from *Mecp2*$^{Stop/y}$ mice. (A and B) Example action potentials recorded from a layer V RS neuron of a wild-type (WT, A) or *Mecp2*$^{Stop/y}$ (KO, B) mouse. Top, action potentials elicited by a depolarising current pulse (+0.2 nA, 500 ms). Bottom, spontaneous action potentials. **(C)** Resting membrane potentials of individual RS neurons. **(D)** Percentage of RS neurons that exhibited spontaneous activity. **(E)** AHP amplitude (left) and duration (right). **(F)** Average EPSP amplitude (left) and frequency (right). **(G)** Action potential amplitude (left), duration (middle) and spike gradients (right). Each symbol represents an individual neuron; horizontal lines represent the median. Statistics performed using Mann-Whitney tests. ns = not significantly different.

---

action potential generation and / or synaptic transmission in RS neurons under baseline conditions. During intracellular experiments, as well as IB cells, I also recorded pyramidal neurons that generated trains of well-spaced action potentials that do not appear together in groups at threshold in response to a current pulse (Fig. 4.3 A and B). These neurons generated spontaneous, regularly-spaced action potentials in the absence of current pulses also. Based on these observations, I classified these neurons as regular spiking (RS) neurons (McCormick et al. 1985): pyramidal cells that neither burst nor possessed an ADP at the end of their single action potentials. All-together, I recorded 9 RS pyramidal neurons from 4 WT mice and 47 RS pyramidal neurons from 6 KO mice.

I found that RS neurons recorded from KO mice were indistinguishable from those recorded in WT mice, firing regularly spaced single action potentials both spontaneously and in response to a depolarising pulse (Fig. 4.3A and B). The action potentials observed in these cells possessed a large AHP component and no ADP. I found no statistically significant changes in spontaneous action potential firing (p=ns, Fisher's exact test, Fig. 4.3 D) as well as in RMP, AHP amplitude or duration, and EPSP amplitude or frequency. Furthermore, RS cell spike amplitude, duration and gradient were unaffected by the loss of MeCP2 (WT: n = 9 cells, KO: n = 47, p=ns for all, Mann-Whitney test for all, Fig. 4.3 C-G). Together, these findings suggest that loss of MeCP2 function does not affect baseline action potential generation or synaptic transmission in layer V RS pyramidal cells.

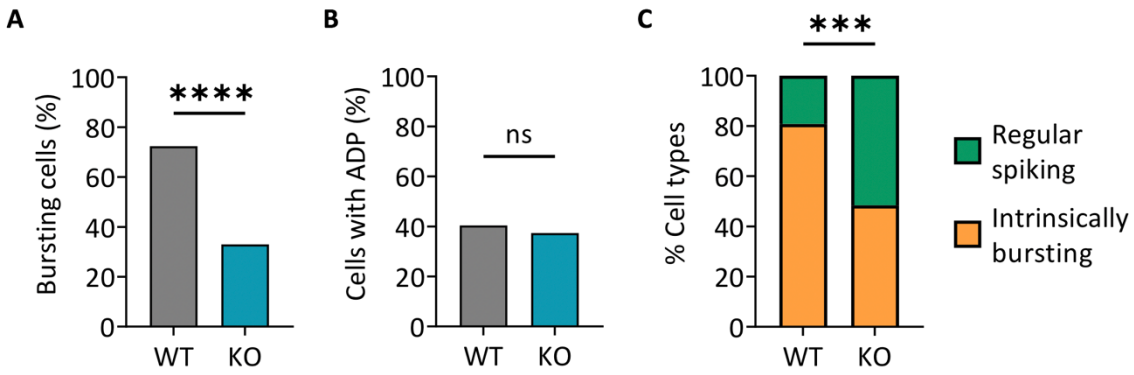

Fig. 4.4: Proportionally fewer IB cells were recorded from *Mecp2*-null brain slices compared to WT slices. (A) Percentage of pyramidal cells that exhibited bursting activity. **(B)** Percentage of cells that exhibited an ADP component on single action potentials. **(C)** Proportion of recorded pyramidal neurons classified as IB (orange) and RS (green) cells. **** = p<0.0001, *** = p<0.001, ns = not significantly different.

4.2.3 Proportionally fewer *Mecp2*-null IB cells were recorded compared to WT cells

During the cellular classification process, I found a statistically significant decrease in the percentage of neurons that generated bursts of action potentials spontaneously or in response to current pulses in KO mice (p<0.0001, Fisher's exact test; Fig. 4.4A). In contrast, I found no significant difference in the number of neurons that exhibited a large ADP associated with a single action potential (p=ns, Fisher's exact test; Fig. 4.4B). Following classification, the *Mecp2*-null population of pyramidal cells contained proportionally fewer putative IB cells compared to the WT cell population (p<0.001, Fisher's exact test; Fig. 4.4C). Together, these data suggest that the bursting properties of IB neurons is impaired in *Mecp2*$^{Stop/y}$ mice.

4.3 Discussion

4.3.1 MeCP2 function has cell-type specificity

The results presented in this chapter suggest that the firing pattern of layer V IB pyramidal neurons is disrupted by the loss of MeCP2 function, whereas the function of

layer V RS cells remains unaffected. Although these cells exhibit distinct differences in their firing patterns and in the processes in which they are involved, they also display many similarities, including their location, general morphology and the fact that they both provide excitatory outputs. With this information, I wanted to ascertain whether it is reasonable to conclude that the global loss of MeCP2 function could have such specific consequences on one individual cell subtype while simultaneously leaving neighbouring cell types largely unaffected.

MeCP2 is a ubiquitous protein that is expressed in every cell in the body, and is highly expressed in the brain (Skene et al. 2010). The *Mecp2*-null mouse model used in this study is a constitutive knockout model whereby, in male mice, MeCP2 function across the entire brain (in fact, the whole body) is lost. However, the consequences of this are not necessarily uniform across the whole brain. The two isoforms of MeCP2 are differentially expressed in particular brain regions in the postnatal mouse brain (Dragich et al. 2007; Olson et al. 2014). Furthermore, in a female heterozygous (*Mecp2*$^{+/-}$) mouse model, the amount of functional MeCP2 protein present in distinct brain regions (eg, cortex, hippocampus, cerebellum and spinal cord) not only differs from WT levels, but also differs in a brain-region specific manner (Wither et al. 2013). This study also showed that MeCP2 levels in the cortex were inversely correlated with phenotypic severity of the animals, highlighting the importance of MeCP2 function in this specific tissue.

Previous studies have also shown that the consequences of MeCP2-loss on gene expression levels is also brain-region specific; that is to say: not all affected genes are equally misregulated across the entire brain. Interestingly, global transcriptome changes are relatively subtle across the entire *Mecp2*-null brain compared to WT controls (Tudor et al. 2002). However, when individual brain regions, including the striatum, hippocampus, cerebellum and hypothalamus, are studied in isolation, overt differences in gene expression levels begin to emerge between WT and KO animals (Smrt et al. 2007; Chahrour et al. 2008; Ben-Shachar et al. 2009; Zhao et al. 2013).

Consistent with the idea that loss of MeCP2 function has differential consequences in different brain regions, previous studies have shown that while auditory event related potentials (ERPs) in the cortex are disrupted in the absence of functional MeCP2 (Stauder et al. 2006; Key et al. 2019; Dong et al. 2020), auditory brainstem responses are preserved (Goffin et al. 2011), suggesting a region-specific role of MeCP2 in sensory processing. At the cellular level, when MeCP2 function was preserved in only forebrain GABAergic interneurons, auditory ERP responses were maintained (Goffin et al. 2014), suggesting that MeCP2 function has cell-type specificity as well as regional specificity.

Also at the cellular level, several studies have examined the morphological consequences of MeCP2 loss on the dendrites of cortical pyramidal cells. A reduction in the number of dendritic arborisations, as well as shorter and less complex branching systems, occurred in layer II/III pyramidal cells of the somatosensory cortex (Fukuda et al. 2005) and layer V pyramidal neurons of the frontal, motor and somatosensory cortex (Armstrong et al. 1995; Stuss et al. 2012; Rietveld et al. 2015). However, none of these studies differentiated between the cellular subtypes that classify as "layer V pyramidal cells". Specifically, they do not clarify whether their results relate to IB or RS cells, and the reader is to presume the data presented represents a mixture of both cell types. The results of the studies discussed in this section suggest that the role of MeCP2 cannot be generalised across all cell-types. It is therefore possible that loss of MeCP2 affects the firing patterns of one cellular subtype (layer V IB neurons) while simultaneously leaving others unaffected, as is proposed by the data presented in this chapter.

The effect of MeCP2 loss on layer V pyramidal cells has previously been studied in an electrophysiological context. Dani et al (2005) showed that spontaneous firing of these cells was significantly reduced; the authors note this data contained both bursting and non-bursting pyramidal cells, and did not differentiate their data based on the two cell types. This study went on to declare that the intrinsic firing properties of these cells was not altered in response to MeCP2 loss, however the authors noted here that these results only pertained to non-bursting cells. Consistent with these findings, the data presented in this chapter (specifically Chapter 4.2.2) highlight that the intrinsic firing properties of layer V RS pyramidal cells is unaffected by the loss of MeCP2 function. It is not discussed in Dani et al (2005) why the intrinsic properties of bursting pyramidal cells were not studied, although it was possibly because the modified ACSF solution required to induce neuronal activity prevented the recording of IB properties. A further study showed that the same layer V pyramidal cells experience reduced cortical connectivity following loss of MeCP2 function (Dani and Nelson, 2009). Here the authors refer to the cells simply as "layer V pyramidal cells", however based on their cell classification system and the example traces provided, this data appears to be of RS cells only.

To my knowledge, the data presented in this thesis represents the first study in which the effects of MeCP2 loss on neuronal properties has been examined specifically in the pyramidal cell subtypes of layer V. In studying both IB and RS cells in isolation, I have shown with confidence that loss of MeCP2 function affects the firing patterns of only IB cells, and not RS cells, in layer V of the mouse somatosensory cortex.

4.3.2 Resting membrane potential modulates IB cell bursting

Earlier in this chapter I reported that layer V IB pyramidal cells in *Mecp2*-null brain slices have a significantly less polarised RMP compared to WT IB cells from the same region (see Fig. 4.1 E). With this information, I wanted to determine whether this alteration would be sufficient to inhibit the bursting mechanisms of these cells, as observed in KO slices (see Fig. 4.1 B). Indeed, it has previously been described how the bursting potential of layer V pyramidal cells can be regulated by RMP (Wang and McCormick, 1993). In this study, intracellular current injections were used to ascertain the RMP at which an IB cell would burst: at RMP values of approximately -60 mV, the cell would fire a burst, however, when held at a less polarised RMP (-55 mV) the firing properties of the cell changed from bursting characteristics to tonic single-spike action potentials (which were associated with an ADP phase, see 4.3.3 for the relevance of this). Furthermore, when held at a significantly more polarised RMP (-64mV), the cell became silent. These results confirm that RMP can influence the mode of action potential generation in layer V IB pyramidal cells, and must be tightly controlled for the generation of burst events.

There is a large amount of resemblance between the data presented in this paper and that which is presented in this chapter: firstly, the average *Mecp2*-null IB RMP was significantly less polarised compared to WT cells. Secondly, many of the putative *Mecp2*-null IB neurons recorded in this project did not display bursting properties, and instead fired single action potentials with a remarkably similar structure to those seen in Wang and McCormick (1993). This is in reference to the large ADP component that was associated with IB single action potentials in both studies. With this in mind, I infer from the results presented in this chapter that the increase in RMP observed in *Mecp2*-null IB cells is at least in part responsible for the disruption of burst generation in these cells. These conclusions raise the question: what causes the increase in RMP in *Mecp2*-null IB cells? The study described above (Wang and McCormick, 1993) also show that activation of mGlu-R and mACh receptors caused an increase in RMP and resulted in the same outcome for bursting cells, and this effect was modulated by changes K^+ currents, including those that are Ca^{2+}-activated. Therefore, in the next chapter of this thesis, the role of Ca^{2+} concentration in layer V IB cells will be investigated in WT and *Mecp2*-null brain slices.

4.3.3 Fewer IB cells were recorded from *Mecp2*-null brain slices compared to WT

During intracellular recordings, I noticed that not only were the firing patterns of KO IB cells altered in the absence of functional MeCP2 compared to WT, but also that proportionally fewer bursting cells were recorded in KO brain slices compared to WT (Fig. 4.4 A). Following classification, I noted that my KO pyramidal cell population contained a significantly smaller proportion of putative IB cells compared to the WT cell population (Fig. 4.4 C).

There are several possible explanations for why this difference was observed in my recorded cell populations. Firstly, one might assume that there are simply fewer IB cells in *Mecp2*-null brain slices, as a result of either disrupted neuronal cell development or poor cellular survival. However, this seemed an unlikely explanation given that previous studies showed no gross anatomical or morphological changes in the brains of human RTT patients (Armstrong et al. 1995). Furthermore, restoration of MeCP2 function in previously null mouse brains was sufficient to reverse the neurological deficits that arise as a result of MeCP2 loss of function (Guy et al. 2007; Robinson et al. 2012), which further supports the theory that the architecture of neuronal networks remains intact in KO slices.

A second explanation as to why fewer IB cells were recorded in KO slices is that the cells are present within the slices, and that I simply struggled to record from them. Reason for this could be that these cells become unstable in the absence of MeCP2 function. During intracellular recordings, even in WT cells, the piercing of the neuronal membrane with a sharp electrode is very invasive and can lead to cell death if the neuronal membrane is ruptured so much that a seal cannot form around the electrode tip. It is possible that the loss of MeCP2 function leads to destabilisation of KO IBs and as a result it is more difficult to find cells that form a seal around the electrode tip and stabilise long enough to record from them.

Finally, the third possible explanation for the observed reduction in the number of IB cells in the KO cell population compared to WT cells is that my cellular classification system is not rigorous enough to correctly identify all of the cells. In previous studies, IB pyramidal neurons were distinguished from RS cells based on their intrinsic bursting properties alone. However, I have shown earlier in this chapter that the bursting

mechanisms of IB cells are disrupted following the loss of MeCP2 function. This led to the conclusion that loss of MeCP2 function reduces the ability and / or likelihood of IB cells producing a burst of action potentials, and as a result, many KO IB cells would be wrongly classified as RS cells if using the conventional classification system only. Consequently, I adjusted my classification system in an attempt to account for this. I included the presence of an ADP component on single action potentials as a feature of IB cells for several reasons. Firstly, previous research studies have commented on the ADP as a common feature of IB cells that is rarely seen in RS cells (Hattox and Nelson, 2007). Another study showed that the cessation of bursting in these cells can be modulated by RMP, where an increase in RMP causes a switch from bursting activity to single-spike action potentials (Wang and McCormick, 1993). Example traces in this paper revealed that these single action potential events were associated with an ADP component at the end. Secondly, I noticed during the data acquisition phase of this project that when both WT and *Mecp2*-null bursting cells fired a single action potential, the event was often associated with an ADP phase. Furthermore, WT cells that did not burst almost never contained an ADP component. Finally, the decision to include ADP phases as a characteristic of IB cells was confirmed by later experiments whereby inhibiting the bursting mechanism of WT IB cells led to the generation of single action potentials that contained a clear ADP component (see Fig 5.2). Additionally, further experiments in non-bursting cells showed that the bursting potential of KO IB cells can be reinstated only when the cell's initial single action potentials were associated with an ADP phase (see Fig 5.5). With this information, I feel confident that including ADP-positive cells within the class of IBs is an acceptable adjustment to the classification system. However, despite this modification, I still recorded significantly fewer IB cells as a proportion of all pyramidal cells in KO slices compared to WT slices, which suggests that the changes made to the cellular classification system remain insufficient for the correct identification of each cell type. To rectify this, I would need to find a new variable that can correctly identify the two pyramidal cell types without relying on the bursting mechanism and / or ADP phase as the defining features.

4.3.4 Interneuron function following MeCP2 loss and implications for delta oscillations

During the experiments outlined in this project, I recorded from only excitatory pyramidal neurons, and not GABAergic interneurons. The reasons for this were two-fold: firstly, interneurons proved to be much less stable compared to excitatory neurons when impaled with the intracell recording electrode and therefore it was very difficult to keep

them long enough to record from. Secondly, due to unforeseen circumstances, intracellular recording experiments had to be terminated earlier than planned, meaning there was not time to learn the correct techniques needed to record from these cells. It would have been preferable to record from these cells given the involvement of GABAergic interneurons in the network processes underlying cortical delta oscillations. Importantly, layer V IB cells receive a barrage of fast IPSPs during the active phase of the delta oscillation from fast-spiking interneurons that results in burst termination, as well as slow IPSPs during the quiescent phase (Carracedo et al., 2013). Some fast-spiking interneurons also fire at theta frequency onto layer V RS cells which establishes the theta rhythms that can be seen nested within the network delta oscillation. These fast-spiking interneurons are known to be parvalbumin-positive (PV+).

Indeed, interneurons have been shown to be influential in the development of RTT-like phenotypes, with many studies showing that conditional loss of MeCP2 from a subset of interneurons leads to a variety of neurological deficits and replicates the phenotype of mice with global MeCP2 loss (Chao et al., 2010; Goffin et al., 2014; Ito-Ishida et al., 2015; Banerjee et al., 2016; Ure et al., 2016; Mossner et al., 2020). Furthermore, global MeCP2 loss leads to abnormal development of interneuron circuitry, with increased density of PV+ interneurons compared to WT mice, and these differences were shown to supersede the onset of RTT-like phenotypes in these animals (Tomassy et al., 2014). In the visual cortex, conditional loss of MeCP2 from only PV+ interneurons did not result in full recapitulation of the RTT-like phenotype but did abolish the experience-dependent critical period of plasticity that is required for the proper development of the visual networks (He et al., 2014). Furthermore, *Mecp2*-null PV+ interneurons exhibited increased intrinsic excitability, reduced ERPs, and fewer synaptic connections with excitatory cells. These findings are replicated in the primary sensory and primary motor cortices also, where PV+ interneurons are more abundant and exhibit atypical plasticity and connectivity with excitatory neurons in the network (Morello et al., 2018). Interestingly, mutations in CDKL5, which are known to cause a subset of atypical RTT cases, also lead to disruption of neuronal network formation including the organisation of PV+ interneurons (Pizzo et al., 2016), highlighting further the importance of interneuron function in the development of RTT-associated neurological deficits. In the visual cortex, PV+ interneurons have reduced responses following loss of MeCP2 in both global and conditional knockout models compared to WT, with both excitatory and inhibitory conductances reduced along with circuit-wide reductions in pyramidal cell response reliability and selectivity (Banerjee et al., 2016). Together these data suggest PV+ interneurons (synonymous with fast-spiking interneurons) have abnormal firing patterns

and connectivity following less of MeCP2 function that affect the excitation/inhibition balance in the cortex and have significant consequences for pyramidal cell firing within the network. Given the role of these inhibitory cells in the generation of cortical delta oscillations, it is predicted that the effects of MeCP2 loss on these cells will contribute to the disruption in cortical delta oscillations seen in *Mecp2*-null animals.

4.3.5 MeCP2 mutations in distinct neuronal circuits and generalisability of results

As previously discussed, MeCP2 is expressed in every cell in the body, however the levels of expression differ between tissue and cell types. In the brain, MeCP2 expression levels vary between brain regions, neuron types and at different developmental stages. As a result, it is unsurprising that the effects of mutations in MeCP2 are not uniform across distinct brain regions. Indeed, individual neuronal circuits are differentially affected by MeCP2 mutations (Shepherd and Katz, 2011). For example, synaptic hyperexcitability is a prominent feature of *Mecp2*-null microcircuits in the brainstem, local ceruleus and hippocampus (Zhang et al., 2008; Taneja et al., 2009; Calfa, Hablitz and Pozzo-Miller, 2011; Kron et al., 2011), while circuits within the sensory and motor cortices exhibit suppressed synaptic activity (Dani et al., 2005; Dani and Nelson, 2009; Wood and Shepherd, 2010). It is also believed that the communication between distinct circuits, such as the brain stem and cortices, is affected by the loss of MeCP2.

Previously, activity-dependent mapping of the immediate early gene Fos (activated following neuronal depolarisation) was used in WT and *Mecp2*-KO mice, to establish the influence of MeCP2 mutations on basal neuronal activity across the brains macrocircuits (Kron et al., 2012). In symptomatic (~ 6 weeks old) *Mecp2*-null mice, a large number of forebrain structures, including the motor, auditory, somatosensory and visual cortices, caudate/putamen and the prelimbic and infralimbic cortices, exhibited reduced Fos levels compared to age-mated WT animals. In cortical regions, the effect of MeCP2 loss on Fos mapping was not specific to cortical lamina, but rather a general reduction occurred in all laminae. Regions such as the hippocampus, thalamus and hypothalamus exhibited no significant difference in Fos levels between WT and *Mecp2*-KO mice. Several structures in the brainstem and cerebellum exhibited a marked increase in Fos labelling compared to WT mice. These findings are in line with the levels of hyper and hypo-excitability in these regions that was discussed in the previous paragraph. Interestingly, pre-symptomatic (~3 weeks old) *Mecp2*-null mice exhibited no differences in Fos mapping across all brain regions studies, and it was also noted that changes in

excitability levels began to develop at the same time that differences in Fos mapping levels began to emerge (Kron et al., 2012). Together these findings mean it is difficult to generalise the findings of the results presented in this thesis to other brain regions or to the whole brain, since it is clear that the effects of MeCP2 loss on all brain regions are not always the same as the effects felt by the somatosensory cortex. This is reflected in the results of previous studies looking at delta oscillations in *Mecp2*-null brains, whereby delta oscillation power was increased, decreased or non-significantly different compared to WT brains, with different studies looking at different brain regions. Furthermore, some studies simply looked at delta oscillations across the whole brain, which does not take into account the regional specificity of the effects of MeCP2 mutations (see Chapter 1.4.7 for more detail). The results discussed in this paragraph compliment the data presented so far in this thesis: the loss of cortically generated delta oscillations (see Chapter 3.2.1) and the disrupted bursting and spontaneous firing of IB cells in the somatosensory cortex of *Mecp2*-null brains is in line with overall reduced neuronal activity in these areas, as shown through Fos mapping in Kron et al. (2012). Furthermore, the findings that thalamic neuronal activity levels did not differ significantly between genotypes corroborates the findings in Chapter 3.2.3 whereby thalamically-generated delta oscillations are preserved in the absence of MeCP2.

Finally, it remains to be discussed whether the findings presented in this thesis, which pertain only to neuronal circuits in the somatosensory cortex, can be generalised to other regions of the cortex. As discussed above, Kron et al. (2012) showed that cortical areas overall experience suppressed neuronal activity following loss of MeCP2 function, which may lead one to think that delta oscillations and IB cell firing patterns will be similarly affected across the cortex. However, different regions of the cortex vary significantly in their structures and circuitry. For example, the motor cortex, which lies just the other side (on the anterior side) of the central sulcus to the somatosensory cortex, is largely devoid of the cortical layer IV, with layer II/III transitioning straight into layer V. Regions such as the somatosensory cortex rely on layer IV as the location for major thalamic inputs as well as input from other cortical areas (see Chapter 1.5.1 and Figure 1.6); in the motor cortex, most thalamic input is instead received by layer V directly. This highlights the fact that microcircuits within the motor cortex are wired differently to those in the somatosensory cortex, and these nuances will impact the processes involved in delta oscillation generation within each region. Indeed, the motor cortex of *Mecp2*-null mouse brains exhibits reduced structural complexity and synchrony and increased inhibitory drive (Tropea et al., 2009; Li et al., 2021), similar to results previously discussed in the somatosensory areas. However, given the structural differences in neuronal

circuitry between the two areas, and the fact that delta oscillation generation relies on such precise and complex circuitry in the somatosensory cortex, the results presented so far in this thesis cannot be generalised to areas of the cortex outside the somatosensory cortex, where the circuitry is not the same.

4.4 Summary

The results of the experiments presented in this chapter have provided substantial evidence for the mechanism in which cortical delta oscillation generation is disrupted following the loss of MeCP2 function. At the cellular level, I showed that the bursting activity of layer V pyramidal IB cells is disrupted in *Mecp2*-null brain slices. Specifically, these cells burst less frequently when artificially stimulated and almost never burst spontaneously. Their cellular characteristics are also affected in the absence of functional MeCP2, including most notably an increase in RMP. In contrast, the firing patterns and cellular properties of layer V RS pyramidal cells were unaffected in these brain slices.

So far in this thesis I have examined the role of MeCP2 on the isolated networks and cells that are responsible for generating delta oscillations in the somatosensory cortex. The next stage of this project will look at the effect of loss of MeCP2 function on the molecular mechanisms that regulate the bursting properties of IB pyramidal cells, including an investigation into the potential cause of increased RMP.

Chapter 5 – Molecular consequences of loss of MeCP2 function in layer V pyramidal neurons

5.1 Aims

In the previous chapters of this thesis, I demonstrated that the generation of neocortical delta rhythms is impaired in isolated cortical slices from *Mecp2*$^{Stop/y}$ mice. This is caused by the disruption of bursting mechanisms in layer V intrinsically bursting (IB) pyramidal neurons that are responsible for generating these rhythms (Carracedo et al. 2013). Given the importance of calcium ion (Ca^{2+}) regulation for the bursting of IB cells, I hypothesise that loss of MeCP2 function impairs Ca^{2+} concentration homeostasis in IB pyramidal neurons. Thus, in this chapter I will assess the implications of modulating Ca^{2+} concentration on layer V IB pyramidal neuron firing and cortical delta oscillation generation in *Mecp2*$^{Stop/y}$ mice.

5.2 Results

5.2.1 Increasing intracellular Ca2+ concentrations inhibit the bursts of spike generation that characterise IB neurons

It has previously been suggested that increased intracellular Ca^{2+} concentrations inhibits the bursting potential of IB neurons (see Chapter 1.5.3). To support these findings, I treated a WT IB neuron from layer V of the S1 cortex with 20 μM cyclopiazonic acid (CPA) – an inhibitor of the sarco-endoplasmic reticulum calcium ATPase (SERCA) pump. Inhibition of SERCA leads to an increase in intracellular Ca^{2+} concentration by preventing the transport of Ca^{2+} into the ER (see Fig. 5.1). CPA treatment led to a progressive, time-dependent loss in the generation of both spontaneous and induced bursting in IB neurons (Fig. 5.2). After 30 minutes of treatment, the IB neuron only exhibited single spontaneous action potentials or single action potentials in response to a current pulse (Fig. 5.2). Notably, these single action potentials always contained an ADP component. These results support the hypothesis that increased intracellular Ca^{2+} concentrations can inhibit the bursting potential of layer V IB pyramidal neurons.

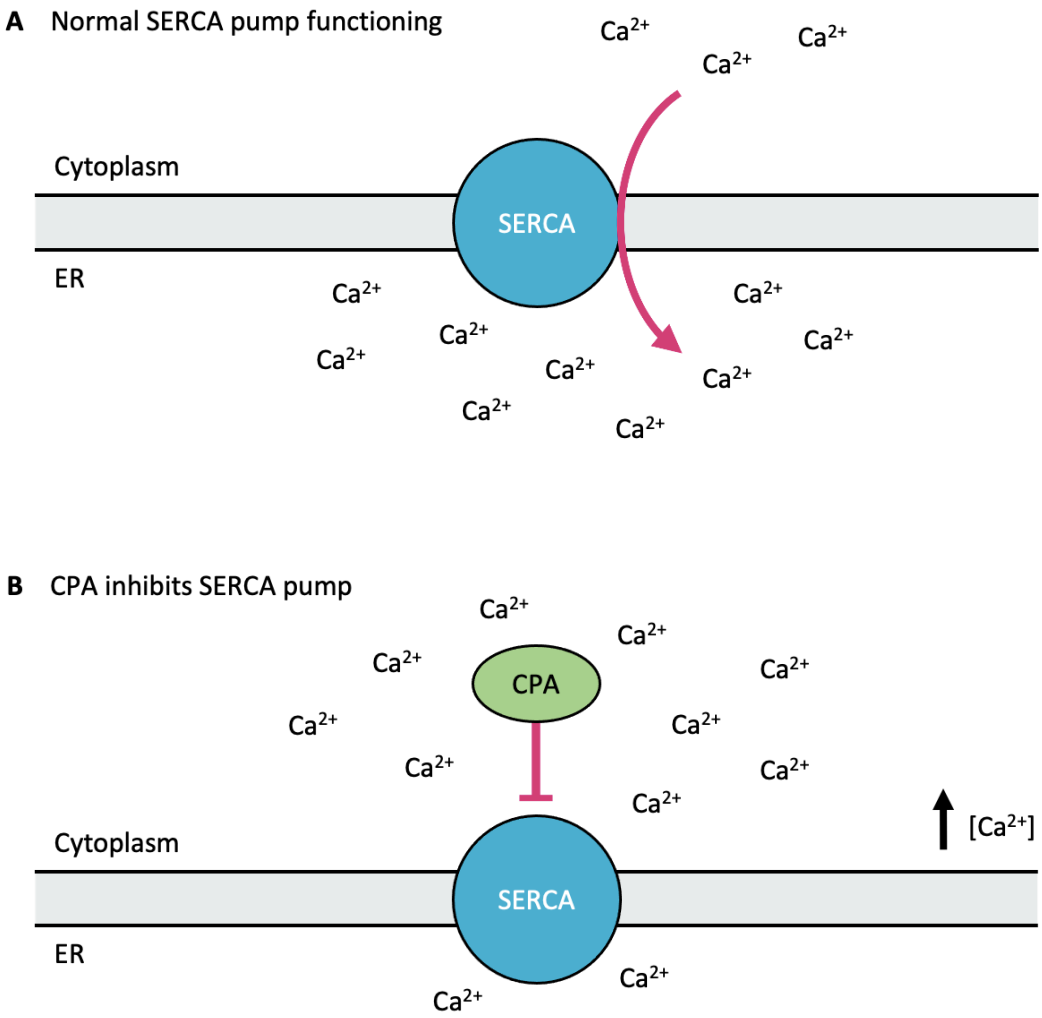

Figure 5.1: Inhibition of the SERCA pump via CPA application. (A) The normal functioning of the SERCA pump serves to transport Ca^{2+} from the cytoplasm to the endoplasmic reticulum (ER) for storage. **(B)** Cyclopiazonic acid (CPA) inhibits the SERCA pump, which leads to an increase in the cytosolic concentration of Ca^{2+}.

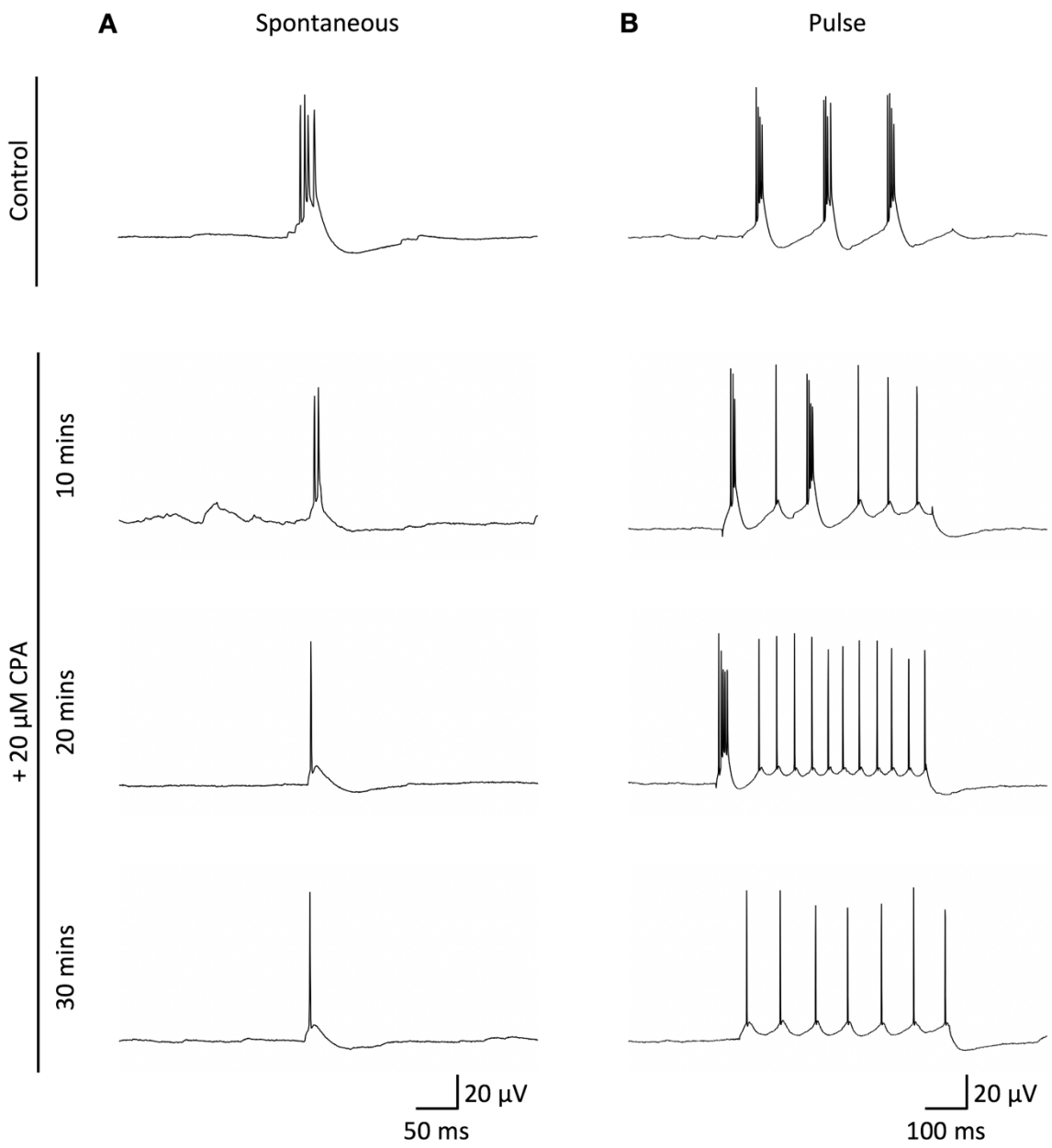

Fig. 5.2: Increasing the intracellular concentration of calcium ions extinguishes the bursting potential of WT IB neurons. (A) Example traces showing the spontaneous activity of a WT IB neuron before (control) and after the application of cyclopiazonic acid (CPA, 20 µM). **(B)** Example traces from the same cell in A in response to a depolarising current pulse (+0.2 nA, 500 ms). Upper traces = control conditions, prior to CPA application; upper middle = 10 minutes post-CPA; lower middle = 20 minutes post-CPA; lower traces = 30 minutes post-CPA.

5.2.2 Increasing intracellular Ca^{2+} concentration inhibits the generation of cortical delta oscillations

With the knowledge that elevated intracellular calcium levels inhibit the bursting mechanism of WT IB cells, I sought to determine whether this was also sufficient to abolish the pharmacologically-induced cortical delta rhythm that was previously recorded and analysed in Chapter 3 of this thesis. To this end, extracellular recording techniques were again utilised, and coronal brain slices containing isolated regions of somatosensory cortex from WT and KO mice were exposed to CCH (4 μM) and SCH-23390 (10 μM) to induce oscillatory activity in the 0.5 - 4 Hz bandwidth. As before, control recordings were taken prior to the addition of CCH and SCH-23390 to confirm the absence of delta oscillations pre-drug treatment (Fig. 5.3 A, upper). Within 120 minutes of CCH and SCH-23390 application, stable delta oscillations were observed (Fig. 5.3 A middle). At this point, 20 μM CPA was added via bath application to the slice and a two-minute recording was taken every five minutes thereafter. After 30 minutes of CPA treatment, the previously established delta rhythm had been abolished (Fig. 5.3 A lower). FFT analysis of the recordings showed that oscillatory activity within the 0.5 - 4 Hz bandwidth was reduced almost back to control levels following treatment with CPA (Fig. 5.3 B). Peak power values of activity within the delta bandwidth at 30 minutes post-CPA treatment was significantly reduced compared to values after CCH and SCH-23390 treatment only ($n=7$, $p<0.001$, One-way ANOVA with Tukey's multiple comparisons test, Fig. 5.3 C), and not significantly different from power values during control recordings ($n=7$, p=ns, One-way ANOVA with Tukey's multiple comparisons test, Fig. 5.3 C). Finally, the frequency at which peak power values were recorded did not differ significantly between either of the three conditions in this experiment ($n=7$, p=ns for all, One-way ANOVA with Tukey's multiple comparisons test, Fig. 5.3 D).

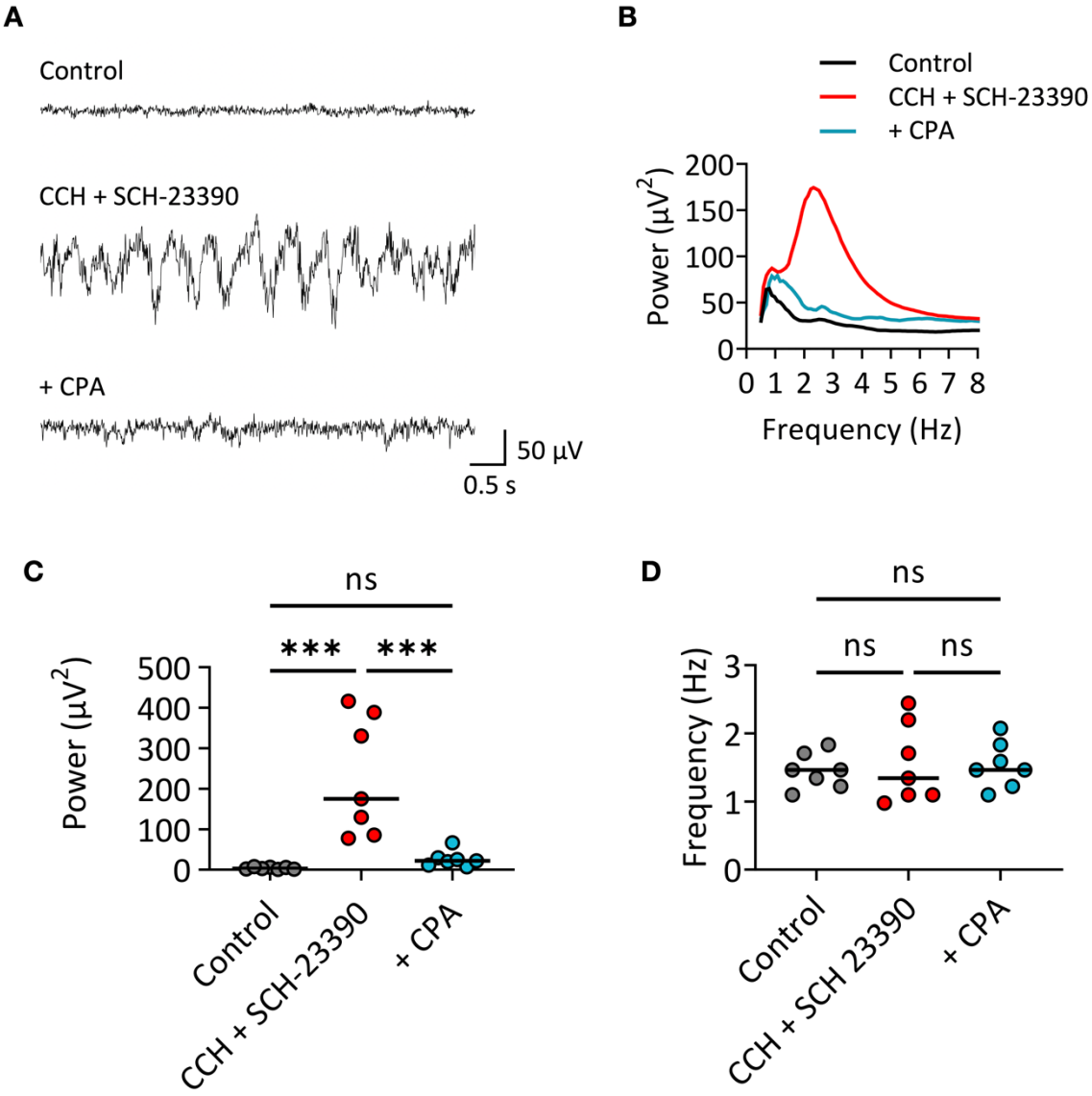

Fig. 5.3: Increasing the intracellular concentration of calcium ions abolishes the pre-existing cortical delta rhythm. (A) 5 second example LFP signal traces (0.3 - 100 Hz bandwidth) from the same WT coronal brain slice containing isolated somatosensory cortex under three sequential conditions: upper = control, no drug-treatment; middle = 120 minutes post-CCH (4 µM) and SCH-23390 (10 µM) treatment; lower = 30 minutes post-CPA (20 µM) treatment. **(B)** Example power spectral density of control (black), post-CCH and SCH-23390 (red), and post-CPA (blue) treatment recordings as seen in A. **(C and D)** Delta oscillation peak power values (C) and the frequency at which these occurred (D) during the three conditions described above. Each symbol represents one data point (one animal), horizontal lines represent median values. *** = $p<0.001$, ns = not significantly different.

5.2.3 Reducing intracellular calcium concentration restores the bursting potential of *Mecp2*-null IB cells

Previously, I have shown that increasing the intracellular concentration of calcium ions can inhibit the bursting mechanism of a previously-bursting WT IB cell and is sufficient to abolish the endogenous cortical delta rhythm in mouse brain slices of isolated somatosensory cortex. Both of these results in WT cells and slices mimic closely the firing patterns and oscillatory activity seen in KO brain slices, which led to the theory that MeCP2 loss causes increased intracellular Ca^{2+} concentration. This in turn would prevent KO IB cells from bursting and inhibit the generation of the cortical delta rhythm. To study this theory further, I applied 0.1M EGTA intracellularly to several non-bursting KO cells and recorded the effects of this through the previously described intracellular recording techniques. EGTA acts as a calcium-chelator: it binds to free Ca^{2+} ions in the cytoplasm and prevents the ions from interacting with any other cytosolic or membrane-bound binding partners, therefore effectively reducing the concentration of free Ca^{2+} in the cytosol (Fig. 5.4).

When EGTA was applied to a non-bursting KO cell it had one of two effects. Firstly, when applied to what would later be identified as an IB cell, EGTA induced bursting activity within 5 minutes of application (Fig. 5.5 A upper middle). This cell was previously very spontaneously active but firing only single action potentials each with a large ADP

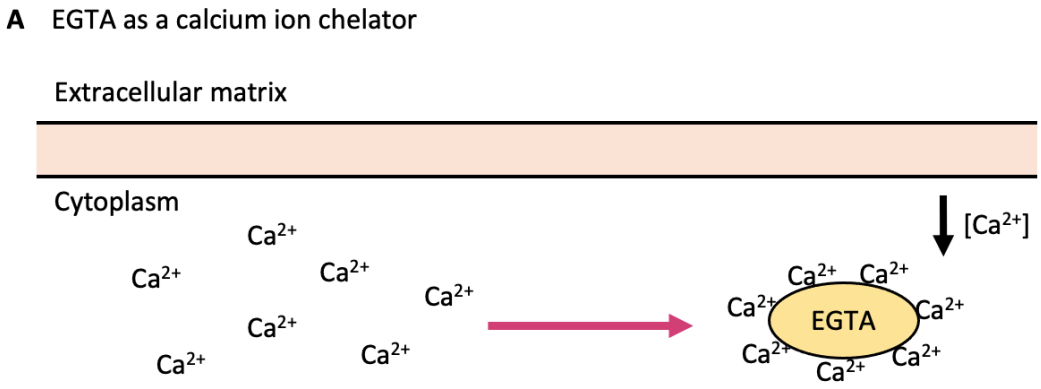

Fig 5.4: Reduction of intracellular calcium ion concentration via the addition of the calcium chelator EGTA. (A) Addition of EGTA to the cytoplasm acts as a Ca^{2+} chelator and therefore reduces the concentration of free Ca^{2+} in the cytoplasm.

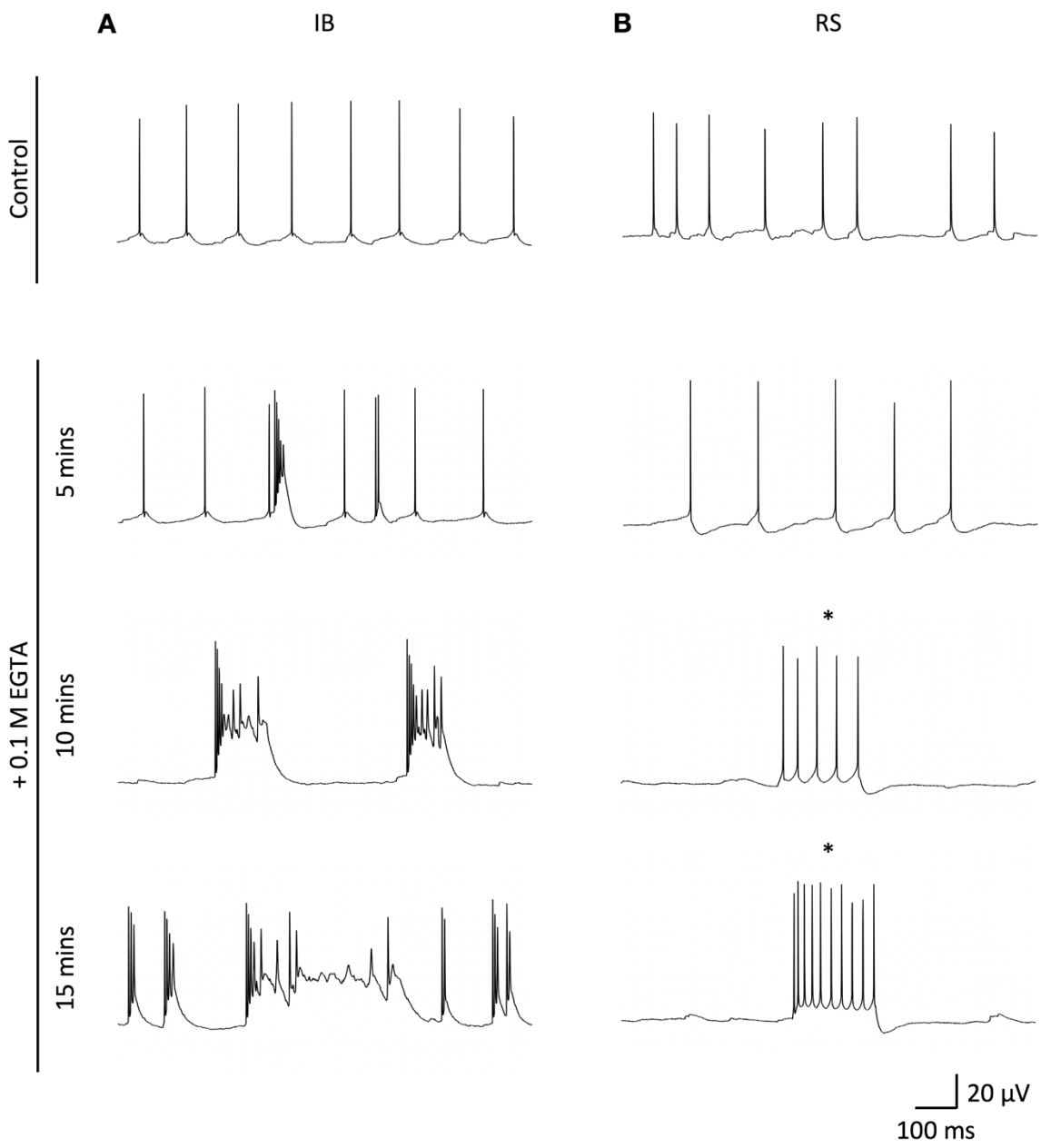

Fig. 5.5: Reducing the intracellular concentration of calcium ions is sufficient to re-establish the bursting potential of KO IB neurons, but does not alter the firing patterns of KO RS cells. (A) Example traces showing the spontaneous activity of a KO IB cell before (control, upper trace) and after (lower three traces) the application of EGTA (0.1M). **(B)** Example traces from a KO RS cell, under the same conditions as those described in A. Traces marked with * represent activity in response to stimulation via pulse depolarisation (+0.2 nA, 500ms) since the cell was no longer spontaneously active. Upper traces = control conditions, prior to EGTA application; upper middle = 5 minutes post-EGTA; lower middle = 10 minutes post-EGTA; lower traces = 15 minutes post-EGTA.

component under control conditions (Fig. 5.5 A upper). After 5 minutes of EGTA treatment, this cell exhibited small bursts of activity interspersed with single action potentials, followed by almost exclusively burst events after 10 minutes (Fig. 5.5 A lower middle). Finally, after 15 minutes of treatment, the cell remained very spontaneously active with large bursting events that lasted a very long duration (Fig. 5.5 A lower). Shortly after this time the cell was lost. In contrast, when EGTA was applied to a non-bursting KO cell that would later be identified as an RS cell, EGTA had little effect on the firing pattern of the cell. This cell was spontaneously firing single action potentials without an ADP under control conditions (Fig. 5.5 B upper) and continued to fire in the same manner after 5 minutes of EGTA treatment (Fig. 5.5 B upper middle). After 10 and 15 minutes of treatment, the cell had ceased firing spontaneously, however under pulse depolarisation conditions continued to only fire single action potentials with no ADP component (Fig. 5.5 B lower middle and lower respectively).

5.2.4 Cortical delta oscillations are restored in *Mecp2*$^{Stop/y}$ mice by pharmacological blockade of voltage-gated calcium channels

With the knowledge that reducing the intracellular concentration of Ca^{2+} ions is sufficient to restore the bursting potential of KO IB cells, I next sought to determine whether this would also be sufficient to reinstate the cortical delta rhythm at the level of the network. To this end, extracellular recording techniques were again utilised. Additional pharmacological entities known to selectively inhibit Ca^{2+} entry into the cell were used in conjunction with CCH and SCH-23390 to determine whether reducing the intracellular Ca^{2+} concentration could indeed lead to the generation of cortical delta oscillations in the isolated somatosensory cortex from *Mecp2*-null mice. These pharmacological agents target Ca^{2+} entry via the inhibition of VGCCs (Fig. 5.6).

As before, control recordings were taken before the application of any drugs to verify the absence of oscillatory activity under control conditions. All activity elicited after drug application was compared against baseline recordings (despite only one example control recording shown on Fig. 5.7 A, first trace) and also against the oscillatory activity elicited after CCH and SCH-23390 alone were added (Fig. 5.7 A second trace). Firstly, I added amlodipine (4 μM), an N-type VGCC blocker, in conjunction with CCH and SCH-23390, and found that within two hours of drug treatment, clear and robust oscillatory activity could be identified in *Mecp2*-null brain slices (Fig. 5.7 A third trace). FFT analysis of these recordings revealed that this oscillatory activity fell within the delta (0.5 - 4 Hz)

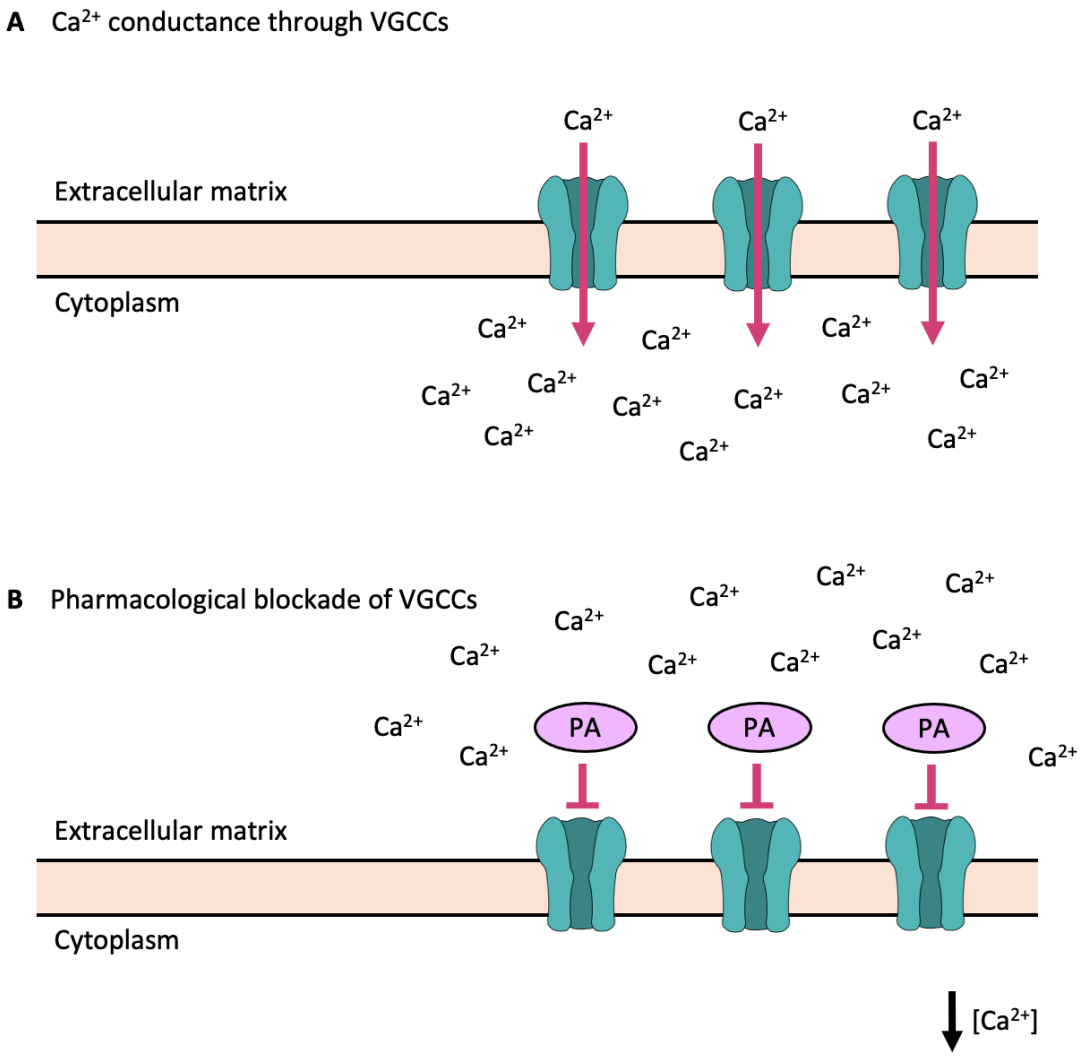

Fig. 5.6: Pharmacological blockade of voltage gated calcium channels inhibits calcium ion entry into the cell. (A) Calcium ions enter the cell via the activation of voltage gated calcium channels (VGCCs, blue channel). **(B)** The addition of pharmacological agents (PA, eg: amlodipine, nifedipine, SNX-482 or NNC 55-0396) inhibit the transport of Ca^{2+} across the plasma membrane via VGCCS and therefore reduce the intracellular ion concentration.

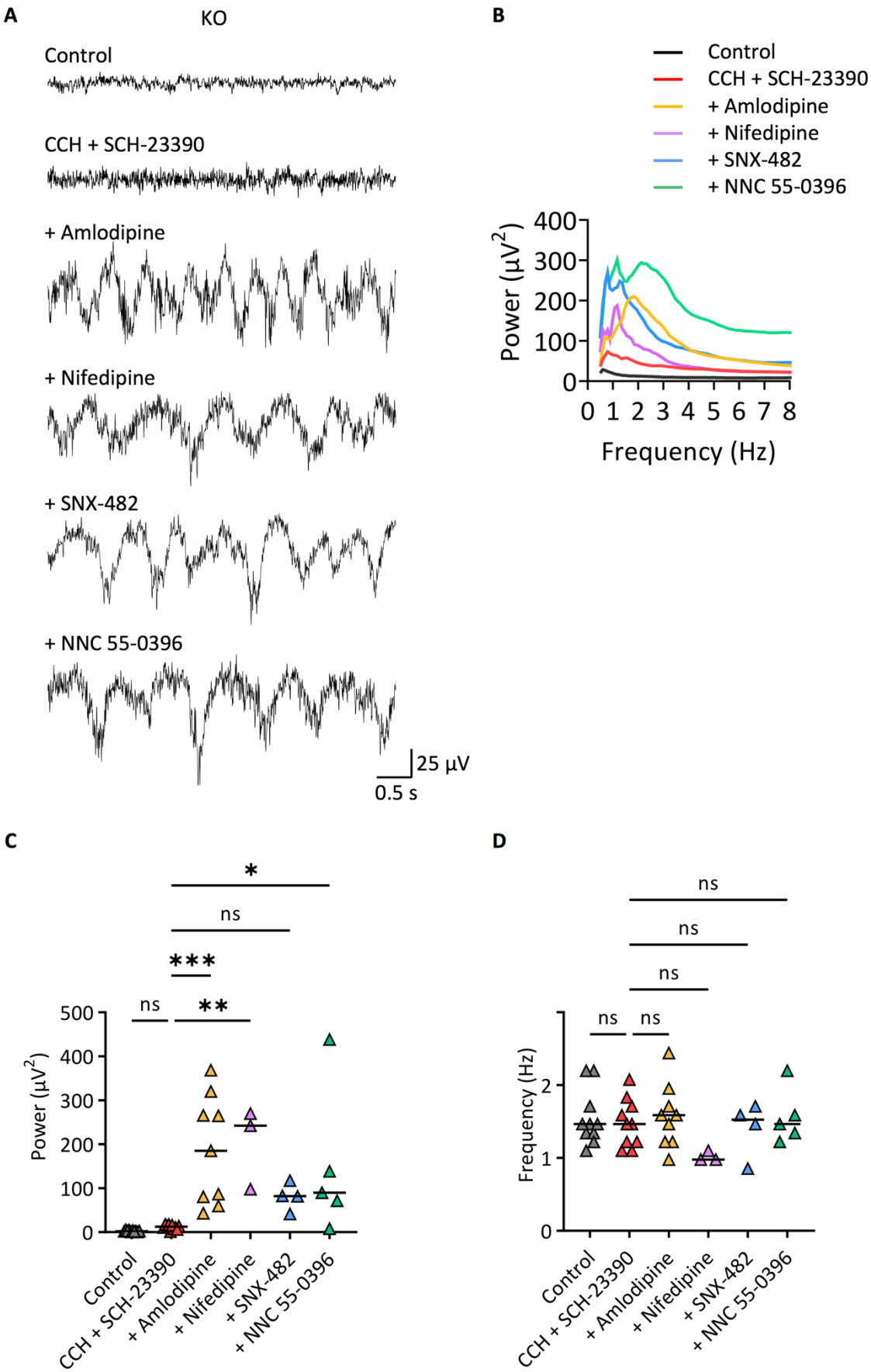
A
KO
Control
CCH + SCH-23390
+ Amlodipine
+ Nifedipine
+ SNX-482
+ NNC 55-0396
25 µV
0.5 s
B
Control
CCH + SCH-23390
+ Amlodipine
+ Nifedipine
+ SNX-482
+ NNC 55-0396
Power (µV²)
400
300
200
100
0
0 1 2 3 4 5 6 7 8
Frequency (Hz)
C
*
ns
***
ns
**
Power (µV²)
500
400
300
200
100
0
Control
CCH + SCH-23390
+ Amlodipine
+ Nifedipine
+ SNX-482
+ NNC 55-0396
D
ns
ns
ns
ns
ns
Frequency (Hz)
2
1
0
Control
CCH + SCH-23390
+ Amlodipine
+ Nifedipine
+ SNX-482
+ NNC 55-0396

Fig. 5.7: Reducing the intracellular concentration of calcium ions is sufficient to re-establish the neocortical delta rhythm in *Mecp2*-null coronal brain slices. (A) 5 second example LFP signal traces (0.3 - 100 Hz bandwidth) from KO coronal brain slices containing isolated somatosensory cortex, under the following conditions: first trace: control, pre-drug treatment; second trace: post-CCH (4 μM) and SCH-23390 (10 μM) treatment; third trace: +amlodipine (4 μM); forth trace: +nifedipine (20 μM); fifth trace: +SNX-482 (3 nM); sixth trace: +NNC 55-0396 (4 μM). **(B)** Example power spectral density of control (black), post-CCH and SCH-23390 (red), +amlodipine (yellow), +nifedipine (purple), +SNX-482 (blue) and +NNC 55-0396 (green) treatment, as seen in A. **(C and D)** Delta oscillation peak power values (C) and the frequency at which these occurred (D) during the six conditions described above. Each symbol represents one data point (one animal), horizontal lines represent median values. *** = $p<0.001$, ** = $p<0.01$, * = $p<0.05$, ns = not significantly different.

---

bandwidth (Fig. 5.7 B), and was significantly greater than the low power activity elicited by CCH and SCH-23390 alone (CCH and SCH-3390: n=7, +Amlodipine: n=9, $p<0.001$, One-way ANOVA with Holm-Šídák's multiple comparisons test, Fig. 5.7 C). These results show that by targeting and inhibiting the N-type calcium channel on the neuronal plasma membrane, I could re-establish the cortical delta rhythm and therefore rescue the oscillatory-phenotype of *Mecp2*-null brain slices.

I next sought to determine whether the proposed increase in intracellular Ca^{2+} levels in *Mecp2*-null IB cells is specific to the function of N-type VGCC. Specifically, is it the case that calcium entry through these channels alone is misregulated in the absence of MeCP2 function, or is the general process of calcium homeostasis dysfunctional? If the latter is the case, adding other pharmacological entities (alongside CCH and SCH-23390) that target and inhibit other sites of calcium entry into the cell would also be sufficient to re-establish the cortical delta rhythm. To this end, I repeated these experiments using three other VGCC inhibitors: nifedipine (20 μM), an L-type calcium channel blocker, SNX-482 (3 nM), an R-type calcium channel blocker, and NNC 55-0396 (4 μM), a T-type calcium channel blocker. The addition of each of these drugs in conjunction with CCH and SCH-23390 was sufficient to induce delta oscillations in KO slices of somatosensory cortex (Fig 5.7 A forth, fifth and six traces respectively). FFT analysis showed that, much like the effects of amlodipine, the effects of nifedipine, NNC 55-0396 and SNX-482 resulted in a large peak of oscillation power within the delta (0.5

- 4 Hz) bandwidth (Fig. 5.7 B). At the time point where these oscillations reached their peak power, nifedipine-induced oscillations were significantly greater in power than those with CCH and SCH-23390 alone (CCH and SCH-3390: n=7, +Nifedipine: n=3, $p<0.01$, One-way ANOVA with Holm-Šídák's multiple comparisons test, Fig. 5.7 C), as were NNC 55-0396-induced delta oscillations (CCH and SCH-3390: n=7, +NNC 55-0396: n=5, $p<0.05$, One-way ANOVA with Holm-Šídák's multiple comparisons test, Fig. 5.7 C). Despite the observation of delta oscillations in slices treated with SNX-482, the power of these oscillations was not deemed significantly different from the activity elicited from CCH and SCH-23390 alone (CCH and SCH-3390: n=7, +SNX-482: n=4, p=ns, One-way ANOVA with Holm-Šídák's multiple comparisons test, Fig. 5.7 C), which was attributed to small sample sizes confounding the statistical analysis. As with previous experiments, the frequency at which peak oscillation power values occurred did not differ significantly between any drug condition (p=ns for all conditions, One-way ANOVA with Holm-Šídák's multiple comparisons test, Fig. 5.7 D). Overall, these results suggest that the general process of calcium regulation within KO cells is disrupted by the loss of MeCP2 function. As a result, the intracellular Ca^{2+} concentration in layer V IB cells is significantly increased. This is responsible for inhibiting the generation of cortical delta oscillations by preventing the bursting of the IB pyramidal neurons that generate these rhythms. By reducing intracellular Ca^{2+} levels via a variety of different membrane-bound calcium channels, it is possible to re-establish the cortical delta rhythm in *Mecp2*-null brain slices.

5.2.5 Intracellular calcium concentrations must be tightly regulated for delta oscillations to be generated

The previous results of this chapter described how the addition of calcium-regulating drugs such as amlodipine, nifedipine, SNX-482 and NNC 55-0396 in conjunction with CCH and SCH-23390 was sufficient to re-establish the cortical delta rhythm that could not be generated with CCH and SCH-23390 alone in *Mecp2*-null mouse brain slices. The final stage of this series of experiments was to assess the effects of these drugs in WT slices to determine whether their effect on KO slices was dependent or independent of MeCP2 function. Specifically, if the addition of these drugs also increased the power of WT delta oscillations compared to CCH and SCH-23390 alone, then the mechanism by which these drugs induce delta oscillations in the KO slices, though still highly relevant, would be deemed independent of MeCP2 function.

As with previous experiments, control recordings were taken before the application of any drugs (despite only one example control recording shown on Fig. 5.8 A first trace). The recordings taken with amlodipine, nifedipine, SNX-482 or NNC 55-0396 in conjunction with CCH and SCH-23390 were compared both to their respective control recordings and also against the oscillatory activity elicited after CCH and SCH-23390 alone were added (Fig. 5.8 A second trace). Interestingly, the application of each of these drugs prevented the induction of high-power delta oscillations in WT brain slices. Although small levels of oscillatory activity could often be observed in these recordings, these were neither consistent nor high power (Fig 5.8 A, lower four traces). FFT analysis of this data confirmed that peaks of activity existed in these recordings that corresponded to the 0.5 - 4 Hz bandwidth, but the average power of these oscillations was much reduced compared to when CCH and SCH-23390 were applied alone (Fig. 5.8 B). At the time points where these oscillations reached their peak power, CCH and SCH-23390-induced oscillations had a significantly greater power compared to all four calcium-regulating drugs (CCH + SCH-23390: n=12, +Amlodipine: n=5, +Nifedipine: n=5, +SNX-482: n=3, +NNC 55-0396: n=5, comparison to CCH + SCH-23390: +Amlodipine: $p<0.0001$, +Nifedipine: $p<0.001$, +SNX-482: $p<0.001$, +NNC 55-0396: $p<0.01$, One-way ANOVA with Holm-Šídák's multiple comparisons test, Fig. 5.8 C). These results not only confirm that the delta-inducing effect of these drugs in KO slices targets an MeCP2-dependent mechanism, but also highlights that intracellular calcium levels must be tightly regulated in order for cortical delta oscillations to be generated robustly and consistently. I have shown previously that when the intracellular calcium concentration is too high (as I hypothesise is the case in *Mecp2*-null IB cells), cortically-generated delta oscillations cannot be established within the network. Here, I also show in WT cells that reducing calcium levels below their usual levels is equally effective at preventing the generation of cortical delta oscillations.

5.3 Discussion

5.3.1 The role of Ca^{2+} in burst generation during IB cell firing

In the previous chapter, I discussed how the bursting potential of layer V IB pyramidal cells is modulated by the cell's resting membrane potential, which is itself modulated (at least in part) by Ca^{2+}-activated potassium conductance (Wang and McCormick, 1993). This theory is supported by the findings of other studies that also showed that cortical pyramidal cell bursting is dependent on calcium concentration (Rhodes and Gray, 1994;

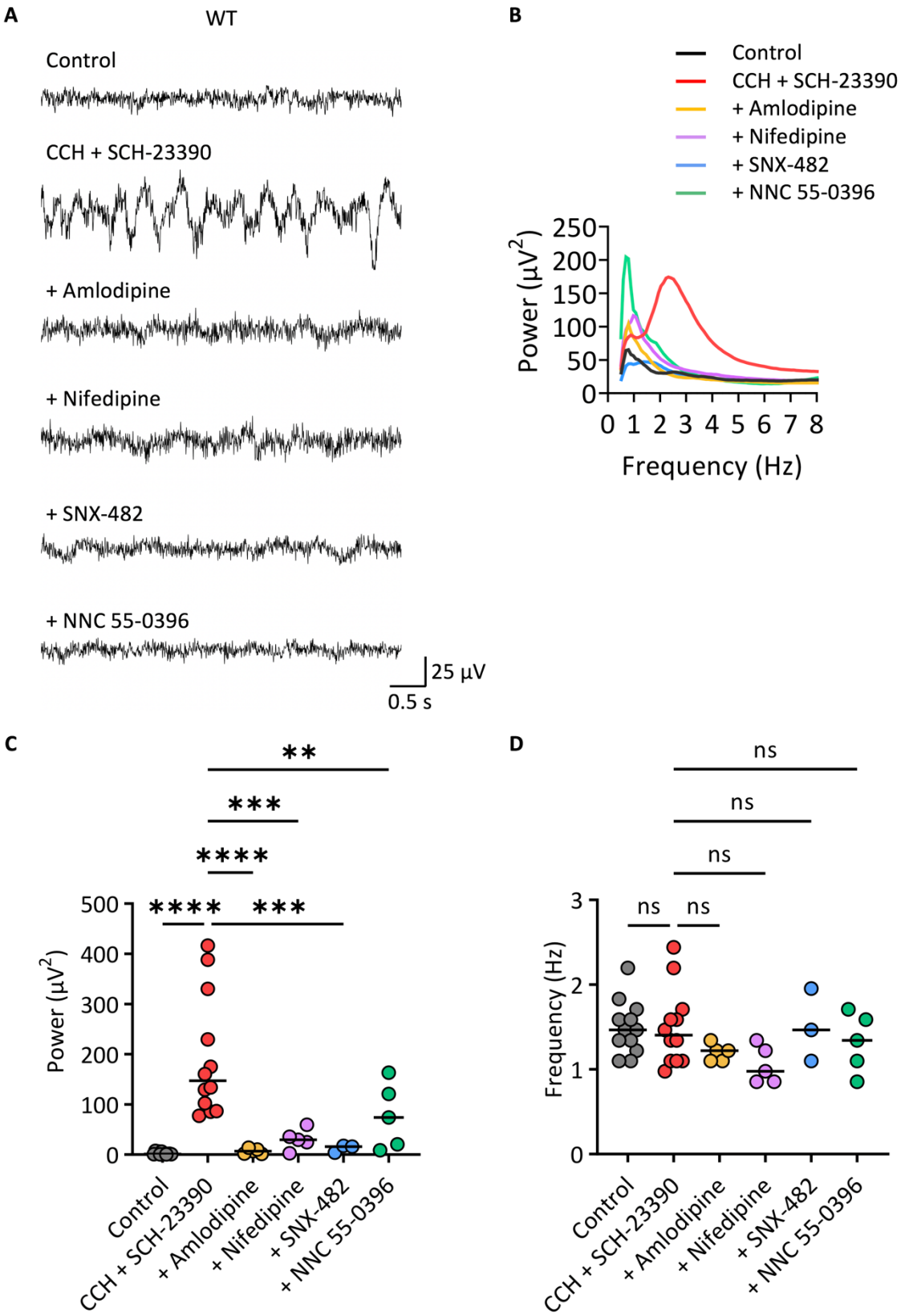

Fig. 5.8: WT delta oscillations cannot be generated when intracellular calcium ion concentrations are too low. (A) 5 second example LFP signal traces (0.3 - 100 Hz bandwidth) from WT coronal brain slices containing isolated somatosensory cortex,

under the following conditions: first trace: control, pre-drug treatment; second trace: post-CCH (4 μM) and SCH-23390 (10 μM) treatment; third trace: +amlodipine (4 μM); forth trace: +nifedipine (20 μM); fifth trace: +SNX-482 (3 nM); sixth trace: +NNC 55-0396 (4 μM). **(B)** Example power spectral density of control (black), post-CCH and SCH-23390 (red), +amlodipine (yellow), +nifedipine (purple), +SNX-482 (blue) and +NNC 55-0396 (green) treatment, as seen in A. **(C and D)** Delta oscillation peak power values (C) and the frequency at which these occurred (D) during the six conditions described above. Each symbol represents one data point (one animal), horizontal lines represent median values. **** = $p<0.0001$, *** = $p<0.001$, ** = $p<0.01$, ns = not significantly different.

Helmchen et al. 1999; Wang et al. 1998; Kole et al. 2007). The results presented in the first part of this chapter also confirm this theory by showing that increasing the intracellular Ca^{2+} concentration inhibits the bursting mechanism of WT IB cells, and results in the activation of single action potential firing (see Fig. 5.2).

In this chapter, I have shown that reducing the intracellular concentration of calcium ions can reinstate the bursting potential of *Mecp2*-null IB cells (see Fig. 5.5) and that this is also sufficient to re-establish the endogenous cortical delta rhythm in these slices (see Fig. 5.7). Therefore, I conclude from these findings that loss of MeCP2 function leads to an increase in the intracellular Ca^{2+} concentration in layer V IB pyramidal cells, and the effects of this are sufficient to disrupt IB cell bursting and consequently the generation of cortical delta oscillations. It has previously been suggested that Ca^{2+} currents in these cells modulate the bursting mechanism via their influence on potassium conductance (Wang and McCormick, 1993). Based on these results and the results presented in this thesis so far, I further hypothesise that the proposed increase in intracellular Ca^{2+} concentration reduces Ca^{2+} conductance into the neuron through the cell membrane, as a result of the diminished concentration gradient. The consequences of this are reduced activation of Ca^{2+}-activated potassium channels, and hence reduced K^+ conductance out of the cell. Since potassium currents through these channels are responsible for membrane repolarisation, the neuronal membrane of *Mecp2*-null IB cells does not repolarise sufficiently, leading to a less polarised RMP and consequently the inhibition of burst firing. This theory is corroborated by the findings presented in the previous chapter of this thesis that showed that the RMP of *Mecp2*-null IB cells is significantly less polarised than WT IB cells.

The present study is not the first to suggest that calcium currents are important for the generation of delta oscillations during NREM sleep. Previously, mice lacking the $\alpha 1_G$-subunit of the T-type VGCC exhibited loss of delta oscillations and reduced sleep spindle activity during both natural sleep and urethane-induced anaesthesia (Lee et al. 2004). Furthermore, the architecture of sleep was disrupted in these animals, who overall spent less time in slow-wave sleep (Stage 3 NREM) and exhibited an increase in the incidence of brief awakenings (>16 s) compared to WT animals. These characteristics have remarkable similarity to RTT patients and *Mecp2*-null animals, who also spend a reduced amount of time in Stage 3 NREM sleep and exhibit frequent sleep disturbances (Young et al. 2007; Wither et al. 2012; Ammanuel et al. 2015; Wong et al. 2015). Importantly, theta oscillations (the hallmark of REM sleep) were unaffected in mutant animals, as was the architecture of REM sleep states (Lee et al. 2004). These data suggest that the T-type VGCC, and specifically the $\alpha 1_G$-subunit, is required for the generation of NREM-associated brain rhythms and the maintenance of behavioural states during sleep. Interestingly, the authors of this study claim that these disruptions in sleep-related brain rhythms are modulated by thalamic T-type calcium currents, since the same $\alpha 1_G$-subunit knockout model previously revealed the absence of low-threshold spiking in thalamocortical cells (Kim et al. 2001). This low-threshold spiking modulates the refractory period of these cells, and subsequently encodes the firing patterns of thalamocortical networks. Indeed, these cells exhibit reduced burst firing in the absence of the $\alpha 1_G$-subunit. With this information, in the more recent study the authors declare that the loss of delta oscillations in EEG recordings relates to thalamically-generated delta, and cortically-generated delta oscillations are not mentioned. While this is a reasonable conclusion to make based on the findings of their earlier paper, it is worth noting that during *in vivo* recordings, it is difficult to differentiate between delta oscillations that have a thalamic and cortical origin. Furthermore, the two delta oscillation generators are known to function independently of each other, and therefore the global loss of delta oscillations in Lee et al. (2004) suggests that loss of function in the $\alpha 1_G$-subunit also disrupts cortical delta generators too. Overall, these findings suggest an important role for T-type calcium channel currents in pyramidal cell bursting and delta oscillation generation.

Previously in this thesis I showed that cortically-generated delta oscillations are disrupted following the loss of MeCP2 function, whereas thalamically-generated delta oscillations remain intact (see Chapter 3). I also discussed how the function of MeCP2 differs with brain region and even cell-type specificity (see Chapter 4.3), meaning that the loss of MeCP2 function does not have the same consequences in all regions and

cell types within the brain. Therefore, it is possible that the global loss of MeCP2 has important implications that are specific only to the cortex, such as disrupted calcium homeostasis that leads to the disruption of IB cell bursting and consequently cortical delta oscillation generation, as proposed in this chapter. The studies discussed above implicate T-type Ca^{2+} channels in the generation of these neuronal events and rhythms, however the data I presented at the end of this chapter showed that IB cell burst firing and cortical delta oscillations could be reinstated by modulating one of four different type of VGCC: N-, T-, L- and R-type channels (see Fig. 5.7). This suggests the root of the problem in *Mecp2*-null IB cells does not lie solely with T-type channels, but rather in the general mechanism of calcium ion regulation. As MeCP2 functions (at least in part) as a master regulator of gene expression, I next will discuss the implications of this on Ca^{2+} homeostasis in *Mecp2*-null animals and RTT patients.

5.3.2 Gene expression changes and Ca^{2+} regulation in *Mecp2*-null neurons

Previously it has been shown that global changes in gene expression levels across the whole brain are relatively subtle following the loss of MeCP2 function (Tudor et al. 2002). However, genotype differences in transcriptome architecture begin to emerge when individual brain regions are sampled in isolation, with the differences between brain regions relating to differential genes affected in each area, not just the same genes affected by different amounts (Smrt et al. 2007; Chahrour et al. 2008; Ben-Shachar et al. 2009). It has been postulated that the difference in gene expression levels between brain regions in *Mecp2*-null mice is greater than the overall difference between *Mecp2*-null and WT mouse brains (Zhao et al. 2013), highlighting the degree to which MeCP2 function is brain-region, and possibly even cell-type, specific. The observed differences in MeCP2-mediated gene regulation between different brain regions is perhaps not so surprising given that the distribution of mC, the major genomic binding target of MeCP2, varies considerably between regions and cell-types, which is correlated with the brain region specificity of MeCP2 expression (Olson et al. 2014).

Many of the genes whose expression levels are affected by the loss of MeCP2 could directly contribute to neurological dysfunction and disease (Jordan et al. 2007). Post-mortem analysis of the brains of RTT patients revealed several hundred genes whose expression levels were misregulated with respect to WT brains, and within these, there exists specific clusters of genes who share a common functional role (Colantuoni et al.

2001). For example, a large group of genes involved in synaptic development had significantly dysregulated expression levels and are thought to contribute to the abnormalities in dendritic morphology observed in *Mecp2*-null animals (Armstrong et al. 1995; Kishi and Macklis, 2004; Zhou et al. 2006). Interestingly, alterations in gene expression levels occur at the post-, but not pre-, symptomatic stage in *Mecp2*-null animals (Sanfeliu et al. 2019) and coincide with the postnatal peak in MeCP2 abundance (Zhao et al. 2013), again highlighting the importance of MeCP2-mediated gene regulation in neurological function. Furthermore, in clonal cells from RTT patients, those with similar mutation types (eg, MBD vs TRD mutations) exhibited similar changes in gene expression levels and could be differentiated from one-another based on these transcriptome differences, as could patients who met the criteria for a clinical RTT diagnosis without an MeCP2 mutation (Ballestar et al. 2005; Nectoux et al. 2010).

Given that inhibition of four different types of VGCC was sufficient to reinstate the cortical delta oscillation in *Mecp2*-null IB cells (see Fig. 5.7), the results in this chapter suggest that the general mechanism of Ca^{2+} homeostasis is disrupted following the loss of MeCP2 function. With this information and the knowledge that one of the proposed functions of MeCP2 is in the regulation of gene expression, I sought to determine whether loss of MeCP2 leads to misregulation of genes involved in calcium homeostasis.

It has previously been discussed in this thesis how MeCP2 binds across the entire neuronal genome, and consequently has an unknown number of binding targets, though it is generally accepted this number lies within the thousands. The result of this is that gene expression analysis (usually via RNA sequencing) of *Mecp2*-null neuronal transcriptomes revealed hundreds, sometimes thousands, of genes whose expression levels were either up- or down-regulated compared to WT (Colantuoni et al. 2001; Ballestar et al. 2005; Jordan et al. 2007; Chahrour et al. 2008; Ben-Shachar et al. 2009; Pacheco et al. 2017). The function of these genes ranges vastly, and includes processes such as cellular differentiation, metabolic regulation, ion transport, synaptic vesicle cycling and neurotransmitter production, among others. Unfortunately, this can make it difficult to define the exact mechanism by which MeCP2 loss-of-function leads to the phenotypes seen in RTT and the associated animal models. Indeed, with regards to the data presented in this thesis, we are unlikely to find a single gene whose expression levels are misregulated in the KO model, which would solely account for the proposed increase in intracellular Ca^{2+} concentration in layer V IB cells. Nevertheless, it is reassuring that several studies have identified clusters of genes involved in calcium ion

regulation and signalling whose expression levels are misregulated following the loss of MeCP2 (Chahrour et al. 2008; Ben-Shachar et al. 2009; Zhao et al. 2013; Pacheco et al. 2017). For example, in the cortex, the *CACNB3* gene that encodes the β3-subunit, which is common to several VGCCs, is increased following the loss of MeCP2 function (Pacheco et al. 2017), which supports the theory of increased VGCC activity in *Mecp2*-null cells. Interestingly, in the hypothalamus, the *CACNB3* gene is downregulated in *Mecp2*-null animals (Chahrour et al. 2008), further highlighting the regional-specificity in which MeCP2 functions. In these two studies, several genes encoding calcium binding proteins, including *CALB1* and *CALR*, as well as various genes involved in the CaM-kinase signalling pathway are also misregulated following the loss of MeCP2.

Of particular note, the *CACNA1G* gene, which encodes the T-type α1G-subunit, is downregulated in the hypothalamus of *Mecp2*-null brains (Chahrour et al. 2008), which suggests that MeCP2 serves to upregulate this gene in this brain region in WT brains. This is interesting in the context of the present study and given the role of this subunit in delta oscillation generation (Lee et al. 2004). Since I hypothesise an increase in intracellular calcium ion concentration in *Mecp2*-null IB cells, we would expect an increase in *CACNA1G* gene expression following the loss of MeCP2 if this gene it to be the root of the issue, which is the opposite to the results in Chahrour et al. (2008). However, it is worth noting that Chahrour et al. (2008) studied gene expression changes in the hypothalamus, while the cells of interest in the present study are located in the cortex. As the function of MeCP2 has regional specificity, it is plausible that MeCP2 loss in the cortex causes an increase in the *CACNA1G*, or indeed other genes involved in Ca^{2+} entry into the cell. Interestingly, it is worth noting that some of the affected calcium-related genes were up-regulated in *Mecp2*-null samples, suggesting a repressive effect of MeCP2, while others were down-regulated, which suggests an activating role for MeCP2. Gene activation could be a direct consequence of MeCP2 association with CREB1 at the gene promoter (Chahrour et al. 2008), or it could simply be an indirect effect of losing the function of MeCP2, which usually represses a repressor protein.

Calcium ion regulation was noted as one of the main processes in which several genes clustered following the loss of MeCP2 (Zhao et al. 2013; Pacheco et al. 2017). In the first study, most down-regulated genes (ie, those that are activated by MeCP2) clustered in functional groups involved in ion and chemical homeostasis, whereas those up-regulated following the loss of MeCP2 were more likely to cluster into cell development and differentiation functional groups (Zhao et al. 2013). In the second study, many different types of calcium-interacting proteins were found to have differential expression

patterns in *Mecp2*-null samples, including Ca^{2+} binding proteins, chaperone proteins, ion channels and transport proteins (Pacheco et al. 2017). The results of this study are very useful for interpreting the data presented in this thesis, as it exhibits transcriptome data solely from the cortex, whereas other studies have focussed on either the whole brain or subcortical structures such as the cerebellum, striatum or hypothalamus. This is the only study to date which has assessed the consequences of MeCP2 loss on gene expression levels specifically in the cortex. However, given the variety of different cell-types and functions across the many regions of the cortex, and the fact that MeCP2 expression is unlikely to be uniform across the whole cortex, a greater degree of regional (and cell-type) specificity would be required in future to determine the exact effects of MeCP2 loss on gene expression levels in pyramidal cells of the somatosensory cortex.

Overall, gene expression analysis studies have revealed that many genes involved in Ca^{2+} homeostasis are misregulated following the loss of MeCP2 function. The data presented in this chapter suggest that the intracellular calcium ion concentration is significantly increased in layer V IB cells. However, as some calcium regulating genes appear to be up-regulated by MeCP2, whereas others appear to be down-regulated, a clear trend in the effect of MeCP2 on calcium homeostasis is yet to be elucidated. This is likely in part due to the difficulty in conducting gene expression analyses with a high degree of regional or cell-type specificity. In the previous chapter I discussed how the functional role of MeCP2 may vary between cell-types, and therefore it is likely that the effect of MeCP2 on transcription levels will also vary between cell-types. However, separating different types of cells during the purification stage of a transcriptome analysis study is incredibly difficult. Zhang et al (2014) showed that it was possible to differentiate between neurons, glia and vascular cells during the purification stage, and therefore examined gene expression levels from the mouse cerebral cortex with a degree of cellular specificity. However, it is yet to be determined whether individual sub-types of neurons (for example, excitatory vs inhibitory, or even more specifically, IB vs RS) could be differentially purified so that their transcriptomes could be analysed in isolation.

5.3.3 The relationship between MeCP2 and Ca^{2+}

The results of this study are not the first time that the functions of MeCP2 and Ca^{2+} have been linked. *Mecp2*-null astrocytes exhibit increased calcium oscillations, increased basal cytosolic Ca^{2+} concentration, and defective intracellular Ca^{2+} signalling compared

to WT cells (Dong et al. 2018; Rakela et al. 2018). This was attributed to an abnormal increase in the activation of store-operated calcium channels that replenish Ca^{2+} ions from extracellular supplies when endoplasmic stores are depleted (Dong et al. 2018). The consequences of this increase in astrocyte Ca^{2+} activity are excessive activation of extra-synaptic NMDA receptors in neighbouring neurons, which in turn leads to hyperexcitability within the network, which is a common feature among *Mecp2*-null cells and networks (Calfa et al. 2011; Zhang et al. 2014). Very early in development, neuronal excitation leads to increases in intracellular Ca^{2+} concentrations, as well as the activation of Ca^{2+}-dependent signal transduction pathways that regulate neuronal activity (Spitzer et al. 2004). At this stage, disturbances in calcium regulation also occur in *Mecp2*-null neuronal networks (Mironov et al. 2009). iPSC-derived neurons from RTT patient fibroblasts also exhibit altered calcium currents that are excitation-dependent (Marchetto et al. 2010).

The results presented in this thesis and the findings of the studies discussed earlier in this chapter suggest that MeCP2 modulates calcium signalling through differential expression of genes that regulate Ca^{2+}levels. However, it has been suggested that calcium signalling can itself regulate MeCP2 function. Specifically, MeCP2 activity is dependent on the phosphorylation status of the Serine 421 residue, which is in turn regulated by calcium signalling via the CaM-kinase signal transduction pathway (Buchthal et al. 2012). These phosphorylation-state changes can be induced in an activity-dependent manner, for example: MeCP2 selectively binds to the BDNF promoter and inhibits its expression, until membrane depolarisation induces Ca^{2+}-dependent phosphorylation of the MeCP2 protein, which causes MeCP2 to dissociate from the BDNF promoter, allowing the gene to be transcribed (Chen et al. 2003; Zhou et al. 2006). These findings reveal that the role of MeCP2 in transcriptional regulation is sensitive to calcium signalling, despite the fact that many calcium-related proteins (eg, binding partners, ion channel proteins and downstream signalling proteins) are regulated by MeCP2 at the transcriptional level. Interestingly, the MeCP2-CaM-kinase relationship of mutual activation has been implicated in cognitive function by regulating synaptogenesis during learning (Lee et al. 2021).

5.3.4 Ca^{2+}-modulating drugs as a therapeutic target for sleep disturbances in RTT

Earlier in this chapter I showed that it is possible to reinstate the cortical delta oscillation in *Mecp2*-null brain slices by modulating the intracellular concentration of calcium ions (see Fig. 5.7). Specifically, this was achieved through the action of four different pharmacological agents that each inhibits a different type of VGCC in the central nervous system: N-type channels were targeted by amlodipine, L-type channels were targeted by nifedipine, R-type channels were targeted by SNX-482 and T-type channels were targeted by NNC 55-0396. The result of this was decreased calcium conductance into the cell, and hence a reduction in intracellular Ca^{2+} concentration, which was sufficient to re-establish delta oscillations in brain slices of isolated somatosensory cortex. Given the role of delta oscillations in Stage 3 NREM sleep and the fact that patients suffering RTT exhibit significant sleep disturbances including a reduced amount of time spent in Stage 3 NREM, the results from these experiments pose the question whether the use of these drugs could be administered in RTT patients to alleviate sleep disturbances and deficits in NREM architecture.

With this in mind, it is worth noting that all the experiments conducted in 5.2.4 lead to epileptic events in *Mecp2*-null brain slices following the induction of cortical delta oscillations (data not shown). Following the application of a Ca^{2+}-modulating drug alongside delta-inducing drugs (CCH and SCH-23390), a two-minute recording was taken every ten minutes for at least two hours. Each recording was analysed to determine the power of the delta oscillations and the presence of epileptic events within the trace. With amlodipine and NNC 55-0396, the average time of onset of epileptic events occurred at the same time as the peak power of delta oscillations. With nifedipine and SNX-482, epileptic events were established within ten minutes of the peak delta power recording. These seizure-like epochs of neuronal activity gradually increased in incidence, amplitude, duration and complexity, and coincided with a reduction in the incidence of delta activity within the trace. Eventually this epileptic activity culminated in one large event after which no discernible neuronal activity was recorded from the brain slice and the experiment was ended. These results suggest that reducing the intracellular calcium ion concentration in *Mecp2*-null IB cells induces cortical delta oscillations that are not sustainable. It is possible that, while modulating calcium activity is sufficient to reinstate IB cell bursting and therefore the generation of transient delta oscillations, the overall process of producing sustainable rhythms is affected by the loss of MeCP2 in a

partially calcium-independent manner. This is not unlikely given the sheer volume of genes whose expression levels are affected by the loss of MeCP2 function. The implications of this are that modulating intracellular Ca^{2+} levels alone would be insufficient for treatment of sleep disturbances in RTT, as the full root of the problem has yet to be elucidated.

It is also possible that adding pharmacological agents that modulate Ca^{2+} signalling to the entire brain slice (via bath application, rather than individually to IB cells which would not be experimentally possible) might have had neurological consequences outside of the delta-generating process that led to epileptic events. Ca^{2+} signalling is integral to the function of all cells, particularly excitable cells, and so it is perhaps not surprising that modulating overall cellular calcium activity throughout the entire network leads to dysfunctional and uncoordinated neuronal activity such as that seen in the seizure-like events in these experiments. Furthermore, in WT experiments in this chapter where CPA was added to show that increasing intracellular Ca^{2+} levels disrupts pre-existing delta oscillations (see Fig. 5.3), the effects of CPA also culminated in epileptic events followed by the cessation of neuronal activity within the brain slice. The use of CPA in these experiments is thought to mimic the conditions in which *Mecp2*-null IB cells do not burst (ie, as a result of increased intracellular Ca^{2+} concentration), which results in the loss of cortical delta oscillations. However, it is worth noting that in KO brain slices treated only with CCH and SCH-23390, these slices rarely exhibited epileptic activity. The fact that increased Ca^{2+} levels in KO brains slices does not lead to epileptic events while CPA application to WT slices does suggests that these seizure-like events are not a consequence of the disrupted delta-generating process, but instead are a consequence of overall disrupted calcium signalling. This serves to further support the idea that disrupting calcium homeostasis and calcium-dependent signalling pathways has negative consequences on neuronal function. With this in mind, the use of calcium-modulating drugs as a therapeutic target for any neurological disorder must be rigorously tested and controlled if it is to be approved.

Three of the four Ca^{2+}-modulating drugs used in this study already have clinical relevance: amlodipine, nifedipine, and mibefradil (a structural analogue of NNC 55-0396 which has been studied more widely in a clinical setting) are all NICE approved drugs used in the treatment of hypertension and angina, and hence their effect outside of the brain (and specifically in the circulatory system) have been extensively studied. However, relatively few studies exist where the effects of these drugs have been studied in the brain. Amlodipine has previously been investigated for its potential used in stroke

management and prevention: treatment reduced oxidative stress in several studied brain regions and overall reduced the magnitude of stroke events (Hirooka et al. 2006; Mogi et al. 2006), however these findings were attributed to increased cerebral blood flow rather than the effects of amlodipine directly on neurons or glia. The lack of brain-specific effects of amlodipine are likely due to the fact that this drug fails to cross the blood-brain barrier (Uchida et al. 1997), although recent studies have developed tools to circumvent this (Alawdi et al. 2019).

Nifedipine on the other hand is thought to be a useful pharmacological tool for treating calcium signalling in neurological disease as it is effectively taken up from plasma into the brain via the blood-brain barrier (Uchida et al. 1997). Similar to amlodipine, nifedipine is a useful treatment following stroke as it relieves restrictions in cerebral blood flow and reduces oxidative stress following ischemic brain damage (Sal'nikov, 2005; Yamato et al. 2011). Nifedipine treatment has also been shown to have brain-specific effects, including the dose-dependent facilitation of neurotransmitter release in a manner that is independent of L-type VGCCs of calcium signalling (Hirasawa and Pittman, 2003). Interestingly, previous studies have shown that nifedipine treatment can increase oscillatory activity in the delta band (Fulga and Stroescu, 1997), although the details of this study could not be accessed while writing this thesis. Given this information and the interplay of neocortical delta oscillations with hippocampal function during memory consolidation, it is not surprising that nifedipine treatment also improved memory performance on a hippocampus-dependent memory task in female Wistar rats (Quevedo et al. 1998). Despite these interesting findings, the support for a role of nifedipine in delta oscillation generation and learning and memory is lacking as few studies have investigated this further, making the assessment of nifedipine as a potential therapeutic target in RTT difficult.

Like amlodipine and nifedipine, mibefradil (a structural analogue of NNC 55-0396) has also been implicated in the treatment of hypertension and stroke prevention (Richer et al. 1996; Vacher et al. 1996; Karch et al. 1997; Oparil et al. 1997; Lindqvist et al. 2007), due to its effects in cardiac and vascular cells of the sympathetic nervous system. Both mibefradil and NNC 55-0396 appear to be incapable of traversing the blood-brain barrier, since they have to be administered by intracerebroventricular routes in order to study their effects on the brain in an experimental setting (Bancila et al. 2011; Matsuda et al. 2019), which complicates their potential for use in therapeutic treatment for sleep disturbances in RTT.

The three drugs discussed above, with the exception briefly of nifedipine, have not previously been studied in the whole brain or in relation to sleep-related brain rhythms. Therefore, although they have NICE approval, their efficacy in the brain for the treatment of delta oscillation disruptions in RTT would require extensive research. Nifedipine so far provides the most promising hope, since this drug already possesses the ability to traverse the blood-brain barrier. For amlodipine and mifebradil, researchers would first need to find a safe and effective way of delivering these drugs to the brain, before their efficacy as a therapeutic target for sleep disturbances could even be determined.

Unlike amlodipine, nifedipine and NNC 55-0396, SNX-482 does not currently have use in a clinical setting, possibly because it is a toxin taken from the tarantula spider *Hysteriocrate gigas*. The effects of SNX-482 were studied *in vitro* in hippocampal networks to reveal the role of R-type channels in synaptic transmission (Gasparini et al. 2001), and also *in vivo* to examine its effect on nociceptive signal transduction in the rat dorsal horn (Matthews et al. 2007). However, the effects of SNX-482 in the whole brain are yet to be established, as is its ability to cross the blood-brain barrier. A recent review article stated that a highly selective antagonist for R-type calcium channels is yet to be found (Schneider et al. 2020), making this channel an unlikely therapeutic target in neurological disease.

5.3.4.1 Pharmacological properties of Ca^{2+} modulating drugs

During the experiments outlined in this chapter, several pharmacological agents were used with the aim of blocking calcium entry into the cell via VGCCs. In *Mecp2*-null brain slices, reducing intracellular calcium concentration via this mechanism resulted in restoration of the previously absent cortical delta oscillation. This led to the suggestion that calcium-modulating drugs such as these (amlodipine, nifedipine, NNC-55-0396 and SNX-482) could be used as a therapeutic target for sleep disturbances in RTT. I have previously discussed the potential for the use of these drugs in a clinical setting with regards to side effects (notably the seizure-like events that occurred following the application of all drugs) and the logistics of using these drugs to act on brain tissue given most of them do not currently possess the ability to cross the blood-brain barrier. It is also important to recognise the pharmacological properties of these drugs that would also need to be considered during their assessment for clinical use.

Amlodipine is a VGCC inhibitor which targets L-type receptors in the peripheral nervous system and other non-brain-specific tissues, but targets N-type VGCCs in the brain. It exerts its effects on N-type VGCCs in an activity-dependent manner: inhibition of VGCC

activity by amlodipine is dependent on potassium conductances during the course of the action potential (Burges, Dodd and Gardiner, 1989). In the experiments described in this chapter, amlodipine was applied at a working concentration of 4 μM, much higher (~2000 times higher) than its IC50 value of 1.9 nM (Burges, Dodd and Gardiner, 1989). The implication of this is that the potency of amlodipine in these experiments was very high, with a large proportion of N-type VGCCs in the brain tissue likely becoming inhibited at any one time. In treating human conditions, each prescribed amlodipine tablet delivers between 2.5 - 10 mg of drug to the body which, in the average human body, equates to a concentration in the blood of approximately 1.2 - 4.9 μM, assuming all of the drug is absorbed from the tablet into the blood. Therefore, the administration of 4 μM amlodipine in the experiments described in this chapter appears reasonable. Cases of amlodipine overdose (Stanek, Nelson and DeNofrio, 1997; Upreti et al., 2013) stated between 25 and 100 μM concentrations (again assuming average human body size). The most serious and potentially fatal effects of these overdoses were largely due to the effects of amlodipine on cardiac muscle, the respiratory system and renal tissues. Amlodipine has a slow onset of action when administered for medication, but also has a slow half-life and therefore a slow plasma elimination rate (35 - 50 hours). One 5 mg tablet taken once a day is thought to be sufficient to maintain plasma concentrations for optimal drug therapy.

Nifedipine was also used in the experiments described in this chapter for its propensity to target L-type VGCCs in the brain. As previously mentioned, unlike the other three, nifedipine is the only calcium modulating drug used in this study which naturally has the ability to pass the blood-brain barrier, which automatically makes it a front runner as a potential therapeutic target in the brain. The inhibitory action of nifedipine is dependent on the state of the L-type VGCC: nifedipine binds to the inactive state of the VGCC and prevents it from becoming activated (Sanguinetti and Kass, 1984). The IC50 value of nifedipine is thought to be around 6 - 8 nM (Larsson-Backström, Arrhenius and Sagge, 1985; Burges et al., 1987), which, similar to amlodipine, is more than 2000 fold smaller than the concentration of nifedipine used in these experiments. A single tablet of prescribed nifedipine medication contains between 5 - 90 mg of drug, which equates to a blood-concentration level of approximately 3 - 50 μM in an average-sized adult human body (again, assuming 100% absorption into the blood). Therefore, the administration of 20 μM nifedipine in the above experiments is a reasonable comparison to the concentration of nifedipine delivered for standard therapeutic use. Similar to amlodipine, nifedipine overdose at more than ten times the recommended dose leads to profound cardiovascular and pulmonary dysfunction (Herrington, Insley and Weinmann, 1986)

owing to the effects of nifedipine on tissues outside the brain. Interestingly, and unlike amlodipine, nifedipine has a very quick onset of action and a short elimination half-life (approximately 2 hours) meaning it is removed from the plasma relatively quickly. It is therefore not an ideal drug for long-term therapy that requires consistent drug levels in the system, as medication would have to be constantly topped up.

NNC 55-0396 has an IC50 value of 80 nM (Son et al., 2014), meaning the 4 μM concentration used in the experiments described in this chapter represent almost a total inhibition of all T-type channels. Unlike amlodipine and nifedipine, NNC 55-0396 is not currently approved for medical use, and its analogue mibefradil was previously withdrawn from the market due to the unwanted side effects that arise from its interaction with other medications. Overall, the use of NNC 55-0396 in this current study was an important step to highlight the potential use of targeting T-type calcium channels in the treatment of sleep disturbances in RTT. However, the current literature suggests that NNC 55-0396 and its analogues are unlikely to represent a realistic target for this role. It would be worthwhile investigating other T-type VGCC blockers such as ethosuximide or trimethadione, which are already approved drugs for the treatment of epilepsy (Kopecky, Liang and Bao, 2014).

To date, SNX-482 has not been extensively investigated for its therapeutic properties, and of the four VGCC inhibitors tested in this project, least is known about SNX-482. R-type VGCCs are thought to be inhibited by SNX-482 in a dose-dependent manner, and SNX-482 has an IC50 value of 4.1 nM (Wang et al., 1999). This is not dissimilar to the 3 nM concentration that was used in the current study, suggesting that the experiments with SNX-482 represent the effects of the drug when less than half of the R-type VGCCs are inhibited. Interestingly, SNX-482 was the only drug not to exert statistically significant effects on the delta-activity in *Mecp2*-null mice compared to no calcium-related drug-treatment, despite the fact that delta oscillations appeared evident in the recorded traces. SNX-482 was also the only drug not used at a (much) larger concentration than its IC50 value. It would be interesting to see if repeating these experiments with a much larger SNX-482 concentration (therefore inhibiting a larger proportion of R-type VGCCs) would change the delta oscillation properties in *Mecp2*-null mice in such a way that the difference became statistically significant. It is worth noting, however, that even at 3 nM, SNX-482 application, like the other three drugs, resulted in epileptic and seizure-like events in the KO brain slices shortly after delta oscillations were observed in the recordings, and these negative consequences of

altering calcium concentrations would only be intensified by increasing the concentration of SNX-482.

Finally, one of the more challenging aspects of drug pharmacology to contend with in this project is in relation to drug specificity. For example, although amlodipine (in high concentrations) targets N-type VGCCs in the brain, it is better known and used for its inhibitory effects on L-type VGCCs in non-brain tissues (Furukawa et al., 1999; Bkaily and Jacques, 2009). Similarly, nifedipine has been shown in some instances to target T-type VGCCs as well as L-type channels (Shcheglovitov et al., 2005). While there is only a small amount of literature surrounding NNC 55-0396, its analogue mibefradil not only blocks L-type VGCCS alongside the T-type channels it was designed to target in this study, but also is thought to block some sub-types of voltage-gated sodium channels too (McNulty and Hanck, 2004). SNX-482 appears to be selective for the R-type VGCC (Wang et al., 1999), although the supplier notes its involvement in inhibiting nociceptive fibres. The some-what lack of specificity for each drug to its intended VGCC may appear to call into question the results and conclusions presented in this chapter. However, given that application of each drug was sufficient to reinstate cortical delta oscillations in *Mecp2*-null brain slices (which was the overall aim of the experiment), each drug represents an avenue towards a potential therapeutic target for sleep disturbances. This suggests that it is not necessary to target individual subtypes of the VGCC, and that the lack of target specificity is therefore unlikely to be an issue going forwards.

5.4 Summary

The results of the experiments in this chapter provide substantial evidence for the mechanism in which cortical delta oscillation generation is disrupted following the loss of MeCP2 function. At the molecular level, I showed that intracellular calcium concentration is increased in *Mecp2*-null IB cells, a factor which is sufficient to prevent WT IBs from bursting and abolish the WT cortical delta oscillation. Indeed, in KO IB cells, reducing the intracellular Ca^{2+} concentration reinstated the bursting potential of these cells, and at the level of the network was sufficient to re-establish the cortical delta rhythm. I confirm that the results of these experiments target an MeCP2-dependent mechanism in KO slices, and highlight the fact that intracellular calcium concentration must be tightly regulated for cortical delta oscillations to be generated robustly. These results highlight the precise mechanism by which cortical delta oscillations are disrupted by the loss of function in MeCP2 and go some way to explaining the presence of sleep disturbances in patients suffering MeCP2-related disorders. Further research is needed

to determine whether Ca^{2+}-modulating drugs could be used as a therapeutic target for these neurological conditions.

So far in this thesis I have examined the role of MeCP2 on the isolated networks and cells that are responsible for generating delta oscillations in the somatosensory cortex, and the molecular consequences of MeCP2-loss on IB pyramidal cells. The final stage of this project will look at the effect of loss of MeCP2 function on the coordination of sleep-related brain rhythms in the whole brain via *in vivo* electrophysiological recordings.

Chapter 6 – *In vivo* assessment of the role of MeCP2 on sleep-related brain rhythms and memory consolidation

6.1 Aims

In the opening chapter of this thesis, the importance of sleep-related brain rhythms for memory consolidation was discussed. In MeCP2-related disorders, including RTT, neurological abnormalities such as reduced network connectivity and irregular neuronal morphology are prevalent, as are memory deficits. I have previously shown in isolated neuronal networks that the generation of cortical delta oscillations is disrupted in the absence of functional MeCP2, while the thalamic delta generator remains intact. With this in mind, the aim of this chapter is to understand how the brain's potential to generate sleep-related neuronal activity in the whole intact brain is affected by the loss of MeCP2 function, with particular attention on three NREM-associated rhythms: delta oscillations, sleep spindles and hippocampal SPW-Rs. Furthermore, as the association of these rhythms to each other is important for sleep-related memory consolidation, this chapter will investigate whether loss of MeCP2 reduces the likelihood of delta oscillation, spindle and SPW-R event coupling. Finally, behavioural performance on a hippocampus-dependent novel location recognition task will shed further light on hippocampo-cortical function following the loss of MeCP2, and how these neurological deficits are manifested in the RTT-like phenotype of *Mecp2*-null animals.

6.1.1 Detection of Delta Waves

Delta waves were detected as described in Maingret et al. (2016). Briefly, broadband LFP recorded during NREM sleep was filtered between 0 – 6 Hz and z-scored. The putative beginning, peak and end of delta waves were defined based on upward-downward-upward zero-crossings of the first derivative of the z-scored filtered signal. Events lasting less than 150 ms or more than 500 ms were discarded. Delta waves corresponded to epochs where the peak amplitude exceeded 2 and the end amplitude was less than 0; or where the peak amplitude exceeded 1 and the end amplitude was less than -1.5. Threshold levels were set after careful consideration of filtered traces (Fig. 6.1).

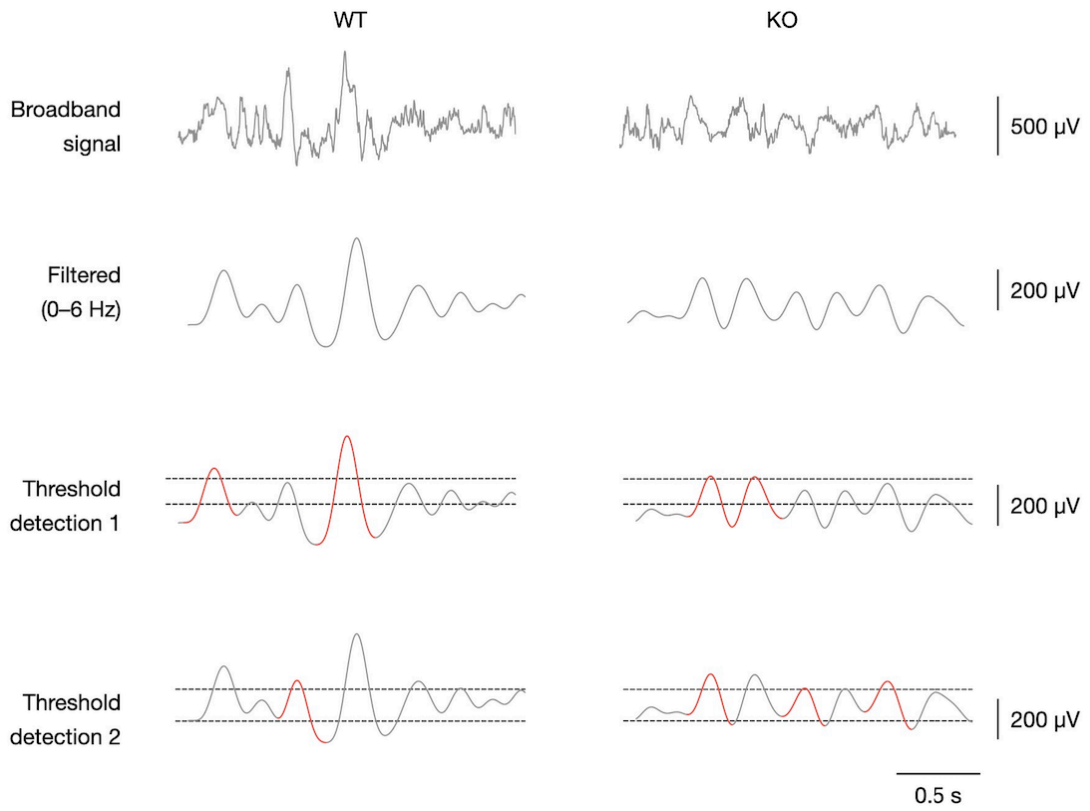

Figure 6.1: Detection of delta waves during NREM sleep. Illustrative detection of delta waves that occur during NREM sleep in wild-type mice (WT, left column) and *Mecp2*$^{Stop/y}$ mice (KO, right column). Top row: broadband LFP. Second row: LFP filtered and z-scored. Third and fourth row: Delta waves corresponded to epochs where the peak amplitude exceeded 2 and the end amplitude was less than 0 (horizontal lines, third row); or where the peak amplitude exceeded 1 and the end amplitude was less than -1.5 (horizontal lines, fourth row). Detected delta waves using the two sets of thresholds are highlighted in red.

6.1.2 Detection of Spindles

Spindles were detected as described in Maingret et al. (2016) with minor modifications. Briefly, broadband LFP recorded during NREM sleep was filtered between 9 – 17 Hz and z-scored. The instantaneous amplitude was extracted via the Hilbert transform and smoothed using a 100 ms Gaussian window. Putative spindles were defined as smoothed instantaneous amplitude peaks exceeding 4. The start/end times of putative spindles were defined when the smoothed instantaneous amplitude fell below 1.5.

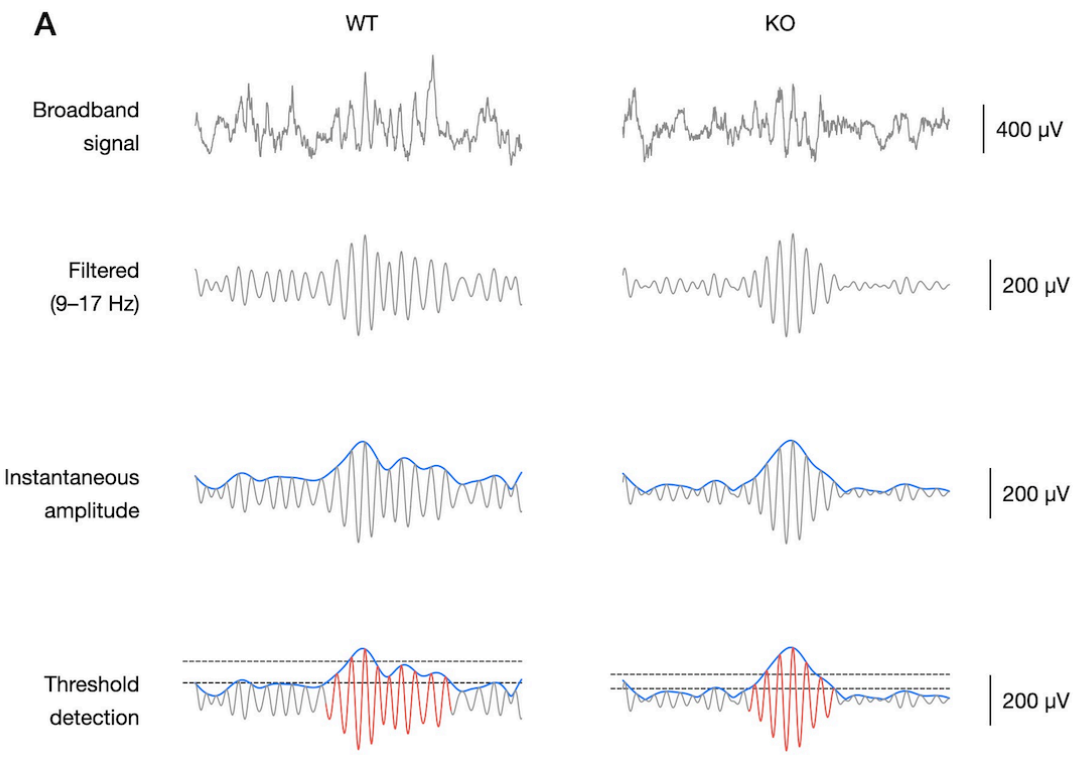

Figure 6.2: Detection of sleep spindles during NREM sleep. Illustrative detection of spindles that occur during NREM sleep in wild-type mice (WT, left column) and *Mecp2*$^{Stop/y}$ mice (KO, right column). Top row: Broadband LFP. Second row: LFP filtered and z-scored. Third row: instantaneous amplitude was extracted via the Hilbert transform and smoothed using a 100-ms Gaussian window (blue trace). Fourth row: putative spindles were defined as smoothed instantaneous amplitude peaks exceeding 4 (top horizontal black line). The start/end times of putative spindles were defined when the smoothed instantaneous amplitude fell below 1.5 (bottom horizontal black line). A detected spindle is highlighted (red trace).

Events separated by less than 0.2 s were merged. Events lasting less than 0.4 seconds or more than 2 seconds were discarded. Threshold levels were set after careful consideration of filtered and instantaneous amplitude traces (Fig. 6.2).

6.1.3 Detection of Sharp Wave-Ripples (SPW-Rs)

SPW-Rs were defined as events in which a ripple occurred concomitant with a sharp-wave and were detected as previously described (Fernández-Ruiz et al. 2019). Briefly,

broadband LFP recorded from the pyramidal cell layer was filtered between 80 - 250 Hz, clipped at mean + 4SD, rectified, and low-pass filtered (pi cycles of the mean band-pass: 52.5 Hz). The mean and standard deviation (SD) of the clipped power was calculated. The power of the non-clipped signal was then computed. All events exceeding mean + 4SD were included as candidate ripples. The start/end times of putative ripples were defined when the non-clipped power fell below 1. Events lasting less than 15 ms were discarded. Sharp waves were detected using the LFP from a channel located in the stratum radiatum. The broadband LFP was band-pass filtered between 5 – 40 Hz. Putative sharp waves were defined as the mean + 2SD of the signal. The start/end times of putative sharp waves were defined when the signal fell below mean + 0.5SD. Events lasting <20 ms or >500 ms were discarded.

6.2 Results

To better understand the role of MeCP2 in the coordination of NREM sleep-related brain rhythms, *in vivo* recordings were taken from WT and *Mecp2*-null mice during both awake and sleep states, with 16 electrode contact points spanning the entire somatosensory cortical column and hippocampal CA1 region. Recordings were sleep-scored to identify periods of wakefulness, REM and NREM sleep, following which delta oscillations, sleep spindles and hippocampal SPW-Rs were analysed as described above. In total, 6 WT and 5 *Mecp2*-null mice were used in these studies, and 5 seven-hour long recordings were taken per animal.

6.2.1 Loss of MeCP2 decreases the number of cortical delta waves during NREM sleep

Analysis of delta waves recorded during NREM sleep revealed that both WT and *Mecp2*-null mice exhibited clear and robust delta oscillations in the somatosensory cortex during NREM phases of sleep (Fig. 6.3A and G). Additionally, CSD analysis in KO recordings revealed that these events originated within the same cortical layer (layer V) and possessed the same pattern of sources and sinks as WT recordings (WT: n = 6, KO: n = 5, p = ns for both, Mann-Whitney test for both, Fig. 6.3H and I). Spectrogram analysis taken from the electrode positioned within layer V confirms that the activity seen in this channel corresponds to delta waves, as the frequency falls within the 0.5 – 4 Hz bandwidth (Fig. 6.3D). Analysis of the characteristics of these delta wave events revealed that the duration (Fig. 6.3B), amplitude (Fig. 6.3E) and frequency (Fig. 6.3F) of delta

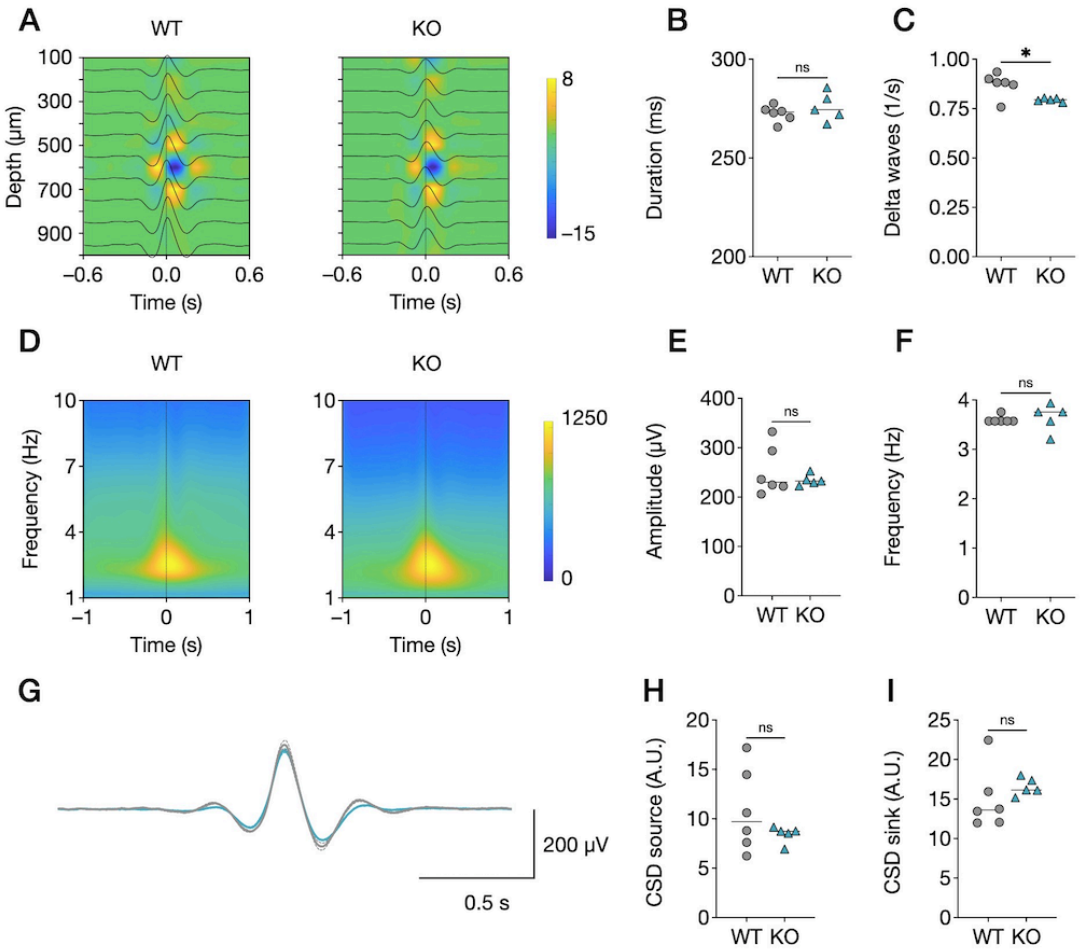

Figure 6.3: Loss of MeCP2 decreases the number of cortical delta waves during NREM sleep. (A) Example depth profile (100 µm spacing) of averaged delta wave LFPs (black lines) superimposed on CSD colour maps in a wild-type mouse (WT; left) and *Mecp2*$^{Stop/y}$ mouse (KO; right). The strong sink of the delta wave corresponds to layer V of the somatosensory cortex. **(B)** Duration of delta waves in WT (n = 6) and KO (n = 5) mice. **(C)** Number of delta waves detected per second. **(D)** Example delta wave-triggered wavelet spectrograms in layer V. **(E)** Maximal delta wave-triggered wavelet power. **(F)** Maximal delta wave-triggered wavelet frequency. **(G)** Delta wave peak-triggered LFP. **(H)** Delta wave peak-triggered CSD source magnitude. **(I)** Delta wave peak-triggered CSD sink magnitude. Statistics performed using Mann-Whitney test.

---

waves are not affected by the loss of MeCP2 function (WT: n = 6, KO: n = 5, p = ns for all conditions, Mann-Whitney test for all). However, I found a statistically significant decrease in the occurrence of delta waves during NREM sleep in KO mice compared to WT (WT: n = 6, KO: n = 5, $p < 0.05$, Mann-Whitney test, Fig. 6.3 C). These results suggest

that, in the whole intact brain, loss of MeCP2 function reduces the incidence of delta waves in the somatosensory cortex during NREM sleep. However, when these events do occur, their architecture remains unaffected compared to WT.

6.2.2 The incidence and amplitude of sleep spindles is decreased in *Mecp2*$^{Stop/y}$ mice

Sleep spindles were also identified in both WT and *Mecp2*-null mice during NREM sleep. Like delta waves, these events were also manifested in layer V of the somatosensory cortex (Fig. 6.4 A and G). Initial analysis of these events quickly identified significant differences in the architecture of these events following the loss of MeCP2 function. Spectrogram analysis revealed that sleep spindles in both genotypes occurred at approximately 12 Hz, however the amplitude of these events was significantly reduced in KO animals (Fig. 6.4D). Quantification of sleep-spindle architecture revealed that the incidence and instantaneous amplitude of sleep spindles were both significantly reduced in KO mice compared to WT (WT: n = 6, KO: n = 5, $p < 0.01$ for both, Mann-Whitney test for both, Fig 6.4B and E respectively). In contrast, I found no significant difference in either the duration or frequency of spindle events between the two genotypes (WT: n = 6, KO: n = 5, p = ns for both, Mann-Whitney test for both, Fig 6.4C and F respectively). Despite alterations in sleep spindle power and incidence, CSD analysis revealed no significant difference in the location of current sources or sinks during these events (WT: n = 6, KO: n = 5, p = ns for both, Mann-Whitney test for both, Fig 6.4H and I).

6.2.3 Loss of MeCP2 results in a decrease in the frequency and incidence of CA1 ripple oscillations during NREM sleep

Hippocampal SPW-Rs were recorded in lower electrodes that extended beyond the cortex into the CA1 region of the hippocampus. Specifically, these events were identified in channels located in the stratum radiatum (sharp wave, Fig. 6.5G lower) and pyramidal cell layer (ripples, Fig. 6.5G upper). SPW-Rs were present in both WT and *Mecp2*-null mice during NREM sleep (Fig. 6.5A and G). Spectrogram analysis confirmed the presence of high frequency (> 100 Hz) oscillations in both WT and KO animals (Fig. 6.5D), but also hinted at subtle differences in the two which were later elucidated. I found a statistically significant decrease in the incidence of SPW-Rs during NREM sleep in KO mice compared to WT littermates (WT: n = 6, KO: n = 5, $p < 0.05$, Mann-Whitney test, Fig 6.5B). I also found a significant decrease in the spectral frequency of SPW-Rs

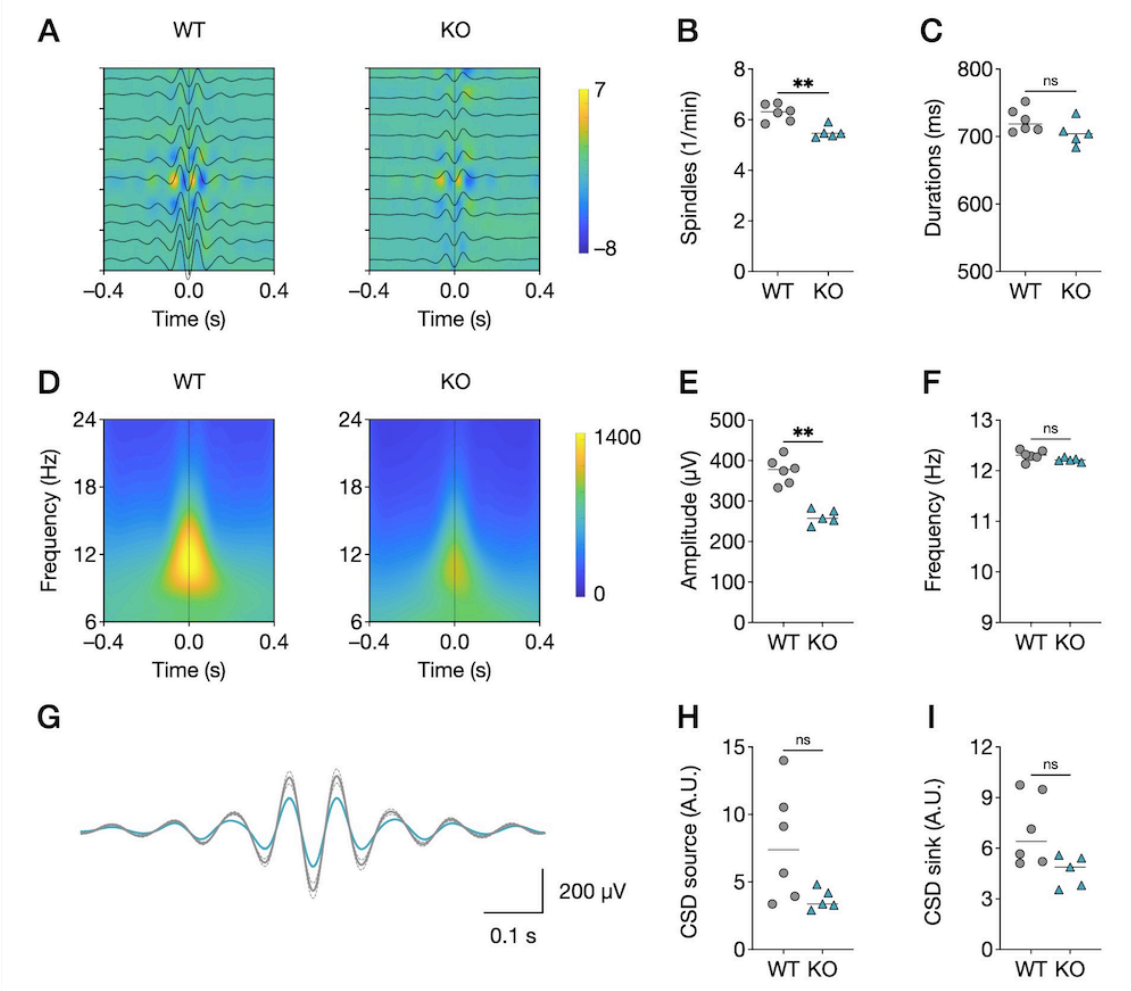

Figure 6.4: The power and incidence of sleep spindles is decreased in *Mecp2*$^{Stop/y}$ mice. (A) Example depth profile (100 μm spacing) of averaged spindles (black lines) superimposed on CSD color maps in a wild-type mouse (WT; left) and *Mecp2*$^{Stop/y}$ mouse (KO; right). The strong sink of the spindle corresponds to layer V of the somatosensory cortex. **(B)** Duration of spindles in WT (n = 6) and KO (n = 5) mice. **(C)** Number of spindles detected per minute. **(D)** Example spindle-triggered wavelet spectrograms in layer V. **(E)** Maximal spindle-triggered wavelet power. **(F)** Maximal spindle-triggered wavelet frequency. **(G)** Spindle peak-triggered LFP. **(H)** Spindle peak-triggered CSD source magnitude. **(I)** Spindle peak-triggered CSD sink magnitude. Statistics performed using Mann-Whitney test.

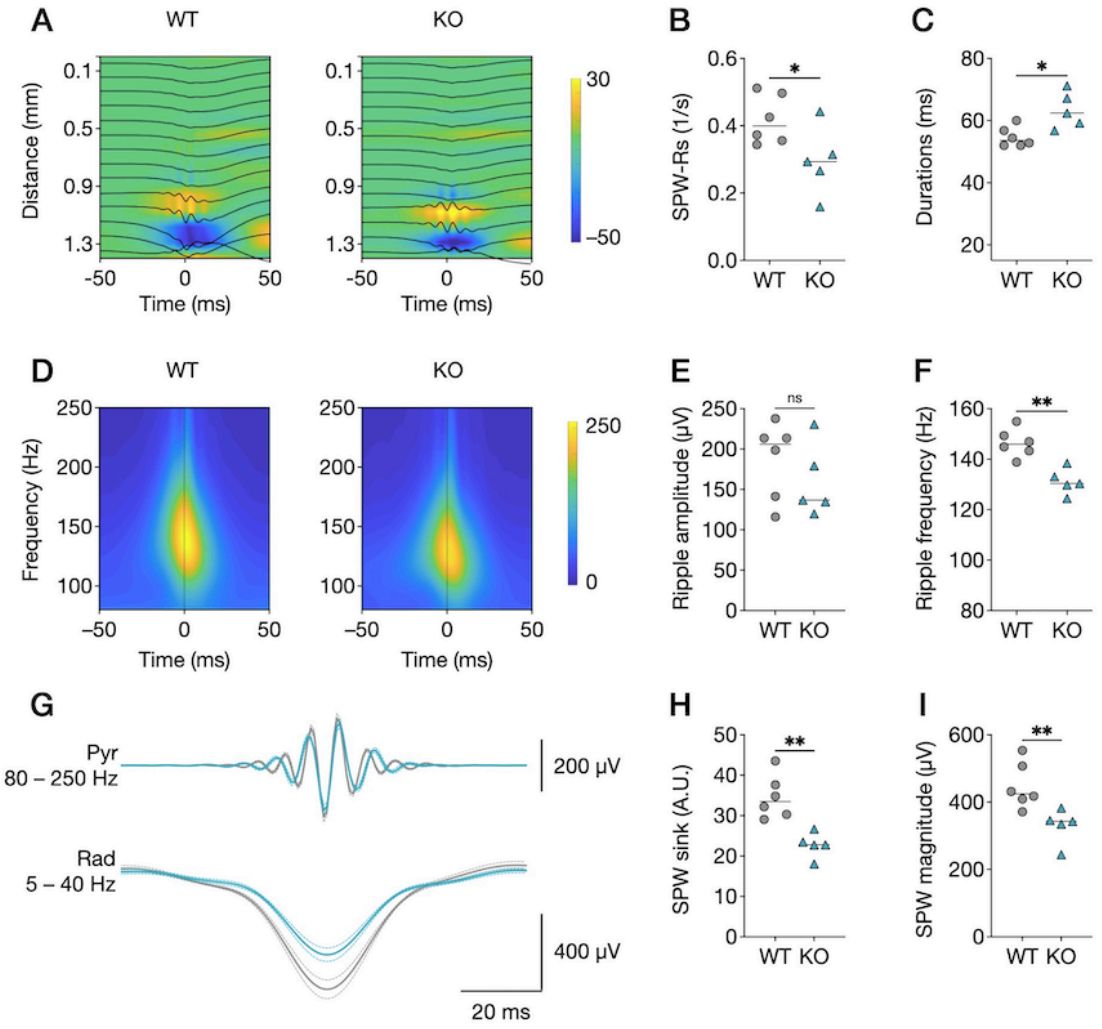

Figure 6.5: Loss of MeCP2 results in a decrease in the frequency and incidence of CA1 ripple oscillations during NREM sleep. (A) Example depth profile (100 μm spacing) of averaged SPW-Rs (black lines) superimposed on CSD colour maps in a wild-type mouse (WT; left) and *Mecp2*$^{Stop/y}$ mouse (KO; right). The strong sink of the SPW-R corresponds to stratum pyramidale. **(B)** Duration of SPW-Rs in WT (n = 6) and KO (n = 5) mice. **(C)** Number of SPW-Rs detected per second. **(D)** Example SPW-R-triggered wavelet spectrograms in stratum pyramidale. **(E)** Maximal SPW-R-triggered wavelet power. **(F)** Maximal SPW-R-triggered wavelet frequency. **(G)** Top, ripple peak-triggered (80 – 250 Hz filtered) LFP from the pyramidal cell layer of all animals. Bottom, ripple peak-triggered (5 –40 Hz filtered) LFP from the stratum radiatum across all animals. **(H)** SPW trough-triggered CSD sink magnitude. **(I)** Maximal SPW magnitude. Statistics performed using Mann-Whitney test.

following the loss of MeCP2 function (WT: n = 6, KO: n = 5, $p < 0.01$, Mann-Whitney test, Fig 6.5F). The amplitude of ripple events was not significantly different between WT and *Mecp2*-null animals (WT: n = 6, KO: n = 5, p = ns, Mann-Whitney test, Fig 6.5E). Finally, I found a significant increase in the duration of SPW-R events in KO mice compared to WT littermates (WT: n = 6, KO: n = 5, $p < 0.05$, Mann-Whitney test, Fig 6.5C). CSD analysis revealed a significant divergence in the location of sources and sinks involved in SPW-R generation (WT: n = 6, KO: n = 5, $p < 0.01$ for both, Mann-Whitney test for both, Fig 6.5H and I).

6.2.4 Hippocampo-cortical oscillatory coupling is normal in *Mecp2*$^{Stop/y}$ mice

It has previously been shown that the temporal association of delta oscillations, sleep spindles and hippocampal SPW-Rs during NREM sleep is required for sleep-related memory consolidation (Sirota et al. 2003; Axmacher et al. 2008; Maingret et al. 2016; Latchoumane et al. 2017), and forms the basis of the Two-Stage Theory of memory consolidation (Buzsáki, 1986; Buzsáki, 1989; review: Navarrete et al 2020). Therefore, the final stage of *in vivo* experiments in this study was to analyse the degree to which these three NREM-associated rhythms (delta oscillations, sleep spindles and hippocampal SPW-Rs) couple to each other during NREM sleep.

Consistent with previous reports, I found that delta waves often occur following the end of a hippocampal SPW-R (Fig. 6.6A), as did spindle-coupled-delta events (Fig. 6.6B). When SPW-Rs and spindle events occurred in temporal association, they occurred almost simultaneously (Fig. 6.6C). Spindle events that were coupled to delta waves occurred both before and after the delta wave (Fig. 6.6D). Interestingly, despite the observed differences in the characteristics of each rhythm (described above), the degree to which delta, spindle and hippocampal SPW-R events coupled to each other was not affected by the loss of MeCP2 function.

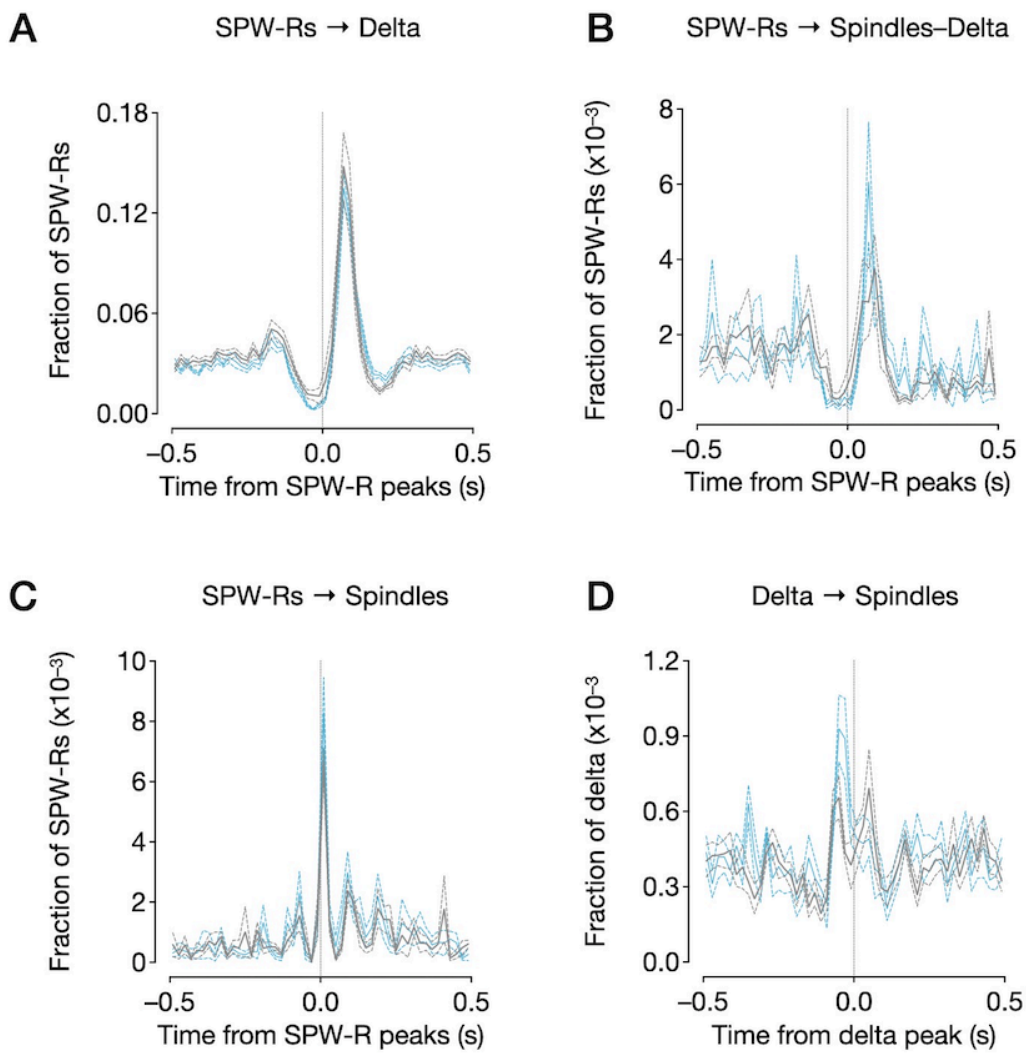

Figure 6.6: Hippocampo-cortical oscillatory coupling is normal in *Mecp2*$^{Stop/y}$ mice. **(A)** Temporal cross-correlation between SPW-Rs and delta waves. **(B)** Temporal cross-correlation between SPW-Rs and delta-spindle sequences. **(C)** Temporal cross-correlation between SPW-Rs and spindles. **(D)** Temporal cross-correlation between delta waves and spindles. Grey = WT, blue = *Mecp2*-knock out.

6.2.5 *Mecp2*-null mice exhibit impaired performance in a novel location recognition task

Previous work has shown that hippocampo-cortical coupling during sleep mediates the processes of memory consolidation that are required for spatial recognition (Barker and

Warburton, 2011; Maingret et al. 2016). Given the previously described deficits in delta wave, spindle and SPW-R characteristics, I examined recall memory using a hippocampus-dependent novel location recognition task (Barker and Warburton, 2011), as described in Chapter 2.5. During the encoding phase of the task, mice were exposed to two identical objects located in adjacent corners of a square box for 20 minutes (see Figure 2.4). During the recall phase, which occurred the 24-hours later, one of the objects was displaced to the opposite corner, and the mice were allowed to explore the test arena. To quantify time spent interacting with objects, an interaction was defined as any event lasting more than 0.5 seconds, where the animal was facing the object in close proximity, sniffing, touching or in any way exploring the object. Climbing onto the object was taken as an interaction, but if the animal then sat on the object without exploring or used it as a means to peer over the edge of the arena walls, the interaction was deemed to have ended. Quantification was performed during the first 5 minutes of each phase so as to only assess exploration of familiarity versus novelty.

Consistent with previous studies (Maingret et al. 2016), I found that WT mice spent a significantly greater proportion of exploration time with the displaced object during the recall phase compared to the encoding phase (WT: n = 12, KO: n = 13, $p<0.01$, two-way ANOVA with Šídák's multiple comparisons test; Fig. 6.7 A), indicating the ability of WT animals to distinguish between objects placed in a novel location verses those in a familiar location.

In contrast, I found that *Mecp2*$^{Stop/y}$ mice spent a similar amount of time exploring both the displaced object and the stationary object during the recall phase of the task, which was not significantly different from the encoding phase (WT: n = 12, KO: n = 13, p = ns, two-way ANOVA with Šídák's multiple comparisons test; Fig. 6.7 A). This suggests that loss of MeCP2 function impairs hippocampal-dependent spatial memory and results in a lack of discrimination between novelty and familiarity in a spatial recognition task. It is unlikely that the lack of discrimination in *Mecp2*$^{Stop/y}$ mice occurred due to phenotype-related motor defects, since I found no significant difference in the total amount of time spent exploring either object between WT and KO animals (WT: n = 12, KO: n = 13, p = ns, two-way ANOVA with Šídák's multiple comparisons test; Fig. 6.7 B).

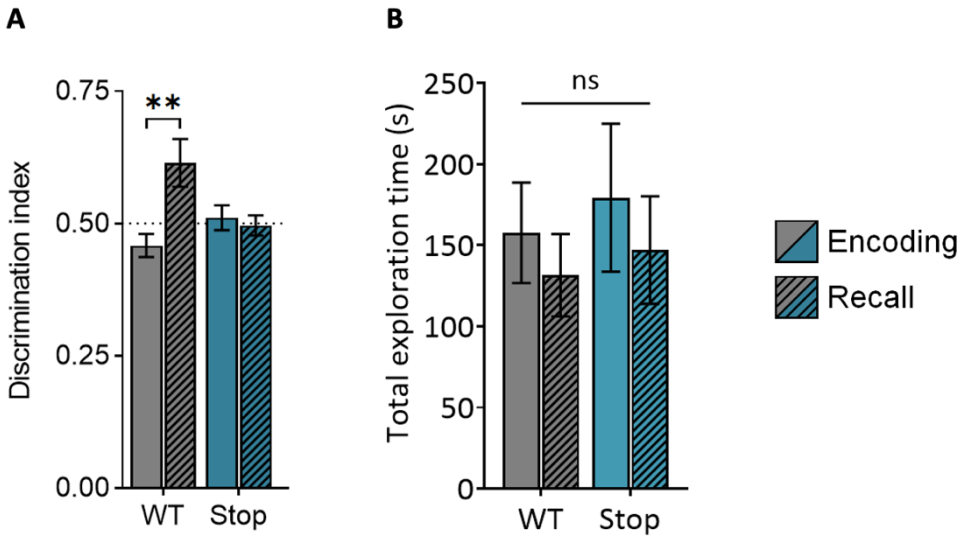

Figure 6.7: Loss of MeCP2 function impairs performance on a hippocampus-dependent spatial memory task. (A) Discrimination index for the displaces object was calculated as the total amount of time spent exploring Object 2 as a proportion of the total amount of time spent exploring either object. In the absence of discrimination, index values would be expected to sit around 0.5 (black dotted line). **(B)** Total exploration time was calculated as the amount of time spent exploring the objects within the test cage, irrespective of object identity. Grey = WT, Blue = *Mecp2*$^{Stop/y}$. Solid bars = encoding phase, stiped bars = recall phase. ** = $p < 0.01$, ns = not significantly different.

6.3 Discussion

6.3.1 Reduced delta oscillation incidence following loss of MeCP2 function

As previously mentioned in earlier chapters of this thesis, the current literature surrounding the effect of MeCP2 loss on delta oscillations is somewhat contradictory. These studies, which mainly comprise EEG data from both RTT patients and *Mecp2*-null mice, sometimes showed an increase (Ammanuel et al. 2015; Roche et al. 2019; Dong et al. 2020), sometimes a decrease (Johnston et al. 2014), and other times found no significant difference (Liao et al. 2012; Wither et al. 2012) in delta power following the loss of MeCP2 function. The data presented in this thesis contribute to this field of understanding by aligning with Liao et al. (2012) and Wither et al. (2012) in also showing that delta power in *Mecp2*-null mice is not significantly different from WT animals. The major difference between these previous studies and the current project is that previous

studies assessed delta power across the whole brain through EEG analysis, whereas the current study used an implanted electrode to study oscillations specifically in the somatosensory cortex and CA1 region of the hippocampus. Therefore, the current project cannot comment on delta power across the whole brain; it could be possible that delta power is affected in other brain regions in differential ways to the somatosensory cortex, and hence may overall be increased or decreased following loss of MeCP2. To make a conclusion on this would be beyond the scope of this project.

The current project also differs from previous studies in that delta power was not the only metric analysed in response to the loss of MeCP2 function: delta wave frequency, incidence and the duration of delta epochs were also subject to investigation. Overall, the characteristics of delta activity in the somatosensory cortex during NREM were largely similar to those in WT animals, with the only significant difference being a reduction in delta wave incidence in *Mecp2*-null mice compared to their WT littermates. Given the results shown in Chapter 3, whereby the entire cortical delta generator is malfunctional in the absence of MeCP2, these results were somewhat surprising. It was predicted prior to the undertaking of these experiments that *in vivo* delta oscillations would be significantly attenuated without a functional cortical generator. The results obtained led me to question whether the thalamic delta oscillation generator (which in Chapter 3 was found to be unaffected by the loss of MeCP2 function) could compensate for the dysfunction of the cortical generator. To understand whether this is the case, researchers would first need to identify a way of studying the two oscillation generators *in vivo* in isolation from each other, which as previously mentioned (see Chapter 3.3.3) is very difficult given that the two brain regions are inexplicably interconnected. It is also not fully understood what functional role each delta rhythm generator plays and in which behavioural states they are active. I previously posed the theory that thalamocortical delta oscillations may likely occur during active brain states such as wakefulness and REM sleep, since overall thalamocortical communication is enhanced during these periods. In contrast, cortical delta oscillations may predominate NREM sleep since the transfer of information to the cortex via the thalamus is markedly reduced during this time. The findings presented in this chapter do not support this theory, since delta oscillations (presumably via the thalamic generator, as the results in Chapter 3 showed that the cortical generator does not function in the absence of MeCP2) are prevalent during NREM sleep in *Mecp2*-null mice. It could therefore be suggested from the results presented in this chapter that cortically-generated delta oscillations do not occur during NREM sleep, since oscillations during this period appear largely unaffected by the loss of MeCP2. Perhaps it is the case instead that thalamocortical delta oscillations

predominate NREM sleep and cortically-generated delta rhythms occur during REM and wakefulness. It was not investigated in this project whether the characteristics of delta oscillations in REM sleep and wakefulness are affected by the loss of MeCP2, which may provide more insight into the temporal and functional role of the two distinct delta generators (see Chapter 7.4.4).

Irrespective of mode of generation, the finding that delta wave incidence is reduced while all other features are unaffected by the loss of MeCP2 function suggests the mechanisms that underlie delta wave generation remain functional in the *in vivo Mecp2*-null brain. Rather, it suggests that the activation of these mechanisms within the somatosensory or thalamic network is suppressed, hence reducing the overall occurrence of delta events. It has previously been shown that loss of MeCP2 function leads to an imbalance in the balance of excitatory and inhibitory drive within cortical networks, with an overall favouring of increased inhibition (Dani et al. 2005), caused by an enhancement of $GABA_A$-mediated signalling at the post-synapse (Lo et al. 2016). Furthermore, MeCP2 has been shown to be important for the excitation-inhibition balance in thalamic networks also: development of GABAergic circuits is disrupted in the thalamus of *Mecp2*-null mice (Zhang et al. 2010), although later results suggest that mice lacking functional MeCP2 protein actually lack intrinsic thalamic GABAergic connections (Hou et al. 2016), which implies a favouring of excitation rather than inhibition. It is plausible that a similar disruption to the excitation-inhibition balance is being observed in the current study whereby reduced excitatory drive onto the somatosensory and / or thalamic networks suppresses the delta-generating mechanisms, despite these mechanisms being fully capable of producing delta oscillations when appropriately activated. It has previously been shown that the intrinsic properties of reticular thalamic neurons, which provide inhibitory feedback to thalamocortical cells to regulate their clock-like firing at delta frequency, are unaffected by the loss of MeCP2 function (Zhang et al. 2010). It has not yet been identified whether the cellular characteristics and intrinsic firing patterns of thalamocortical cells is affected by the loss of MeCP2, though I hypothesise from the findings in Chapter 1 that there would be no difference between these cells in WT and *Mecp2*-null animals. If we assume that the delta oscillations recorded during NREM sleep in *Mecp2*-null animals possess a thalamic origin, the knowledge that neurons within the thalamus do not have altered intrinsic properties following loss of MeCP2, in conjunction with the knowledge that MeCP2 regulates the excitatory/inhibitory balance within the thalamus, supports the hypothesis that thalamic networks possess the ability to produce delta oscillations, but are less likely to do so due to misregulated excitation and inhibition patterns. This

hypothesis is supported by the findings in the current chapter that NREM-associated delta oscillations in *Mecp2*-null animals do not differ significantly from WT oscillations in any feature other than incidence, where they are significantly reduced. Of course, to confirm this theory researchers would need to verify that thalamocortical cell properties are unaffected in *Mecp2*-null mice and investigate further the precise changes in glutamatergic and GABAergic signalling in this network following the loss of MeCP2 function (see Chapter 7.4.1).

In previous chapters of this thesis, I used intracellular current clamp recordings to study the effect of MeCP2 loss on the cells responsible for generating delta oscillations with a purely cortical origin. These results showed that the intrinsic properties of these cells are affected, specifically through disrupted burst firing as is typical of IB pyramidal cells. Since this was attributable to misregulated calcium ion homeostasis, I sought to determine whether calcium ion signalling or homeostasis has previously been linked specifically to excitatory or inhibitory inputs. With the data presented in this thesis and in the previous studies mentioned above, it could be hypothesised that intracellular calcium signalling is increased following the receipt of inhibitory (GABAergic) input. However, this hypothesis is not supported by the findings of previous literature. $GABA_A$-receptor mediated signalling actively inhibits activity-dependent Ca^{2+} currents in prefrontal layer V pyramidal neurons (Marlin and Carter, 2014). Furthermore, a substantial amount of research evidence has linked calcium ion regulation to glutamatergic signalling. NMDA receptors contain ionotropic channels that, alongside Na^+ and K^+, are permeable to Ca^{2+}, which allows for localised fluctuations of intracellular Ca^{2+} levels at the dendritic spines. Also, activation of phospholipase C-associated-mGluRs can lead to the production of inositol triphosphate (IP_3), which causes the release of Ca^{2+} ions from ER-stores via activation of the IP_3-receptor. Hence, these are two processes whereby glutamatergic signalling leads to an increase in the cytosolic concentration of calcium ions. With all of this in mind, further research is needed to identify the precise role of MeCP2 function on the balance of excitatory and inhibitory inputs into the cortical network, and the potential consequences of these effects on calcium ion homeostasis.

6.3.2 Loss of MeCP2 function also affects the properties of other NREM-associated brain rhythms

The *in vivo* protocols used in experiments in this chapter allowed for the recording of multiple different types of brain rhythm, and hence sleep spindles and hippocampal

SPW-Rs were also subject to investigation during NREM sleep. These rhythms were chosen for assessment since their coupling to each other and to delta oscillations are known to enhance sleep-related memory consolidation (see Chapter 6.3.3). Like delta oscillations, both sleep spindles and hippocampal SPW-Rs were also significantly reduced in incidence in *Mecp2*-null animals compared to WT, which may also reflect the proposed MeCP2-related imbalance of excitation and inhibition that was discussed in the previous section. Unlike delta oscillations, sleep spindles also exhibited significantly reduced amplitude and spectral power. Since sleep spindles and thalamically-generated delta oscillations arise from cells within the same thalamic networks, the findings in this thesis that thalamic delta oscillations are unaffected by the loss of MeCP2 while sleep spindles are attenuated in these animals highlights the way in which the loss of MeCP2 has differential effects on the same cells in relation to alternative neurological processes. Furthermore, the consequences of these findings is the knowledge that the cells in this network are not completely dysfunctional in the absence of MeCP2, but rather can become temporarily dysfunctional depending on the type of neuronal activity occurring at the time. Interestingly, while both rhythms rely on reciprocal connections between the thalamus and the cortex, there exists distinct differences in the mechanisms that underlie these two rhythms: sleep spindles are generated by reticular thalamic neurons reciprocally connected to thalamic relay cells, whereas thalamically-generated delta oscillations originate in thalamocortical cells and relies on their connections to reticular thalamic cells. As previously mentioned, the intrinsic properties of reticular thalamic cells are unaffected by the loss of MeCP2 function (Zhang et al. 2010). With this in mind, one might predict that loss of MeCP2 hinders the function of thalamic relay cells, since these are vital for sleep spindle generation in projecting rhythms to the cortex and facilitating the integration of feedback from cortical regions and are less involved in the generation of thalamic delta oscillations. This theory provides further rationale for the intracellular study of the effect of MeCP2 loss on different neuronal subtypes in the thalamocortical network (see Chapter 7.4.1). To date, few studies have investigated the implications of MeCP2 loss on the generation of sleep spindles, and none have explicitly explored the role of MeCP2 in coordinating the underlying mechanisms that regulate sleep spindle generation. One previous study using longitudinal EEG studies in RTT patients showed that sleep spindles appear normal at the pre-symptomatic stage and become progressively less prevalent during disease progression compared to aged-matched controls (Ishizaki et al. 1989). These findings are mirrored by the data presented in this chapter which show that the incidence of spindle activity is significantly reduced in *Mecp2*-null mice compared to WT.

Also in this chapter, hippocampal function during NREM sleep was assessed through the occurrence of SPW-Rs in the CA1. The hippocampus has previously been subject to investigation in mouse models of RTT, both in relation to synaptic plasticity and LTP processes as well as in an electrophysiological context with regards to the generation of gamma oscillations. Similar to cortical and thalamic networks, the hippocampal network exhibits alterations in the balance of excitation and inhibition, and are also prone to hyperexcitability and seizure-like activity (Zhang et al. 2008; Calfa et al. 2011; Ho et al. 2014). Previously, MeCP2 was shown to regulate hippocampal connectivity and the relationship between excitatory and inhibitory synapses (Goffin and Zhou, 2012). Compared to other hippocampus-related processes and rhythms, less is known about the role of MeCP2 in the production of hippocampal SPW-Rs. The results presented in this chapter show that SPW-R frequency is significantly reduced, and duration is significantly increased in *Mecp2*-null mice compared to WT. Also, as previously mentioned, the occurrence of SPW-R events was significantly reduced in these animals also, similar to the occurrence of delta oscillations and sleep spindles. These findings are supported by the findings of a previous study, also in our lab, which investigated the consequences of MeCP2 loss on network activity within the hippocampus. This study, which also examined the characteristics of SPW-Rs during NREM sleep, also showed that loss of MeCP2 did not affect the depolarisation of CA1 pyramidal cell apical dendrites, as the location and amplitude of current sources and sinks did not differ between *Mecp2*-null mice and their WT littermates (data not published). Interestingly, this study did however find that loss of MeCP2 function reduced the rate of CA1 pyramidal cell firing during SPW-Rs, while inhibitory cell firing rate was not affected (data not shown), which supports the idea that MeCP2 loss causes an imbalance of excitatory and inhibitory activity within the hippocampal network. The importance of these experiments and the data presented in this thesis is enhanced given that the hippocampus is the brain's central hub of memory and that hippocampal SPW-Rs have been implicated in processes of memory consolidation, particularly those relating to the encoding of spatial information (Girardeau et al. 2009; Ego-Stengel and Wilson, 2010; van de Ven et al. 2016). Previously, *Mecp2*$^{+/-}$ hippocampal place cells (a form of pyramidal neuron found in the CA1 and CA3 regions which are activated upon entering a new location) exhibited an increased basal firing rate during periods of ripple activity, leading to hypersynchrony of the network (Kee et al. 2018). This prevented the significant increase in ripple synchrony across the hippocampus in response to a novel location paradigm, which in WT animals is required for spatial memory consolidation. As a result, these animals exhibited poor performance on a hippocampus-dependent spatial memory behavioural task compared to their WT littermates. These findings further

highlight the relationship between hippocampal SPW-Rs and spatial memory and identify the role of MeCP2 in supporting these processes.

6.3.3 Coupling of NREM-associated rhythms is unaffected by the loss of MeCP2 function

Although the investigation of sleep spindles and hippocampal SPW-Rs *in vivo* following the loss of MeCP2 function would provide useful and novel information about the role of MeCP2 in the generation of different brain rhythms, the main reason for studying them in this project was to investigate the coupling of these rhythms to each other and to delta oscillations during NREM sleep. Surprisingly, despite deficits in the characteristics of all three rhythms in *Mecp2*-null mice, their coupling together was not attenuated. Specifically, this means that when one rhythm occurred, the likelihood that another rhythm will also occur with exquisitely close temporal association was not significantly different between WT and *Mecp2*-null animals. This was true for all four coupling events: SPW-R:delta, SPW-R:spindle, delta:spindle and SPW-R:spindle:delta. This was a very surprising finding given that the coupling of these rhythms is known to facilitate sleep-related memory consolidation (Buzsáki, 1986; Axmacher et al. 2008; Maingret et al. 2016; Latchoumane et al. 2017; reviewed: Navarrete et al. 2020), and that both RTT patients and *Mecp2*-null animals exhibit significant deficits the same processes (Moretti et al. 2006; Stearns et al. 2007; Kee et al. 2018).

Interestingly, although there was no significant difference in the probability of one rhythm coupling to another between WT and *Mecp2*-null mice, the incidence rate of delta oscillations, sleep spindles and hippocampal SPW-Rs were all individually reduced. During the data analysis stage of this project, the overall incidence of rhythm-coupled events was not measured or compared between genotypes; only the probability that when one rhythm occurred another rhythm would follow in close temporal proximity. However, the finding that all three rhythms occur less frequently in *Mecp2*-null mice would mean that the overall incidence of coupled events would also be reduced. For example, the probability that a cortical delta wave closely followed a hippocampal SPW-R was found to be approximately 0.15 for both WT and *Mecp2*-null animals. But if, individually, both rhythms occur less frequently, the occurrence of delta-coupled-SPW-R events would also be reduced, even though the probability of them occurring together was not significantly different to WT animals. These findings provide insight into the role of MeCP2 in coordinating NREM-associated brain rhythms: MeCP2 function does not directly affect the rhythm coupling processes, but rather influences the individual

characteristics of delta oscillations, sleep spindles and SPW-Rs which in turn affects the occurrence of coupling events. These conclusions have large implications for the role of MeCP2 in sleep-related memory consolidation, with specific attention paid to the processes of encoding spatial information. This provides context for the behavioural deficits associated with loss of MeCP2 function whereby these animals perform atypically on a hippocampus-dependent novel location recognition test.

6.3.4 The importance of MeCP2 function for performance on a hippocampus-dependent learning and memory task

In humans, learning and memory capabilities are often assessed through cued or prompted behaviours, such as spoken language, written language or performance of a learnt task. However, when studying animals, behaviour cannot be prompted or communicated by the subject, and often the behaviours in question are subjective, open to interpretation and even anthropomorphised. The novel location recognition test examines the differences in exploration behaviours of objects in familiar and novel locations, and therefore provides a relatively easy way to measure learning and memory through the distinction of familiarity versus novelty. This behavioural paradigm is a popular method of studying memory-induced behaviours, as it utilises a simple set-up, with very little equipment required, and is one of the least stress-inducing behavioural paradigms known. Rodents in particular have a general and natural preference for novelty, and therefore the novel location recognition paradigm provides a simple way to induce behaviour without the need for reward or reinforcement. This behavioural test can also be modified to suit the requirements of the study, for example: reducing the retention time between the encoding and recall phases to assess short-term memory, or lengthening it to assess long-term memory.

In line with the deficits observed in delta oscillation, sleep spindle and hippocampal SPW-R generation, the loss of MeCP2 function in *Mecp2*$^{Stop/y}$ mice also lead to overt differences in performance during a hippocampus-dependent learning and memory task. It has previously been shown that increased coupling of hippocampo-cortical events can be used as a marker for learning and memory, and correlates with improved performance on the same novel location recognition task as the one used in this study (Maingret et al. 2016). Previous studies have shown that hippocampal function is vital for spatial memory and object-location recognition (Barker and Warburton, 2011), hence

it was shown in the current study that *Mecp2*-null animals whose hippocampal function is hindered also perform atypically on a spatial memory behavioural test.

Previous studies have identified that learning and memory deficits exist in *Mecp2*-null animals, and hippocampus-dependent learning tasks are routinely used to assess this (review: Robinson and Pozzo-Miller, 2019). The role of MeCP2 in spatial memory, which is regulated by the hippocampus, has previously been assessed using the Morris water maze test: *Mecp2*-null mice exhibited slower rates of platform identification in successive tests compared to WT controls (Moretti et al. 2006). Several studies and review articles have questioned the validity of these (and related) results given that the RTT-like phenotype associated with *Mecp2*-null animals involved severe motor deficits, which may interfere with task performance in a manner that is not related to memory processes. In acknowledgement of this, Moretti et al. (2006) also reported that *Mecp2*-null mice displayed swimming speeds that were not significantly different from WT animals. Furthermore, on the first iteration of the Morris water maze test, WT and *Mecp2*-null animals found the platform with average times that were not significantly different from each other. These findings confirm that deficits in test performance were attributable to spatial memory deficits alone, and not confounded by the RTT-like phenotype of the mutant animals.

With this in mind, motor performance was also assessed during the experiments presented in this thesis, to ensure that the observed deficits in spatial memory performance were not confounded by the phenotype of the RTT model. Motor deficits were evident in many *Mecp2*$^{Stop/y}$ mice, and this cohort exhibited a large amount of variability among phenotype severity despite all animals being of a similar age. Despite this, motor deficits did not appear to influence the outcome of behavioural testing, as the total amount of time spent exploring the objects irrespective of object identity did not differ significantly between the two genotypes in either phase of the test (see Fig. 6.7 B). The main influence of RTT-associated motor deficits was observed to be that when not exploring the objects, *Mecp2*$^{Stop/y}$ mice spent a large portion of their time not moving, whereas WT animals continually explored the rest of the test arena.

The results presented in this chapter, whereby loss of MeCP2 function impairs performance on a novel location recognition task, supports the findings of previous studies that also showed that functional MeCP2 is required for recognising spatial novelty in an open field behavioural test (Stearns et al. 2007). Interestingly, it has further been shown that memory tasks involved in spatial learning induce alternative splicing

events in a use-dependent manner, and that MeCP2 is required to regulate this process (Brito et al. 2020). Not only do *Mecp2*-null mice exhibit performance deficits in spatial memory tasks, the authors of this paper also identified misregulations in alternative splicing events in mature hippocampal neurons compared to WT controls. Many of the affected genes were shown to be involved in neuronal structure and function. These findings suggest that, in response to a spatial learning paradigm, MeCP2 directly modulates the expression levels of individual transcripts that regulate synaptic plasticity, thus identifying the precise mechanism by which MeCP2 influences spatial memory consolidation.

Among the studies that utilise these exploration-based behavioural paradigms (even those using the same type of test), it can be hard to compare the results given the difficulty of defining what constitutes "exploratory behaviour" and that gathering this data is subjective to the researcher. Because of this, there are no clear standardised criteria for analysing these behaviours, and as such each study tends to have its own unique method. In this project, an interaction was noted if the animal was facing the object in close proximity, sniffing, touching, climbing on the object, or doing anything else that was perceived as exploration of the object. The duration of the interaction was recorded from the moment of first contact (or close proximity if just sniffing) until the animal was no longer actively interacting with the object (or turned away if just sniffing). If an animal climbed on the object and just sat there, or simply used the height advantage to try and peer over the top of the arena, this was not considered a continuation of the interaction, despite the animal being in contact with the object. Leger et al. (2013) suggested that a minimal exploration time be reached before an interaction is recorded, as one way of standardising the criteria for this variable. This criterion was implemented in the present study, with any interactions lasting less than 0.5 seconds not included in the analysis. This ensured that all interactions recorded were intentional and meaningful.

6.4 Summary

The data presented in this chapter highlight the role of MeCP2 in coordinating NREM-associated brain rhythms and the consequences of MeCP2 loss of function on sleep-related memory consolidation. Using *in vivo* experimental protocols, I simultaneously recorded across the entire hippocampus CA1 region and all layers of the somatosensory cortex during awake and sleep states, in *Mecp2*-null mice and their WT littermates. I showed that loss of MeCP2 function leads to a reduction in the incidence of delta waves that originate in layer V of the somatosensory cortex during NREM sleep. I also showed

that both the incidence and amplitude of sleep spindle events are reduced in *Mecp2*-null mice compared to WT. Hippocampal SPW-Rs were found to have a significantly reduced incidence and frequency, and a significantly increased duration in *Mecp2*-null animals compared to WT. Interestingly, despite the alterations observed in the individual architecture of these three rhythms, I was intrigued to find that the loss of MeCP2 did not affect the coupling of either of these rhythms to each other. However, as all three rhythms were reduced in incidence in *Mecp2*-null animals, it can be inferred that the overall rate of coupled events would also be reduced as a result. Since rhythm coupling facilitates sleep-related memory consolidation, a reduction in coupled events would likely have down-stream effects on learning and memory processes in *Mecp2*-null animals. In support of this, I showed that hippocampal-dependent spatial memory is impaired following the loss of MeCP2 function.

Overall, the results in this chapter build on those previously presented in this thesis in providing further insight into the role of MeCP2 in coordinating NREM-associated brain rhythms. These findings shed light on the potential mechanisms by which learning and memory deficits occur in RTT and other MeCP2-related disorders, and provide the starting blocks for future research projects that would deliver further understanding in these topics. The future directions and wider implications of the results presented in this thesis will be discussed in the following chapter.

Chapter 7 – General discussion

7.1 Overview

To date, the physiology of sleep and the structure of the sleep cycle has been studied in depth, as has the importance of obtaining high-quality, uninterrupted sleep on neurological and cognitive function. Furthermore, it is well established that sleep disturbances are prevalent among at least 80% of RTT patients, as well as those suffering other MeCP2-related disorders. Previous research has shown that RTT patients spend less time in Stage 3 NREM sleep, however, until now, the importance of MeCP2 on the mechanisms that underlie the generation of NREM-related brain rhythms has yet to be fully elucidated.

With this in mind, the overarching aim of this thesis was to investigate the consequences of MeCP2-loss on the neuronal networks involved in generating delta oscillations, which are the main constituent of Stage 3 NREM. Moreover, I explored the repercussions of MeCP2 mutations on the cellular and molecular features of this rhythm. Finally, I investigated whether other neuronal oscillations that occur during NREM sleep, including sleep spindles and hippocampal SPW-Rs, are also affected by the loss of MeCP2 function, as well as the coupling of these three rhythms to each other, a process which is known to facilitate sleep-related memory consolidation. In this final chapter, I will discuss the implications of the data presented in this thesis in the context of wider research, and propose avenues for future research that would aid further understanding of the themes presented in this thesis.

7.1.1 Summary of findings

In conclusion, the results of this thesis have provided new insights into the role of MeCP2 (and the consequences of MeCP2 loss) in the generation of sleep-related brain rhythms and memory consolidation. It was demonstrated in Chapter 3 that loss of MeCP2 function leads to the disruption in the generation of cortical delta oscillations from the mouse somatosensory cortex in an *in vitro* model of pharmacologically-induced delta oscillations. On the contrary, delta oscillations produced via the thalamic generator were preserved in *Mecp2*-null mice. Interestingly, the comparison of cortical delta oscillation architecture between juvenile (less than 28 days) and adult (over 60 days) mice revealed an age-dependent reduction in delta power in both WT and *Mecp2*-null brain slices.

Furthermore, at both ages, the power of cortical delta oscillations was significantly reduced in *Mecp2*-null brain slices compared to WT, suggesting that deficits in cortical delta oscillation generation precede the onset of RTT-like symptoms in *Mecp2*-null animals. The deficits in cortical delta oscillations were attributed to the results of Chapter 4 which showed that the firing pattern of layer V IB pyramidal cells, which are responsible for generating the cortical delta rhythm, is significantly attenuated following the loss of MeCP2. Furthermore, in Chapter 5 it was revealed that IB cell bursting could be re-established in *Mecp2*-null slices by reducing the intracellular concentration of calcium ions, which was also sufficient to reinstate the cortical delta rhythm. Finally, in Chapter 6, I examined the effect of MeCP2 loss on *in vivo* sleep-related brain rhythms by studying delta oscillations, sleep spindles and hippocampal SPW-Rs during NREM sleep. Although the coupling of these events to one another was not altered, subtle changes exist in the architecture of each rhythm, including reduced incidence of all three rhythms, and therefore reduced incidence in coupled-events as a result. Since these rhythms are involved in the coordination of sleep-related memory consolidation, I lastly showed that the loss of MeCP2 leads to poor performance on a hippocampus-dependent novel location recognition task paradigm.

7.2 Wider implications

When studying a disease model, such as the RTT-model used in this project, the overarching aim is to further the understanding of disease progression and pathophysiology. As RTT is still a relatively “new” neurological disorder in the world of research (it is only a little over two decades since the genetic basis of RTT was discovered), there are still many unanswered questions regarding the processes that underlie the RTT pathology. It remains largely unknown how mutations in a single protein, MeCP2, can have such drastic consequences for neurological function and how the outward disease phenotype is so heterogeneous among the RTT population. Only once researchers fully understand the consequences of MeCP2 loss of function on vital neurological processes can we hope to identify truly effective therapeutic targets for RTT and other MeCP2-related disorders.

To address this, I sought to understand how the loss of MeCP2 function affects the brain's ability to generate NREM-associated neuronal rhythms, with the majority of experiments focussed on delta oscillations in the somatosensory cortex. The major significant findings within this thesis show that the cortical delta oscillation generator is disrupted in the absence of functional MeCP2, and that deficits in sleep-related memory

consolidation arise through the reduced incidence of NREM-associated rhythms, whose coupling together facilitates spatial learning. To my knowledge, this study is the first in-depth investigation into the electrophysiological consequences of MeCP2 loss on these specific rhythms (cortical and thalamocortical delta oscillations, sleep spindles and hippocampal SPW-Rs) in localised areas of the brain (mainly somatosensory cortex, with hippocampal assessment for SPW-Rs), as well as the mechanisms underlying their dysregulation in RTT and the resultant effect on memory consolidation. With the knowledge that modulating calcium ion levels in pyramidal neurons can re-establish the previously defective cortical delta rhythm, the findings of this thesis not only reveal one of the molecular consequences of loss of MeCP2 function but also identify a potential therapeutic target for sleep disturbances in RTT. Further research would be needed to identify whether this is a realistic aim for the future of RTT treatment (see Chapter 5.3.4 and 7.4.7).

Although the rhythms investigated in this project were studied in a singular disease model, the findings presented here extend beyond RTT research. Sleep disturbances are common features of many health conditions, and often contribute to the severity of a disorder given the importance of gaining high-quality, uninterrupted sleep on memory consolidation, metabolic function and immune function, among other things. The data presented here highlight how misregulation of NREM-associated brain rhythms, irrespective of mechanistic origin, contribute to neurological dysfunction and ill health. Finally, the data presented in this thesis also has implications beyond neuropathology. Given the heterogeneity of MeCP2 function in epigenetics, alternative splicing, chromatin remodelling and microRNA processing, the findings discussed here contribute to the wider scientific field of neurobiology by aiding the understanding of these molecular processes on neurological function.

7.3 Strengths and weaknesses of this project

During the course of this project, I used a large variety of experimental techniques to assess the consequences of MeCP2 loss on sleep-related brain rhythms and the implications of this on memory consolidation. I have utilised all of the electrophysiological recording techniques available to me, including *ex vivo* extracellular (local field potential), *ex vivo* intracellular, and *in vivo* recordings. I have also used non-electrophysiological experimental techniques (behavioural testing) to assess the wider implications of the results seen in the previous electrophysiology experiments. I believe the breadth of experimental techniques utilised in this thesis to be one of the overarching

strengths of this project, as I have studied the effect of MeCP2 loss on multiple levels: from the molecular and cellular consequences, to the effects on individual neuronal networks, the whole brain and finally beyond the brain to behavioural phenotypes.

There are however several limitations to the experiments set out in this thesis which are relevant across multiple chapters. Firstly, due to several extraneous factors (including the Covid-19 pandemic among other things), some of the data sets presented in this thesis are not as extensive as I would have liked. These include the use of the 16-channel microelectrode array in coronal brain slices (Fig. 3.1), juvenile versus adult cortical delta oscillations (Fig. 3.4), modulation of intracellular calcium concentration in intracellular recordings (Fig. 5.2 and 5.5), modulation of intracellular calcium concentration in extracellular local field potential recordings (Fig. 5.7 and 5.8), and *in vivo* single-shank 16 channel electrode recordings (Fig. 5.3-6). Where statistical analyses were performed, a minimum repeat number of at least three (though usually more) was obtained. However, given the inter-individual variability that occurs during electrophysiological experiments (particularly *in vivo* recordings), a minimum repeat number of eight would be preferable. The experiment where CPA was added to a WT IB cell during intracellular recordings was unfortunately a singular repeat, which certainly would have been repeated many more times if possible. The fact that only one data point was gathered for this experiment was due to the fact that CPA was added via bath application, meaning that only one cell in the whole slice could be recorded both pre- and post-CPA treatment. Following this singular CPA recording, intracell experiments were paused due to a standard break in animal supply. Unfortunately, for various unforeseen reasons, intracell experiments could not be re-started for the remainder of this project. In an attempt to rectify this very small data set, CPA was added during extracellular local field potential experiments to show that CPA application destroys the pre-existing cortical delta rhythm, with the implications that this occurs via the inhibition of IB cell bursting, as displayed by the singular repeat in intracellular recordings. Despite this, the lack of multiple repeats for intracellular CPA experiments is acknowledged as a weakness of this project.

With regards to intracellular experiments, basic pyramidal cell firing patterns and cellular characteristics (Fig. 4.1-3) were recorded in control conditions, without any pharmacological manipulation. I would have liked to be able to record from these cells concurrently with LFPs following the application of CCH and SCH-23390, to show the phase-coupling between IB cell burst firing and delta oscillations, and the lack of coupling in *Mecp2*-null slices. Similarly, experiments where the addition of Ca^{2+}-

modulating drugs reinstated the cortical delta rhythm in *Mecp2*-null slices would have been improved if intracellular recordings of IB cell bursting could have been achieved simultaneously. As previously mentioned, intracellular experiments were terminated prematurely due to unforeseen circumstances, meaning these simultaneous LFP-intracell recordings could not be taken. In addition to this, it would have also been interesting to record from GABAergic interneurons since cortical delta oscillations are generated by layer V IB cells which both receive and activate a source of $GABA_B$-receptor mediated inhibition. During the course of intracellular recordings in this project, it quickly became apparent that due to the instability of interneurons during this type of experiment it would be very difficult to impale and keep one of these cells for long enough to record. As a result, I was only able to record two interneurons per genotype, which is not enough data for meaningful analysis.

One of the long-running limitations of *in vitro* electrophysiology is the lack of consistent reproducibility that occurs as a result of the fragility of slice recordings in relation to the ergonomic set up of the experiment. During the early stages of this project, the rate in which delta oscillations were successfully recorded from WT brain slices was relatively low, which could have been attributed to a range of variables that might influence the chance of successfully evoking oscillations. These variables include quality of slice preparation, temperature and quality of oxygen supply, among other things. The initial difficulty in successfully evoking delta oscillations from WT brain slices posed difficulties in interpreting the results from coronal *Mecp2*-null brain slices: it was hard to determine whether the lack of oscillatory activity was indeed a phenotypic trait or simply a consequence of experimental conditions that prevented the generation of endogenous rhythms from each slice. With time, experimental conditions were fine-tuned and experimenter-errors were minimised such that delta oscillations were consistently generated from WT brain slices in a reproducible manner. Once this was achieved, it became easier to confirm the lack of cortical delta oscillations in *Mecp2*-null slices by comparison.

7.4 Future directions

7.4.1 Differential influence of MeCP2 on cortical and thalamocortical networks

The results in Chapter 3.2 suggest that MeCP2 plays a significant role in the generation of cortical, but not thalamocortical, delta oscillations. Despite this, in Chapter 6.2 I

showed that the *in vivo* delta rhythm recorded in the somatosensory cortex during NREM sleep showed only subtle changes (reduced delta wave incidence, with no difference in delta power, frequency or duration) in *Mecp2*-null animals compared to WT. These findings led to inquiries into whether thalamocortical delta oscillations might be able to compensate for the loss of cortically-generated delta oscillations (see Chapter 6.3.1). In this section, the precise (and still unknown) functional role of each delta oscillation generator was also discussed, as was the role of MeCP2 in regulating the balance of excitatory and inhibitory inputs into the thalamic and cortical networks. The factors discussed previously (see Chapter 3.3.3) mean that to date it has not been possible to identify the precise functional differences between thalamocortical and cortical delta oscillations, as researchers cannot study cortical delta oscillations *in vivo* without input from the thalamus and vice versa. In order to fully understand the exact role of MeCP2 in coordinating NREM-associated brain rhythms such as delta oscillations, the precise function of cortical and thalamocortical delta oscillations must first be elucidated. This includes identifying the different behavioural states and / or neurological processes in which each type of delta generator functions.

It would also be fruitful to study intracellularly the neurons that define the thalamocortical network during periods of delta activity, namely thalamocortical and reticular thalamic cells. As discussed in the opening chapter of this thesis, thalamocortical delta oscillations are governed by two intrinsic cellular properties, one of which is the low-threshold Ca^{2+} current known as I_t. Since Ca^{2+} (mis-)regulation was implicated in the disruption of cortical IB cells bursting and delta oscillation generation in *Mecp2*-null brain slices (see Chapter 5.2), it would be worth investigating whether Ca^{2+} oscillations in functionally-related networks are also affected by the loss of MeCP2 function. With thalamocortical delta oscillations preserved in *Mecp2*-null brain slices, it is hypothesised that I_t currents in thalamocortical cells would also be maintained. Nevertheless, confirmation of this would still further our understanding of the role of MeCP2 in calcium regulation, and shed further light on the regional and cell-type specificity with which MeCP2 functions. Furthermore, since NREM-associated delta oscillations (presumably with a thalamic origin) have a significantly reduced incidence in *Mecp2*-null mice compared to WT, it would be advantageous to study the intrinsic properties of thalamocortical neurons and the mechanisms of glutamatergic and GABAergic signalling in this network in the presence and absence of MeCP2. This would help determine the influence of MeCP2 on the balance of excitation versus inhibition within the thalamocortical network. Also, since the thalamus functions in gating sensory input and propagating this information to the cortex, thalamic activity does not just occur in

relation to delta oscillations. Intracellular investigation into the firing patterns and intrinsic properties of cells within the thalamic and thalamocortical networks would provide insight into the potential role of MeCP2 in wider (ie non-delta related) sensory processing. Finally, although the generation of delta oscillations in the thalamus appear unaffected by the loss of MeCP2 function, other NREM-associated thalamically-generated rhythms do exhibit marked differences following loss of MeCP2 function, and the mechanisms underlying this could be investigated further to better understand the role of MeCP2 in coordinating sleep-related brain rhythms (see Chapter 7.4.9).

7.4.2 Age-dependent reduction in delta oscillation power

In line with the data presented in Chapter 3.2.2, it has previously been shown that a natural age-dependent reduction in delta oscillations occurs during development, and particularly during the transition from juvenile to adulthood (Campbell and Feinberg, 2009; Baker et al. 2012; Zhang et al. 2013). Since this phenomenon occurred in both WT and *Mecp2*-null brain slices in the current project, this age-dependent process functions independent of MeCP2. Despite many previous studies showing these findings, little is known about the underlying causes of this age-dependent reduction in delta oscillation power. One theory is that a process of synaptic pruning during later-development enhances neuronal activity by eliminating unneeded and inefficient synaptic connections (Feinberg and Campbell, 2010; Chu et al. 2014; Cirelli and Tononi, 2015). This coincides with an increase in oscillation coherence across the brain within multiple frequency bandwidths (Tarokh et al. 2010). Reducing the number of synaptic connections would indeed account for reduced delta oscillation power, however several studies have shown that both apical dendrite length and complexity continue to increase long into development (Wise et al. 1979; Koenderink and Uylings, 1995; Zhu, 2000), beyond the time point where delta oscillation power begins to reduce, which counteracts the idea of synaptic downscaling. Clarification on the precise timing of these processes would provide better insight into the mechanisms that underlie the age-dependent changes in oscillatory architecture between juvenile and adulthood. Furthermore, the precise functioning of the cells and mechanisms that are responsible for cortical delta oscillation generation have not been extensively studied and compared between both age groups. It would therefore be interesting to investigate the firing patterns and intrinsic cellular properties of layer V IB pyramidal cells at the juvenile stage via intracellular recording experiments. This would identify whether the cellular properties of these cells differ to those recorded in adult brain slices, and whether these potential differences contribute to increased delta oscillation power in the younger age group. These experiments would

clarify whether the reduction in delta oscillation power with age is attributable to changes in synaptic strength, changes in intrinsic cellular properties, or a combination of the two.

7.4.3 Delta oscillations in other brain regions

Delta oscillations were first discovered in the somatosensory cortex and have been extensively studied in this region given the findings that delta power reaches its greatest value in this region during deep (Stage 3 NREM) sleep (Ioannides et al. 2009). Indeed, the *in vitro* model of delta oscillations that was used in this project was established in the rat somatosensory cortex for this reason (Carracedo et al. 2013). With this in mind, in conjunction with the knowledge that neuronal network connectivity changes have already been revealed in an *Mecp2*-null mouse model (Dani et al. 2005; Dani and Nelson, 2009), the somatosensory cortex was chosen as the brain region of interest in this study. However, delta oscillations do not exclusively occur in this brain region, and have been studied in other areas of the cortex including the motor and visual cortices (Whittingstall and Logothetis, 2009; Saleh et al. 2010; Morillon et al. 2019), and subcortical structures such as the hippocampus (Watrous et al. 2011). It would therefore be interesting to probe further the mechanisms by which delta oscillation generation is affected by the loss of MeCP2 function. In the present study, the results implicate the somatosensory cortex and layer V IB pyramidal cells specifically as (at least) one of the components in this process whose function is disrupted in *Mecp2*-null brain slices. Given that the function of MeCP2, and as a result the consequences of MeCP2 loss, have regional and possibly cell-type specificity, it would be interesting to investigate whether the results obtained in the present study are reflective of other brain regions. Specifically, are the same cell-types affected across multiple regions or are the effects observed here specific to the somatosensory cortex? Previous studies in our lab have shown that delta oscillations can be generated in other cortical (parietal association and temporal association) regions via the same methods of pharmacological induction as those used in this study (data not published), hence validating the use of this *in vitro* model of delta oscillations outside of the somatosensory cortex.

7.4.4 Delta oscillations during wakefulness

In terms of neurological activity, delta oscillations are the main constituent of Stage 3 NREM sleep (Chauvette et al. 2011), and have been highly implicated in processes relating to sleep-related memory consolidation (Huber et al. 2004; Marshall et al. 2006). For these reasons, delta oscillations have mainly been studied in the context of Stage 3

NREM sleep. However, delta oscillations do also occur during wakefulness where they have been implicated in a range of processes, including motivation, hunger, arousal and addiction (review: Knyazev, 2012). They have also been implicated in emotional processing: delta (and delta-coupled-theta) oscillations are increased following the presentation of a happy or sad face compared to a neutral face (Knyazev et al. 2009). Delta oscillations are also involved in facial recognition (Başar et al. 2007, Başar et al. 2008). In these studies, delta responses were increased following the presentation of an image of a known person compared to the image of a stranger, and increased further if the image is of a loved one rather than simply an acquaintance. Finally, delta oscillations are also thought to function during the awake state to enhance attentional and cognitive processing (Lakatos et al. 2008), and inhibit unwanted sensory information that occurs out of phase to the endogenous rhythm (Schroeder and Lakatos, 2009).

With all of this in mind, it would be interesting to determine whether the overall mechanisms that underlie the generation of delta oscillations in the awake state differ to those during sleep, and whether or not the impact of MeCP2 function on these processes also differs. In the present study, during *in vivo* recording protocols, only delta oscillations recorded during NREM sleep were subject to analysis and hence the awake state data could also be analysed in the future to shed light on the influence of MeCP2 in slow rhythm generation during wakefulness. As previously discussed, these analyses are confounded by the limitations of *in vivo* investigations into delta oscillations, whereby the cortical and thalamocortical components of these rhythms cannot be studied in isolation. These limitations would still apply to the analysis of delta oscillations that occur during the awake state also.

7.4.5 Delta oscillations couple to higher frequency rhythms

One of the functions of delta oscillations that was not discussed in this thesis is the role of delta oscillations as a carrier for high-frequency oscillations during both awake and sleep states. In both of these states, delta oscillations associate temporally with a range of different rhythms. In the auditory cortex, a hierarchical system occurs whereby delta oscillations modulate the phase of concurrent theta oscillations, which in turn modulate the phase of gamma oscillations to process sensory information and organise stimulus-related responses (Lakatos et al. 2005). The power of fast oscillations in this system is determined by the power of the delta rhythm (Lakatos et al. 2008). In humans, the power of these delta-modulated gamma oscillations correlates with improved performance on a visual discrimination task (Händel and Haarmeier, 2009), highlighting the role of this

reciprocal relationship between fast and slow rhythms in attention and sensory information processing. EEG, LFP and multi-unit activity analysis in the macaque visual cortex during a visual stimulation paradigm showed that rhythm coupling occurred only between slow (delta and theta) and fast (gamma) oscillations, and not with oscillations of moderate frequencies such as alpha or beta (Whittingstall and Logothetis, 2009). During the course of this project, delta oscillations were studied in association with sleep spindles and hippocampal SPW-Rs since their coupling during NREM sleep has been implicated in sleep-related memory consolidation. Due to the time constraints of this project, delta oscillations were not studied in conjunction with any other rhythm. Given the disruption of cortical delta oscillations observed in this project, investigation into the occurrence of delta-coupled-oscillations would provide insight into the role of MeCP2 in coordinating the interactions between rhythms of multiple frequencies.

Of particular relevance to this project is the association between delta and theta rhythms, which has previously been discussed in Chapter 1.4.5.2. During establishment of the neocortical model of delta oscillations, Carracedo et al. (2013) noted that theta oscillations are nested within the cortical column during periods of delta activity, with the phase of the theta rhythm dictated by the delta oscillation. This is the same neocortical model which was used in this project to study delta oscillations *in vitro* in *Mecp2*-null mice. With this in mind and the knowledge that cortical delta oscillations are disrupted in the absence of MeCP2, it would be interesting to determine whether the generation of these delta-coupled-theta oscillations is equally affected. This could be studied in both isolated brain slices of somatosensory cortex (as in Carracedo et al. 2013) or in *in vivo* studies such as those conducted in this project. Since the incidence of cortical delta waves is reduced during NREM sleep *in vivo*, it is reasonable to hypothesise that the incidence of delta-associated-theta oscillations would be equally affected.

7.4.6 Loss of MeCP2 function on beta oscillations

Previously, the effect of MeCP2 loss of function on other neuronal oscillations have also been studied, including gamma, alpha, beta and theta oscillations (D'Cruz et al. 2010; Goffin et al. 2011; Liao et al. 2012; Ammanuel et al 2015; Roche et al. 2019; Dong et al. 2020). Although these studies found significant differences in oscillation architecture, some of the results appear to contradict each other. Furthermore, the mechanisms underlying the observed differences to WT were not extensively explored, as the majority of these studies used EEG methods of recording which lacked a high-degree of regional

and cell-type specificity. Interestingly, although beta oscillations are generally one of the lesser-studied rhythms, they appear to be mechanistically relevant to the results presented in this thesis. Beta II oscillations (20 - 30 Hz) can be generated in an *in vitro* model of the rodent somatosensory cortex, specifically via the activity of layer V IB pyramidal neurons (Roopun et al. 2006). These are the same cells that are required for the generation of cortical delta oscillations, whose firing patterns are affected by the loss of MeCP2 function, as shown by the results in this thesis. The beta II rhythm evoked in these cells is induced via pharmacological activation of kainate receptors, rather than through low cholinergic tone and dopaminergic antagonisation, as is required for delta oscillation generation. This suggests that the function of IB cells within this network is multifaceted, and is dependent on the type of neuronal input received by the IB cell. Therefore, the experiments presented in this thesis could be extended to include the investigation of the function of IB cells in the generation of beta II oscillations. This would help to identify whether the loss of MeCP2 function disrupts IB cell firing patterns irrespective of network activity, or whether the effects of MeCP2 loss on the bursting mechanisms of these cells is specific to the mechanisms involved in delta oscillation generation.

7.4.7 Effect of Ca^{2+}-modulating drugs *in vivo* during sleep and on hippocampus-dependent memory consolidation

The chronology of experiments conducted in this project were such that *in vitro* investigation into the effects of modulating Ca^{2+} levels was one of the last experimental series to be undertaken. These therefore occurred after the termination of *in vivo* protocols. As it has been shown previously in this thesis, reducing the intracellular concentration of calcium ions in layer V IB pyramidal cells in the somatosensory cortex is sufficient to reinstate IB cell bursting and re-establish a neocortical delta rhythm that was previously absent in *Mecp2*-null brain slices. With this in mind, the logical next step for the continuation of this research would include the investigation into the effects of Ca^{2+}-modulating drugs on sleep-related brain rhythms in these animals in an *in vivo* setting and the consequences of this on memory consolidation. This has the potential to provide huge insight into the possible use of Ca^{2+}-modulating drugs as a therapeutic target for sleep disturbances in RTT. Specifically, these experiments would answer several questions: can pharmacological application of these drugs ameliorate the deficits in delta oscillations seen in the whole brain? Furthermore, would these drugs have any effect on sleep spindle and /or SPW-R architecture? Importantly, it would be most interesting to determine whether the application of these drugs would be sufficient

to negate the impact of MeCP2 loss on individual performance during a novel location recognition task designed to assess hippocampus-dependent memory consolidation, such as the one used in this project.

Of course, the decision to undertake an experimental study such as this is not one to be taken lightly. The use of pharmacological agents such as these in an *in vivo* setting would require specific ethical approval, and can only be undertaken if it falls within the current personal, project and establishment licences, as approved by the Home Office. Also, as discussed in the Chapter 5, the specificity, efficacy and safety of these drugs in the whole brain has yet to be fully determined, and for some of them their current inability to cross the blood-brain barrier poses a logistical challenge in itself. As a result, while these experiments would provide a large amount of insight into the potential use of Ca^{2+}-modulating drugs in the treatment of sleep disturbances in RTT, the logistics of carrying out a study such as this require a large amount of planning that was beyond the realms of this current project.

7.4.8 Quantification of intracellular Ca^{2+} concentration misregulation in *Mecp2*-null cells

In the fifth chapter of this thesis I put forward the hypothesis that the disrupted layer V IB pyramidal cell bursting seen in *Mecp2*-null brain slices is caused by a significant increase in the intracellular concentration of calcium ions in these cells. Indeed, reducing the intracellular Ca^{2+} concentration via VGCC inhibition was sufficient to reinstate IB cell bursting and re-established the cortical delta rhythm in subsequent LFP recordings. To confirm the hypothesis that calcium ion homeostasis is disrupted in *Mecp2*-null IB cells, it would be useful to quantify the ionic concentration in *Mecp2*-null IB cells and compare this to WT cells. This can be achieved through the use of ratiometric dyes such as Fura-2 which emit two different wavelengths of light depending on when they are bound and unbound to Ca^{2+}. Similarly, alternative dyes such a Flou-4 can be used, whose fluorescence is greatly enhanced upon binding to Ca^{2+}. Green-emitting dyes such as Flou-4 are generally considered preferable to Fura-2 since they do not require the experimenter to switch between excitation wavelengths, and therefore provide better temporal resolution (review: Lock et al. 2015). These experiments are usually conducted on cultured cells in suspension, however *Mecp2*-null neuronal cell cultures were not available during the course of this project. Furthermore, the lack of functioning neuronal networks (even simple isolated networks such as those maintained in neocortical brain slices) would render the results somewhat invalid since Ca^{2+} oscillations and signalling

within neurons are largely activity-dependent. Brain slice preparations can be used for these analyses provided they are prepared without cardiac perfusion and are sliced thinner than is required for electrophysiological recording (300 μm thick rather than 450 μm). This could pose some issues in that 450 μm is thought to be the minimum thickness required for the preservation of functional neuronal networks when recording electrophysiological activity of the slices. Hence, a 300 μm brain slice preparation, similar to cultured neuronal cells, may not contain enough reciprocally-connected viable cells to provide Ca^{2+} oscillations that are representative of the *in vivo* environment. Previous studies have successfully demonstrated the efficacy of Fura-2 and Flou-4 in brain slice preparations (Cameron et al. 2016), showing that it would be possible to quantify Ca^{2+} concentrations in *Mecp2*-null neurons and compare them to WT. Whether it would be possible to distinguish individual cell-types, or record specifically from IB neurons is yet to be determined and might be beyond the realms of this experimental design.

7.4.9 Further exploration into the effect of MeCP2 on sleep spindles

Although the majority of the research presented in this thesis focuses on the role of MeCP2 on the generation of delta oscillations, the *in vivo* experiments presented in in Chapter 6 allowed for the simultaneous recording of other NREM-associated brain rhythms, including sleep spindles. Interestingly, sleep spindle frequency and power were both found to be significantly reduced in *Mecp2*-null animals compared to WT, as was their incidence. Sleep spindles are generated via the reciprocal connections between thalamic reticular neurons, thalamocortical neurons and cortical pyramidal neurons, with the rhythms occurring in both regions phase-locked to each other (Contreras and Steriade, 1996; Destexhe et al. 1998; Andrillon et al. 2011). Like delta oscillations, it is thought that local generators of sleep spindles exist in both the thalamus (Steriade et al. 1985; Steriade et al. 1987) and the cortex (Contreras et al. 1996). It would be interesting to investigate further the precise mechanisms by which loss of MeCP2 affects the characteristics of sleep spindles, which could be conducted *in vitro* via extracellular LFP and intracellular recordings, similar to those used for studying delta oscillations in this thesis. Of particular relevance to the results presented in this thesis, sleep spindle rhythmogenesis is thought to be reliant on transient calcium conductances, particularly low-threshold calcium currents through T-type VGCCs (Lee et al. 2004; Lee and Shin, 2007; Astori et al. 2011; Pellegrini et al. 2016). Therefore, investigation into the effects of MeCP2 loss on the cells responsible for the generation of sleep spindles would build on

the findings of the current project in elucidating further the relationship between MeCP2 and calcium homeostasis.

7.4.10 Further exploration into the effect of MeCP2 on hippocampal SPW-Rs

During the course of this project, the somatosensory cortex was chosen as the main brain region of interest, since cortical (and projected thalamocortical) delta oscillations occur here during Stage 3 NREM sleep. In Chapter 6, electrophysiological studies were expanded to include recording of the hippocampus, with specific attention on the generation of hippocampal SPW-Rs and the coupling of cortico-hippocampal activity during deep sleep. The final experiments presented in this study investigated the behavioural implications of the results in the previous experiments by assessing spatial memory consolidation in a hippocampus-dependent memory task. Since the hippocampus is widely known as the central hub of learning and memory, research projects involved in memory consolidation would usually include a large portion of hippocampal research. It has previously been shown that loss of MeCP2 function leads to impaired synaptic plasticity and disrupted learning and memory processes (including LTP) in hippocampal networks (Asaka et al. 2006; Moretti et al. 2006; Chao et al. 2007; Weng et al. 2011). Furthermore, hippocampal pyramidal neurons exhibit the typical alterations in dendritic spine morphology as seen in other brain regions (Armstrong et al. 1995; Smrt et al. 2007; Chapleau et al. 2009; Stuss et al. 2012). However, the intrinsic cellular properties of cells within the hippocampal network in the absence of MeCP2 function have yet to be fully investigated. With this in mind, a potential future direction of the current research project is to utilise intracellular recording techniques with hippocampal brain slice preparations to study the firing patterns and cellular characteristics of cells within this network. Particularly relevant to the current project would be the investigation of pyramidal cells in the CA1 and CA3 regions of the hippocampus, since these cells are responsible for the generation of hippocampal SPW-Rs. These experiments would clarify the precise role of MeCP2 in the generation of hippocampal brain rhythms and by definition the exact mechanisms by which MeCP2 influences consolidation-related processes in the learning and memory centre of the brain.

List of abbreviations

ACh	Acetylcholine
ACSF	Atrificial cerebrospinal fluid
	nACSF: normal
	sACSF: sucrose-based
ADP	After-depolarisation
AHP	After-hyperpolarisation
AMPA	Alpha-amino-3-hydroxy-5-methyl-4-isoxazolepropionic acid
CCH	Carbachol
CSD	Current source density
EEG	Electroencephalogram
EPSP	Excitatory postsynaptic potential
ERP	Event related potential
FFT	Fast Fourier transform
GABA	Gamma-aminobutyric acid
HDAC	Histone deacetylase
IB cell	Intrinsically bursting cell
I_h	Hyperpolarisation-activated cation current
IPSP	Inhibitory postsynaptic potential
I_t	Low-threshold calcium current
KO	Knock-out
LFP	Local field potential
LTP	Long-term potentiation
mAChR	Muscarinic acetylcholine receptor
MBD	Methyl-CpG binding domain
mC	Methyl-cytosine
MDS	MeCP2 duplication syndrome
MeCP2	Methyl-CpG binding protein 2
	Protein: MeCP2
	Human gene: *MECP2*
	Mouse gene: *Mecp2*
mGluR	Metabotropic glutamate receptor
nAChR	Nicotinic acetylcholine receptor
NMDA	Non-N-methyl-D-aspartate
NREM sleep	Non-rapid eye movement sleep

REM sleep	Rapid eye movement sleep
RMP	Resting membrane potential
RS cell	Regular spiking cell
RTT	Rett syndrome
S1 cortex	Primary somatosensory cortex
S2 cortex	Secondary somatosensory cortex
SERCA	Sarco/endoplasmic reticulum Ca^{2+}-ATPase
SPW-R	Sharp-wave ripple
SWO	Slow wave oscillation
SWS	Slow wave sleep
TRD	Transcriptional repression domain
VGCC	Voltage gated calcium channel
WT	Wild-type
Xi	X-chromosome inactivation

Bibliography

Ackermann, S. and Rasch, B. (2014) 'Differential effects of non-REM and REM sleep on memory consolidation?', *Current neurology and neuroscience reports*, 14(2), p. 430.

Adamantidis, A. R., Gutierrez Herrera, C. and Gent, T. C. (2019) 'Oscillating circuitries in the sleeping brain', *Nature reviews. Neuroscience*, 20(12), pp. 746–762.

Adrian, E. D. and Matthews, B. H. C. (1934) 'THE BERGER RHYTHM: POTENTIAL CHANGES FROM THE OCCIPITAL LOBES IN MAN', *Brain: a journal of neurology*, 57(4), pp. 355–385.

Aeschbach, D., Cutler, A. J. and Ronda, J. M. (2008) 'A role for non-rapid-eye-movement sleep homeostasis in perceptual learning', *The Journal of neuroscience: the official journal of the Society for Neuroscience*, 28(11), pp. 2766–2772.

Aghajanian, G. K. and Rasmussen, K. (1989) 'Intracellular studies in the facial nucleus illustrating a simple new method for obtaining viable motoneurons in adult rat brain slices', *Synapse* , 3(4), pp. 331–338.

Agmon, A. and Connors, B. W. (1989) 'Repetitive burst-firing neurons in the deep layers of mouse somatosensory cortex', *Neuroscience letters*, 99(1-2), pp. 137–141.

Agmon, A. and Connors, B. W. (1991) 'Thalamocortical responses of mouse somatosensory (barrel) cortexin vitro', *Neuroscience*, 41(2), pp. 365–379.

Agmon, A. and Connors, B. W. (1992) 'Correlation between intrinsic firing patterns and thalamocortical synaptic responses of neurons in mouse barrel cortex', *The Journal of neuroscience: the official journal of the Society for Neuroscience*, 12(1), pp. 319–329.

Ahmed, M. S. and Siegelbaum, S. A. (2009) 'Recruitment of N-Type Ca2+ Channels during LTP Enhances Low Release Efficacy of Hippocampal CA1 Perforant Path Synapses', *Neuron*, 63(3), pp. 372–385.

Akbarian, S. *et al.* (2001) 'Expression pattern of the Rett syndrome gene MeCP2 in primate prefrontal cortex', *Neurobiology of disease*, 8(5), pp. 784–791.

Alawdi, S. H. *et al.* (2019) 'Loading Amlodipine on Diamond Nanoparticles: A Novel Drug Delivery System', *Nanotechnology, science and applications*, 12, pp. 47–53.

Alhola, P. and Polo-Kantola, P. (2007) 'Sleep deprivation: Impact on cognitive performance', *Neuropsychiatric disease and treatment*, 3(5), pp. 553–567.

Alonso, A. and García-Austt, E. (1987) 'Neuronal sources of theta rhythm in the entorhinal cortex of the rat: I. Laminar distribution of theta field potentials', *Experimental brain research. Experimentelle Hirnforschung. Experimentation cerebrale*, 67(3), pp. 493–501.

Amir, R. E. *et al.* (1999) 'Rett syndrome is caused by mutations in X-linked MECP2, encoding methyl-CpG-binding protein 2', *Nature genetics*, 23, p. 185.

Amir, R. E. *et al.* (2005) 'Mutations in exon 1 of MECP2 are a rare cause of Rett syndrome', *Journal of medical genetics*, 42(2), p. e15.

Ammanuel, S. *et al.* (2015) 'Heightened Delta Power during Slow-Wave-Sleep in Patients with Rett Syndrome Associated with Poor Sleep Efficiency', *PloS one*, 10(10), p. e0138113.

Amzica, F., Nun˜ez, A. and Steriade, M. (1992) 'Delta frequency (1–4 Hz) oscillations of perigeniculate thalamic neurons and their modulation by light', *Neuroscience*, 51(2), pp. 285–294.

Amzica, F. and Steriade, M. (1998) 'Electrophysiological correlates of sleep delta waves', *Electroencephalography and clinical neurophysiology*, 107(2), pp. 69–83.

Andrillon, T. *et al.* (2011) 'Sleep spindles in humans: insights from intracranial EEG and unit recordings', *The Journal of neuroscience: the official journal of the Society for Neuroscience*, 31(49), pp. 17821–17834.

Aran, D. *et al.* (2011) 'Replication timing-related and gene body-specific methylation of active human genes', *Human molecular genetics*, 20(4), pp. 670–680.

Ariani, F. *et al.* (2008) 'FOXG1 is responsible for the congenital variant of Rett syndrome', *American journal of human genetics*, 83(1), pp. 89–93.

Armstrong, D. *et al.* (1995) 'Selective dendritic alterations in the cortex of Rett syndrome', *Journal of neuropathology and experimental neurology*, 54(2), pp. 195–201.

Armstrong, D. D. *et al.* (1999) 'Organ growth in Rett syndrome: a postmortem examination analysis', *Pediatric neurology*, 20(2), pp. 125–129.

Aronoff, R. *et al.* (2010) 'Long-range connectivity of mouse primary somatosensory barrel cortex: Long-range connectivity of barrel cortex', *The European journal of neuroscience*, 31(12), pp. 2221–2233.

Asaka, Y. *et al.* (2006) 'Hippocampal synaptic plasticity is impaired in the Mecp2-null mouse model of Rett syndrome', *Neurobiology of disease*, 21(1), pp. 217–227.

Ashcroft, F. M. *et al.* (1994) 'Stimulus-secretion coupling in pancreatic β cells', *Journal of cellular biochemistry*, 55(S1994A), pp. 54–65.

Astori, S., Wimmer, R. D. and Prosser, H. M. (2011) 'The CaV3. 3 calcium channel is the major sleep spindle pacemaker in thalamus', *Proceedings of the*. Available at: https://www.pnas.org/content/108/33/13823.short.

Axmacher, N. *et al.* (2006) 'Memory formation by neuronal synchronization', *Brain research reviews*, 52(1), pp. 170–182.

Axmacher, N., Elger, C. E. and Fell, J. (2008) 'Ripples in the medial temporal lobe are relevant for human memory consolidation', *Brain: a journal of neurology*, 131(Pt 7), pp. 1806–1817.

Azimi, A., Alizadeh, Z. and Ghorbani, M. (2021) 'The essential role of hippocampo-cortical connections in temporal coordination of spindles and ripples', *NeuroImage*, 243, p. 118485.

Baker, F. C., Turlington, S. R. and Colrain, I. (2012) 'Developmental changes in the sleep electroencephalogram of adolescent boys and girls', *Journal of sleep research*, 21(1), pp. 59–67.

Baker, S. A. *et al.* (2013) 'An AT-hook domain in MeCP2 determines the clinical course of Rett syndrome and related disorders', *Cell*, 152(5), pp. 984–996.

Baker, S. N. *et al.* (1999) 'The role of synchrony and oscillations in the motor output', *Experimental brain research. Experimentelle Hirnforschung. Experimentation cerebrale*, 128(1-2), pp. 109–117.

Ballestar, E. *et al.* (2005) 'The impact of MECP2 mutations in the expression patterns of Rett syndrome patients', *Human genetics*, 116(1-2), pp. 91–104.

Ballestar, E., Yusufzai, T. M. and Wolffe, A. P. (2000) 'Effects of Rett syndrome mutations of the methyl-CpG binding domain of the transcriptional repressor MeCP2 on selectivity for association with methylated DNA', *Biochemistry*, 39(24), pp. 7100–7106.

Ball, M. P. *et al.* (2009) 'Targeted and genome-scale strategies reveal gene-body methylation signatures in human cells', *Nature biotechnology*, 27(4), pp. 361–368.

Bancila, M. *et al.* (2011) 'Two structurally different T-type Ca 2+ channel inhibitors, mibefradil and pimozide, protect CA1 neurons from delayed death after global ischemia in rats', *Fundamental & clinical pharmacology*, 25(4), pp. 469–478.

Banerjee, A. *et al.* (2016) 'Jointly reduced inhibition and excitation underlies circuit-wide changes in cortical processing in Rett syndrome', *Proceedings of the National Academy of Sciences of the United States of America*, 113(46), pp. E7287–E7296.

Barker, G. R. I. and Warburton, E. C. (2011) 'When is the hippocampus involved in recognition memory?', *Journal of Neuroscience*. Available at: https://www.jneurosci.org/content/31/29/10721.short.

Başar, E. *et al.* (2007) 'Brain oscillations differentiate the picture of one's own grandmother', *International journal of psychophysiology: official journal of the International Organization of Psychophysiology*, 64(1), pp. 81–90.

Başar, E. *et al.* (2008) 'Brain oscillations evoked by the face of a loved person', *Brain research*, 1214, pp. 105–115.

Baubec, T. *et al.* (2013) 'Methylation-dependent and -independent genomic targeting principles of the MBD protein family', *Cell*, 153(2), pp. 480–492.

Behrens, C. J. *et al.* (2005) 'Induction of sharp wave-ripple complexes in vitro and reorganization of hippocampal networks', *Nature neuroscience*, 8(11), pp. 1560–1567.

Bekkers, J. M. (2011) 'Pyramidal neurons', *Current biology: CB*, 21(24), p. R975.

Belden, W. J. *et al.* (2011) 'CHD1 remodels chromatin and influences transient DNA methylation at the clock gene frequency', *PLoS genetics*, 7(7), p. e1002166.

Belluscio, M. A. *et al.* (2012) 'Cross-Frequency Phase-Phase Coupling between Theta and Gamma Oscillations in the Hippocampus', *Journal of Neuroscience*, pp. 423–435. doi: 10.1523/jneurosci.4122-11.2012.

Ben-Shachar, S. *et al.* (2009) 'Mouse models of MeCP2 disorders share gene expression changes in the cerebellum and hypothalamus', *Human molecular genetics*, 18(13), pp. 2431–2442.

Benshalom, G. and White, E. L. (1986) 'Quantification of thalamocortical synapses with spiny stellate neurons in layer IV of mouse somatosensory cortex', *The Journal of comparative neurology*, 253(3), pp. 303–314.

Besedovsky, L., Lange, T. and Born, J. (2012) 'Sleep and immune function', *Pflugers Archiv: European journal of physiology*, 463(1), pp. 121–137.

Bibbig, A. *et al.* (2001) 'Self-Organized Synaptic Plasticity Contributes to the Shaping of γ and β Oscillations In Vitro', *The Journal of neuroscience: the official journal of the Society for Neuroscience*, 21(22), pp. 9053–9067.

Bibbig, A., Traub, R. D. and Whittington, M. A. (2002) 'Long-range synchronization of gamma and beta oscillations and the plasticity of excitatory and inhibitory synapses: a network model', *Journal of neurophysiology*, 88(4), pp. 1634–1654.

Bird, A. *et al.* (1985) 'A fraction of the mouse genome that is derived from islands of nonmethylated, CpG-rich DNA', *Cell*, 40(1), pp. 91–99.

Bird, A. (2002) 'DNA methylation patterns and epigenetic memory', *Genes & development*, 16(1), pp. 6–21.

Bird, A. P. (1980) 'DNA methylation and the frequency of CpG in animal DNA', *Nucleic acids research*, 8(7), pp. 1499–1504.

Bird, A. P. (1986) 'CpG-rich islands and the function of DNA methylation', *Nature*, 321(6067), pp. 209–213.

Bkaily, G. and Jacques, D. (2009) 'L-type calcium channel antagonists and suppression of expression of plasminogen receptors: is the missing link the L-type calcium channel?', *Circulation research*, pp. 112–113.

Bock, C. *et al.* (2012) 'DNA methylation dynamics during in vivo differentiation of blood and skin stem cells', *Molecular cell*, 47(4), pp. 633–647.

Bönsch, D. *et al.* (2007) 'Daily variations of homocysteine concentration may influence methylation of DNA in normal healthy individuals', *Chronobiology international*, 24(2), pp. 315–326.

Borbély, A. A. *et al.* (1981) 'Sleep deprivation: effect on sleep stages and EEG power density in man', *Electroencephalography and clinical neurophysiology*, 51(5), pp. 483–495.

Borbély, S. *et al.* (2018) 'Sleep deprivation decreases neuronal excitability and responsiveness in rats both in vivo and ex vivo', *Brain research bulletin*, 137, pp. 166–177.

Bornhövd, K. *et al.* (2002) 'Painful stimuli evoke different stimulus–response functions in the amygdala, prefrontal, insula and somatosensory cortex: a single-trial fMRI study', *Brain: a journal of neurology*, 125(6), pp. 1326–1336.

Breman, A. M. *et al.* (2011) 'MECP2 duplications in six patients with complex sex chromosome rearrangements', *European journal of human genetics: EJHG*, 19(4), pp. 409–415.

Brero, A. *et al.* (2005) 'Methyl CpG–binding proteins induce large-scale chromatin reorganization during terminal differentiation', *The Journal of cell biology*, 169(5), pp. 733–743.

Briggs, F. (2010) 'Organizing principles of cortical layer 6', *Frontiers in neural circuits*, 4, p. 3.

Brini, M. *et al.* (2014) 'Neuronal calcium signaling: function and dysfunction', *Cellular and molecular life sciences: CMLS*, 71(15), pp. 2787–2814.

Brito, D. V. C. *et al.* (2020) 'MeCP2 gates spatial learning-induced alternative splicing events in the mouse hippocampus', *Molecular brain*, 13(1), p. 156.

Brosenitsch, T. A. and Katz, D. M. (2001) 'Physiological patterns of electrical stimulation can induce neuronal gene expression by activating N-type calcium channels', *The Journal of neuroscience: the official journal of the Society for Neuroscience*, 21(8), pp. 2571–2579.

Brown, R. E. *et al.* (2012) 'Control of sleep and wakefulness', *Physiological reviews*, 92(3), pp. 1087–1187.

Buchmann, A. *et al.* (2011) 'EEG sleep slow-wave activity as a mirror of cortical maturation', *Cerebral cortex* , 21(3), pp. 607–615.

Buchthal, B. *et al.* (2012) 'Nuclear calcium signaling controls methyl-CpG-binding protein 2 (MeCP2) phosphorylation on serine 421 following synaptic activity', *The Journal of biological chemistry*, 287(37), pp. 30967–30974.

Buhl, E. H., Tamás, G. and Fisahn, A. (1998) 'Cholinergic activation and tonic excitation induce persistent gamma oscillations in mouse somatosensory cortex in vitro', *The Journal of physiology*, 513 (Pt 1), pp. 117–126.

Bullock, T. H., Buzsáki, G. and McClune, M. C. (1990) 'Coherence of compound field potentials reveals discontinuities in the CA1-subiculum of the hippocampus in freely-moving rats', *Neuroscience*, 38(3), pp. 609–619.

Burges, R.A. *et al.* (1987) 'Calcium channel blocking properties of amlodipine in vascular smooth muscle and cardiac muscle in vitro: evidence for voltage modulation of vascular dihydropyridine receptors', *Journal of cardiovascular pharmacology*, 9(1), pp. 110–119.

Burges, R.A., Dodd, M.G. and Gardiner, D.G. (1989) 'Pharmacologic profile of amlodipine', *The American journal of cardiology*, 64(17), p. 10I–18I; discussion 18I–20I.

Buyse, I.M. et al. (2000) 'Diagnostic testing for Rett syndrome by DHPLC and direct sequencing analysis of the MECP2 gene: identification of several novel mutations and polymorphisms', American journal of human genetics, 67(6), pp. 1428–1436.

Buzsáki, G. (1986) 'Hippocampal sharp waves: their origin and significance', *Brain research*, 398(2), pp. 242–252.

Buzsáki, G. (1989) 'Two-stage model of memory trace formation: A role for "noisy" brain states', *Neuroscience*, 31(3), pp. 551–570.

Buzsáki, G. *et al.* (1992) 'High-frequency network oscillation in the hippocampus', *Science*, 256(5059), pp. 1025–1027.

Buzsáki, G. (2002) 'Theta oscillations in the hippocampus', *Neuron*, 33(3), pp. 325–340.

Buzsaki, G. (2006) *Rhythms of the Brain*. Oxford University Press.

Buzsáki, G., Leung, L. W. and Vanderwolf, C. H. (1983) 'Cellular bases of hippocampal EEG in the behaving rat', *Brain research*, 287(2), pp. 139–171.

Calfa, G., Hablitz, J. J. and Pozzo-Miller, L. (2011) 'Network hyperexcitability in hippocampal slices from Mecp2 mutant mice revealed by voltage-sensitive dye imaging', *Journal of neurophysiology*, 105(4), pp. 1768–1784.

Cameron, M. *et al.* (2016) 'Calcium Imaging of AM Dyes Following Prolonged Incubation in Acute Neuronal Tissue', *PloS one*, 11(5), p. e0155468.

Campbell, I. G. and Feinberg, I. (2009) 'Longitudinal trajectories of non-rapid eye movement delta and theta EEG as indicators of adolescent brain maturation', *Proceedings of the National Academy of Sciences of the United States of America*, 106(13), pp. 5177–5180.

Campbell, I. G., Guinan, M. J. and Horowitz, J. M. (2002) 'Sleep deprivation impairs long-term potentiation in rat hippocampal slices', *Journal of neurophysiology*, 88(2), pp. 1073–1076.

Canolty, R. T. *et al.* (2006) 'High gamma power is phase-locked to theta oscillations in human neocortex', *Science*, 313(5793), pp. 1626–1628.

Carney, R. M. *et al.* (2003) 'Identification of MeCP2 mutations in a series of females with autistic disorder', *Pediatric neurology*, 28(3), pp. 205–211.

Carracedo, L. M. *et al.* (2013) 'A neocortical delta rhythm facilitates reciprocal interlaminar interactions via nested theta rhythms', *The Journal of neuroscience: the official journal of the Society for Neuroscience*, 33(26), pp. 10750–10761.

Carr, M. F., Karlsson, M. P. and Frank, L. M. (2012) 'Transient slow gamma synchrony underlies hippocampal memory replay', *Neuron*, 75(4), pp. 700–713.

Chahrour, M. *et al.* (2008) 'MeCP2, a key contributor to neurological disease, activates and represses transcription', *Science*, 320(5880), pp. 1224–1229.

Chahrour, M. and Zoghbi, H. Y. (2007) 'The story of Rett syndrome: from clinic to neurobiology', *Neuron*, 56(3), pp. 422–437.

Chao, H.-T., Zoghbi, H. Y. and Rosenmund, C. (2007) 'MeCP2 controls excitatory synaptic strength by regulating glutamatergic synapse number', *Neuron*, 56(1), pp. 58–65.

Chao, H.-T. *et al.* (2010) 'Dysfunction in GABA signalling mediates autism-like stereotypies and Rett syndrome phenotypes', *Nature*, 468(7321), pp. 263–269.

Chapleau, C. A. *et al.* (2009) 'Dendritic spine pathologies in hippocampal pyramidal neurons from Rett syndrome brain and after expression of Rett-associated MECP2 mutations', *Neurobiology of disease*, 35(2), pp. 219–233.

Chauvette, S. *et al.* (2011) 'Properties of slow oscillation during slow-wave sleep and anesthesia in cats', *The Journal of neuroscience: the official journal of the Society for Neuroscience*, 31(42), pp. 14998–15008.

Cheadle, J.P. et al. (2000) 'Long-read sequence analysis of the MECP2 gene in Rett syndrome patients: correlation of disease severity with mutation type and location', Human molecular genetics, 9(7), pp. 1119–1129.

Cheng, T.-L. *et al.* (2014) 'MeCP2 suppresses nuclear microRNA processing and dendritic growth by regulating the DGCR8/Drosha complex', *Developmental cell*, 28(5), pp. 547–560.

Chen, L. *et al.* (2015) 'MeCP2 binds to non-CG methylated DNA as neurons mature, influencing transcription and the timing of onset for Rett syndrome', *Proceedings of the National Academy of Sciences of the United States of America*, 112(17), pp. 5509–5514.

Chen, R. Z. *et al.* (2001) 'Deficiency of methyl-CpG binding protein-2 in CNS neurons results in a Rett-like phenotype in mice', *Nature genetics*, 27(3), pp. 327–331.

Chen, T. L. *et al.* (2008) 'Human secondary somatosensory cortex is involved in the processing of somatosensory rare stimuli: an fMRI study', *NeuroImage*, 40(4), pp. 1765–1771.

Chen, W. G. *et al.* (2003) 'Derepression of BDNF transcription involves calcium-dependent phosphorylation of MeCP2', *Science*, 302(5646), pp. 885–889.

Chovsepian, A. *et al.* (2017) 'Heterotopic Transcallosal Projections Are Present throughout the Mouse Cortex', *Frontiers in cellular neuroscience*, 11, p. 36.

Christie, B. R., Schexnayder, L. K. and Johnston, D. (1997) 'Contribution of voltage-gated Ca2+ channels to homosynaptic long-term depression in the CA1 region in vitro', *Journal of neurophysiology*, 77(3), pp. 1651–1655.

Chrobak, J. J. and Buzsáki, G. (1998) 'Gamma oscillations in the entorhinal cortex of the freely behaving rat', *The Journal of neuroscience: the official journal of the Society for Neuroscience*, 18(1), pp. 388–398.

Chu, C. J. *et al.* (2014) 'The maturation of cortical sleep rhythms and networks over early development', *Clinical neurophysiology: official journal of the International Federation of Clinical Neurophysiology*, 125(7), pp. 1360–1370.

Cirelli, C. (2009) 'The genetic and molecular regulation of sleep: from fruit flies to humans', *Nature reviews. Neuroscience*, 10(8), pp. 549–560.

Cirelli, C. and Tononi, G. (2015) 'Cortical development, electroencephalogram rhythms, and the sleep/wake cycle', *Biological psychiatry*, 77(12), pp. 1071–1078.

Claveria-Gimeno, R. et al. (2017) 'The intervening domain from MeCP2 enhances the DNA affinity of the methyl binding domain and provides an independent DNA interaction site', Scientific reports, 7(1), pp. 1–16.

Cohen, D. *et al.* (2002) 'MECP2 mutation in a boy with language disorder and schizophrenia', *The American journal of psychiatry*, 159(1), pp. 148–149.

Cohen, S. *et al.* (2011) 'Genome-wide activity-dependent MeCP2 phosphorylation regulates nervous system development and function', *Neuron*, 72(1), pp. 72–85.

Colantuoni, C. *et al.* (2001) 'Gene expression profiling in postmortem Rett Syndrome brain: differential gene expression and patient classification', *Neurobiology of disease*, 8(5), pp. 847–865.

Collins, A. L. *et al.* (2004) 'Mild overexpression of MeCP2 causes a progressive neurological disorder in mice', *Human molecular genetics*, 13(21), pp. 2679–2689.

Colten, H. R., Altevogt, B. M. and Institute of Medicine (US) Committee on Sleep Medicine and Research (2006) *Sleep Physiology*. National Academies Press (US).

Connelly, J. C. *et al.* (2020) 'Absence of MeCP2 binding to non-methylated GT-rich sequences in vivo', *Nucleic acids research*, 48(7), pp. 3542–3552.

Contreras, D. *et al.* (1996) 'Control of Spatiotemporal Coherence of a Thalamic Oscillation by Corticothalamic Feedback', *Science*, pp. 771–774. doi: 10.1126/science.274.5288.771.

Contreras, D. and Steriade, M. (1996) 'Spindle oscillation in cats: the role of corticothalamic feedback in a thalamically generated rhythm', *The Journal of physiology*, 490 (Pt 1), pp. 159–179.

Cooper, L. N. and Bear, M. F. (2012) 'The BCM theory of synapse modification at 30: interaction of theory with experiment', *Nature reviews. Neuroscience*, 13(11), pp. 798–810.

Coulondre, C. *et al.* (1978) 'Molecular basis of base substitution hotspots in Escherichia coli', *Nature*, 274(5673), pp. 775–780.

Couvert, P. *et al.* (2001) 'MECP2 is highly mutated in X-linked mental retardation', *Human molecular genetics*, 10(9), pp. 941–946.

Csicsvari, J. *et al.* (2000) 'Ensemble patterns of hippocampal CA3-CA1 neurons during sharp wave-associated population events', *Neuron*, 28(2), pp. 585–594.

Cuddapah, V. A. *et al.* (2014) 'Methyl-CpG-binding protein 2 (MECP2) mutation type is associated with disease severity in Rett syndrome', *Journal of medical genetics*, 51(3), pp. 152–158.

Dani, V. S. *et al.* (2005) 'Reduced cortical activity due to a shift in the balance between excitation and inhibition in a mouse model of Rett syndrome', *Proceedings of the National Academy of Sciences of the United States of America*, 102(35), pp. 12560–12565.

Dani, V. S. and Nelson, S. B. (2009) 'Intact long-term potentiation but reduced connectivity between neocortical layer 5 pyramidal neurons in a mouse model of Rett syndrome', *The Journal of neuroscience: the official journal of the Society for Neuroscience*, 29(36), pp. 11263–11270.

D'Cruz, J. A. *et al.* (2010) 'Alterations of cortical and hippocampal EEG activity in MeCP2-deficient mice', *Neurobiology of disease*, 38(1), pp. 8–16.

Deaton, A. M. and Bird, A. (2011) 'CpG islands and the regulation of transcription', *Genes & development*, 25(10), pp. 1010–1022.

De Gennaro, L. *et al.* (2001) 'Antero-posterior EEG changes during the wakefulness–sleep transition', *Clinical neurophysiology: official journal of the International Federation of Clinical Neurophysiology*, 112(10), pp. 1901–1911.

De Gennaro, L. and Ferrara, M. (2003) 'Sleep spindles: an overview', *Sleep medicine reviews*, 7(5), pp. 423–440.

De Gennaro, L., Ferrara, M. and Bertini, M. (2001) 'The boundary between wakefulness and sleep: quantitative electroencephalographic changes during the sleep onset period', *Neuroscience*, 107(1), pp. 1–11.

Deschênes, M., Roy, J. P. and Steriade, M. (1982) 'Thalamic bursting mechanism: an inward slow current revealed by membrane hyperpolarization', *Brain research*, 239(1), pp. 289–293.

D'Esposito, M. *et al.* (1996) 'Isolation, physical mapping, and northern analysis of the X-linked human gene encoding methyl CpG-binding protein, MECP2', *Mammalian genome: official journal of the International Mammalian Genome Society*, 7(7), pp. 533–535.

Destexhe, A. *et al.* (1994) 'A model of spindle rhythmicity in the isolated thalamic reticular nucleus', *Journal of neurophysiology*, 72(2), pp. 803–818.

Destexhe, A. *et al.* (1996) 'In vivo, in vitro, and computational analysis of dendritic calcium currents in thalamic reticular neurons', *The Journal of Neuroscience*, pp. 169–185. doi: 10.1523/jneurosci.16-01-00169.1996.

Destexhe, A., Contreras, D. and Steriade, M. (1998) 'Mechanisms underlying the synchronizing action of corticothalamic feedback through inhibition of thalamic relay cells', *Journal of neurophysiology*, 79(2), pp. 999–1016.

Dicke, U. and Roth, G. (2016) 'Neuronal factors determining high intelligence', *Philosophical transactions of the Royal Society of London. Series B, Biological sciences*, 371(1685), p. 20150180.

Diekelmann, S. and Born, J. (2010) 'The memory function of sleep', *Nature reviews. Neuroscience*, 11(2), pp. 114–126.

Dong, H.-W. *et al.* (2020) 'Detection of neurophysiological features in female R255X MeCP2 mutation mice', *Neurobiology of disease*, 145, p. 105083.

Dong, Q. *et al.* (2018) 'Mechanism and consequence of abnormal calcium homeostasis in Rett syndrome astrocytes', *eLife*, 7. doi: 10.7554/eLife.33417.

Dotti, M. T. *et al.* (2002) 'A Rett syndrome MECP2 mutation that causes mental retardation in men', *Neurology*, 58(2), pp. 226–230.

Douvlataniotis, K. *et al.* (2020) 'No evidence for DNA N6-methyladenine in mammals', *Science Advances*, 6(12), p. eaay3335.

Dragich, J., Houwink-Manville, I. and Schanen, C. (2000) 'Rett syndrome: a surprising result of mutation in MECP2', Human molecular genetics, 9(16), pp. 2365–2375.

Dragich, J. M. *et al.* (2007) 'Differential distribution of the MeCP2 splice variants in the postnatal mouse brain', *The Journal of comparative neurology*, 501(4), pp. 526–542.

Dworak, M. *et al.* (2011) 'Delta oscillations induced by ketamine increase energy levels in sleep-wake related brain regions', *Neuroscience*, 197, pp. 72–79.

Ebersole, J. S. and Ebersole, S. M. (2010) 'Combining MEG and EEG source modeling in epilepsy evaluations', *Journal of clinical neurophysiology: official publication of the American Electroencephalographic Society*, 27(6), pp. 360–371.

Ego-Stengel, V. and Wilson, M. A. (2010) 'Disruption of ripple-associated hippocampal activity during rest impairs spatial learning in the rat', *Hippocampus*, 20(1), pp. 1–10.

Ellaway, C. *et al.* (2001) 'Sleep dysfunction in Rett syndrome: lack of age related decrease in sleep duration', *Brain and Development*, pp. S101–S103. doi: 10.1016/s0387-7604(01)00356-4.

Engel, A. K., König, P., *et al.* (1991) 'Interhemispheric synchronization of oscillatory neuronal responses in cat visual cortex', *Science*, 252(5009), pp. 1177–1179.

Engel, A. K., Kreiter, A. K., *et al.* (1991) 'Synchronization of oscillatory neuronal responses between striate and extrastriate visual cortical areas of the cat', *Proceedings of the National Academy of Sciences of the United States of America*, 88(14), pp. 6048–6052.

Evans, J. C. *et al.* (2005) 'Early onset seizures and Rett-like features associated with mutations in CDKL5', *European journal of human genetics: EJHG*, 13(10), pp. 1113–1120.

Faulkner, H. J., Traub, R. D. and Whittington, M. A. (1999) 'Anaesthetic/amnesic agents disrupt beta frequency oscillations associated with potentiation of excitatory synaptic potentials in the rat hippocampal slice', *British journal of pharmacology*, 128(8), pp. 1813–1825.

Feinberg, I. and Campbell, I. G. (2010) 'Sleep EEG changes during adolescence: an index of a fundamental brain reorganization', *Brain and cognition*, 72(1), pp. 56–65.

Fernández-Ruiz, A. *et al.* (2019) 'Long-duration hippocampal sharp wave ripples improve memory', *Science*. doi: 10.1126/science.aax0758.

Ferrara, M. *et al.* (2012) 'Hippocampal sleep features: relations to human memory function', *Frontiers in neurology*, 3, p. 57.

Fischer, S. *et al.* (2002) 'Sleep forms memory for finger skills', *Proceedings of the National Academy of Sciences of the United States of America*, 99(18), pp. 11987–11991.

Fogel, S. M. *et al.* (2007) 'Sleep spindles and learning potential', *Behavioral neuroscience*, 121(1), pp. 1–10.

Fogel, S. M. and Smith, C. T. (2006) 'Learning-dependent changes in sleep spindles and Stage 2 sleep', *Journal of sleep research*, 15(3), pp. 250–255.

Fogel, S. M., Smith, C. T. and Cote, K. A. (2007) 'Dissociable learning-dependent changes in REM and non-REM sleep in declarative and procedural memory systems', *Behavioural brain research*, 180(1), pp. 48–61.

Franceschetti, S. *et al.* (1993) 'Expression of intrinsic bursting properties in neurons of maturing sensorimotor cortex', *Neuroscience letters*, 162(1), pp. 25–28.

Fries, P. *et al.* (2001) 'Modulation of oscillatory neuronal synchronization by selective visual attention', *Science*, 291(5508), pp. 1560–1563.

Fukuda, T. *et al.* (2005) 'Delayed maturation of neuronal architecture and synaptogenesis in cerebral cortex of Mecp2-deficient mice', *Journal of neuropathology and experimental neurology*, 64(6), pp. 537–544.

Fulga, I. G. and Stroescu, V. (1997) 'Effect of nifedipine on electrical activity of the brain in rat', *Romanian journal of physiology: physiological sciences / [Academia de Stiinte Medicale]*, 34(1-4), pp. 115–125.

Furukawa, T. *et al.* (1999) 'Selectivities of dihydropyridine derivatives in blocking Ca(2+) channel subtypes expressed in Xenopus oocytes', *The Journal of pharmacology and experimental therapeutics*, 291(2), pp. 464–473.

Gabbott, P. L. and Somogyi, P. (1986) 'Quantitative distribution of GABA-immunoreactive neurons in the visual cortex (area 17) of the cat', *Experimental brain research. Experimentelle Hirnforschung. Experimentation cerebrale*, 61(2), pp. 323–331.

Gabel, H. W. *et al.* (2015) 'Disruption of DNA-methylation-dependent long gene repression in Rett syndrome', *Nature*, 522(7554), pp. 89–93.

Gais, S. and Born, J. (2004) 'Declarative memory consolidation: mechanisms acting during human sleep', *Learning & memory* , 11(6), pp. 679–685.

Galli, C. *et al.* (1995) 'Apoptosis in cerebellar granule cells is blocked by high KCl, forskolin, and IGF-1 through distinct mechanisms of action: the involvement of intracellular calcium and RNA synthesis', *The Journal of neuroscience: the official journal of the Society for Neuroscience*, 15(2), pp. 1172–1179.

Gamelli, A. E. *et al.* (2011) 'Deletion of the L-type calcium channel Ca(V) 1.3 but not Ca(V) 1.2 results in a diminished sAHP in mouse CA1 pyramidal neurons', *Hippocampus*, 21(2), pp. 133–141.

Gardiner-Garden, M. and Frommer, M. (1987) 'CpG Islands in vertebrate genomes', *Journal of molecular biology*, 196(2), pp. 261–282.

Gasparini, S. *et al.* (2001) 'Presynaptic R-type calcium channels contribute to fast excitatory synaptic transmission in the rat hippocampus', *The Journal of neuroscience: the official journal of the Society for Neuroscience*, 21(22), pp. 8715–8721.

del Gaudio, D. *et al.* (2006) 'Increased MECP2 gene copy number as the result of genomic duplication in neurodevelopmentally delayed males', *Genetics in medicine: official journal of the American College of Medical Genetics*, 8(12), pp. 784–792.

Gentet, L. J. and Ulrich, D. (2004) 'Electrophysiological characterization of synaptic connections between layer VI cortical cells and neurons of the nucleus reticularis thalami in juvenile rats', *The European journal of neuroscience*, 19(3), pp. 625–633.

Girardeau, G. *et al.* (2009) 'Selective suppression of hippocampal ripples impairs spatial memory', *Nature neuroscience*, 12, p. 1222.

Gisiger, T. and Boukadoum, M. (2011) 'Mechanisms Gating the Flow of Information in the Cortex: What They Might Look Like and What Their Uses may be', *Frontiers in computational neuroscience*, 5, p. 1.

Gleichmann, M. and Mattson, M. P. (2011) 'Neuronal Calcium Homeostasis and Dysregulation', *Antioxidants & redox signaling*, 14(7), pp. 1261–1273.

Goffin, D. *et al.* (2011) 'Rett syndrome mutation MeCP2 T158A disrupts DNA binding, protein stability and ERP responses', *Nature neuroscience*, 15(2), pp. 274–283.

Goffin, D. *et al.* (2014) 'Cellular origins of auditory event-related potential deficits in Rett syndrome', *Nature neuroscience*, 17(6), pp. 804–806.

Goffin, D. and Zhou, Z. J. (2012) 'The neural circuit basis of Rett syndrome', *Frontiers of biology*, 7(5), pp. 428–435.

Gonzales, M.L. et al. (2012) 'Phosphorylation of distinct sites in MeCP2 modifies cofactor associations and the dynamics of transcriptional regulation', Molecular and cellular biology, 32(14), pp. 2894–2903.

Good, K.V., Vincent, J.B. and Ausió, J. (2021) 'MeCP2: The Genetic Driver of Rett Syndrome Epigenetics', Frontiers in genetics, 12, p. 620859.

Graef, I. A. *et al.* (1999) 'L-type calcium channels and GSK-3 regulate the activity of NF-ATc4 in hippocampal neurons', *Nature*, 401(6754), pp. 703–708.

Gross, D. W. and Gotman, J. (1999) 'Correlation of high-frequency oscillations with the sleep–wake cycle and cognitive activity in humans', *Neuroscience*, 94(4), pp. 1005–1018.

Gross, J. *et al.* (2007) 'Gamma oscillations in human primary somatosensory cortex reflect pain perception', *PLoS biology*, 5(5), p. e133.

Grunstein, M. (1997) 'Histone acetylation in chromatin structure and transcription', *Nature*, 389(6649), pp. 349–352.

Guo, J. U. *et al.* (2014) 'Distribution, recognition and regulation of non-CpG methylation in the adult mammalian brain', *Nature neuroscience*, 17(2), pp. 215–222.

Gupta, T. *et al.* (2016) 'Functional conservation of MBD proteins: MeCP2 and Drosophila MBD proteins alter sleep', *Genes, brain, and behavior*, 15(8), pp. 757–774.

Guy, J. *et al.* (2001) 'A mouse Mecp2-null mutation causes neurological symptoms that mimic Rett syndrome', *Nature genetics*, 27(3), pp. 322–326.

Guy, J. *et al.* (2007) 'Reversal of neurological defects in a mouse model of Rett syndrome', *Science*, 315(5815), pp. 1143–1147.

Haenschel, C. *et al.* (2000) 'Gamma and beta frequency oscillations in response to novel auditory stimuli: A comparison of human electroencephalogram (EEG) data with in vitro models', *Proceedings of the National Academy of Sciences of the United States of America*, 97(13), pp. 7645–7650.

Hagberg, B. *et al.* (1983) 'A progressive syndrome of autism, dementia, ataxia, and loss of purposeful hand use in girls: Rett's syndrome: report of 35 cases', *Annals of neurology*, 14(4), pp. 471–479.

Hall, S. P. *et al.* (2018) 'Enhanced interlaminar excitation or reduced superficial layer inhibition in neocortex generates different spike-and-wave-like electrographic events in vitro', *Journal of neurophysiology*, 119(1), pp. 49–61.

Händel, B. and Haarmeier, T. (2009) 'Cross-frequency coupling of brain oscillations indicates the success in visual motion discrimination', *NeuroImage*, 45(3), pp. 1040–1046.

Hanlon, E. C. *et al.* (2009) 'Effects of skilled training on sleep slow wave activity and cortical gene expression in the rat', *Sleep*, 32(6), pp. 719–729.

Harvey, C. G. *et al.* (2007) 'Sequence variants within exon 1 of MECP2 occur in females with mental retardation', *American journal of medical genetics. Part B, Neuropsychiatric genetics: the official publication of the International Society of Psychiatric Genetics*, 144B(3), pp. 355–360.

Hattox, A. M. and Nelson, S. B. (2007) 'Layer V neurons in mouse cortex projecting to different targets have distinct physiological properties', *Journal of neurophysiology*, 98(6), pp. 3330–3340.

Havekes, R. *et al.* (2016) 'Sleep deprivation causes memory deficits by negatively impacting neuronal connectivity in hippocampal area CA1', *eLife*, 5. doi: 10.7554/eLife.13424.

Hayashi, Y. *et al.* (2000) 'Driving AMPA receptors into synapses by LTP and CaMKII: requirement for GluR1 and PDZ domain interaction', *Science*, 287(5461), pp. 2262–2267.

He, L.-J. *et al.* (2014) 'Conditional deletion of Mecp2 in parvalbumin-expressing GABAergic cells results in the absence of critical period plasticity', *Nature communications*, 5, p. 5036.

Hellman, A. and Chess, A. (2007) 'Gene body-specific methylation on the active X chromosome', *Science*, 315(5815), pp. 1141–1143.

Helmchen, F. *et al.* (1999) 'In vivo dendritic calcium dynamics in deep-layer cortical pyramidal neurons', *Nature neuroscience*, 2(11), pp. 989–996.

Helton, T. D., Xu, W. and Lipscombe, D. (2005) 'Neuronal L-Type Calcium Channels Open Quickly and Are Inhibited Slowly', *The Journal of neuroscience: the official journal of the Society for Neuroscience*, 25(44), pp. 10247–10251.

Hendrich, B. and Bird, A. (1998) 'Identification and characterization of a family of mammalian methyl-CpG binding proteins', *Molecular and cellular biology*, 18(11), pp. 6538–6547.

Henrie, J. A. and Shapley, R. (2005) 'LFP power spectra in V1 cortex: the graded effect of stimulus contrast', *Journal of neurophysiology*, 94(1), pp. 479–490.

Hermes, D. *et al.* (2015) 'Stimulus Dependence of Gamma Oscillations in Human Visual Cortex', *Cerebral cortex* , 25(9), pp. 2951–2959.

Herrington, D.M., Insley, B.M. and Weinmann, G.G. (1986) 'Nifedipine overdose', *The American journal of medicine*, 81(2), pp. 344–346.

Hirasawa, M. and Pittman, Q. J. (2003) 'Nifedipine facilitates neurotransmitter release independently of calcium channels', *Proceedings of the National Academy of Sciences of the United States of America*, 100(10), pp. 6139–6144.

Hirata, A. and Castro-Alamancos, M. A. (2010) 'Neocortex network activation and deactivation states controlled by the thalamus', *Journal of neurophysiology*, 103(3), pp. 1147–1157.

Hirooka, Y. *et al.* (2006) 'Amlodipine-induced reduction of oxidative stress in the brain is associated with sympatho-inhibitory effects in stroke-prone spontaneously hypertensive rats', *Hypertension research: official journal of the Japanese Society of Hypertension*, 29(1), pp. 49–56.

Ho, E. C. Y. *et al.* (2014) 'Network models predict that reduced excitatory fluctuations can give rise to hippocampal network hyper-excitability in MeCP2-null mice', *PloS one*, 9(3), p. e91148.

Horike, S.-I. *et al.* (2005) 'Loss of silent-chromatin looping and impaired imprinting of DLX5 in Rett syndrome', *Nature genetics*, 37(1), pp. 31–40.

Hou, G., Smith, A. G. and Zhang, Z.-W. (2016) 'Lack of Intrinsic GABAergic Connections in the Thalamic Reticular Nucleus of the Mouse', *The Journal of neuroscience: the official journal of the Society for Neuroscience*, 36(27), pp. 7246–7252.

Howard, M. W. *et al.* (2003) 'Gamma oscillations correlate with working memory load in humans', *Cerebral cortex* , 13(12), pp. 1369–1374.

Hsiao, S. S., O'Shaughnessy, D. M. and Johnson, K. O. (1993) 'Effects of selective attention on spatial form processing in monkey primary and secondary somatosensory cortex', *Journal of neurophysiology*, 70(1), pp. 444–447.

Huber, R. *et al.* (2004) 'Local sleep and learning', *Nature*, 430(6995), pp. 78–81.

Huber, R. *et al.* (2006) 'Arm immobilization causes cortical plastic changes and locally decreases sleep slow wave activity', *Nature neuroscience*, 9(9), pp. 1169–1176.

Huppke, P. et al. (2000) ‘Rett syndrome: analysis of MECP2 and clinical characterization of 31 patients’, Human molecular genetics, 9(9), pp. 1369–1375.

Huppke, P. *et al.* (2006) ‘Very mild cases of Rett syndrome with skewed X inactivation’, *Journal of medical genetics*, 43(10), pp. 814–816.

Ichiyanagi, T. *et al.* (2013) ‘Accumulation and loss of asymmetric non-CpG methylation during male germ-cell development’, *Nucleic acids research*, 41(2), pp. 738–745.

Imessaoudene, B. *et al.* (2001) ‘MECP2 mutation in non-fatal, non-progressive encephalopathy in a male’, *Journal of medical genetics*, 38(3), pp. 171–174.

Inostroza, M. and Born, J. (2013) ‘Sleep for preserving and transforming episodic memory’, *Annual review of neuroscience*, 36, pp. 79–102.

Ioannides, A. A. *et al.* (2009) ‘MEG identifies dorsal medial brain activations during sleep’, *NeuroImage*, 44(2), pp. 455–468.

Ishizaki, A. *et al.* (1989) ‘Longitudinal observation of electroencephalograms in the Rett syndrome’, *Brain & development*, 11(6), pp. 407–412.

Isomura, Y. *et al.* (2006) ‘Integration and segregation of activity in entorhinal-hippocampal subregions by neocortical slow oscillations’, *Neuron*, 52(5), pp. 871–882.

Ito-Ishida, A. *et al.* (2015) ‘Loss of MeCP2 in Parvalbumin-and Somatostatin-Expressing Neurons in Mice Leads to Distinct Rett Syndrome-like Phenotypes’, *Neuron*, 88(4), pp. 651–658.

Jang, H. S. *et al.* (2017) ‘CpG and Non-CpG Methylation in Epigenetic Gene Regulation and Brain Function’, *Genes*, 8(6). doi: 10.3390/genes8060148.

Jeffery, L. and Nakielny, S. (2004) ‘Components of the DNA methylation system of chromatin control are RNA-binding proteins’, *The Journal of biological chemistry*, 279(47), pp. 49479–49487.

Jensen, M. S., Azouz, R. and Yaari, Y. (1996) ‘Spike after-depolarization and burst generation in adult rat hippocampal CA1 pyramidal cells’, *The Journal of physiology*, 492 (Pt 1), pp. 199–210.

Jensen, O. *et al.* (2002) ‘Oscillations in the alpha band (9-12 Hz) increase with memory load during retention in a short-term memory task’, *Cerebral cortex* , 12(8), pp. 877–882.

Jensen, O. and Mazaheri, A. (2010) ‘Shaping functional architecture by oscillatory alpha activity: gating by inhibition’, *Frontiers in human neuroscience*, 4, p. 186.

Jensen, O. and Tesche, C. D. (2002) ‘Frontal theta activity in humans increases with memory load in a working memory task’, *The European journal of neuroscience*, 15(8), pp. 1395–1399.

Jiang, M. *et al.* (2013) ‘Dendritic arborization and spine dynamics are abnormal in the mouse model of MECP2 duplication syndrome’, *The Journal of neuroscience: the official journal of the Society for Neuroscience*, 33(50), pp. 19518–19533.

Ji, D. and Wilson, M. A. (2006) ‘Coordinated memory replay in the visual cortex and hippocampus during sleep’, *Nature neuroscience*, 10(1), pp. 100–107.

Ji, Y. *et al.* (2010) ‘Methylation analyses on promoters of mPer1, mPer2, and mCry1 during perinatal development’, *Biochemical and biophysical research communications*, 391(4), pp. 1742–1747.

Johnston, M. V. *et al.* (2014) ‘Twenty-four hour quantitative-EEG and in-vivo glutamate biosensor detects activity and circadian rhythm dependent biomarkers of pathogenesis in Mecp2 null mice’, *Frontiers in systems neuroscience*, 8, p. 118.

Jones, E. G. and Friedman, D. P. (1982) ‘Projection pattern of functional components of thalamic ventrobasal complex on monkey somatosensory cortex’, *Journal of neurophysiology*, 48(2), pp. 521–544.

Jones, O. T. *et al.* (1997) ‘N-Type calcium channels in the developing rat hippocampus: subunit, complex, and regional expression’, *The Journal of neuroscience: the official journal of the Society for Neuroscience*, 17(16), pp. 6152–6164.

Jones, P. A. (2012) ‘Functions of DNA methylation: islands, start sites, gene bodies and beyond’, *Nature reviews. Genetics*, 13(7), pp. 484–492.

Jones, P. L. *et al.* (1998) ‘Methylated DNA and MeCP2 recruit histone deacetylase to repress transcription’, *Nature genetics*, 19(2), pp. 187–191.

Jordan, C. *et al.* (2007) ‘Cerebellar gene expression profiles of mouse models for Rett syndrome reveal novel MeCP2 targets’, *BMC medical genetics*, 8, p. 36.

Jouvet, M. (1969) ‘Biogenic amines and the states of sleep’, *Science*, 163(3862), pp. 32–41.

Kahana, M. J. *et al.* (1999) 'Human theta oscillations exhibit task dependence during virtual maze navigation', *Nature*, 399(6738), pp. 781–784.

Kaiser, D. A. (2005) 'Basic principles of quantitative EEG', *Journal of adult development*, 12(2-3), pp. 99–104.

Kankirawatana, P. *et al.* (2006) 'Early progressive encephalopathy in boys and MECP2 mutations', *Neurology*, 67(1), pp. 164–166.

Karch, F. E. *et al.* (1997) 'Comparative efficacy and tolerability of two long-acting calcium antagonists, mibefradil and amlodipine, in essential hypertension', *Clinical therapeutics*, 19(6), pp. 1368–1378.

Kasper, E. M. *et al.* (1994) 'Pyramidal neurons in layer 5 of the rat visual cortex. I. Correlation among cell morphology, intrinsic electrophysiological properties, and axon targets: MORPHOLOGY AND PHYSIOLOGY OF ADULT LAYER 5 PYRAMIDAL NEURONS', *The Journal of comparative neurology*, 339(4), pp. 459–474.

Kattler, H., Dijk, D. J. and Borbély, A. A. (1994) 'Effect of unilateral somatosensory stimulation prior to sleep on the sleep EEG in humans', *Journal of sleep research*, 3(3), pp. 159–164.

Kawaguchi, Y. (1995) 'Physiological subgroups of nonpyramidal cells with specific morphological characteristics in layer II/III of rat frontal cortex', *The Journal of neuroscience: the official journal of the Society for Neuroscience*, 15(4), pp. 2638–2655.

Kee, S. E. *et al.* (2018) 'Impaired spatial memory codes in a mouse model of Rett syndrome', *eLife*, 7. doi: 10.7554/eLife.31451.

Keinrath, C. *et al.* (2006) 'Post-movement beta synchronization after kinesthetic illusion, active and passive movements', *International journal of psychophysiology: official journal of the International Organization of Psychophysiology*, 62(2), pp. 321–327.

Key, A. P., Jones, D. and Peters, S. (2019) 'Spoken word processing in Rett syndrome: Evidence from event-related potentials', *International Journal of Developmental Neuroscience*, pp. 26–31. doi: 10.1016/j.ijdevneu.2019.01.001.

Khader, P. H. *et al.* (2010) 'Theta and alpha oscillations during working-memory maintenance predict successful long-term memory encoding', *Neuroscience letters*, 468(3), pp. 339–343.

Kim, D. *et al.* (2001) 'Lack of the burst firing of thalamocortical relay neurons and resistance to absence seizures in mice lacking alpha(1G) T-type Ca(2+) channels', *Neuron*, 31(1), pp. 35–45.

Kinde, B. *et al.* (2016) 'DNA methylation in the gene body influences MeCP2-mediated gene repression', *Proceedings of the National Academy of Sciences of the United States of America*, 113(52), pp. 15114–15119.

Kishi, N. and Macklis, J. D. (2004) 'MECP2 is progressively expressed in post-migratory neurons and is involved in neuronal maturation rather than cell fate decisions', *Molecular and cellular neurosciences*, 27(3), pp. 306–321.

Kishi, N. and Macklis, J. D. (2010) 'MeCP2 functions largely cell-autonomously, but also non-cell-autonomously, in neuronal maturation and dendritic arborization of cortical pyramidal neurons', *Experimental neurology*, 222(1), pp. 51–58.

Klauck, S. M. *et al.* (2002) 'A mutation hot spot for nonspecific X-linked mental retardation in the MECP2 gene causes the PPM-X syndrome', *American journal of human genetics*, 70(4), pp. 1034–1037.

Kleefstra, T. *et al.* (2004) 'MECP2 analysis in mentally retarded patients: implications for routine DNA diagnostics', *European journal of human genetics: EJHG*, 12(1), pp. 24–28.

Knyazev, G. G. (2012) 'EEG delta oscillations as a correlate of basic homeostatic and motivational processes', *Neuroscience and biobehavioral reviews*, 36(1), pp. 677–695.

Knyazev, G. G., Slobodskoj-Plusnin, J. Y. and Bocharov, A. V. (2009) 'Event-related delta and theta synchronization during explicit and implicit emotion processing', *Neuroscience*, 164(4), pp. 1588–1600.

Koch, G. L. (1990) 'The endoplasmic reticulum and calcium storage', *BioEssays: news and reviews in molecular, cellular and developmental biology*, 12(11), pp. 527–531.

Koenderink, M. J. and Uylings, H. B. (1995) 'Postnatal maturation of layer V pyramidal neurons in the human prefrontal cortex. A quantitative Golgi analysis', *Brain research*, 678(1-2), pp. 233–243.

Kokura, K. *et al.* (2001) 'The Ski protein family is required for MeCP2-mediated transcriptional repression', *The Journal of biological chemistry*, 276(36), pp. 34115–34121.

Kole, M. H. P., Bräuer, A. U. and Stuart, G. J. (2007) 'Inherited cortical HCN1 channel loss amplifies dendritic calcium electrogenesis and burst firing in a rat absence epilepsy model', *The Journal of physiology*, 578(Pt 2), pp. 507–525.

Komuro, H. and Rakic, P. (1992) 'Selective role of N-type calcium channels in neuronal migration', *Science*, 257(5071), pp. 806–809.

Kopecky, B.J., Liang, R. and Bao, J. (2014) 'T-type calcium channel blockers as neuroprotective agents', *Pflugers Archiv: European journal of physiology*, 466(4), pp. 757–765.

Kopell, N. *et al.* (2000) 'Gamma rhythms and beta rhythms have different synchronization properties', *Proceedings of the National Academy of Sciences of the United States of America*, 97(4), pp. 1867–1872.

Kramer, M. A. *et al.* (2008) 'Rhythm generation through period concatenation in rat somatosensory cortex', *PLoS computational biology*, 4(9), p. e1000169.

Kriaucionis, S. and Bird, A. (2004) 'The major form of MeCP2 has a novel N-terminus generated by alternative splicing', *Nucleic acids research*, 32(5), pp. 1818–1823.

Kriaucionis, S. and Heintz, N. (2009) 'The nuclear DNA base 5-hydroxymethylcytosine is present in Purkinje neurons and the brain', *Science*, 324(5929), pp. 929–930.

Krishnan, K. *et al.* (2015) 'MeCP2 regulates the timing of critical period plasticity that shapes functional connectivity in primary visual cortex', *Proceedings of the National Academy of Sciences of the United States of America*, 112(34), pp. E4782–91.

Kron, M. *et al.* (2011) 'Altered responses of MeCP2-deficient mouse brain stem to severe hypoxia', *Journal of neurophysiology*, 105(6), pp. 3067–3079.

Kron, M. *et al.* (2012) 'Brain activity mapping in Mecp2 mutant mice reveals functional deficits in forebrain circuits, including key nodes in the default mode network, that are reversed with ketamine treatment', *Journal of Neuroscience*, 32(40), pp. 13860–13872.

Kroon, T. *et al.* (2019) 'Early postnatal development of pyramidal neurons across layers of the mouse medial prefrontal cortex', *Scientific reports*, 9(1), pp. 1–16.

Kudo, S. *et al.* (2001) 'Functional analyses of MeCP2 mutations associated with Rett syndrome using transient expression systems', *Brain and Development*, pp. S165–S173. doi: 10.1016/s0387-7604(01)00345-x.

Kume, K. *et al.* (2005) 'Dopamine is a regulator of arousal in the fruit fly', *The Journal of neuroscience: the official journal of the Society for Neuroscience*, 25(32), pp. 7377–7384.

Künzle, H. (1977) 'Projections from the primary somatosensory cortex to basal ganglia and thalamus in the monkey', *Experimental brain research. Experimentelle Hirnforschung. Experimentation cerebrale*, 30(4), pp. 481–492.

Kurth, S. *et al.* (2010) 'Mapping of cortical activity in the first two decades of life: a high-density sleep electroencephalogram study', *The Journal of neuroscience: the official journal of the Society for Neuroscience*, 30(40), pp. 13211–13219.

Kyle, S.M., Vashi, N. and Justice, M.J. (2018) 'Rett syndrome: a neurological disorder with metabolic components', Open biology, 8(2). doi:10.1098/rsob.170216.

Lagger, S. *et al.* (2017) 'MeCP2 recognizes cytosine methylated tri-nucleotide and di-nucleotide sequences to tune transcription in the mammalian brain', *PLoS genetics*, 13(5), p. e1006793.

Lakatos, P. *et al.* (2005) 'An oscillatory hierarchy controlling neuronal excitability and stimulus processing in the auditory cortex', *Journal of neurophysiology*, 94(3), pp. 1904–1911.

Lakatos, P. *et al.* (2008) 'Entrainment of neuronal oscillations as a mechanism of attentional selection', *Science*, 320(5872), pp. 110–113.

Larson, J., Wong, D. and Lynch, G. (1986) 'Patterned stimulation at the theta frequency is optimal for the induction of hippocampal long-term potentiation', *Brain research*, 368(2), pp. 347–350.

Larsson-Backström, C., Arrhenius, E. and Sagge, K. (1985) 'Comparison of the calcium-antagonistic effects of terodiline, nifedipine and verapamil', *Acta pharmacologica et toxicologica*, 57(1), pp. 8–17.

Latchoumane, C.-F. V. *et al.* (2017) 'Thalamic Spindles Promote Memory Formation during Sleep through Triple Phase-Locking of Cortical, Thalamic, and Hippocampal Rhythms', *Neuron*, 95(2), pp. 424–435.e6.

Laurent, L. *et al.* (2010) 'Dynamic changes in the human methylome during differentiation', *Genome research*, 20(3), pp. 320–331.

LeBlanc, J. J. *et al.* (2015) 'Visual evoked potentials detect cortical processing deficits in Rett syndrome', *Annals of Neurology*, pp. 775–786. doi: 10.1002/ana.24513.

Lee, J., Kim, D. and Shin, H.-S. (2004) 'Lack of delta waves and sleep disturbances during non-rapid eye movement sleep in mice lacking α1G-subunit of T-type calcium channels', *Proceedings of the National Academy of Sciences of the United States of America*, 101(52), pp. 18195–18199.

Lee, J. and Shin, H.-S. (2007) 'T-type calcium channels and thalamocortical rhythms in sleep: a perspective from studies of T-type calcium channel knockout mice', *CNS & neurological disorders drug targets*, 6(1), pp. 63–69.

Lee, L.-C. *et al.* (2021) 'Association of CaMK2A and MeCP2 signaling pathways with cognitive ability in adolescents', *Molecular brain*, 14(1), p. 152.

Leger, M. *et al.* (2013) 'Object recognition test in mice', *Nature protocols*, 8(12), pp. 2531–2537.

Lei, S. *et al.* (2003) 'Depolarization-induced long-term depression at hippocampal mossy fiber-CA3 pyramidal neuron synapses', *The Journal of neuroscience: the official journal of the Society for Neuroscience*, 23(30), pp. 9786–9795.

Lena, I., Parrot, S. and Deschaux, O. (2005) 'Variations in extracellular levels of dopamine, noradrenaline, glutamate, and aspartate across the sleep–wake cycle in the medial prefrontal cortex and nucleus …', *Journal of*. Available at: https://onlinelibrary.wiley.com/doi/abs/10.1002/jnr.20602?casa_token=NfMIkNkKrBEAAAAA:t72idNXRlIkN6gZuzsRsWlU6Mm0rujc7JLBo8fbckb5gpqyFk19ml5c_M4U6EkhCVEfhDl0vkJzSjw.

Leresche, N. *et al.* (1991) 'Low-frequency oscillatory activities intrinsic to rat and cat thalamocortical cells', *The Journal of physiology*, 441, pp. 155–174.

Levesque, M. *et al.* (1996) 'Corticostriatal projections from layer V cells in rat are collaterals of long-range corticofugal axons', *Brain research*, 709(2), pp. 311–315.

Lewis, J. D. *et al.* (1992) 'Purification, sequence, and cellular localization of a novel chromosomal protein that binds to methylated DNA', *Cell*, 69(6), pp. 905–914.

Li, J. *et al.* (2021) 'Collapse of complexity of brain and body activity due to excessive inhibition and MeCP2 disruption', *Proceedings of the National Academy of Sciences of the United States of America*, 118(43). doi:10.1073/pnas.2106378118.

Liao, W. *et al.* (2012/4) 'MeCP2+/– mouse model of RTT reproduces auditory phenotypes associated with Rett syndrome and replicate select EEG endophenotypes of autism spectrum disorder', *Neurobiology of disease*, 46(1), pp. 88–92.

Lindqvist, M. *et al.* (2007) 'Long-term calcium antagonist treatment of human hypertension with mibefradil or amlodipine increases sympathetic nerve activity', *Journal of hypertension*, 25(1), pp. 169–175.

Lipscombe, D., Kongsamut, S. and Tsien, R. W. (1989) 'Alpha-adrenergic inhibition of sympathetic neurotransmitter release mediated by modulation of N-type calcium-channel gating', *Nature*, 340(6235), pp. 639–642.

Li, Q. *et al.* (2015) 'Circadian rhythm disruption in a mouse model of Rett syndrome circadian disruption in RTT', *Neurobiology of disease*, 77, pp. 155–164.

Lister, R. *et al.* (2009) 'Human DNA methylomes at base resolution show widespread epigenomic differences', *Nature*, 462(7271), pp. 315–322.

Lister, R. *et al.* (2011) 'Hotspots of aberrant epigenomic reprogramming in human induced pluripotent stem cells', *Nature*, 471(7336), pp. 68–73.

Lister, R. *et al.* (2013) 'Global epigenomic reconfiguration during mammalian brain development', *Science*, 341(6146), p. 1237905.

Liu, Z. *et al.* (2016) 'Autism-like behaviours and germline transmission in transgenic monkeys overexpressing MeCP2', *Nature*, 530(7588), pp. 98–102.

Lock, J. T., Parker, I. and Smith, I. F. (2015) 'A comparison of fluorescent Ca2+ indicators for imaging local Ca2+ signals in cultured cells', *Cell calcium*, 58(6), pp. 638–648.

Lo, F.-S., Blue, M. E. and Erzurumlu, R. S. (2016) 'Enhancement of postsynaptic GABAA and extrasynaptic NMDA receptor-mediated responses in the barrel cortex of Mecp2-null mice', *Journal of neurophysiology*, 115(3), pp. 1298–1306.

Logothetis, N. K. *et al.* (2012) 'Hippocampal–cortical interaction during periods of subcortical silence', *Nature*, 491(7425), pp. 547–553.

Lohmann, C. and Kessels, H. W. (2014) 'The developmental stages of synaptic plasticity', *The Journal of physiology*, 592(1), pp. 13–31.

Loomis, A. L., Harvey, E. N. and Hobart, G. (1935) 'POTENTIAL RHYTHMS OF THE CEREBRAL CORTEX DURING SLEEP', *Science*, 81(2111), pp. 597–598.

Lugtenberg, D. *et al.* (2009) 'Structural variation in Xq28: MECP2 duplications in 1% of patients with unexplained XLMR and in 2% of male patients with severe encephalopathy', *European journal of human genetics: EJHG*, 17(4), pp. 444–453.

Lu, H. *et al.* (2007) 'Synchronized delta oscillations correlate with the resting-state functional MRI signal', *Proceedings of the National Academy of Sciences of the United States of America*, 104(46), pp. 18265–18269.

Lyst, M. J. *et al.* (2013) 'Rett syndrome mutations abolish the interaction of MeCP2 with the NCoR/SMRT co-repressor', *Nature neuroscience*, 16(7), pp. 898–902.

Lyst, M. J. *et al.* (2016) 'Sequence-specific DNA binding by AT-hook motifs in MeCP2', *FEBS letters*, 590(17), pp. 2927–2933.

Lyst, M. J. and Bird, A. (2015) 'Rett syndrome: a complex disorder with simple roots', *Nature reviews. Genetics*, 16(5), pp. 261–275.

MacKay, W. A. and Mendoncc¸a, A. J. (1995) 'Field potential oscillatory bursts in parietal cortex before and during reach', *Brain research*, 704(2), pp. 167–174.

Madsen, P. L. *et al.* (1991) 'Cerebral O2 metabolism and cerebral blood flow in humans during deep and rapid-eye-movement sleep', *Journal of applied physiology*, 70(6), pp. 2597–2601.

Magee, J. C. and Carruth, M. (1999) 'Dendritic voltage-gated ion channels regulate the action potential firing mode of hippocampal CA1 pyramidal neurons', *Journal of neurophysiology*, 82(4), pp. 1895–1901.

Maingret, N. *et al.* (2016) 'Hippocampo-cortical coupling mediates memory consolidation during sleep', *Nature neuroscience*, 19, p. 959.

Maquet, P. (1995) 'Sleep function(s) and cerebral metabolism', *Behavioural brain research*, 69(1-2), pp. 75–83.

Marchetto, M. C. N. *et al.* (2010) 'A model for neural development and treatment of Rett syndrome using human induced pluripotent stem cells', *Cell*, 143(4), pp. 527–539.

Maret, S. *et al.* (2011) 'Sleep and waking modulate spine turnover in the adolescent mouse cortex', *Nature neuroscience*, 14(11), pp. 1418–1420.

Mari, F. *et al.* (2005) 'CDKL5 belongs to the same molecular pathway of MeCP2 and it is responsible for the early-onset seizure variant of Rett syndrome', *Human molecular genetics*, 14(14), pp. 1935–1946.

Marin-Padilla, M. and Marin-Padilla, T. M. (1982) 'Origin, prenatal development and structural organization of layer I of the human cerebral (motor) cortex. A Golgi study', *Anatomy and embryology*, 164(2), pp. 161–206.

Marlin, J. J. and Carter, A. G. (2014) 'GABA-A receptor inhibition of local calcium signaling in spines and dendrites', *The Journal of neuroscience: the official journal of the Society for Neuroscience*, 34(48), pp. 15898–15911.

Marshall, J. *et al.* (2003) 'Calcium channel and NMDA receptor activities differentially regulate nuclear C/EBPbeta levels to control neuronal survival', *Neuron*, 39(4), pp. 625–639.

Marshall, L. *et al.* (2004) 'Transcranial direct current stimulation during sleep improves declarative memory', *The Journal of neuroscience: the official journal of the Society for Neuroscience*, 24(44), pp. 9985–9992.

Marshall, L. *et al.* (2006) 'Boosting slow oscillations during sleep potentiates memory', *Nature*, 444(7119), pp. 610–613.

Martínez de Paz, A. *et al.* (2019) 'MeCP2-E1 isoform is a dynamically expressed, weakly DNA-bound protein with different protein and DNA interactions compared to MeCP2-E2', *Epigenetics & chromatin*, 12(1), p. 63.

Massimini, M. *et al.* (2004) 'The sleep slow oscillation as a traveling wave', *The Journal of neuroscience: the official journal of the Society for Neuroscience*, 24(31), pp. 6862–6870.

Matsuda, S. *et al.* (2019) 'NNC 55-0396, a T-type calcium channel blocker, protects against the brain injury induced by middle cerebral artery occlusion and reperfusion in mice', *Journal of pharmacological sciences*, 140(2), pp. 193–196.

Matthews, E. A. *et al.* (2007) 'The Cav2.3 calcium channel antagonist SNX-482 reduces dorsal horn neuronal responses in a rat model of chronic neuropathic pain', *The European journal of neuroscience*, 25(12), pp. 3561–3569.

Maunakea, A. K. *et al.* (2013) 'Intragenic DNA methylation modulates alternative splicing by recruiting MeCP2 to promote exon recognition', *Cell research*, 23(11), pp. 1256–1269.

McCarley, R. W. (2007) 'Neurobiology of REM and NREM sleep', *Sleep medicine*, 8(4), pp. 302–330.

McCormick, D. A. *et al.* (1985) 'Comparative electrophysiology of pyramidal and sparsely spiny stellate neurons of the neocortex', *Journal of neurophysiology*, 54(4), pp. 782–806.

McCormick, D. A. and Pape, H. C. (1990) 'Properties of a hyperpolarization-activated cation current and its role in rhythmic oscillation in thalamic relay neurones', *The Journal of physiology*, 431, pp. 291–318.

McNulty, M.M. and Hanck, D.A. (2004) 'State-dependent mibefradil block of Na+ channels', *Molecular pharmacology*, 66(6), pp. 1652–1661.

Medic, G., Wille, M. and Hemels, M. E. H. (2017) 'Short-and long-term health consequences of sleep disruption', *Nature and science of sleep*, 9, p. 151.

Meehan, R. R. *et al.* (1989) 'Identification of a mammalian protein that binds specifically to DNA containing methylated CpGs', *Cell*, 58(3), pp. 499–507.

Meehan, R. R., Lewis, J. D. and Bird, A. P. (1992) 'Characterization of MeCP2, a vertebrate DNA binding protein with affinity for methylated DNA', *Nucleic acids research*, 20(19), pp. 5085–5092.

Mellén, M. *et al.* (2012) 'MeCP2 binds to 5hmC enriched within active genes and accessible chromatin in the nervous system', *Cell*, 151(7), pp. 1417–1430.

Meloni, I. *et al.* (2000) 'A mutation in the rett syndrome gene, MECP2, causes X-linked mental retardation and progressive spasticity in males', *American journal of human genetics*, 67(4), pp. 982–985.

Mencarelli, M. A. *et al.* (2010) 'Novel FOXG1 mutations associated with the congenital variant of Rett syndrome', *Journal of medical genetics*, 47(1), pp. 49–53.

Metz, A. E. *et al.* (2005) 'R-type calcium channels contribute to afterdepolarization and bursting in hippocampal CA1 pyramidal neurons', *The Journal of neuroscience: the official journal of the Society for Neuroscience*, 25(24), pp. 5763–5773.

Michels, L. *et al.* (2013) 'Developmental changes of functional and directed resting-state connectivities associated with neuronal oscillations in EEG', *NeuroImage*, 81, pp. 231–242.

Miller, K. D. (2003) 'Understanding Layer 4 of the Cortical Circuit: A Model Based on Cat V1', *Cerebral cortex* , 13(1), pp. 73–82.

Mills, L. R. *et al.* (1994) 'N-type Ca2+ channels are located on somata, dendrites, and a subpopulation of dendritic spines on live hippocampal pyramidal neurons', *The Journal of neuroscience: the official journal of the Society for Neuroscience*, 14(11 Pt 2), pp. 6815–6824.

Mironov, S. L. *et al.* (2009) 'Remodelling of the respiratory network in a mouse model of Rett syndrome depends on brain-derived neurotrophic factor regulated slow calcium buffering', *The Journal of physiology*, 587(Pt 11), pp. 2473–2485.

Mitchell, S. J. and Ranck, J. B., Jr (1980) 'Generation of theta rhythm in medial entorhinal cortex of freely moving rats', *Brain research*, 189(1), pp. 49–66.

Mnatzakanian, G. N. *et al.* (2004) 'A previously unidentified MECP2 open reading frame defines a new protein isoform relevant to Rett syndrome', *Nature genetics*, 36(4), pp. 339–341.

Mochida, S. *et al.* (1996) 'Inhibition of neurotransmission by peptides containing the synaptic protein interaction site of N-type Ca2+ channels', *Neuron*, 17(4), pp. 781–788.

Mogi, M. *et al.* (2006) 'Amlodipine Treatment Reduces Stroke Size in Apolipoprotein E–Deficient Mice*', *American journal of hypertension*, 19(11), pp. 1144–1149.

Molderings, G. J., Likungu, J. and Göthert, M. (2000) 'N-Type calcium channels control sympathetic neurotransmission in human heart atrium', *Circulation*, 101(4), pp. 403–407.

Mölle, M. *et al.* (2004) 'Learning increases human electroencephalographic coherence during subsequent slow sleep oscillations', *Proceedings of the National Academy of Sciences of the United States of America*, 101(38), pp. 13963–13968.

Monesterolo, N. E. *et al.* (2008) 'Activation of PMCA by calmodulin or ethanol in plasma membrane vesicles from rat brain involves dissociation of the acetylated tubulin/PMCA complex', *The FEBS journal*, 275(14), pp. 3567–3579.

Moog, U. *et al.* (2003) 'Neurodevelopmental disorders in males related to the gene causing Rett syndrome in females (MECP2)', *European journal of paediatric neurology: EJPN: official journal of the European Paediatric Neurology Society*, 7(1), pp. 5–12.

Moore, L. D., Le, T. and Fan, G. (2012) 'DNA Methylation and Its Basic Function', *Neuropsychopharmacology: official publication of the American College of Neuropsychopharmacology*, 38(1), pp. 23–38.

Moore, S. J. and Murphy, G. G. (2020) 'The role of L-type calcium channels in neuronal excitability and aging', *Neurobiology of learning and memory*, 173, p. 107230.

Morello, N. *et al.* (2018) 'Loss of Mecp2 Causes Atypical Synaptic and Molecular Plasticity of Parvalbumin-Expressing Interneurons Reflecting Rett Syndrome-Like Sensorimotor Defects', *eNeuro*, 5(5). doi:10.1523/ENEURO.0086-18.2018.

Moretti, P. *et al.* (2006) ‘Learning and Memory and Synaptic Plasticity Are Impaired in a Mouse Model of Rett Syndrome’, *The Journal of neuroscience: the official journal of the Society for Neuroscience*, 26(1), pp. 319–327.

Morillon, B. *et al.* (2019) ‘Prominence of delta oscillatory rhythms in the motor cortex and their relevance for auditory and speech perception’, *Neuroscience and biobehavioral reviews*, 107, pp. 136–142.

Morison, R. S. and Bassett, D. L. (1946) ‘ELECTRICAL ACTIVITY OF THE THALAMUS AND BASAL GANGLIA IN DECORTICATE CATS’, *The Journal of Nervous and Mental Disease*, p. 452. doi: 10.1097/00005053-194610000-00018.

Mormann, F. *et al.* (2008) ‘Independent delta/theta rhythms in the human hippocampus and entorhinal cortex’, *Frontiers in human neuroscience*, 2, p. 3.

Mossner, J.M. *et al.* (2020) ‘Developmental loss of MeCP2 from VIP interneurons impairs cortical function and behavior’, *eLife*, 9, p. e55639.

Mountcastle, V. B. (1997) ‘The columnar organization of the neocortex’, *Brain: a journal of neurology*, 120 (Pt 4), pp. 701–722.

Mulert, C. *et al.* (2004) ‘Integration of fMRI and simultaneous EEG: towards a comprehensive understanding of localization and time-course of brain activity in target detection’, *NeuroImage*, 22(1), pp. 83–94.

Münzel, M. *et al.* (2010) ‘Quantification of the sixth DNA base hydroxymethylcytosine in the brain’, *Angewandte Chemie* , 49(31), pp. 5375–5377.

Myoga, M. H. and Regehr, W. G. (2011) ‘Calcium microdomains near R-type calcium channels control the induction of presynaptic long-term potentiation at parallel fiber to purkinje cell synapses’, *The Journal of neuroscience: the official journal of the Society for Neuroscience*, 31(14), pp. 5235–5243.

Na, E. S. *et al.* (2012) ‘A mouse model for MeCP2 duplication syndrome: MeCP2 overexpression impairs learning and memory and synaptic transmission’, *Journal of*. Available at: https://www.jneurosci.org/content/32/9/3109.short.

Na, E. S. and Monteggia, L. M. (2011) ‘The role of MeCP2 in CNS development and function’, *Hormones and behavior*, 59(3), pp. 364–368.

Naka, A. and Adesnik, H. (2016) 'Inhibitory Circuits in Cortical Layer 5', *Frontiers in neural circuits*, 10, p. 35.

Nakamura, A. *et al.* (1998) 'Somatosensory Homunculus as Drawn by MEG', *NeuroImage*, 7(4), pp. 377–386.

Nan, X. *et al.* (1998) 'Transcriptional repression by the methyl-CpG-binding protein MeCP2 involves a histone deacetylase complex', *Nature*, 393(6683), pp. 386–389.

Nan, X., Meehan, R. R. and Bird, A. (1993) 'Dissection of the methyl-CpG binding domain from the chromosomal protein MeCP2', *Nucleic acids research*, 21(21), pp. 4886–4892.

Navarrete, M., Valderrama, M. and Lewis, P. A. (2020) 'The role of slow-wave sleep rhythms in the cortical-hippocampal loop for memory consolidation', *Current Opinion in Behavioral Sciences*, 32, pp. 102–110.

Nazor, K. L. *et al.* (2012) 'Recurrent variations in DNA methylation in human pluripotent stem cells and their differentiated derivatives', *Cell stem cell*, 10(5), pp. 620–634.

Nectoux, J. *et al.* (2010) 'Cell cloning-based transcriptome analysis in Rett patients: relevance to the pathogenesis of Rett syndrome of new human MeCP2 target genes', *Journal of cellular and molecular medicine*, 14(7), pp. 1962–1974.

Nelson, E. D., Kavalali, E. T. and Monteggia, L. M. (2006) 'MeCP2-dependent transcriptional repression regulates excitatory neurotransmission', *Current biology: CB*, 16(7), pp. 710–716.

Neul, J. L. *et al.* (2008) 'Specific mutations in methyl-CpG-binding protein 2 confer different severity in Rett syndrome', *Neurology*, 70(16), pp. 1313–1321.

Neul, J. L. *et al.* (2010) 'Rett syndrome: revised diagnostic criteria and nomenclature', *Annals of neurology*, 68(6), pp. 944–950.

Neul, J. L. (2012) 'The relationship of Rett syndrome and MECP2 disorders to autism', *Dialogues in clinical neuroscience*, 14(3), pp. 253–262.

Neul, J. L. and Zoghbi, H. Y. (2004) 'Rett syndrome: a prototypical neurodevelopmental disorder', *The Neuroscientist: a review journal bringing neurobiology, neurology and psychiatry*, 10(2), pp. 118–128.

Nomura, Y. (2005) 'Early behavior characteristics and sleep disturbance in Rett syndrome', *Brain & development*, 27 Suppl 1, pp. S35–S42.

Normann, C. *et al.* (2000) 'Associative long-term depression in the hippocampus is dependent on postsynaptic N-type Ca2+ channels', *The Journal of neuroscience: the official journal of the Society for Neuroscience*, 20(22), pp. 8290–8297.

Nowak, L. *et al.* (1984) 'Magnesium gates glutamate-activated channels in mouse central neurones', *Nature*, 307(5950), pp. 462–465.

Nyhus, E. and Curran, T. (2010) 'Functional role of gamma and theta oscillations in episodic memory', *Neuroscience and biobehavioral reviews*, 34(7), pp. 1023–1035.

Olson, C. O. *et al.* (2014) 'Brain Region-Specific Expression of MeCP2 Isoforms Correlates with DNA Methylation within Mecp2 Regulatory Elements', *PloS one*, 9(3). doi: 10.1371/journal.pone.0090645.

Olufsen, M. S. *et al.* (2003) 'New roles for the gamma rhythm: population tuning and preprocessing for the Beta rhythm', *Journal of computational neuroscience*, 14(1), pp. 33–54.

Oparil, S. *et al.* (1997) 'Dose-response characteristics of mibefradil, a novel calcium antagonist, in the treatment of essential hypertension', *American journal of hypertension*, 10(7 Pt 1), pp. 735–742.

Opitz, T., De Lima, A. D. and Voigt, T. (2002) 'Spontaneous development of synchronous oscillatory activity during maturation of cortical networks in vitro', *Journal of neurophysiology*, 88(5), pp. 2196–2206.

Orrico, A. *et al.* (2000) 'MECP2 mutation in male patients with non-specific X-linked mental retardation', *FEBS letters*, 481(3), pp. 285–288.

Orzeł-Gryglewska, J. (2010) 'Consequences of sleep deprivation', *International journal of occupational medicine and environmental health*, 23(1), pp. 95–114.

Osipova, D. *et al.* (2006) 'Theta and gamma oscillations predict encoding and retrieval of declarative memory', *The Journal of neuroscience: the official journal of the Society for Neuroscience*, 26(28), pp. 7523–7531.

Pacheco, N. L. *et al.* (2017) 'RNA sequencing and proteomics approaches reveal novel deficits in the cortex of Mecp2-deficient mice, a model for Rett syndrome', *Molecular autism*, 8, p. 56.

Panagiotaropoulos, T. I. *et al.* (2012) 'Neuronal discharges and gamma oscillations explicitly reflect visual consciousness in the lateral prefrontal cortex', *Neuron*, 74(5), pp. 924–935.

Parajuli, L. K. *et al.* (2012) 'Quantitative Regional and Ultrastructural Localization of the Cav2.3 Subunit of R-type Calcium Channel in Mouse Brain', *Journal of Neuroscience*, pp. 13555–13567. doi: 10.1523/jneurosci.1142-12.2012.

Paré, D. and Collins, D. R. (2000) 'Neuronal Correlates of Fear in the Lateral Amygdala: Multiple Extracellular Recordings in Conscious Cats', *The Journal of neuroscience: the official journal of the Society for Neuroscience*, 20(7), pp. 2701–2710.

Park, H. *et al.* (2016) 'Formation of visual memories controlled by gamma power phase-locked to alpha oscillations', *Scientific reports*, 6, p. 28092.

Patil, V., Ward, R. L. and Hesson, L. B. (2014) 'The evidence for functional non-CpG methylation in mammalian cells', *Epigenetics: official journal of the DNA Methylation Society*, 9(6), pp. 823–828.

Patterson, K. C. *et al.* (2016) 'MeCP2 deficiency results in robust Rett-like behavioural and motor deficits in male and female rats', *Human molecular genetics*, 25(24), pp. 5514–5515.

Pellegrini, C. *et al.* (2016) 'Suppression of Sleep Spindle Rhythmogenesis in Mice with Deletion of CaV3.2 and CaV3.3 T-type Ca2+ Channels', *Sleep*, 39(4), pp. 875–885.

Penfield, W. and Boldrey, E. (1937) 'Somatic motor and sensory representation in the cerebral cortex of man as studied by electrical stimulation', *Brain: a journal of neurology*.

Percy, A. (2014) 'The American history of Rett syndrome', *Pediatric neurology*, 50(1), pp. 1–3.

Perez-Reyes, E. *et al.* (1998) 'Molecular characterization of a neuronal low-voltage-activated T-type calcium channel', *Nature*, 391(6670), pp. 896–900.

Perez-Reyes, E. (2003) 'Molecular physiology of low-voltage-activated t-type calcium channels', *Physiological reviews*, 83(1), pp. 117–161.

Philippe, C. et al. (2006) 'Spectrum and distribution of MECP2 mutations in 424 Rett syndrome patients: a molecular update', European journal of medical genetics, 49(1), pp. 9–18.

Philippe, C. *et al.* (2010) 'Phenotypic variability in Rett syndrome associated with FOXG1 mutations in females', *Journal of medical genetics*, 47(1), pp. 59–65.

Pizzo, R. *et al.* (2016) 'Lack of Cdkl5 Disrupts the Organization of Excitatory and Inhibitory Synapses and Parvalbumin Interneurons in the Primary Visual Cortex', *Frontiers in cellular neuroscience*, 10, p. 261.

Platt, B. and Riedel, G. (2011) 'The cholinergic system, EEG and sleep', *Behavioural brain research*, 221(2), pp. 499–504.

Ploner, M. *et al.* (2000) 'Differential organization of touch and pain in human primary somatosensory cortex', *Journal of neurophysiology*, 83(3), pp. 1770–1776.

Quaderi, N. A. *et al.* (1994) 'Genetic and physical mapping of a gene encoding a methyl CpG binding protein, Mecp2, to the mouse X chromosome', *Genomics*, 22(3), pp. 648–651.

Quenard, A. *et al.* (2006) 'Deleterious mutations in exon 1 of MECP2 in Rett syndrome', *European journal of medical genetics*, 49(4), pp. 313–322.

Quevedo, J. *et al.* (1998) 'L-type voltage-dependent calcium channel blocker nifedipine enhances memory retention when infused into the hippocampus', *Neurobiology of learning and memory*, 69(3), pp. 320–325.

Qureshi, I. A. and Mehler, M. F. (2014) 'Epigenetics of sleep and chronobiology', *Current neurology and neuroscience reports*, 14(3), p. 432.

Rakela, B., Brehm, P. and Mandel, G. (2018) 'Astrocytic modulation of excitatory synaptic signaling in a mouse model of Rett syndrome', *eLife*, 7. doi: 10.7554/eLife.31629.

Ramocki, M. B. *et al.* (2009) 'Autism and other neuropsychiatric symptoms are prevalent in individuals with MeCP2 duplication syndrome', *Annals of neurology*, 66(6), pp. 771–782.

Ramocki, M. B., Tavyev, Y. J. and Peters, S. U. (2010) 'The MECP2 duplication syndrome', *American journal of medical genetics. Part A*, 152A(5), pp. 1079–1088.

Randall, A. D. and Tsien, R. W. (1997) 'Contrasting biophysical and pharmacological properties of T-type and R-type calcium channels', *Neuropharmacology*, 36(7), pp. 879–893.

Rett, A. (1966) '[On a unusual brain atrophy syndrome in hyperammonemia in childhood]', *Wiener medizinische Wochenschrift* , 116(37), pp. 723–726.

Rhodes, P. A. and Gray, C. M. (1994) 'Simulations of intrinsically bursting neocortical pyramidal neurons', *Neural computation*, 6(6), pp. 1086–1110.

Richer, C. *et al.* (1996) 'Cerebroprotective effects of a calcium antagonist, mibefradil. In the stroke-prone spontaneously hypertensive rat', *Fundamental & clinical pharmacology*, 2(10), p. 212.

Riddle, J. *et al.* (2020) 'Causal Evidence for a Role of Theta and Alpha Oscillations in the Control of Working Memory', *Current biology: CB*, 30(9), pp. 1748–1754.e4.

Rieckhof, G. E. *et al.* (2003) 'Presynaptic N-type calcium channels regulate synaptic growth', *The Journal of biological chemistry*, 278(42), pp. 41099–41108.

Rietveld, L. *et al.* (2015) 'Genotype-specific effects of Mecp2 loss-of-function on morphology of Layer V pyramidal neurons in heterozygous female Rett syndrome model mice', *Frontiers in cellular neuroscience*, 9, p. 145.

Rizzuto, D. S. *et al.* (2006) 'Human neocortical oscillations exhibit theta phase differences between encoding and retrieval', *NeuroImage*, 31(3), pp. 1352–1358.

Robinson, H. A. and Pozzo-Miller, L. (2019) 'The role of MeCP2 in learning and memory', *Learning & memory* , 26(9), pp. 343–350.

Robinson, L. *et al.* (2012) 'Morphological and functional reversal of phenotypes in a mouse model of Rett syndrome', *Brain: a journal of neurology*, 135(Pt 9), pp. 2699–2710.

Roche, K. J. *et al.* (2019) 'Electroencephalographic spectral power as a marker of cortical function and disease severity in girls with Rett syndrome', *Journal of neurodevelopmental disorders*, 11(1), p. 15.

Rodriguez, A. V. *et al.* (2016) 'Why Does Sleep Slow-Wave Activity Increase After Extended Wake? Assessing the Effects of Increased Cortical Firing During Wake and Sleep', *The Journal of neuroscience: the official journal of the Society for Neuroscience*, 36(49), pp. 12436–12447.

Roopun, A. K. *et al.* (2006) 'A beta2-frequency (20-30 Hz) oscillation in nonsynaptic networks of somatosensory cortex', *Proceedings of the National Academy of Sciences*, pp. 15646–15650. doi: 10.1073/pnas.0607443103.

Roopun, A. K. *et al.* (2008) 'Period concatenation underlies interactions between gamma and beta rhythms in neocortex', *Frontiers in cellular neuroscience*, 2, p. 1.

Rosanova, M. and Ulrich, D. (2005) 'Pattern-specific associative long-term potentiation induced by a sleep spindle-related spike train', *The Journal of neuroscience: the official journal of the Society for Neuroscience*, 25(41), pp. 9398–9405.

Rossiter, H. E. *et al.* (2013) 'Gamma oscillatory amplitude encodes stimulus intensity in primary somatosensory cortex', *Frontiers in human neuroscience*, 7, p. 362.

Saleh, M. *et al.* (2010) 'Fast and slow oscillations in human primary motor cortex predict oncoming behaviorally relevant cues', *Neuron*, 65(4), pp. 461–471.

Sal'nikov, S. N. (2005) 'Effect of nifedipine on cerebral saturation parameters', *Bulletin of experimental biology and medicine*, 140(4), pp. 423–424.

Sanfeliu, A. *et al.* (2019) 'Transcriptomic Analysis of Mecp2 Mutant Mice Reveals Differentially Expressed Genes and Altered Mechanisms in Both Blood and Brain', *Frontiers in psychiatry / Frontiers Research Foundation*, 10, p. 278.

Sanguinetti, M.C. and Kass, R.S. (1984) 'Voltage-dependent block of calcium channel current in the calf cardiac Purkinje fiber by dihydropyridine calcium channel antagonists', *Circulation research*, 55(3), pp. 336–348.

Sann, S. B. *et al.* (2008) 'Neurite outgrowth and in vivo sensory innervation mediated by a Cav2. 2–laminin β2 stop signal', *Journal of*. Available at: https://www.jneurosci.org/content/28/10/2366.short.

Saunders, C. J. *et al.* (2009) 'Novel exon 1 mutations in MECP2 implicate isoform MeCP2_e1 in classical Rett syndrome', *American journal of medical genetics. Part A*, 149A(5), pp. 1019–1023.

Sauseng, P. *et al.* (2010) 'Control mechanisms in working memory: a possible function of EEG theta oscillations', *Neuroscience and biobehavioral reviews*, 34(7), pp. 1015–1022.

Saxonov, S., Berg, P. and Brutlag, D. L. (2006) 'A genome-wide analysis of CpG dinucleotides in the human genome distinguishes two distinct classes of promoters', *Proceedings of the National Academy of Sciences of the United States of America*, 103(5), pp. 1412–1417.

Schabus, M. *et al.* (2004) 'Sleep spindles and their significance for declarative memory consolidation', *Sleep*, 27(8), pp. 1479–1485.

Schanen, C. *et al.* (2004) 'Phenotypic manifestations of MECP2 mutations in classical and atypical Rett syndrome', *American journal of medical genetics. Part A*, 126A(2), pp. 129–140.

Schlingloff, D. *et al.* (2014) 'Mechanisms of sharp wave initiation and ripple generation', *The Journal of neuroscience: the official journal of the Society for Neuroscience*, 34(34), pp. 11385–11398.

Schneider, T. *et al.* (2020) 'Cav2.3 R-type calcium channels: from its discovery to pathogenic de novo CACNA1E variants: a historical perspective', *Pflügers Archiv - European Journal of Physiology*, 472(7), pp. 811–816.

Schroeder, C. E. and Lakatos, P. (2009) 'Low-frequency neuronal oscillations as instruments of sensory selection', *Trends in neurosciences*, 32(1), pp. 9–18.

Schübeler, D. (2015) 'Function and information content of DNA methylation', *Nature*, 517(7534), pp. 321–326.

Schultz, W. (1998) 'Predictive reward signal of dopamine neurons', *Journal of neurophysiology*, 80(1), pp. 1–27.

Schwartzman, J. S. *et al.* (2001) 'Rett syndrome in a boy with a 47,XXY karyotype confirmed by a rare mutation in the MECP2 gene', *Neuropediatrics*, 32(3), pp. 162–164.

Sederberg, P. B. *et al.* (2007) 'Hippocampal and neocortical gamma oscillations predict memory formation in humans', *Cerebral cortex* , 17(5), pp. 1190–1196.

Shaffery, J. P. *et al.* (2002) 'Rapid eye movement sleep deprivation modifies expression of long-term potentiation in visual cortex of immature rats', *Neuroscience*, 110(3), pp. 431–443.

Shahbazian, M. D. *et al.* (2002) 'Insight into Rett syndrome: MeCP2 levels display tissue- and cell-specific differences and correlate with neuronal maturation', *Human molecular genetics*, 11(2), pp. 115–124.

Shaw, F. Z., Chen, R. F. and Yen, C. T. (2001) 'Dynamic changes of touch- and laser heat-evoked field potentials of primary somatosensory cortex in awake and pentobarbital-anesthetized rats', *Brain research*, 911(2), pp. 105–115.

Shcheglovitov, A. *et al.* (2005) 'Contrasting the effects of nifedipine on subtypes of endogenous and recombinant T-type Ca2+ channels', *Biochemical pharmacology*, 69(5), pp. 841–854.

Sheng, Z. H. *et al.* (1994) 'Identification of a syntaxin-binding site on N-type calcium channels', *Neuron*, 13(6), pp. 1303–1313.

Shepherd, G.M.G. and Katz, D.M. (2011) 'Synaptic microcircuit dysfunction in genetic models of neurodevelopmental disorders: focus on Mecp2 and Met', *Current opinion in neurobiology*, 21(6), pp. 827–833.

Siapas, A. G. and Wilson, M. A. (1998) 'Coordinated Interactions between Hippocampal Ripples and Cortical Spindles during Slow-Wave Sleep', *Neuron*, 21(5), pp. 1123–1128.

Siegel, J. M. *et al.* (1998) 'Monotremes and the evolution of rapid eye movement sleep', *Philosophical transactions of the Royal Society of London. Series B, Biological sciences*, 353(1372), pp. 1147–1157.

Signorini, C. *et al.* (2016) 'MECP2 Duplication Syndrome: Evidence of Enhanced Oxidative Stress. A Comparison with Rett Syndrome', *PloS one*, 11(3), p. e0150101.

Sirota, A. *et al.* (2003) 'Communication between neocortex and hippocampus during sleep in rodents', *Proceedings of the National Academy of Sciences of the United States of America*, 100(4), pp. 2065–2069.

Sirota, A. and Buzsáki, G. (2005) 'Interaction between neocortical and hippocampal networks via slow oscillations', *Thalamus & related systems*, 3(4), pp. 245–259.

Skene, P. J. *et al.* (2010) 'Neuronal MeCP2 is expressed at near histone-octamer levels and globally alters the chromatin state', *Molecular cell*, 37(4), pp. 457–468.

Smrt, R. D. *et al.* (2007) 'Mecp2 deficiency leads to delayed maturation and altered gene expression in hippocampal neurons', *Neurobiology of disease*, 27(1), pp. 77–89.

Soltesz, I. *et al.* (1991) 'Two inward currents and the transformation of low-frequency oscillations of rat and cat thalamocortical cells', *The Journal of physiology*, 441, pp. 175–197.

Son, Y.K. *et al.* (2014) 'Ca2+ channel inhibitor NNC 55-0396 inhibits voltage-dependent K+ channels in rabbit coronary arterial smooth muscle cells', *Journal of pharmacological sciences*, 125(3), pp. 312–319.

Spitzer, N. C., Root, C. M. and Borodinsky, L. N. (2004) 'Orchestrating neuronal differentiation: patterns of Ca2+ spikes specify transmitter choice', *Trends in neurosciences*, 27(7), pp. 415–421.

Staiger, J. F. *et al.* (2004) 'Functional diversity of layer IV spiny neurons in rat somatosensory cortex: quantitative morphology of electrophysiologically characterized and biocytin labeled cells', *Cerebral cortex* , 14(6), pp. 690–701.

Stancheva, I. *et al.* (2003) 'A mutant form of MeCP2 protein associated with human Rett syndrome cannot be displaced from methylated DNA by notch in Xenopus embryos', *Molecular cell*, 12(2), pp. 425–435.

Stanek, E.J., Nelson, C.E. and DeNofrio, D. (1997) 'Amlodipine overdose', *The Annals of pharmacotherapy*, 31(7-8), pp. 853–856.

Staresina, B. P. *et al.* (2015) 'Hierarchical nesting of slow oscillations, spindles and ripples in the human hippocampus during sleep', *Nature neuroscience*, 18(11), pp. 1679–1686.

Stark, E. *et al.* (2014) 'Pyramidal cell-interneuron interactions underlie hippocampal ripple oscillations', *Neuron*, 83(2), pp. 467–480.

Staubli, U. and Lynch, G. (1990) 'Stable depression of potentiated synaptic responses in the hippocampus with 1-5 Hz stimulation', *Brain research*, 513(1), pp. 113–118.

Stauder, J. E. A. *et al.* (2006) 'The development of visual- and auditory processing in Rett syndrome: an ERP study', *Brain & development*, 28(8), pp. 487–494.

Stearns, N. A. *et al.* (2007) 'Behavioral and anatomical abnormalities in Mecp2 mutant mice: a model for Rett syndrome', *Neuroscience*, 146(3), pp. 907–921.

von Stein, A. *et al.* (1999) 'Synchronization between temporal and parietal cortex during multimodal object processing in man', *Cerebral cortex* , 9(2), pp. 137–150.

Steriade, M. *et al.* (1985) 'Abolition of spindle oscillations in thalamic neurons disconnected from nucleus reticularis thalami', *Journal of neurophysiology*, 54(6), pp. 1473–1497.

Steriade, M. *et al.* (1987) 'The deafferented reticular thalamic nucleus generates spindle rhythmicity', *Journal of Neurophysiology*, pp. 260–273. doi: 10.1152/jn.1987.57.1.260.

Steriade, M. *et al.* (1993) 'The slow (< 1 Hz) oscillation in reticular thalamic and thalamocortical neurons: scenario of sleep rhythm generation in interacting thalamic and neocortical networks', *The Journal of neuroscience: the official journal of the Society for Neuroscience*, 13(8), pp. 3284–3299.

Steriade, M. (2003) 'The corticothalamic system in sleep', *Frontiers in bioscience: a journal and virtual library*, 8, pp. d878–99.

Steriade, M. (2006) 'Grouping of brain rhythms in corticothalamic systems', *Neuroscience*, 137(4), pp. 1087–1106.

Steriade, M., Amzica, F. and Contreras, D. (1996) 'Synchronization of fast (30-40 Hz) spontaneous cortical rhythms during brain activation', *The Journal of neuroscience: the official journal of the Society for Neuroscience*, 16(1), pp. 392–417.

Steriade, M., Dossi, R. C. and Nunez, A. (1991) 'Network modulation of a slow intrinsic oscillation of cat thalamocortical neurons implicated in sleep delta waves: cortically induced synchronization and brainstem …', *Journal of Neuroscience*. Available at: http://www.jneurosci.org/content/11/10/3200.short.

Steriade, M., McCormick, D. A. and Sejnowski, T. J. (1993) 'Thalamocortical oscillations in the sleeping and aroused brain', *Science*, 262(5134), pp. 679–685.

Steriade, M., Nuñez, A. and Amzica, F. (1993a) 'A novel slow (< 1 Hz) oscillation of neocortical neurons in vivo: depolarizing and hyperpolarizing components', *The Journal of neuroscience: the official journal of the Society for Neuroscience*, 13(8), pp. 3252–3265.

Steriade, M., Nuñez, A. and Amzica, F. (1993b) 'Intracellular analysis of relations between the slow (< 1 Hz) neocortical oscillation and other sleep rhythms of the electroencephalogram', *The Journal of neuroscience: the official journal of the Society for Neuroscience*, 13(8), pp. 3266–3283.

Stuss, D. P. *et al.* (2012) 'MeCP2 mutation results in compartment-specific reductions in dendritic branching and spine density in layer 5 motor cortical neurons of YFP-H mice', *PloS one*, 7(3), p. e31896.

Südhof, T. C. (2012) 'Calcium control of neurotransmitter release', *Cold Spring Harbor perspectives in biology*, 4(1), p. a011353.

Su, H. *et al.* (2001) 'Extracellular calcium modulates persistent sodium current-dependent burst-firing in hippocampal pyramidal neurons', *The Journal of neuroscience: the official journal of the Society for Neuroscience*, 21(12), pp. 4173–4182.

Szulwach, K. E. *et al.* (2011) '5-hmC--mediated epigenetic dynamics during postnatal neurodevelopment and aging', *Nature neuroscience*, 14(12), p. 1607.

Tallon-Baudry, C. and Bertrand, O. (1999) 'Oscillatory gamma activity in humans and its role in object representation', *Trends in cognitive sciences*, 3(4), pp. 151–162.

Tanabe, T. *et al.* (1988) 'Restoration of excitation—contraction coupling and slow calcium current in dysgenic muscle by dihydropyridine receptor complementary DNA', *Nature*, 336(6195), pp. 134–139.

Tanabe, T. *et al.* (1990) 'Regions of the skeletal muscle dihydropyridine receptor critical for excitation–contraction coupling', *Nature*, 346(6284), pp. 567–569.

Taneja, P. *et al.* (2009) 'Pathophysiology of Locus Ceruleus Neurons in a Mouse Model of Rett Syndrome', *The Journal of neuroscience: the official journal of the Society for Neuroscience*, 29(39), pp. 12187–12195.

Tan, L. L. *et al.* (2019) 'Gamma oscillations in somatosensory cortex recruit prefrontal and descending serotonergic pathways in aversion and nociception', *Nature communications*, 10(1), p. 983.

Tarczy-Hornoch, K., Martin, K. A. C. and Stratford, K. J. (1999) 'Intracortical Excitation of Spiny Neurons in Layer 4 of Cat Striate Cortex In Vitro', *Cerebral*. Available at: https://academic.oup.com/cercor/article-abstract/9/8/833/346715.

Tarokh, L. and Carskadon, M. A. (2010) 'Developmental changes in the human sleep EEG during early adolescence', *Sleep*, 33(6), pp. 801–809.

Tarokh, L., Carskadon, M. A. and Achermann, P. (2010) 'Developmental changes in brain connectivity assessed using the sleep EEG', *Neuroscience*, 171(2), pp. 622–634.

Tate, P., Skarnes, W. and Bird, A. (1996) 'The methyl-CpG binding protein MeCP2 is essential for embryonic development in the mouse', *Nature genetics*, 12(2), pp. 205–208.

Tesche, C. D. and Karhu, J. (2000) 'Theta oscillations index human hippocampal activation during a working memory task', *Proceedings of the National Academy of Sciences of the United States of America*, 97(2), pp. 919–924.

Thomson, A. M. *et al.* (2002) 'Synaptic connections and small circuits involving excitatory and inhibitory neurons in layers 2–5 of adult rat and cat neocortex: triple intracellular recordings and …', *Cerebral cortex* . Available at: https://academic.oup.com/cercor/article-abstract/12/9/936/383201.

Tillotson, R. *et al.* (2021) 'Neuronal non-CG methylation is an essential target for MeCP2 function', *Molecular cell*, 81(6), pp. 1260–1275.e12.

Timmermann, L. *et al.* (2001) 'Differential coding of pain intensity in the human primary and secondary somatosensory cortex', *Journal of neurophysiology*, 86(3), pp. 1499–1503.

Timofeev, I. *et al.* (2000) 'Origin of slow cortical oscillations in deafferented cortical slabs', *Cerebral cortex* , 10(12), pp. 1185–1199.

Ting, J. T. *et al.* (2014) 'Acute brain slice methods for adult and aging animals: application of targeted patch clamp analysis and optogenetics', *Methods in molecular biology* , 1183, pp. 221–242.

Tomassy, G.S. *et al.* (2014) 'Developmental abnormalities of cortical interneurons precede symptoms onset in a mouse model of Rett syndrome', *Journal of neurochemistry*, 131(1), pp. 115–127.

Tononi, G. and Cirelli, C. (2003) 'Sleep and synaptic homeostasis: a hypothesis', *Brain research bulletin*, 62(2), pp. 143–150.

Tononi, G. and Cirelli, C. (2006) 'Sleep function and synaptic homeostasis', *Sleep medicine reviews*, 10(1), pp. 49–62.

Tononi, G. and Cirelli, C. (2014) 'Sleep and the price of plasticity: from synaptic and cellular homeostasis to memory consolidation and integration', *Neuron*, 81(1), pp. 12–34.

Topçu, M. *et al.* (2002) 'Somatic mosaicism for a MECP2 mutation associated with classic Rett syndrome in a boy', *European journal of human genetics: EJHG*, 10(1), pp. 77–81.

Tort, A. B. L. *et al.* (2008) 'Dynamic cross-frequency couplings of local field potential oscillations in rat striatum and hippocampus during performance of a T-maze task', *Proceedings of the National Academy of Sciences of the United States of America*, 105(51), pp. 20517–20522.

Traub, R. D. *et al.* (1996) 'Analysis of gamma rhythms in the rat hippocampus in vitro and in vivo', *The Journal of physiology*, 493(2), pp. 471–484.

Tropea, D. *et al.* (2009) 'Partial reversal of Rett Syndrome-like symptoms in MeCP2 mutant mice', *Proceedings of the National Academy of Sciences of the United States of America*, 106(6), pp. 2029–2034.

Tudor, M. *et al.* (2002) 'Transcriptional profiling of a mouse model for Rett syndrome reveals subtle transcriptional changes in the brain', *Proceedings of the National Academy of Sciences of the United States of America*, 99(24), pp. 15536–15541.

Uchida, S. *et al.* (1997) 'Brain pharmacokinetics and in vivo receptor binding of 1,4-dihydropyridine calcium channel antagonists', *Life sciences*, 61(21), pp. 2083–2090.

Upreti, V. *et al.* (2013) 'Shock due to amlodipine overdose', *Indian journal of critical care medicine: peer-reviewed, official publication of Indian Society of Critical Care Medicine*, 17(6), pp. 375–377.

Ure, K. *et al.* (2016) 'Restoration of Mecp2 expression in GABAergic neurons is sufficient to rescue multiple disease features in a mouse model of Rett syndrome', *eLife*, 5. doi:10.7554/eLife.14198.

Vacca, M. et al. (2001) 'MECP2 gene mutation analysis in the British and Italian Rett Syndrome patients: hot spot map of the most recurrent mutations and bioinformatic analysis of a new MECP2 conserved region', Brain & development, 23 Suppl 1, pp. S246–50.

Vacher, E. *et al.* (1996) 'Mibefradil, a selective calcium T-channel blocker, in stroke-prone spontaneously hypertensive rats', *Journal of cardiovascular pharmacology*, 27(5), pp. 686–694.

Valderrama, M. *et al.* (2012) 'Human gamma oscillations during slow wave sleep', *PloS one*, 7(4), p. e33477.

Vandecaetsbeek, I. *et al.* (2011) 'The Ca2+ pumps of the endoplasmic reticulum and Golgi apparatus', *Cold Spring Harbor perspectives in biology*, 3(5). doi: 10.1101/cshperspect.a004184.

Van Esch, H. *et al.* (2005) 'Duplication of the MECP2 region is a frequent cause of severe mental retardation and progressive neurological symptoms in males', *American journal of human genetics*, 77(3), pp. 442–453.

Vanyushin, B. F. *et al.* (1968) '5-Methylcytosine and 6-Methylaminopurine in Bacterial DNA', *Nature*, 218(5146), pp. 1066–1067.

Varley, K. E. *et al.* (2013) 'Dynamic DNA methylation across diverse human cell lines and tissues', *Genome research*, 23(3), pp. 555–567.

van de Ven, G. M. *et al.* (2016) 'Hippocampal Offline Reactivation Consolidates Recently Formed Cell Assembly Patterns during Sharp Wave-Ripples', *Neuron*, 92(5), pp. 968–974.

Villard, L. (2007) 'MECP2 mutations in males', *Journal of medical genetics*, 44(7), pp. 417–423.

de Vivo, L. *et al.* (2014) 'Developmental patterns of sleep slow wave activity and synaptic density in adolescent mice', *Sleep*, 37(4), pp. 689–700, 700A–700B.

Vlahou, E. L. *et al.* (2014) 'Resting-state slow wave power, healthy aging and cognitive performance', *Scientific reports*, 4(1), pp. 1–6.

van Vugt, M. K. *et al.* (2010) 'Hippocampal gamma oscillations increase with memory load', *The Journal of neuroscience: the official journal of the Society for Neuroscience*, 30(7), pp. 2694–2699.

Vulliemoz, S. *et al.* (2010) 'The combination of EEG source imaging and EEG-correlated functional MRI to map epileptic networks', *Epilepsia*, 51(4), pp. 491–505.

Vyazovskiy, V. V. *et al.* (2009) 'Cortical firing and sleep homeostasis', *Neuron*, 63(6), pp. 865–878.

Vyazovskiy, V. V. and Harris, K. D. (2013) 'Sleep and the single neuron: the role of global slow oscillations in individual cell rest', *Nature reviews. Neuroscience*, 14(6), pp. 443–451.

Walker, M. P. (2009) 'The role of slow wave sleep in memory processing', *Journal of clinical sleep medicine: JCSM: official publication of the American Academy of Sleep Medicine*, 5(2 Suppl), pp. S20–6.

Walker, M. P. and Stickgold, R. (2004) 'Sleep-dependent learning and memory consolidation', *Neuron*, 44(1), pp. 121–133.

Wan, M. et al. (1999) ‘Rett Syndrome and Beyond: Recurrent Spontaneous and Familial MECP2 Mutations at CpG Hotspots’, American journal of human genetics, 65(6), pp. 1520–1529.

Wang, H. S. *et al.* (1998) ‘KCNQ2 and KCNQ3 potassium channel subunits: molecular correlates of the M-channel’, *Science*, 282(5395), pp. 1890–1893.

Wang, X. J. (1998) ‘Calcium coding and adaptive temporal computation in cortical pyramidal neurons’, *Journal of neurophysiology*, 79(3), pp. 1549–1566.

Wang, G. *et al.* (1999) ‘An R-type Ca(2+) current in neurohypophysial terminals preferentially regulates oxytocin secretion’, *The Journal of neuroscience: the official journal of the Society for Neuroscience*, 19(21), pp. 9235–9241.

Wang, Y. *et al.* (2018) ‘A simplified morphological classification scheme for pyramidal cells in six layers of primary somatosensory cortex of juvenile rats’, *IBRO reports*, 5, pp. 74–90.

Wang, Z. and McCormick, D. A. (1993) ‘Control of firing mode of corticotectal and corticopontine layer V burst-generating neurons by norepinephrine, acetylcholine, and 1S,3R- ACPD’, *The Journal of neuroscience: the official journal of the Society for Neuroscience*, 13(5), pp. 2199–2216.

Watrous, A. J., Fried, I. and Ekstrom, A. D. (2011) ‘Behavioral correlates of human hippocampal delta and theta oscillations during navigation’, *Journal of neurophysiology*, 105(4), pp. 1747–1755.

Watson, B. O. *et al.* (2016) ‘Network Homeostasis and State Dynamics of Neocortical Sleep’, *Neuron*, 90(4), pp. 839–852.

Weick, J. P. *et al.* (2003) ‘Interactions with PDZ proteins are required for L-type calcium channels to activate cAMP response element-binding protein-dependent gene expression’, *The Journal of neuroscience: the official journal of the Society for Neuroscience*, 23(8), pp. 3446–3456.

Weisskopf, M. G., Bauer, E. P. and LeDoux, J. E. (1999) ‘L-type voltage-gated calcium channels mediate NMDA-independent associative long-term potentiation at thalamic input synapses to the amygdala’, *The Journal of neuroscience: the official journal of the Society for Neuroscience*, 19(23), pp. 10512–10519.

Weng, S.-M. *et al.* (2011) 'Synaptic plasticity deficits in an experimental model of rett syndrome: long-term potentiation saturation and its pharmacological reversal', *Neuroscience*, 180, pp. 314–321.

Whittingstall, K. and Logothetis, N. K. (2009) 'Frequency-band coupling in surface EEG reflects spiking activity in monkey visual cortex', *Neuron*, 64(2), pp. 281–289.

Whittington, M. A. *et al.* (1997) 'Recurrent excitatory postsynaptic potentials induced by synchronized fast cortical oscillations', *Proceedings of the National Academy of Sciences of the United States of America*, 94(22), pp. 12198–12203.

Winson, J. (1974) 'Patterns of hippocampal theta rhythm in the freely moving rat', *Electroencephalography and clinical neurophysiology*, 36(3), pp. 291–301.

Winson, J. (1978) 'Loss of hippocampal theta rhythm results in spatial memory deficit in the rat', *Science*, 201(4351), pp. 160–163.

Wise, S. P., Fleshman, J. W. and Jones, E. G. (1979) 'Maturation of pyramidal cell form in relation to developing afferent and efferent connections of rat somatic sensory cortex', *Neuroscience*, 4(9), pp. 1275–1297.

Witcher, D. R. *et al.* (1993) 'Subunit identification and reconstitution of the N-type Ca2+ channel complex purified from brain', *Science*, 261(5120), pp. 486–489.

Wither, R. G. *et al.* (2012) 'Daily rhythmic behaviors and thermoregulatory patterns are disrupted in adult female MeCP2-deficient mice', *PloS one*, 7(4), p. e35396.

Wither, R. G. *et al.* (2013) 'Regional MeCP2 expression levels in the female MeCP2-deficient mouse brain correlate with specific behavioral impairments', *Experimental neurology*, 239, pp. 49–59.

Wolfart, J. and Roeper, J. (2002) 'Selective coupling of T-type calcium channels to SK potassium channels prevents intrinsic bursting in dopaminergic midbrain neurons', *The Journal of neuroscience: the official journal of the Society for Neuroscience*, 22(9), pp. 3404–3413.

Wong, K. *et al.* (2015) 'The trajectories of sleep disturbances in Rett syndrome', *Journal of sleep research*, 24(2), pp. 223–233.

Wood, L. and Shepherd, G.M.G. (2010) 'Synaptic circuit abnormalities of motor-frontal layer 2/3 pyramidal neurons in a mutant mouse model of Rett syndrome', *Neurobiology of disease*, 38(2), pp. 281–287.

Wuytack, F., Raeymaekers, L. and Missiaen, L. (2002) 'Molecular physiology of the SERCA and SPCA pumps', *Cell calcium*, 32(5-6), pp. 279–305.

Xie, L. *et al.* (2013) 'Sleep drives metabolite clearance from the adult brain', *Science*, 342(6156), pp. 373–377.

Xie, W. *et al.* (2012) 'Base-resolution analyses of sequence and parent-of-origin dependent DNA methylation in the mouse genome', *Cell*, 148(4), pp. 816–831.

Yamadori, A. (1971) 'Role of the spindles in the onset of sleep', *The Kobe journal of medical sciences*, 17(3), pp. 97–111.

Yamamoto, J. *et al.* (2014) 'Successful execution of working memory linked to synchronized high-frequency gamma oscillations', *Cell*, 157(4), pp. 845–857.

Yamato, M. *et al.* (2011) 'Nifedipine treatment reduces brain damage after transient focal ischemia, possibly through its antioxidative effects', *Hypertension research: official journal of the Japanese Society of Hypertension*, 34(7), pp. 840–845.

Yasui, D. H. *et al.* (2014) 'Mice with an isoform-ablating Mecp2 exon 1 mutation recapitulate the neurologic deficits of Rett syndrome', *Human molecular genetics*, 23(9), pp. 2447–2458.

Yeo, S. *et al.* (2007) 'Characterization of DNA methylation change in stem cell marker genes during differentiation of human embryonic stem cells', *Biochemical and biophysical research communications*, 359(3), pp. 536–542.

Young, D. *et al.* (2007) 'Sleep problems in Rett syndrome', *Brain & development*, 29(10), pp. 609–616.

Young, J. I. *et al.* (2005) 'Regulation of RNA splicing by the methylation-dependent transcriptional repressor methyl-CpG binding protein 2', *Proceedings of the National Academy of Sciences of the United States of America*, 102(49), pp. 17551–17558.

Yusufzai, T. M. and Wolffe, A. P. (2000) 'Functional consequences of Rett syndrome mutations on human MeCP2', *Nucleic acids research*, 28(21), pp. 4172–4179.

Zhang, L. *et al.* (2008) 'The MeCP2-null mouse hippocampus displays altered basal inhibitory rhythms and is prone to hyperexcitability', *Hippocampus*. Available at: https://onlinelibrary.wiley.com/doi/abs/10.1002/hipo.20389.

Zhang, W. *et al.* (2013) 'Event-related synchronization of delta and beta oscillations reflects developmental changes in the processing of affective pictures during adolescence', *International journal of psychophysiology: official journal of the International Organization of Psychophysiology*, 90(3), pp. 334–340.

Zhang, W. *et al.* (2014) 'Loss of MeCP2 from forebrain excitatory neurons leads to cortical hyperexcitation and seizures', *The Journal of neuroscience: the official journal of the Society for Neuroscience*, 34(7), pp. 2754–2763.

Zhang, X., Lin, J.-S. and Spruyt, K. (2021) 'Sleep problems in Rett syndrome animal models: A systematic review', *Journal of neuroscience research*, 99(2), pp. 529–544.

Zhang, Y. *et al.* (2014) 'An RNA-Sequencing Transcriptome and Splicing Database of Glia, Neurons, and Vascular Cells of the Cerebral Cortex', *The Journal of neuroscience: the official journal of the Society for Neuroscience*, 34(36), pp. 11929–11947.

Zhang, Z.-W., Zak, J. D. and Liu, H. (2010) 'MeCP2 is required for normal development of GABAergic circuits in the thalamus', *Journal of neurophysiology*, 103(5), pp. 2470–2481.

Zhao, Y.-T. *et al.* (2013) 'Loss of MeCP2 function is associated with distinct gene expression changes in the striatum', *Neurobiology of disease*, 59, pp. 257–266.

Zhou, Z. *et al.* (2006) 'Brain-specific phosphorylation of MeCP2 regulates activity-dependent Bdnf transcription, dendritic growth, and spine maturation', *Neuron*, 52(2), pp. 255–269.

Zhu, J. J. (2000) 'Maturation of layer 5 neocortical pyramidal neurons: amplifying salient layer 1 and layer 4 inputs by Ca2+ action potentials in adult rat tuft dendrites', *The Journal of physiology*, 526 Pt 3, pp. 571–587.

Ziller, M. J. *et al.* (2011) 'Genomic distribution and inter-sample variation of non-CpG methylation across human cell types', *PLoS genetics*, 7(12), p. e1002389.

Zimmerman, J. E. *et al.* (2008) 'Conservation of sleep: insights from non-mammalian model systems', *Trends in neurosciences*, 31(7), pp. 371–376.